New AAA-DDD heterocomplexes

by

Smilja Djurdjevic

Degree of Doctor of Philosophy

School of Chemistry

University of Edinburgh

March 2007

Dedicated to my husband and my children

Posveceno mom muzu i mojoj deci

Table of Contents

Abstract

The basis of this project was to synthesise novel aromatic heterocyclic hosts, with two and three adjacent hydrogen bond acceptor (A) sites in AA and AAA arrangements. They have been used to study the binding affinity with donors (D) in AA-DDD and AAA-DDD heterocomplexes. In order to produce the targeted AA and AAA systems, new synthetic methods and techniques such as flash vacuum pyrolysis (FVP), Buchwald-Hartwig coupling and Suzuki coupling chemistry, *etc.* were employed.

The FVP approach allowed the synthesis of naphthyridine ring systems in only two steps from substituted Meldrum's acid derivatives after cyclisation at high temperature. In the second approach palladium catalyzed coupling was used to provide heterocyclic diarylamines from readily available pyridine or naphthyridine precursors, with subsequent ring closure under acidic conditions. This approach led to the synthesis of new compounds: dipyrido[1,2-*a*;2',3'-*a*]pyrimidin-5-one **106** (AA) and 1,6a,11,12–tetraaza-naphthacene-6-one **110** (an AAA hydrogen bonding unit) in high yields. The Suzuki coupling strategy afforded compounds: dibenzo[*c*,*f*][1,8]naphthyridine **117** (AA) and 1,13,14-triazadibenz[*a*,*j*]anthracene **120** (AAA). Their extended aromatic framework is thought to help overcome stability problems during binding studies.

For the binding studies, the selected DDD counterparts were dihydropyridines **1**, 2,6-bis(hydroxy-methyl)-*p*-cresol **124** and protonated 2,6-diaminopyridine (with a lipophylic tetraarylborate counter-ion) **125** developed as a cationic DDD unit.

K_a values for **1•117** (8.6×10^4 M^{-1}), **1•106** (6.2×10^3 M^{-1}) and **124•120** (2.4×10^4 M^{-1}) were determined by ^{1}H NMR titration experiments in chloroform-*d* solution. The other AAA-DDD heterocomplexes **1•110**, **1•120** and **125•120** display very high binding stabilities ($K_a > 10^5$ M^{-1}) and these K_a values were determined using fluorescence spectroscopy. In this way accurate assignment of $K_a = 1.4 \times 10^6$ M^{-1} for the **1•110** heterocomplex, $K_a = 2.6 \times 10^7$ M^{-1} for the **1•120** heterocomplex and $K_a = 3.8 \times 10^9$ M^{-1} for the cationic **125•120** heterocomplex were determined. The experimental binding constants were in qualitative agreement with molecular modelling calculations for **1•110** and **1•120** heterocomplexes. The extremely high

binding stability of all these heterocomplexes is attributed to the combination of cooperative secondary interactions and strong electrostatic energy. All these factors, with additional cationic charge in the **125•120** heterocomplex, makes binding exceptionally strong in this case so that **125•120** is the most stable AAA-DDD heterocomplex reported so far.

Declaration

The scientific work described in this thesis was carried out in the School of Chemistry at the University of Edinburgh between May 2002 and December 2006. Unless otherwise stated, it is the work of the author and has not been submitted in whole or in support of an application for another degree or qualification of this or any other University or institute of learning.

Lectures and Meetings Attended

1. **Organic Research Seminars**, School of Chemistry, University of Edinburgh, Scotland, 2002-2006.

2. **Firbush Organic Talks**, School of Chemistry, University of Edinburgh, Scotland, 2002-2006.

3. **Perkin Organic Chemistry Conference**, University of Dundee, Scotland, 12/02.

4. **UK Macrocycles and Supramolecular Chemistry Meeting EMMA Scientific Conference**, University of Edinburgh, Scotland, 5/02.

5. **Perkin Organic Chemistry Conference**, School of Chemistry, University of Edinburgh, Scotland, 12/03.

6. **USIC 2004**, Heriot Watt University, Edinburgh, Scotland, 9/04.

7. **RSC Perkin Meeting**, University of St Andrews, Scotland, 11/04, Presented poster entitled: *"Extremely stable triple hydrogen bonded AAA-DDD heterocomplexes."*

8. **Perkin Organic Chemistry Conference**, School of Chemistry, University of Edinburgh, Scotland, 12/04.

9. **229th ACS National Meeting,** San Diego, California, USA, 3/05. 15-minute oral presentation: *"Extremely stable triple hydrogen bonded AAA-DDD heterocomplexes."*

10. **20th International Congress of Heterocyclic Chemistry,** Palermo, Sicily, 8/05. 30-minute oral presentation entitled: *"Novel triple hydrogen bonded AAA-DDD heterocomplex with high binding stability".*

11. **International Symposium on Reactive Intermediates and Unusual Molecules,** 10/05. Presented poster entitled: *"Novel triple hydrogen bonded AAA-DDD heterocomplex with high binding stability".*

Acknowledgements

List of Abbreviations

A	Acceptor
K_a	Association constant
Å	Angstrom
δ	Chemical shift
A-T	Adenine-Thymine
Al_2O_3	Aluminium-oxide
BINAP	2,2'-Bis(diphenylphosphino)-1,1'-binaphthyl
$CsCO_3$	Cesium carbonate
CHN	Carbon, hydrogen, nitrogen analysis
D	Donor
DDQ	Dichlorodicyanoquinone
Ph_2O	Diphenyl oxide
Ph_2	Diphenyl
DMF	*N,N'* -dimethylformamide
DMSO	Dimethylsulfoxide
DNA	Deoxyribonucleic acid
DCM	Dichloromethane
equiv	Equivalent
ESI	Electrospray Ionisation
FVP	Flash vacuum pyrolysis
FAB	Fast Atom Bombardment
T_f	Furnace temperature
$\Delta G°$	Free energy
g	Grams
G-C	Guanidine-Cytosine
h	Hours
δ_H	Hydrogen chemical shift
δ_C	Carbon chemical shift
H-bonding	Hydrogen bonding
HRMS	High Resolution Mass Spectrometry

$CDCl_3$	Deuterated Chloroform
cm	Centimetre
shift, h	Chemical shift of the host
shift, cplx	Chemical shift of the complex
J	Coupling constant
°C	Degree Celsius
IUPAC	International Union of Pure and Applied Chemistry
kcal	Kilocalorie
λ	Lambda
$MgSO_4$	Magnesium sulfate
M	Molar
MeOH	Methanol
Me	Methyl
MA	Meldrum's acid
MMMA	Methoxymethylene Meldrum's acid
mg	Milligram
MHz	MegaHertz
min	Minutes
mL	Millilitres
μm	Micromolar
mmol	Millimoles
mp	Melting point
MS	Mass Spectrometry
m/z	Mass-to-charge ratio
NBS	*N*-Bromosuccinimide
NMR	Nuclear Magnetic Resonance
ppm	Parts per million
p	Pressure
$Pd(OAc)_2$	Palladium acetate
K_2CO_3	Potassium carbonate
$POCl_3$	Phosphorus oxychloride
PCl_5	Phosphorus pentachloride

RNA	Ribonucleic acid
R	Substituent
Na_2CO_3	Sodium carbonate
NaOH	Sodium hydroxide
s	Second
[H]	Starting concentration of the host
[G]	Starting concentration of the guest
Vol_H	Starting volume of the host
T_i	Temperature of inlet tube
t	Time
TBDMS	t-Butyldimethyl silyl ether
TMS	Trimethylsilyl
TMV	Tobacco mosaic virus
TLC	Thin Layer Chromatography
UV	Ultraviolet

General Comments on Experimental Data

Unless stated otherwise, all reagents and anhydrous solvents were purchased from Aldrich Chemicals and used without further purification. Column chromatography was carried out using Kieselgel C60 (Merck, Germany) as the stationary phase, and TLC was performed on precoated silica gel plates (0.25 mm thick, $60F_{254}$, Merck, Germany) and observed under UV light. All ^{1}H and ^{13}C NMR spectra were recorded on a Bruker AV400 instrument at a constant temperature of 25 °C. Chemical shifts are reported in parts per million from low to high field and referenced to TMS. Coupling constants (J) are reported in Hertz (Hz). Standard abbreviations indicating multiplicity were used as follows: m = multiplet, br = broad, d = doublet, q = quartet, t = triplet, s = singlet. All melting points were determined using a Sanyo Gallenkamp apparatus and are reported uncorrected. ESI mass spectrometry was performed with a Micromass Platform II mass spectrometer controlled using Masslynx v2.3 software while FAB mass spectrometry was carried out by the laboratory services at the University of Edinburgh. Elemental analyses were performed on a Perkin-Elmer 2400 Series CHN analyzer. Steady state absorption spectroscopy was conducted by using a Hitachi UV-3300 spectrophotometer and corrected fluorescence spectra were recorded on a Hitachi F-4500 spectrofluorimeter. All the experiments were conducted at ambient temperature and the dichloromethane used for fluorescence spectroscopy was of analytical grade and was filtered through a 1 μm filter before use. The fluorescence cells used were thoroughly cleaned with water, acetone and dichloromethane before use.

Chapter 1:   Complementary hydrogen bond-directed heteroaromatic assemblies
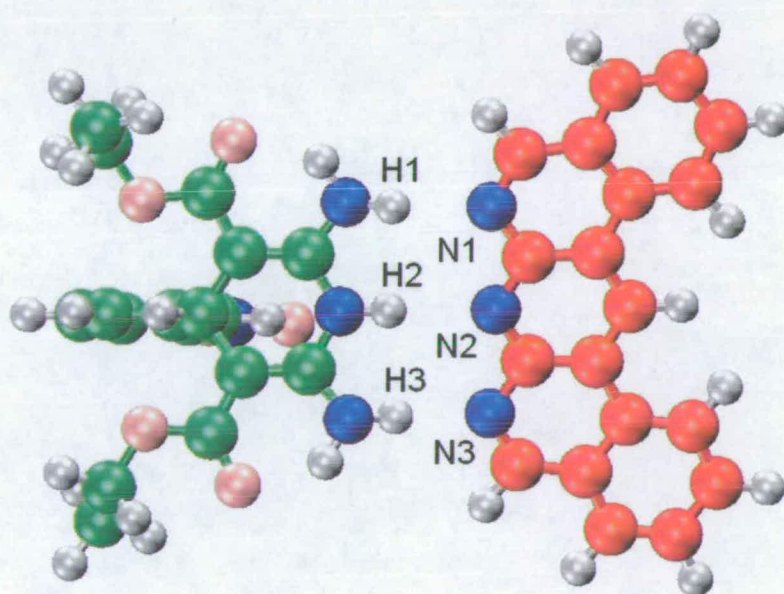
Molecular model of 1•120 heterocomplex

Introduction

In this introduction, the factors influencing the formation of hydrogen bonded complexes will be discussed, followed by a comprehensive review of triple and some quadruple hydrogen bonded systems in all arrangements. The importance the acceptor-acceptor-acceptor (AAA)/ donor-donor-donor (DDD) arrangements will become apparent and this is the subject of the experimental results in this thesis. An excellent review of hydrogen bonded complexes appeared in 2000.[1] The purpose of this chapter is to summarize this account and to update it with advances in the field over the last 6 years.

1.1 Self-assembly challenge

Many examples of self-assembly can be found in biological systems and are used as inspiration for scientists from numerous disciplines in the hope of learning to design and control the behaviour of self assembling systems. "Self-assembly, an essential process for creating and maintaining the organisation of complex biological systems has provided a special challenge for biomimetic chemists" was thus described by Zimmerman and Corbin.[2]

The most striking example is the DNA double helix formed from two complementary deoxyribonucleic acid strands under the right conditions. The thermodynamically stable double helix forms spontaneously and reversibly as the strands are mixed together and hydrogen bonds form between complementary base pairs (Figure 1.1). Self-assembly allows access to very complex architectures not accessible in traditional multi-step synthesis with many potential applications from information storage to drug delivery.[3] Nature's use of purines and pyrimidines as the storage units of genetic information was the inspiration for many chemists to use the heteroaromatic modules as recognition units for self assembly.
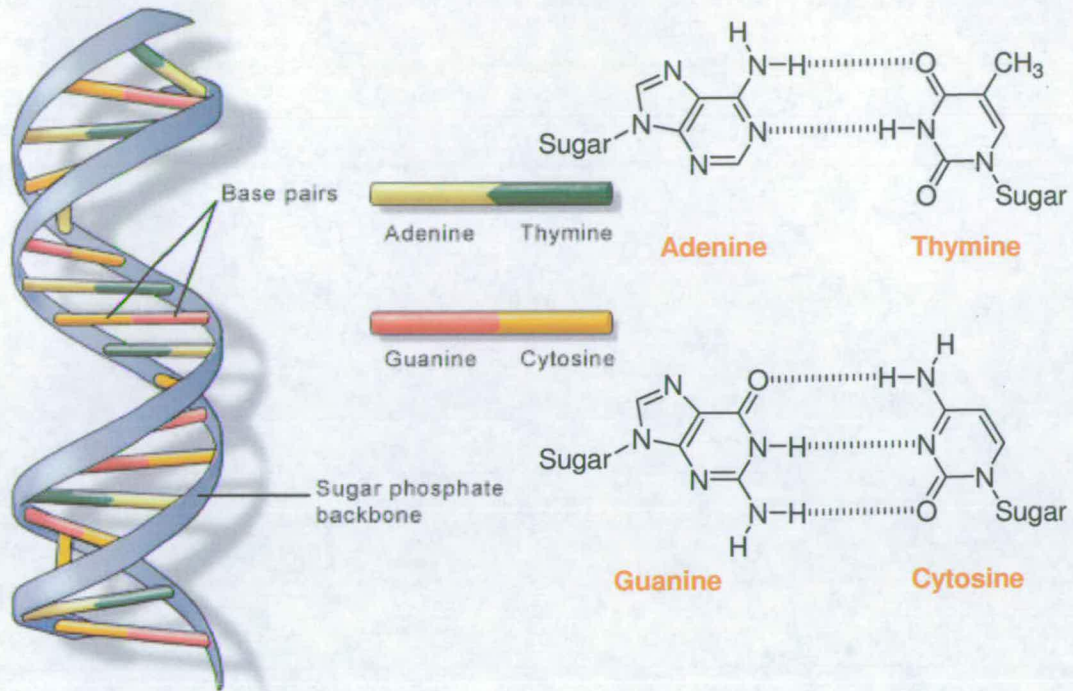
Figure 1.1 Hydrogen-bonded complementary A-T and G-C base pairs in DNA (Image courtesy of the U.S. National Library of Medicine).

A more complex example of self-assembly is found in living systems such as the tobacco mosaic virus (TMV)[4] which consists of a single RNA strand and 2130 protein subunits within the capsomers[5] (Figure 1.2). Virus's superstructure is formed when protein blocks self-assemble around the RNA strand (16.3 proteins per helix turn) driven by non-covalent interactions and hydrophobic forces.
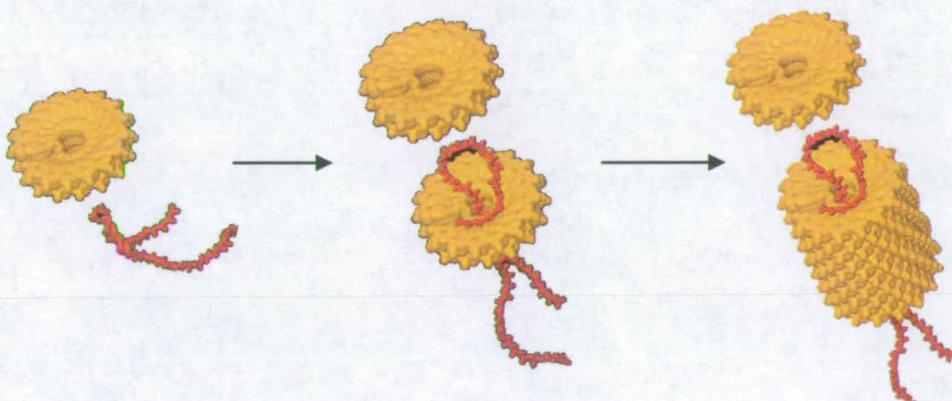
Figure 1.2 The capsomers (orange) grow into a spiral and self-assemble around RNA strands (red) to form the cylindrical shape of the tobacco mosaic virus (Image courtesy of the H. Wang and G. Stubbs from Vanderbilt University).

The DNA and RNA base-pairing systems have been used in numerous model studies providing a considerable body of quantitative binding data as do the many host-guest studies that have targeted the nucleobases with heteroaromatic hosts.[4, 6-10]

Preference for heteroaromatic compounds in binding studies is due to their geometrically well defined, rigid structure often with a linear, array of hydrogen bond *donor* (D) and *acceptor* (A) groups present on the edges of the heterocyclic system. The main disadvantages for using them as building blocks in host-guest studies are solubility problems and difficulties in controlling the tautomeric forms.

This introduction presents a short review of all relevant factors determining stability and strength of hydrogen bonded interactions in the directed heteroaromatic assemblies which have been employed to date, with the focus on heteroaromatics with a linear array of triple hydrogen bonded surface.

1.2 Factors affecting complex stability

The key factor in determining the correct self-assembled structure is the *complementarity* with which individual components assemble. The most important example of complementarity is base pairing in the DNA double helix; adenine complements thymine (A-T) and guanine complements cytosine (G-C) with formation of two and three hydrogen bonds, respectively (Figure 1.1). At the same time many other factors affect the direction and stability of complexation such as: strength and number of individual hydrogen bonds, arrangement of hydrogen bonding sites, geometry of the hydrogen bond surface, cooperativity effect, host preorganisation, tautomeric forms, solvent effect *etc.*, and they will be discussed below.

1.2.1 Hydrogen-bond interactions

The stability of any hydrogen-bonded complex is determined by the strength of the individual hydrogen bonds. Hydrogen bonding arises from a combination of electrostatic, inductive, charge-transfer and dispersion energy effects.[11] Electrostatic interaction between the partially positive hydrogen atom of the donor site and the lone pair of the acceptor site plays the largest role (Figure 1.3). The strength of a single hydrogen bond in the gas phase is typically of the order of 2-20 kcal mol^{-1}, much less than the energy of a covalent bond (35-135 kcal mol^{-1}).

donor   acceptor
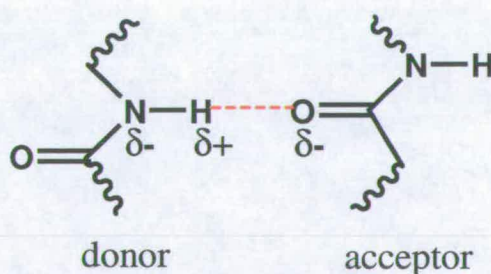
Figure 1.3 Typical hydrogen bond.

Jeffrey and Saenger[12] have concluded that the energy of an individual hydrogen bond between uncharged groups is 1.0-1.4 kcal mol^{-1}, whereas that involving a charged

group is slightly higher (1.5-2.8 kcal mol^{-1}). When both donor and acceptor are charged, the energy of a hydrogen bond rises to 4 kcal mol^{-1}. Six years later Scheiner[13] reports that the energy of the H-bonds when either donor or acceptor is charged becomes much stronger then thought previously in the range of 10-45 kcal mol^{-1}. This allows us to create a model where increasing the positive charge upon the donor proton or increasing the negative charge upon the acceptor atom are both expected to increase the strength of the interaction. In that respect, Wilcox and co-workers[14] investigated the effect of substituents on the strength of hydrogen-bonding interactions between thioureas and a zwitterionic sulfonate (Figure 1.4).

K_a = 6600 M^{-1} (CDCl$_3$) K_a = 10 M^{-1} (CDCl$_3$)
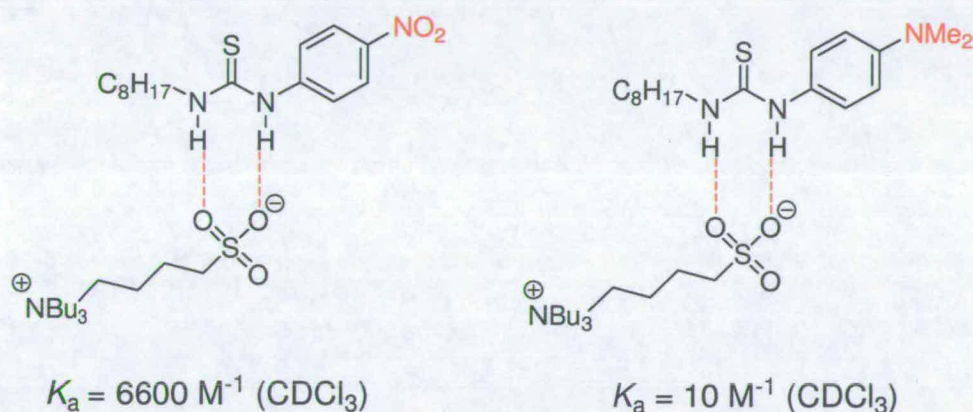
Figure 1.4 Urea-sulfonate dyad studied by Wilcox and co-workers.[14]

The association constant measured in CDCl$_3$ ranged from 6600 M^{-1} for a nitrobenzene-substituted receptor to 10 M^{-1} for a receptor featuring the dimethylanilino substituent. This corresponds to the difference in binding energy of 3.8 kcal mol^{-1} and is due to an increase in hydrogen bond donating capability by the proximal N-H group.

1.2.2 Number of hydrogen bonds

The number of hydrogen bonds in general, plays an important role in determining the strength of complexation. In Figure 1.5 three heterocomplexes involving two **1•2**, three **1•3** and six **4•5** hydrogen bonds are compared, as determined by Zimmerman and co-workers.[6, 15, 16]
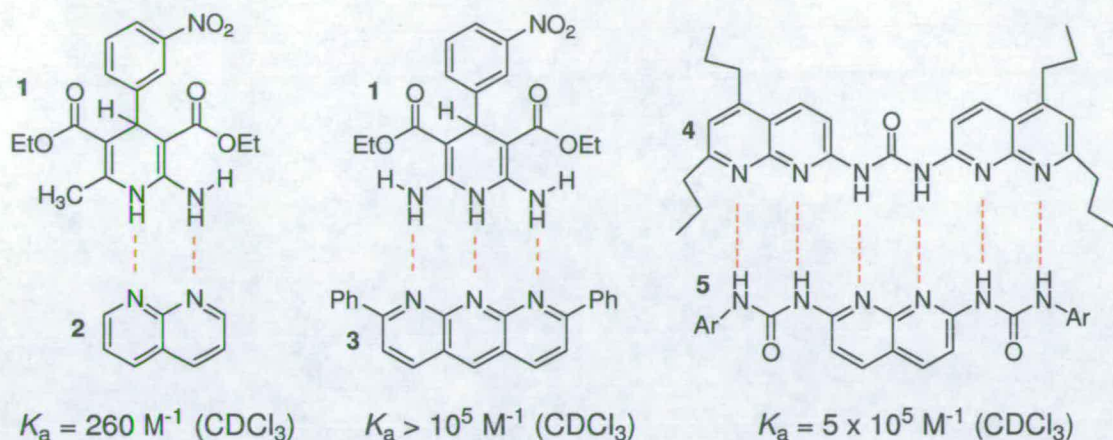
Figure 1.5 Heterocomplexes developed by Zimmerman and co-workers[6, 15, 16] with two, three and six hydrogen bonds.

The triple hydrogen bonded assembly **1•3** exhibits a significantly higher stability ($K_a > 10^5$ M^{-1}) than the corresponding motif based on two H-bonds **1•2** ($K_a = 260$ M^{-1}). However the heterocomplex based on six hydrogen bonds **4•5** has a very similar association constant ($K_a = 5 \times 10^5$ M^{-1}) to that of the triple hydrogen bond motif although three additional hydrogen bonds have been introduced. This indicates that the number of hydrogen bonds is not the only important factor in determining the binding strength.

1.2.3 Arrangement of hydrogen bonding sites

Rich and co-workers[9] systematically compared the experimental binding data available for the 3-H bonded dimeric complexes **6•7**, **8•9** and **3•10** (Figure 1.6) in chloroform-*d* and found very different binding stabilities ranging from 10^2 to 10^4-10^5 M^{-1}. These differences in stabilities have been largely attributed to attractive and repulsive *secondary* interactions as exemplified by the "Jörgensen model"[17, 18] and "Schneider's rule".[19] Jörgensen proposed that secondary electrostatic interactions arising from the arrangement of the hydrogen-bond donor and acceptor groups is a critical factor in determining the complex stability.

Sartorius and Schneider derived a simple empirical rule using the Jorgensen model to predict the binding strength of a given complex. They postulated that free energy for dimerisation consists only of two increments: a contribution of 1.88 kcal mol^{-1} for each H-bond and ± 0.7 kcal mol^{-1} for each attractive or repulsive secondary interaction.[19]

Stabilization arises from electrostatic interaction between positively and negatively polarized atoms in adjacent H-bonds, whereas destabilization is likewise the result of electrostatic repulsion between two positively or negatively polarized atoms (Figure 1.6).
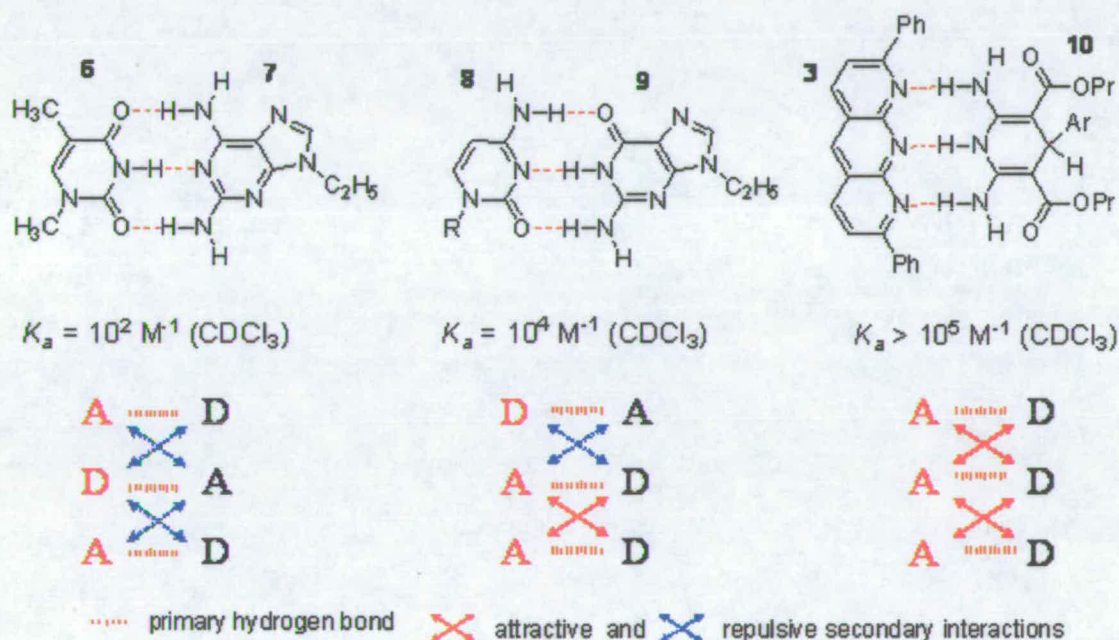
Figure 1.6 The effect of attractive and repulsive secondary interactions on binding strength – demonstration of the "Jorgensen secondary interaction" model.

Formation of the AAD-DDA system involves two attractive and two repulsive secondary interactions whereas in the weakest ADA-DAD complex all secondary interactions are repulsive. The Jorgensen model predicted the highest association constant for an AAA-DDD complex **3•10** with exclusively four attractive secondary interactions and that has been proven experimentally by Zimmerman and Murray.[20]

1.2.4 Cooperativity

Cooperativity[21] plays an important role in maintaining the stability and selectivity of biological systems and is partly responsible for the ready formation of the DNA duplex. Hunter and co-workers[22, 23] employed this approach in developing the "zipper" complex (Figure 1.7a) which is held together by a combination of multiple hydrogen bonding interactions between different amide units with additional edge to face π-π interactions in the spacer. The dimer has an association constant of 1.1×10^3 M^{-1}. The modified approach developed by Gong *et al*[24] involves the covalent synthesis of modules of rigid linear arrays of multiple H-bonding sites (Figure 1.7b) and this dimer has an association constant of 10^9 M^{-1}.

a) $K_a = 1.1 \times 10^3$ M^{-1} (CDCl$_3$)   b) $K_a > 1.3 \times 10^9$ M^{-1} (CDCl$_3$)
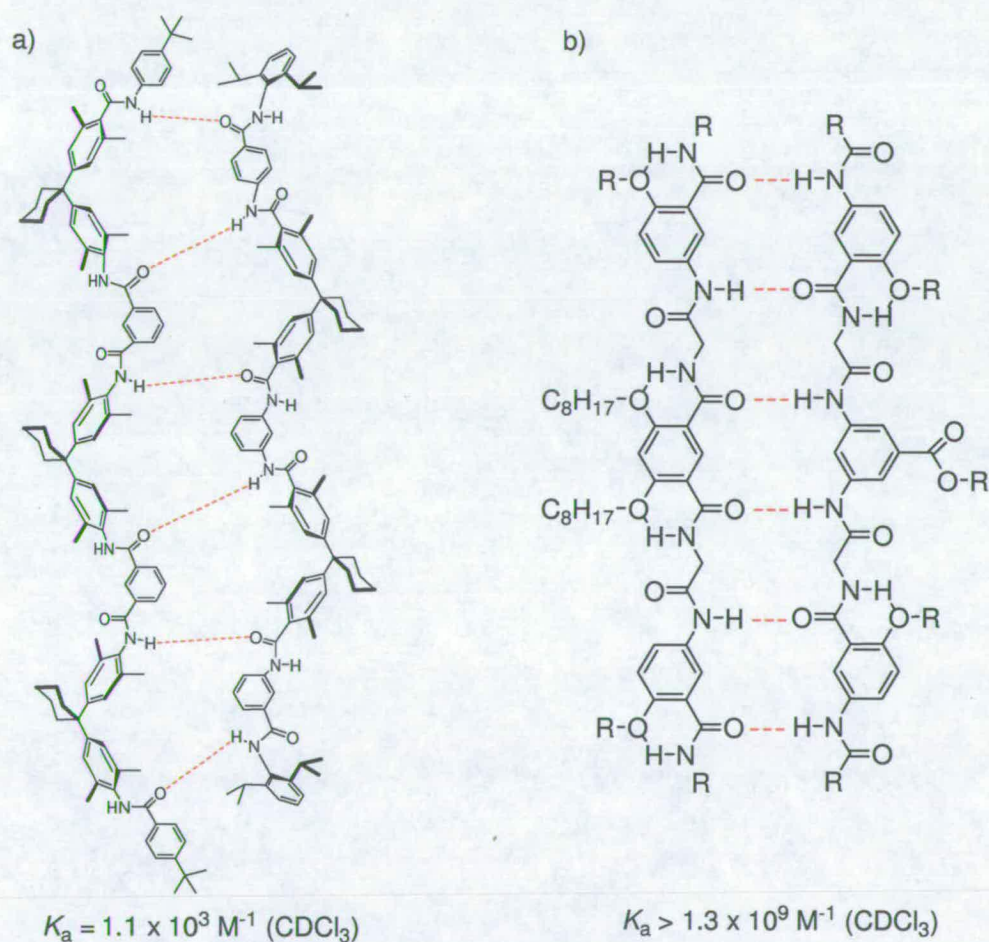
Figure 1.7 Multidentate zipper complexes as reported by a) Hunter and co-workers[22, 23] and b) Gong and co-workers.[24]

These two different strategies use as the key factor, a positive cooperativity effect between individual H-bonding sites to increase the stability of H-bonded assemblies. Although both complexes have the same number and arrangement of hydrogen bonds, the difference in the binding stabilities of 10 kcal mol^{-1} is largely contributed to the rigid geometry of binding sites in the later example.

1.2.5 Other factors

There are a few other factors that will determine the strength with which heteroaromatic modules pair, such as host preorganisation (Part 1.3.2), tautomeric forms of heterocyclic units (Part 1.4), solvent effects and these will be discussed in later sections. Chloroform is the most common solvents used in complexation and self-assembly studies. Chloroform is preferred because it is not highly competitive for hydrogen bond donor and acceptor sites, yet it is a good solvent for dissolving the heteroaromatic compounds. In cases when the complex is not soluble in chloroform the usual way to solubilise it is to synthesise analogues with introduced lipophilic groups as seen in many examples (Figure 1.8, Figure 1.12, Figure 1.20, *etc.*).

1.3 Triple hydrogen bonded heteroaromatic motifs

In this part all relevant examples of heteroaromatic modules with triple hydrogen bond motifs (ADA, DAD, AAD, DDA, DDD and AAA) will be covered. Their complementary dimeric modules (ADA-DAD, AAD-DDA and AAA-DDD) will be considered together with selected examples of their use in supramolecular formation.

1.3.1 ADA and DAD Heteroaromatic motifs

The ADA-DAD system is the most common binding motif used in complexation studies due to a number of available compounds that can used as hydrogen bonded ADA or DAD units. Although the weakest of all triple hydrogen bonded heterocomplexes (Part 1.2.3), it is the best studied and a number of series of

ADA-DAD complexes with their corresponding K_a values have been measured in chloroform-_d_. The first series was developed by Rich and co-workers[9] and is presented in Figure 1.8.

$K_a = 170$ M^{-1} $K_a = 210$ M^{-1} $K_a = 500$ M^{-1}
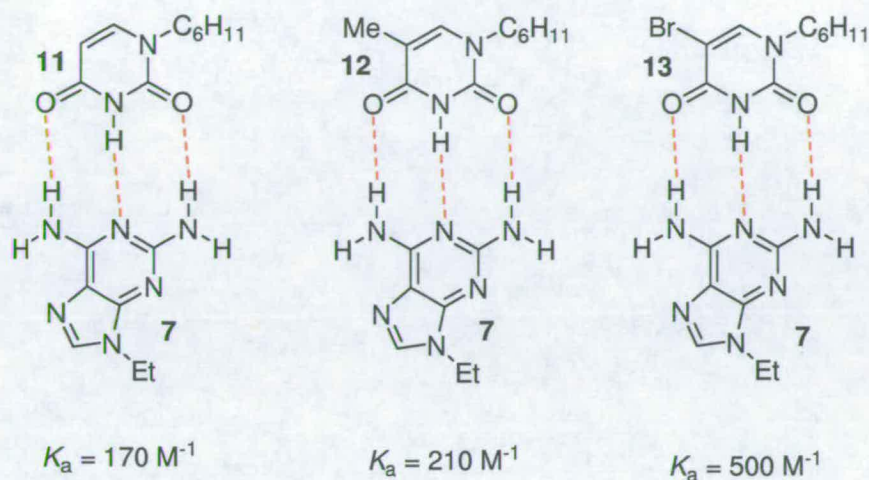
Figure 1.8 Hydrogen bond complexes containing the ADA-DAD arrangement developed by Rich and co-workers.[9] Association constant measured in chloroform-_d_.

The K_a values range from 100 M^{-1} (6•7 complex, Figure 1.6) to 500 M^{-1} for the 13•7 complex although the DAD unit 7 was the same and only the ADA unit has been changed from 6 to 13. The difference in binding strength is attributed to the substituents incorporated into the aromatic ring of units 6, 12 and 13. Binding stability can be enhanced using substituent effects as discussed in Part 1.2.1 and illustrated in heterocomplex 13•7, the strongest in this series.

Hamilton and Engen[25] used new a diamidopyridine based DAD unit (15) in an ADA-DAD array (Figure 1.9a) which is developed as a part of a study of synthetic receptors for biologically active molecules. The binding constant of 14•15 heterocomplex was only 90 M^{-1} but the effort was made to design the complement to the targeted receptors using the strategy of substrate induced organization of the binding site.

a) b)

14

15

$K_a = 90 \text{ M}^{-1}$

16
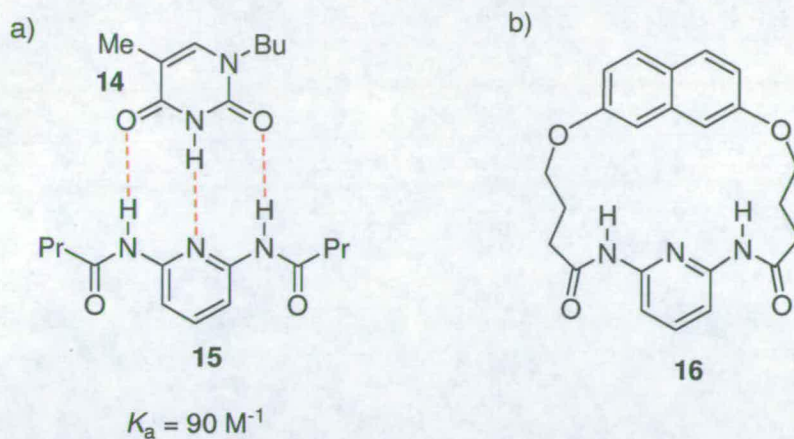
Figure 1.9 Hydrogen bond complex **14•15** in ADA-DAD arrangement with macrocyclic DAD receptor **16** developed by Hamilton and Engen.[25] Association constant measured in chloroform-*d*.

The approach was to assemble hydrogen bonding and hydrophobic groups within a macrocyclic structure such as compound **16** (Figure 1.9b) that can form a cavity complementary to the nucleotide base substrate. After substrate complexation, the naphthalene unit lay approximately parallel to the plane of the thymine unit, as seen in receptors for nucleotide base substrates. The structures of the macrocycle **16** and complex **14•16** have been confirmed by X-ray crystallography (Figure 1.10) and the ADA-DAD pairing was clearly seen in an X-ray analysis of the crystalline complex.

Guest
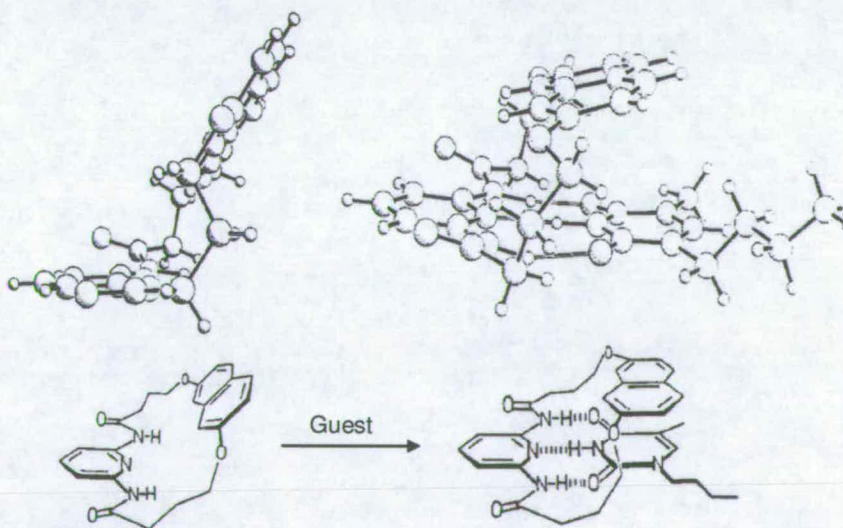
Figure 1.10 X-structures of **16** and **14•16** complex. Figure reprinted from Hamilton A.D and van Engen D.[25]

The binding constant of the complex **14•16** measured in chloroform was 290 M^{-1} (*vs.* 90 M^{-1} for **14•15**, Figure 1.9a), analyzed by Hamilton.[25] The added stability of **14•16** system is in the combination of a hydrogen bonding array and π-stacking interactions, clearly seen in the solid-state structure.

The most commonly used ADA unit within ADA-DAD arrays contains pyrimidine-2,4-dione nucleus such as **11**, **12**, **13** (Figure 1.8) and **17**, **20** (Figure 1.11). They are easily synthesised in one step by *N*-alkylation of thymine or uracil with an alkyl halide. Heterocomplexes **17•18** and **17•19** were developed by Rebek and co-workers,[26] and systems **20•21** and **20•22** were designed by Meijer and co-workers.[27] The K_a values measured in CDCl$_3$ range from 436 to the 900 M^{-1} respectively.
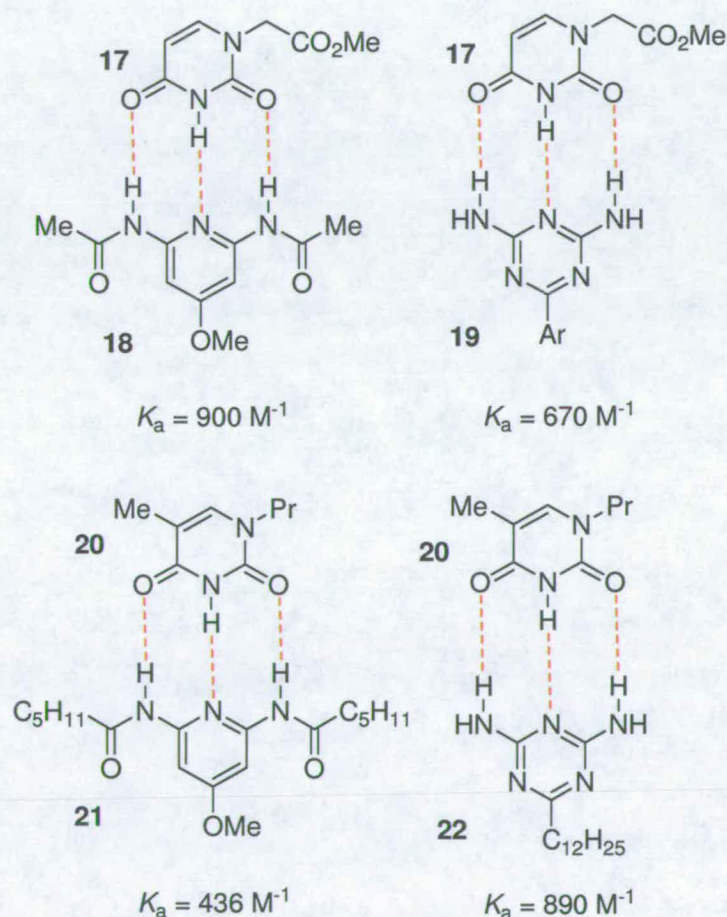
Figure 1.11 Hydrogen bond complexes in ADA-DAD arrangement developed by different authors.[26,27] Association constants were measured in chloroform-*d*.

A number of compounds can serve as DAD units, and many of them are commercially available (*e.g.* diaminopyridine, diaminopyrimidine, melamine *etc.*) or readily available such as diamidopyridine derivatives **15** (Figure 1.9), **18** and **21** (Figure 1.11) and diaminotriazines as **19** and **22** (Figure 1.11).

Dimeric systems containing ADA modules are synthesised by alkylating appropriate thymine or uracil analogues with an alkyl dibromide as illustrated in Leonard's synthesis[28] of bis-thymine **23** (Figure 1.12).
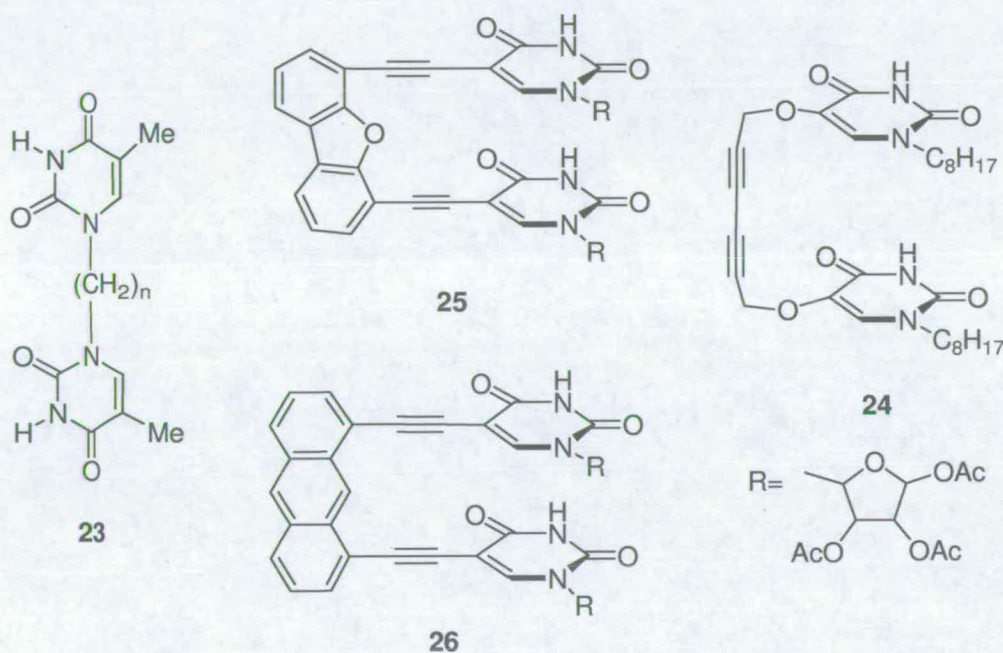
Figure 1.12 Dimeric ADA modules constructed by covalently linking two identical modules, R=

Another example is Hamilton's[29] linking two 1-octyl-5-hydroxythymine units by a diyne spacer to give compound **24**. Sessler[30] introduced anthracene and benzofuran spacers in syntheses of rigid units **25** and **26** to provide a series of "artificial dinucleotides" (See Figure 1.28) some of which form DNA-like complexes, and will be discussed later (Section 1.3.3).

As appropriate counterparts for dimeric ADA modules a number of DAD dimeric systems were developed with some of them illustrated in Figure 1.13.
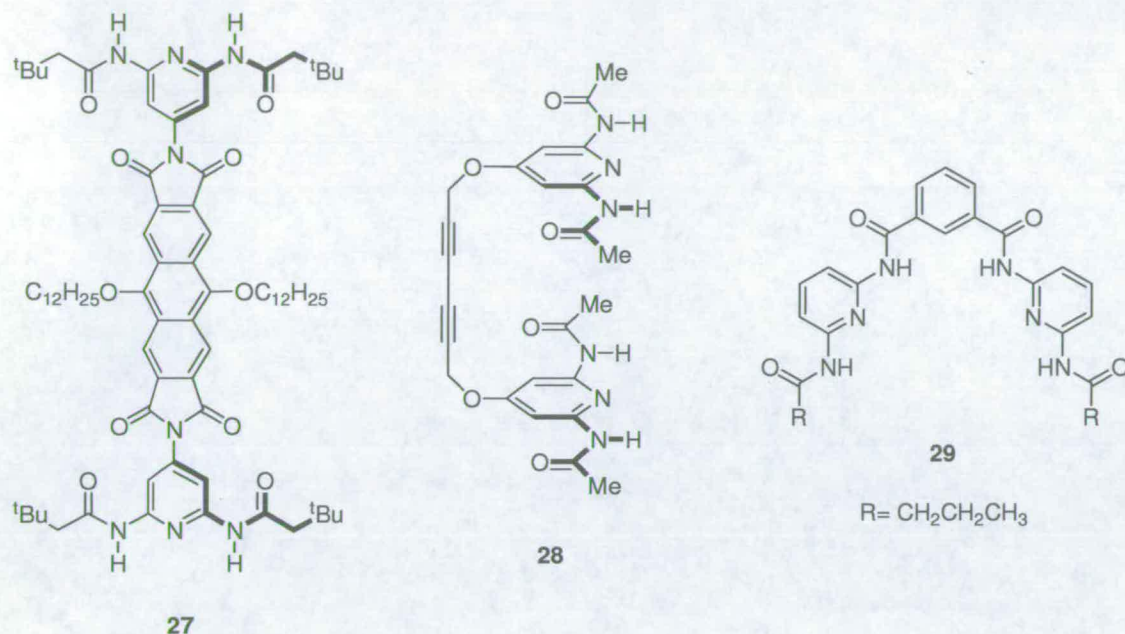
Figure 1.13 Dimeric DAD modules constructed by covalently linking two identical modules.

Compound **28**,[29] was designed as a complementary unit with matching spacer distance of about 10 Å to analogous **24** (See Figure 1.16 for self-assembly structure). Lehn[31] developed the rigid, rod-like bis-diamidopyridine subunit **27** useful for creating polymeric assemblies using hydrogen bonding sites along the axis of the molecule. The dimer **29** was designed to form closed, discrete aggregates with appropriate complementary partners.

The ADA units (Figure 1.14) containing only -N and –NH groups as hydrogen bond acceptor and donor sites are anthyridinone or anthyridan units **30** and **32** respectively, developed by Murray and Zimmerman.[20] Binding constants determined for complexes **30•10**, **32•10** and **30•31** are around 70 M^{-1} and are amongst the lowest for this ADA-DAD arrangement. Several reasons can be attributed to this fact, including low solubility of anthyridones in chloroform and tautomerism of counterpart **10**, as will be addressed later in Chapter 3.
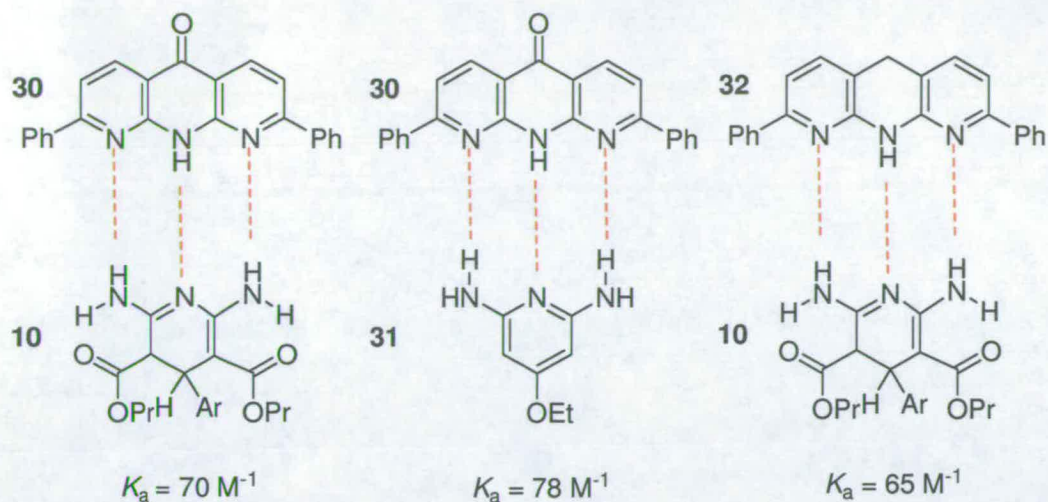
Figure 1.14 Hydrogen bond complexes in ADA-DAD arrangement developed by Zimmerman and co-workers.[20] Association constant measured in chloroform-*d*.

Overall, K_a values of all ADA-DAD heterocomplexes presented so far range from 65 M^{-1} (**32•10**) to 900 M^{-1} for the **17•18** complex. Although this is a narrow range for complexes that contain the same number and arrangement of hydrogen bonds, the free energy ($\Delta G°$) difference is only 1.5 kcal mol^{-1}. Differences in binding stabilities are predominantly attributed to the structural differences of binding units (geometry, introduced substituents, hydrogen bond acceptor and donor groups etc.) and to the measurement methods. Although all binding constants have been measured in chloroform-*d* using ^{1}H NMR titration experiments, they have been done in different labs using different NMR instruments. All this together with variability in the conditions for the binding studies (water content in the chloroform-*d*, solubility and purity of binding components *etc.*) and experimental errors can explain differences in measured binding stabilities.
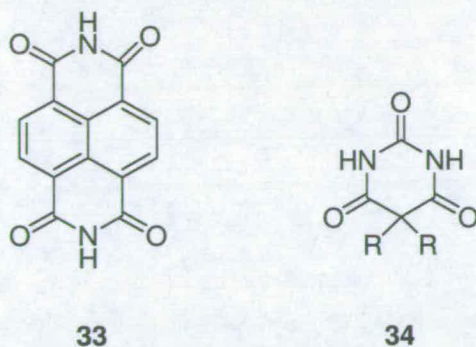
Figure 1.15 Intrinsic ditopic modules containing two ADA modules.

Finally, some ditopic ADA units were found in the commercially available naphthalene diimide **33** and in the substituted barbituric acids **34** (Figure 1.15), extensively used as modules in self-assembly.

1.3.2 Self-assembling ADA-DAD systems

Many of the examples described above were designed to form closed or discrete aggregates such as **24•28**; **35•34**; **37•34**; **38•39**; **37•33** and **27•38**. The linking of modules is an important factor for increasing the complex stability, for example the K_a for **24•28** (Figure 1.16) was 4500 M^{-1}, 10-fold higher than an analogous single base-pair **20•21** (Figure 1.11).
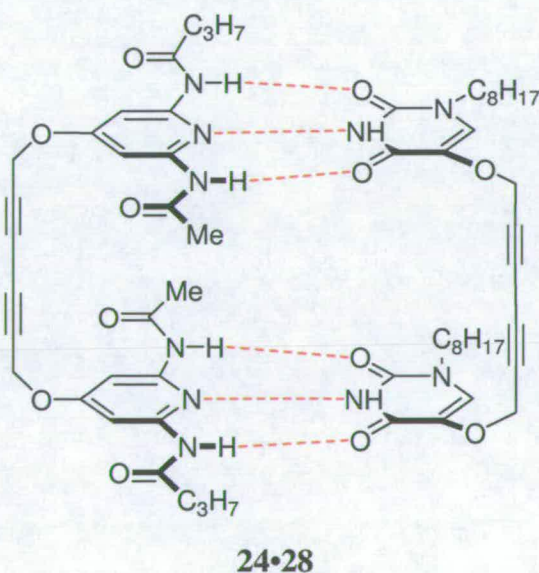
24•28

Figure 1.16 Self-assembled structure of dimeric modules **24•28**.

Very often hydrogen bonding sites in the modules are in approximate parallel planes as seen in **24•28**, but sometimes they are designed to converge as in the **35•34** complex (Figure 1.17) with an association constant of 10^6 M^{-1}.[32] This value is 2-4 orders of magnitude higher than the analogous heterocomplex **29•34** (Figure 1.17).

$K_a = 10^4$ M^{-1}

$K_a = 10^6$ M^{-1}
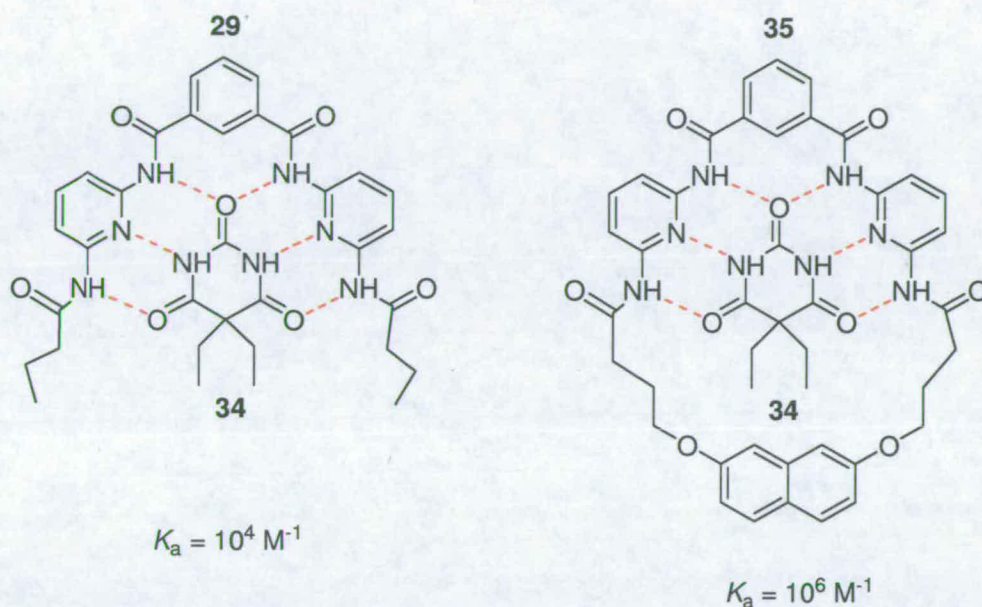
Figure 1.17 Effect of host preorganisation in **29•34** and **35•34** complexes on hydrogen bonding stability. Association constants measured in chloroform-*d*.

This difference of 100-fold smaller K_a for the **29•34** complex compared with the **35•34** complex was explained by different degrees of *host preorganisation* between the two systems. In acyclic host **29** hydrogen bonding sites are free to adapt a number of conformations, making complexation with guests less effective. In macrocyclic host **35** binding sites are pre-organised in such a manner to enhance binding with ligand **34** involving all six hydrogen bonds and resulting in stronger binding. A crystal structure of the complex was obtained (Figure 1.18), providing further evidence for the binding mode.
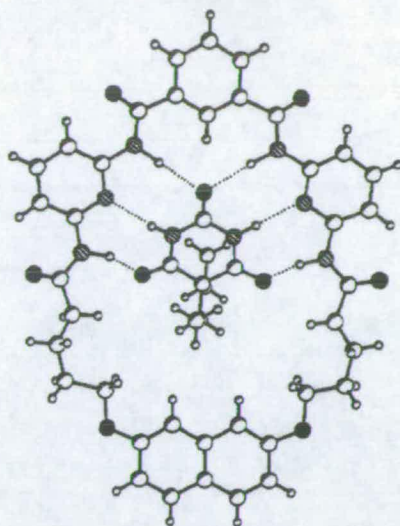
Figure 1.18 Crystal structure of the receptor 35•34 complex, X-ray figure reprinted.[33]

Another strategy for creating closed cyclic assemblies or rosettes, is the use of intrinsic dimeric modules in which two complementary hydrogen-bonding sites are fixed at a 60° angle as in the hexamer **34•36**. This insoluble complex (Ar = 4-*tert*-butylphenyl) is formed after mixing two complementary species, barbituric acid containing ADA triad of hydrogen bonds and melamine with DAD triad in solution (Figure 1.19).[144]
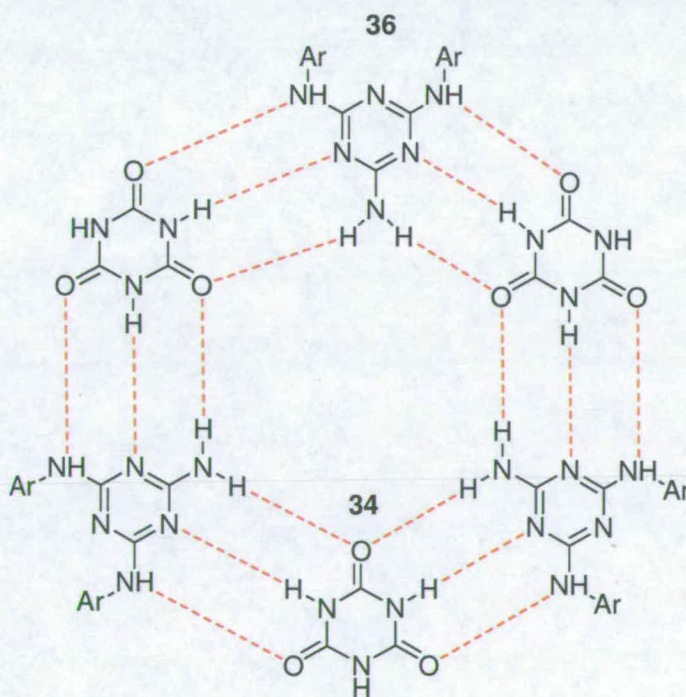
Figure 1.19 Cyclic hexameric aggregate 36•34.

Lehn and co-workers[34] used the same binding mode with some variations for the synthesis of molecular ribbons (Figure 1.20). Barbituric acid **34** and melamine **37** have been modified with alkyl groups blocking one side of molecule and preventing hydrogen bonding on that side of the heterocycles.
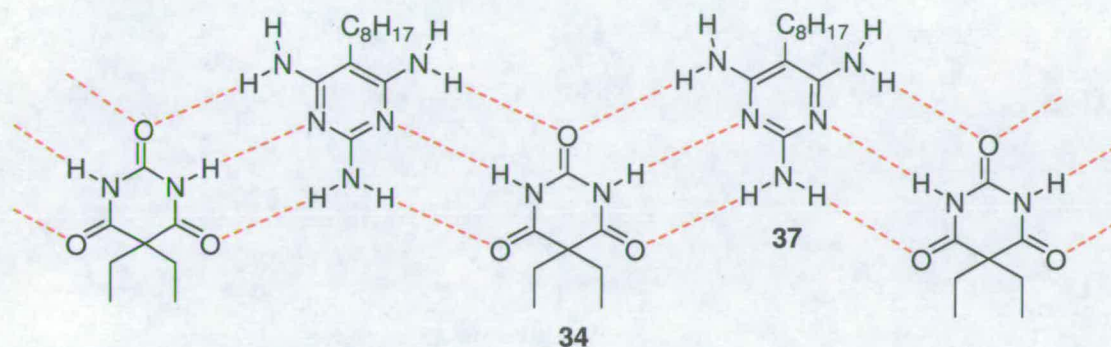
Figure 1.20 Molecular ribbon based on **34•37** repeating unit.

Larger superstructures can be formed by the subsequent aggregation of discrete assemblies as in the Kimizuke and Kunitake example[35] using a 1:1 mixture of melamine and diimide units. The tubular structure (Figure 1.21-inset) is generated by columnar stacking of a cyclic heterododecamer of **33** and **36**. Evidence of three-dimensional helically formed strands with 100 Å diameter were found by electron microscopic observation, very architecturally similar to the structure of tobacco mosaic virus.[36]
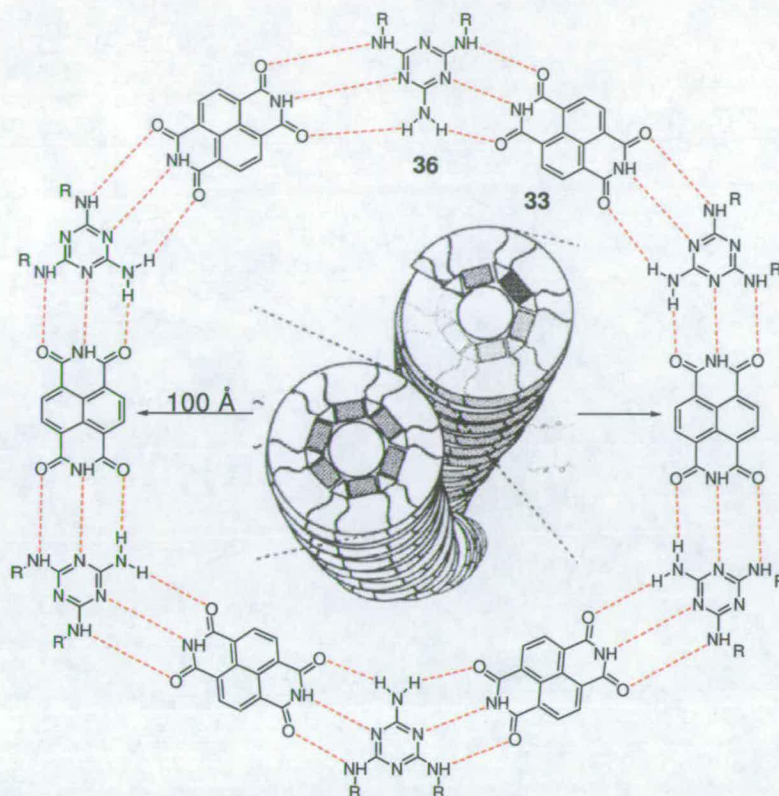
Figure 1.21 One possible structure for the self-assembled material formed from 1:1 mixture of **33** and **36** (R= $C_{12}H_{25}OC_3H_6$ or $C_4H_9(C_2H_5)CHC_3H_6$) with schematic representation.

Finally the first supramolecular polymer was developed by Lehn and co-workers in 1990 (Figure 1.22).[37] The polymer was composed of an equimolar mixture of repeating units **38** and **39**, which associated *via* triple hydrogen bonding in ADA-DAD arrangement.
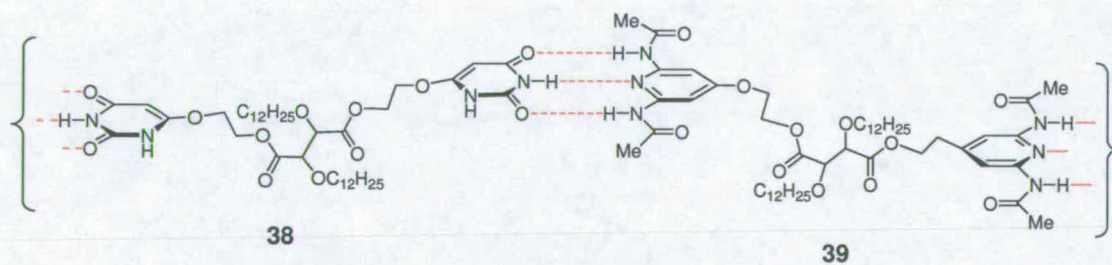
Figure 1.22 First supramolecular polymer.

Lehn's polymer adopted a well defined structure and displayed physical properties similar to conventional polymers and became an important example in the field of supramolecular polymer chemistry. More detailed insight into supramolecular polymers and their properties will be covered in Part 1.5.

Subsequently, the diaminopyridine-uracil triple hydrogen–bonding motif **27•40** has been used in the synthesis of supramolecular rigid rods (Figure 1.23).[31]
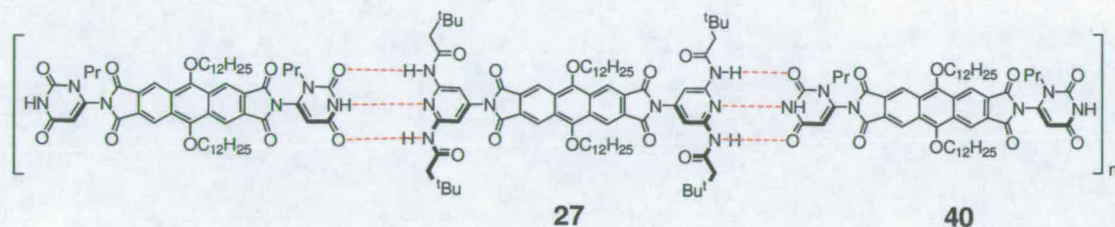
Figure 1.23 Supramolecular rigid rods based on **27•40** unit.

Upon mixing equimolar quantities of repeating components **27** and **40**, they self-assemble in a rigid assembly that forms a lyotropic mesophase.[31]

1.3.3 DAA and ADD Heteroaromatic motifs

The best known DDA-AAD system with high affinity ($K_a \approx 10^4$ M^{-1}) is the DNA base-pair cytosine (C)-guanidine (G) **41•9** (Figure 1.23). Other examples listed were developed by Kelly and co-workers[38] using the AAD array found in 2-amidonaphthyridines (**42** and **43**). They can be readily synthesised by Knorr cyclisation[39] of 2,6-diaminopyridine with 1,3-diketones, that are commercially available. Subsequent reaction with acetic anhydride readily affords AAD products.

$K_a = 10^4 \text{ M}^{-1}$ $K_a = 1.7 \times 10^4 \text{ M}^{-1}$ $K_a = 9.3 \times 10^3 \text{ M}^{-1}$
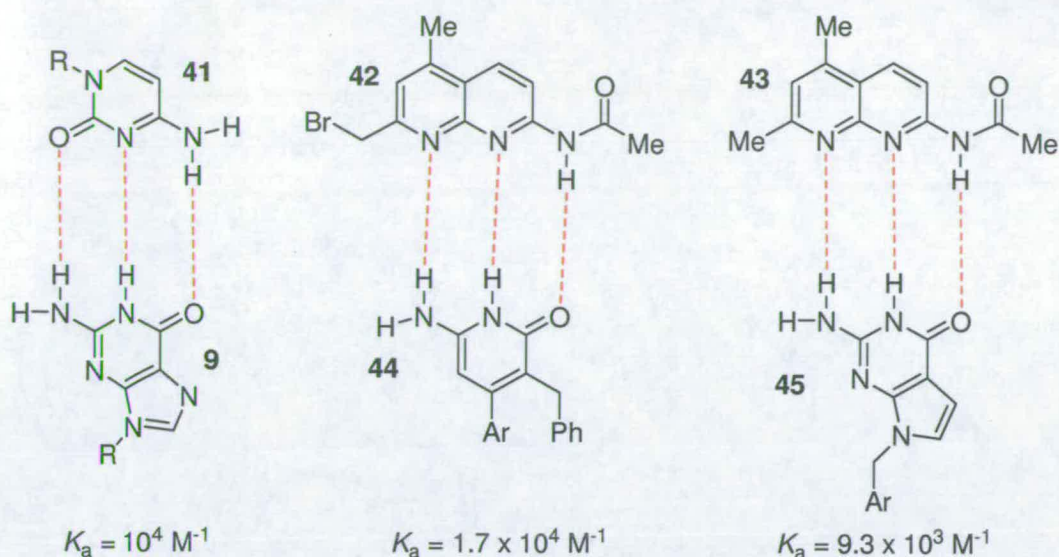
Figure 1.24 Hydrogen bond complexes containing the DDA-AAD motif. Association constant measured in chloroform-_d_.

The DDA arrays used in **42•44** and **43•45** complexes are found in the 6-amino-2(1_H_)-pyridone (**44**), and 7-deaza-guanine (**45**)[20] systems. In general the number of DDA units is very limited and synthetically less accessible apart from commercially available DDA units such as guanine (**9**) and guanosine that must be derivatised to overcome their extremely poor solubility in organic solvents.

Zimmerman and Murray[40] were targeting more soluble DDA units containing only –N and –NH donor and acceptor groups as in compound **46** with a 1,4-dihydronaphthyridine core (Figure 1.25). Unfortunately **46** was extremely unstable undergoing spontaneous oxidation to form the corresponding 2-amino-1,8-naphthyridine. A second attempt was successful and compound **47** proved to be stable and chloroform soluble but was never used in binding studies.
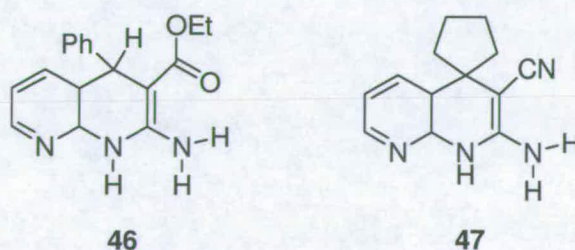
Figure 1.25 More chloroform soluble ADD units.

Several dimeric AAD and DDA modules have been reported that use a porphyrin or porphyrin analogues as the scaffold.[30, 41, 42]

Sessler[43, 44] has used a palladium-catalysed Stille-coupling to connect a porphyrin system to 8-bromoguanosine for use in a self-assembling photosynthetic model system (**48•49** and **50•49** in Figure 1.26).

$K_a = 9 \times 10^3 \, M^{-1}$ $K_a = 1.3 \times 10^4 \, M^{-1}$
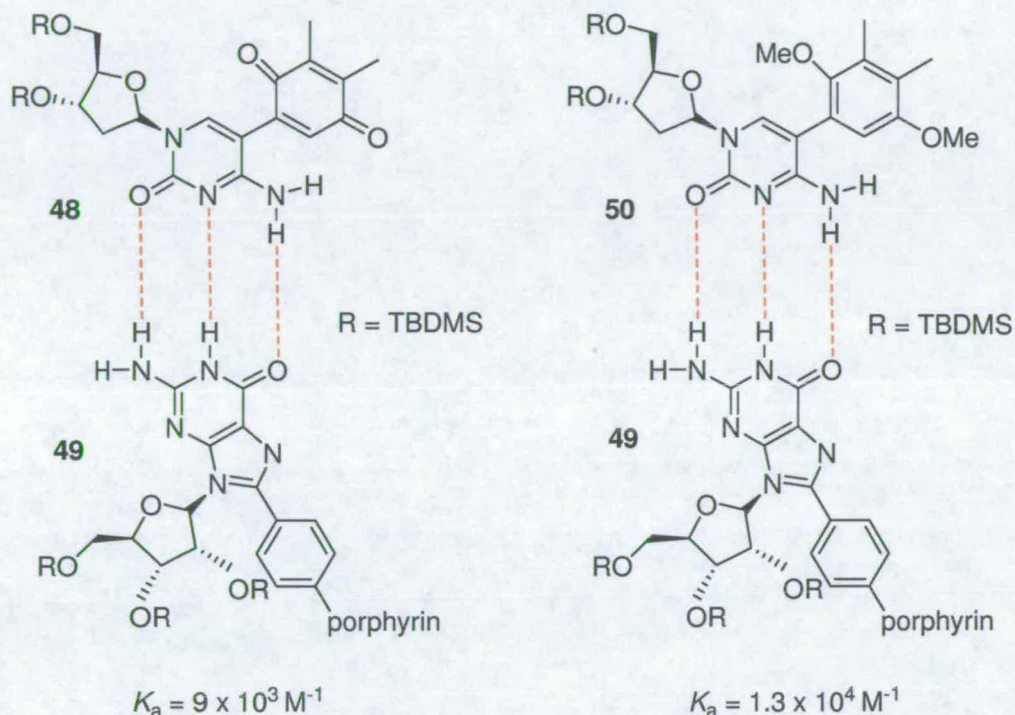
Figure 1.26 Photosynthetic model systems containing the DDA-AAD motif developed by Sessler and co-workers.[43, 44] Association constants were measured in chloroform-*d*.

The K_a values for **48•49** and **50•49** heterocomplexes are in the $10^4 \, M^{-1}$ range as other AAD-DDA examples (Figure 1.24), which are two to three orders of magnitude higher than observed for the ADA-DAD systems. The true values reported seem to be even higher as the self-association of **9, 44, 45** was not taken into account and it is reported that **9** and **45** strongly dimerise in chloroform.[9]

Another interesting example of dimeric AAD and DDA developed by Sessler[30] (Figure 1.27), was cytosine-guanine "heterodimer" **51**, synthesised and studied as part of their effort to create artificial duplexes.
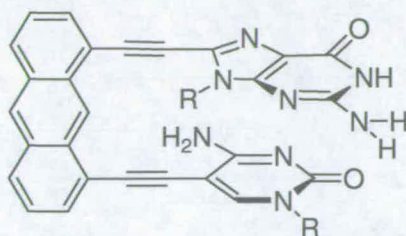
51

Figure 1.27 The cytosine-guanine "heterodimer" **51** is a dimeric DDA module.

In this case the bases are rigidly held apart so that base-pairing is forced to occur intermolecularly. The authors reported that dimer **51•51** (Figure 1.28a) did not show appreciable dissociation upon dilution (^{1}H NMR monitoring) in chloroform-*d*, whereas complex **41•9** (Figure 1.24) do fully dissociates under these conditions (5% DMSO-*d$_6$*/CDCl$_3$)[30]. The most impressive example is dimer **52•52**[45] (Figure 1.28b) which does not dissociate even in the highly competitive solvent DMSO.

a)
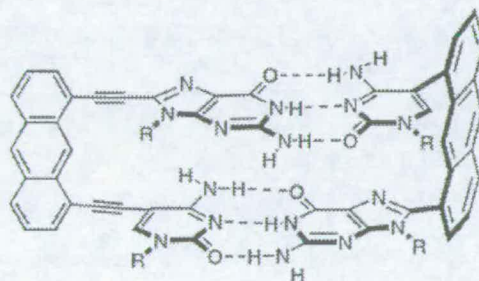
51•51

b)
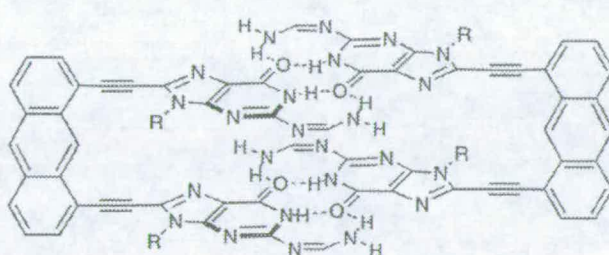
52•52

Figure 1.28 Self-assembled structure of dimeric modules a) **51•51** and b) **52•52**. Figure reprinted from Zimmerman and Corbin.[1]

Solubility problems have been noticed for most of the dimeric AAD modules, which in fact are significant for most guanine-based compounds as pointed out previously. One very interesting and highly rigid dimeric AAD system **53** was developed by Zimmerman and coworkers[46] (Figure 1.29). Synthesis was achieved by reaction of 2,6-diaminopyridine-3-carboxaldehyde (DPC) with tetracyclo-[6.3.0.0^{4,11}.0^{5,9}]undecane-2,7-dione followed by acylation with octanoic anhydride.
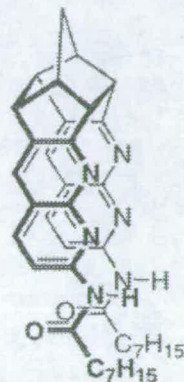
53

Figure 1.29 Rigid dimeric DDA module **53**. Figure reprinted from Zimmerman and Corbin.[1]

1.3.4 Self-assembling DDA-AAD systems

In addition to the dimeric AAD-DDA units, several intrinsic ditopic AAD-DDA units (Figure 1.30) have been reported by Lehn[47] (**56**) and Zimmerman[47, 48] (**54** and **55**). Compounds **54** and **55** contain two cytosine nuclei (AAD array) fused to a central pyridine unit, respectively. Compound **55** is available in three steps from appropriate _N_-alkylureas.[49]
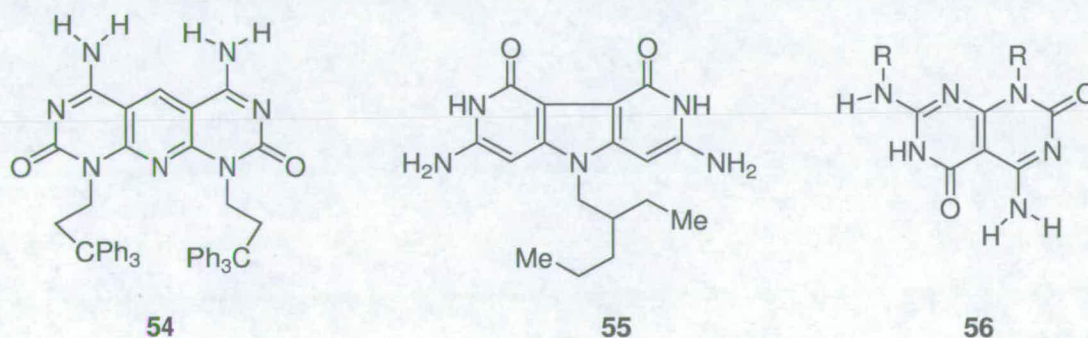
54   **55**   **56**

Figure 1.30 Intrinsic dimeric modules containing DDA and AAD hydrogen bond array.

The ditopic guanine analogues **55** contain two 6-amino-2(1*H*)pyridone rings fused to a central pyrrole unit, respectively, and was designed as complements to **54**.

The groups of Lehn[50] and Mascal[51] both reported self assembly behaviour of compound **57** into a cyclic hexameric structure (Figure 1.31).
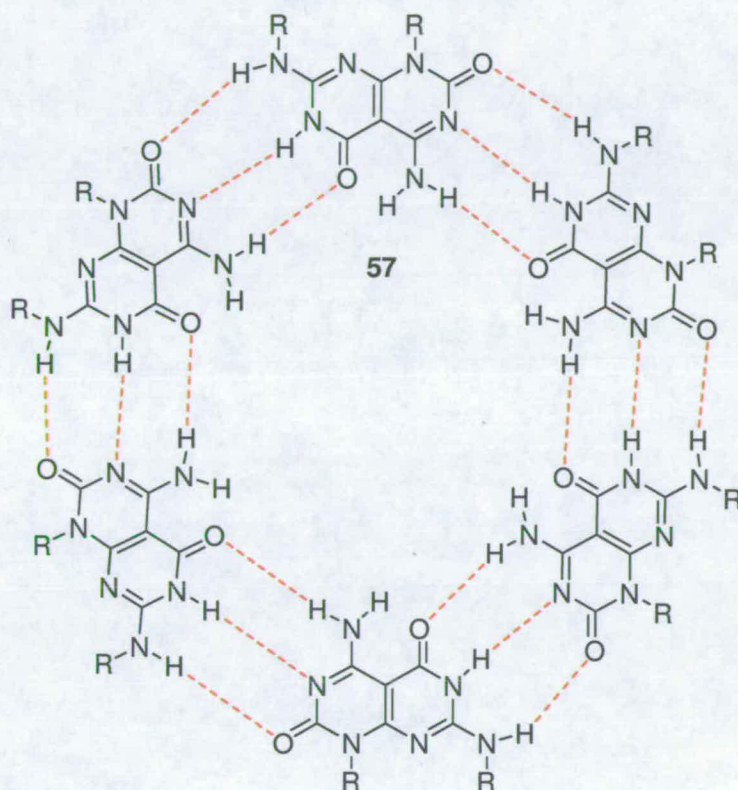
Figure 1.31 Cyclic hexameric aggregate **57•57**, R=C_8H_{17}.

These "Janus" type molecules possess a complementary AAD-DDA array at an angle of 120°. The formation of the cyclic hexamer in the solution and in solid state was confirmed by ^1H NMR spectroscopy measurements[50] and X-ray crystallographic studies.[51]

1.3.5 DDD and AAA Heteroaromatic motifs

The Jörgensen model of secondary interactions indicated that AAA-DDD systems are the strongest of all triple hydrogen bonded complexes. Heterocomplex **1•3** (Figure 1.32) developed by Zimmerman and Murray[52] gave the first experimental

confirmation; the binding constant in chloroform-*d* was estimated to be $K_a > 10^5$ M^{-1}, which is 3 orders of magnitude stronger than ADA-DAD systems. More detailed insight into the binding studies of **1•3** and measuring methods will be discussed in Chapter 3.

$K_a > 10^5$ M^{-1}
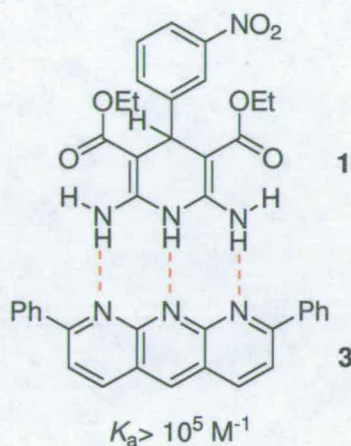
Figure 1.32 Heteroaromatic AAA-DDD modules developed by Zimmerman.[52]

This was the only reported neutral triple hydrogen bonded AAA-DDD system that could be found in literature. Part of reason for that is the very limited number of AAA units present in the literature findings,[52, 53] so it is not surprising that syntheses of new AAA units will become the first target in this thesis.

The AAA unit **3** with the 1,9,10-anthyridine nucleus was synthesised by Caluwe[53] in a single step by a double Friedlander reaction of 2,6-diamino-3,5-pyridinedicarboxaldehyde and ketones. Compound **3** had some stability issues and they will be addressed in Chapter 3 together with a modified synthesis of anthyridines developed by Zimmerman.[52]

Choice for DDD units particularly with only –NH donors is very restricted. Dihydropyridines **1** and **10** can serve as DDD units and are readily available in a single step by a Hantzsch synthesis using methyl carbamimidoyl acetate and 2-nitrobenzaldehyde.[52] The only limitation is the tautomerism of dihydropyridines, which can exist in 1,4-dihydro or 3,4-dihydro forms depending on the solvent.

By ^{1}H NMR experiments in chloroform, **1** exhibited a >20:1 preference for the 1,4-dihydro form, while **10** (Figure 1.6) was a 2:1 mixture of 1,4-dihydro form and 3,4-dihydro form.[52]

Other examples of AAA-DDD systems **61•3** and **58•61** were developed by Anslyn and Bell[54] as cationic AAA-DDD systems (Figure 1.24). In this case the DDD unit was protonated ethyl 2,6-diaminonicotinate **61** with a lipophilic tetraarylborate counter-ion for increasing solubility in chloroform. The ester group in **61** was required to increase solubility and acidity of the 2- and 6-amino groups. The cationic AAA-DDD system **61•3** was estimated to have $K_a > 5 \times 10^5$ M^{-1}, by UV-vis titration experiments.
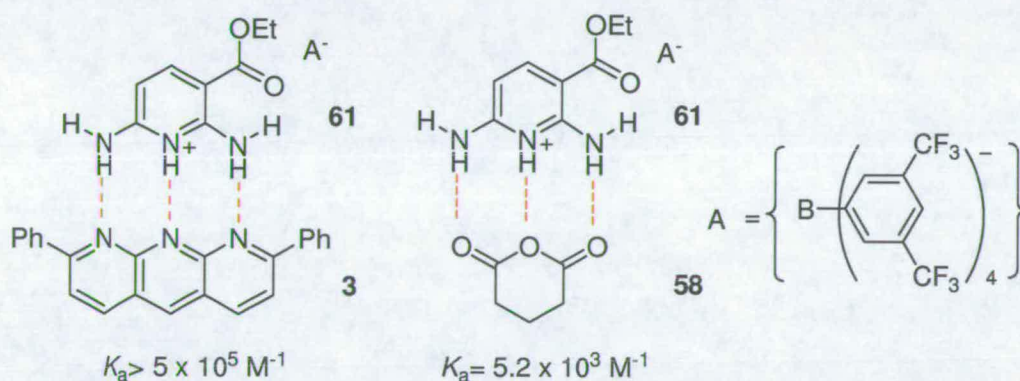
Figure 1.33 Cationic heteroaromatic AAA-DDD modules developed by Anslyn[54].

In complex **58•61** the ^{1}H NMR titration studies in chloroform-d indicated the presence of multiple equilibria in solution, two K_a values were determined $K_{1,1} = 5.2 \times 10^5$ M^{-1} and $K_{1,2} = 1.8 \times 10^2$ M^{-1}, respectively.

1.3.6 Self-assembling AAA-DDD systems

The first example of AAA-DDD systems in self-assembled complexes was designed by Fuyuhiro and Kawata.[55] They generated a metal-containing supramolecular system by the self assembly of anions **60** containing two AAA sets from $[M\text{-}(tdpd)_2(H_2O)_2]^{2-}$ (H$_2$tdpd=1,4,5,6-tetrahydro-5,6-dioxo-2,3-pyrazinedicarbonitrile, M= Ni, Co, Cu) together with melaminium cations **59** containing one DDD set (Figure 1.34).
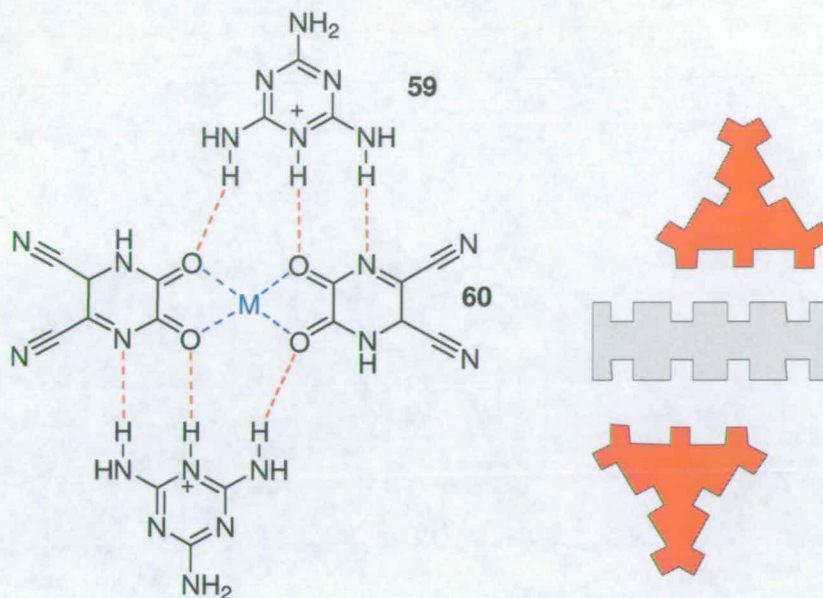
Figure 1.34 Heteroaromatic AAA-DDD modules used in metal mediated supramolecular system, with schematic representation. M= Ni, Co, Cu.

Self-assembling products based on complementary AAA-DDD arrays were formed in the solid state even when recrystallized from competitive solvents such as water. In both cases building mode has been further extended by additional hydrogen-bonding interactions to finally produce 2D layers (Figure 1.35).
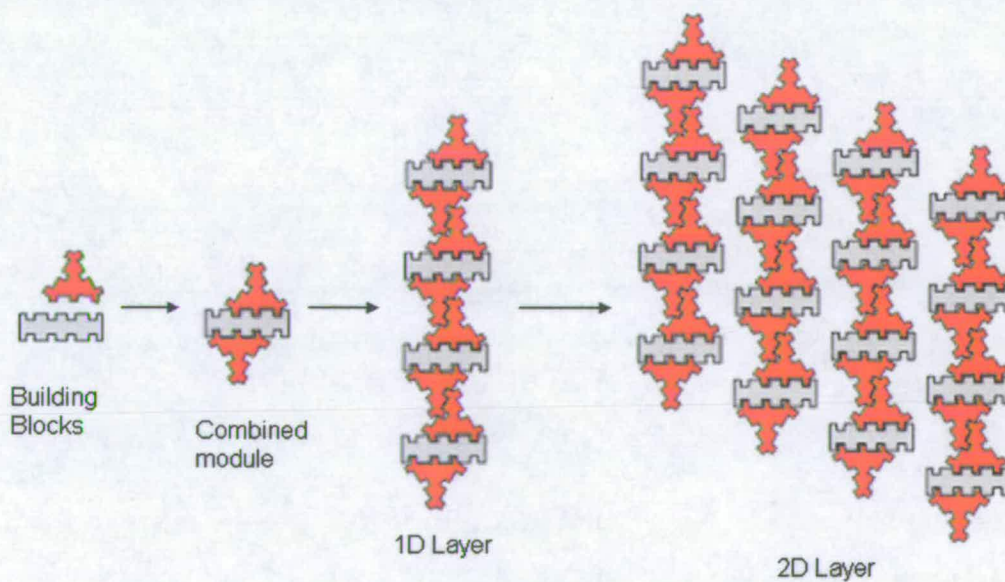
Figure 1.35 Construction of metal containing supramolecular system.

1.4 Selected Quadruple hydrogen bonded motifs

The initial attempts to find stronger triple hydrogen bonded systems led to the accidental discovery of quadruple hydrogen bonded systems. The first to be discovered were dimers of **62a** (Figure 1.36) with binding stability of K_a= 530 M^{-1} which is low considering the number of hydrogen bonds involved.[56]

K_{dim} = 530 M^{-1} K_{dim} = 2 x 10^4 M^{-1}
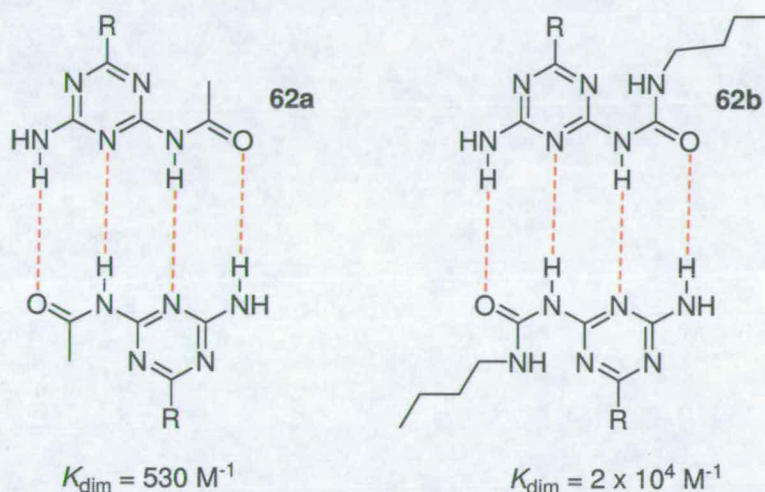
Figure 1.36 First quadruple hydrogen bonded DADA dimers (R= CH$_3$). Association constant measured in chloroform-_d_.

A further increase in binding stability (K_a= 2 × 10^4 M^{-1}) was observed in the reorganised ureidotriazine **62b**. An intramolecular hydrogen bond afforded a planar conformation of the ADAD array, as has been seen in the X-ray crystal structure of **62b** dimer which stacks in columns with hexagonal order.

The simple preparation and relatively strong dimerisation of ureidotriazines were reasons for using them as units in polymeric aggregates with high degrees of polymerisation.[57]

The strongest dimer in an ADAD arrangement was formed using pyrimidine analogues **63** with K_a= 2 × 10^5 M^{-1} (Figure 1.37), though requiring some chromatographic purification and relatively expensive starting material.[58]

$$K_{dim} > 2 \times 10^5 \text{ M}^{-1}$$
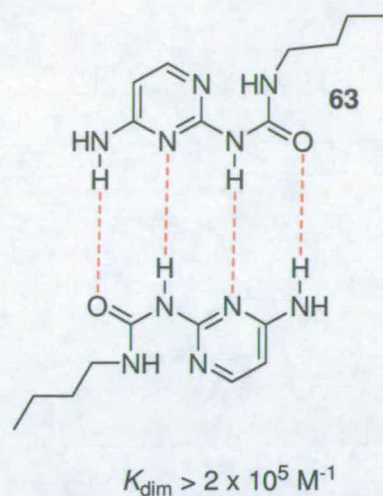
Figure 1.37 The most stable DADA dimer. Association constant measured in chloroform-*d*.

Meijer and co-workers were the first to describe a series of 2-ureido-4(1*H*)-pyrimidone derivatives that can dimerise through the DDAA array.[59] Ureidopyrimidones are easily synthesised in a two step reaction of β-keto esters with guanidine followed by acylation of resulting isocytosine with an isocyanate.

The fact that certain types of the ureidopyrimidones exist in three different tautomeric forms significantly complicates the assembly process. The overall binding energy for dimerisation is therefore reduced by the energy which has to be paid for this conformational change. For example, the 2-ureidopyrimidone **64** exists in tautomeric equilibrium with pyrimidone monomer **64a** (AADD) and the pyrimidin-4-ol monomer **64b** (DADA; Scheme 1.1). Both species **64a** and **64b** are self complementary with dimerisation constants of $K_{dim} > 10^6$ and 4.5×10^5 M^{-1} in chloroform, respectively.
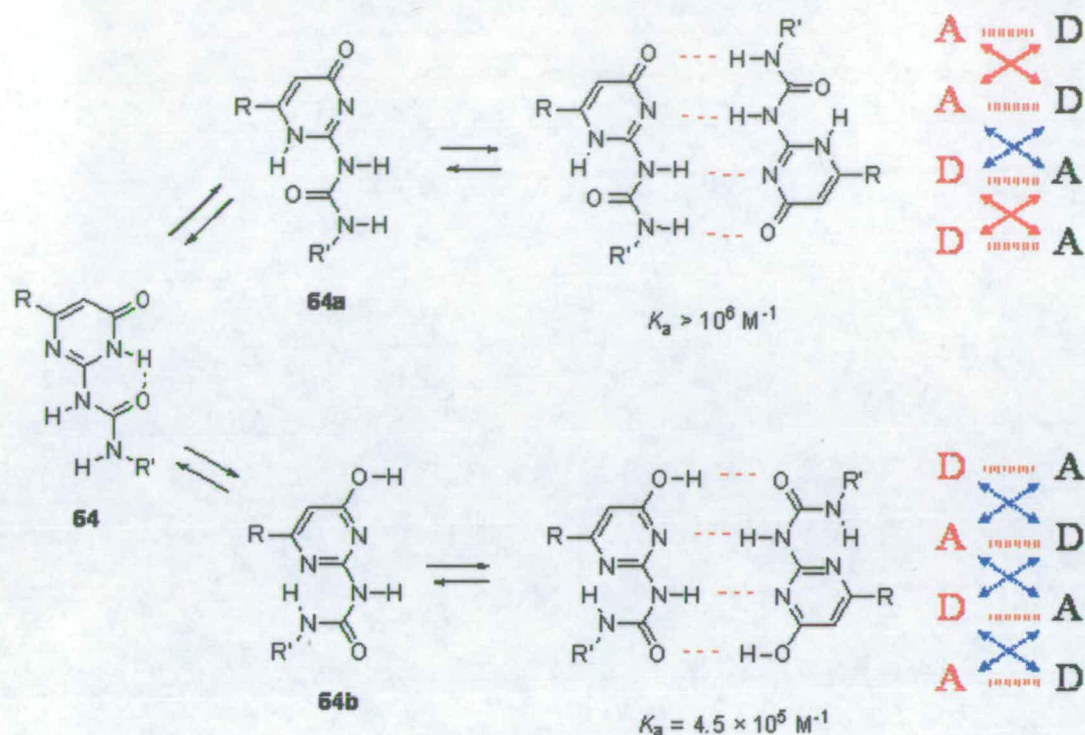
Scheme 1.1 Dimerisation of ureidopyrimidones **64a** and **64b**. Association constant measured in chloroform-*d*.

The extremely efficient self-association of such AADD binding motifs in chloroform now allows direct control of the macroscopic physical properties of large supramolecular architectures.[60, 61]

1.5 Linear supramolecular polymers

In subsequent work, two 2-ureido-4(1*H*)-pyrimidones were covalently coupled through a *m*-xylylene spacer, which resulted in the self-complementary molecule **65** that dimerizes through the formation of eight H-bonds (Figure 1.38).[62] The very high stability of these dimeric systems combined with their easy accessibility makes them ideal candidates for the noncovalent synthesis of supramolecular polymers.
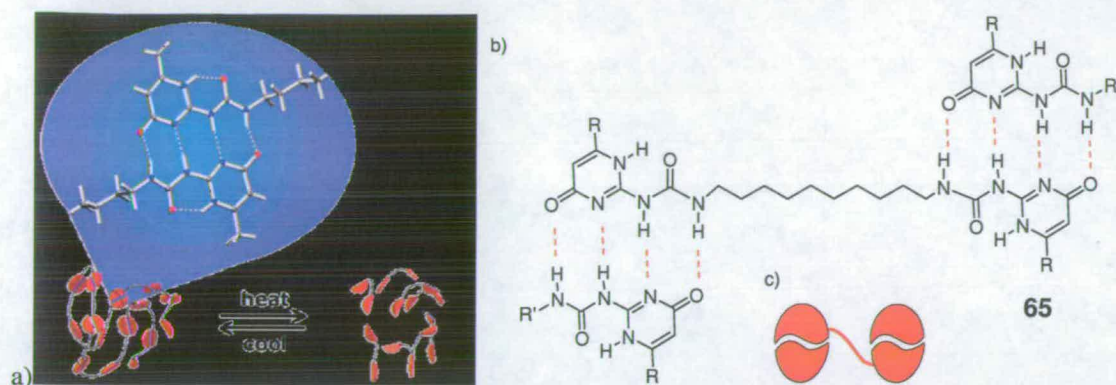
Figure 1.38 a) X-ray crystal structure of **64**,[63] b) self-complementary "Janus molecule" **65** and c) schematic representation.

Compound **65** shows an association number of more than 500 in chloroform[64, 65] as a highly viscous solution and displays all the properties of a classical polymer. However, supramolecular polymers have a strong concentration and temperature dependence on viscosity which is found in conventional polymers. This observation can be explained by the effect of temperature on the strength of the hydrogen bonds. They become first weakened by increased thermal motion and are finally broken, leaving the individual monomers in solution so the solution becomes less viscous (Figure 1.39).
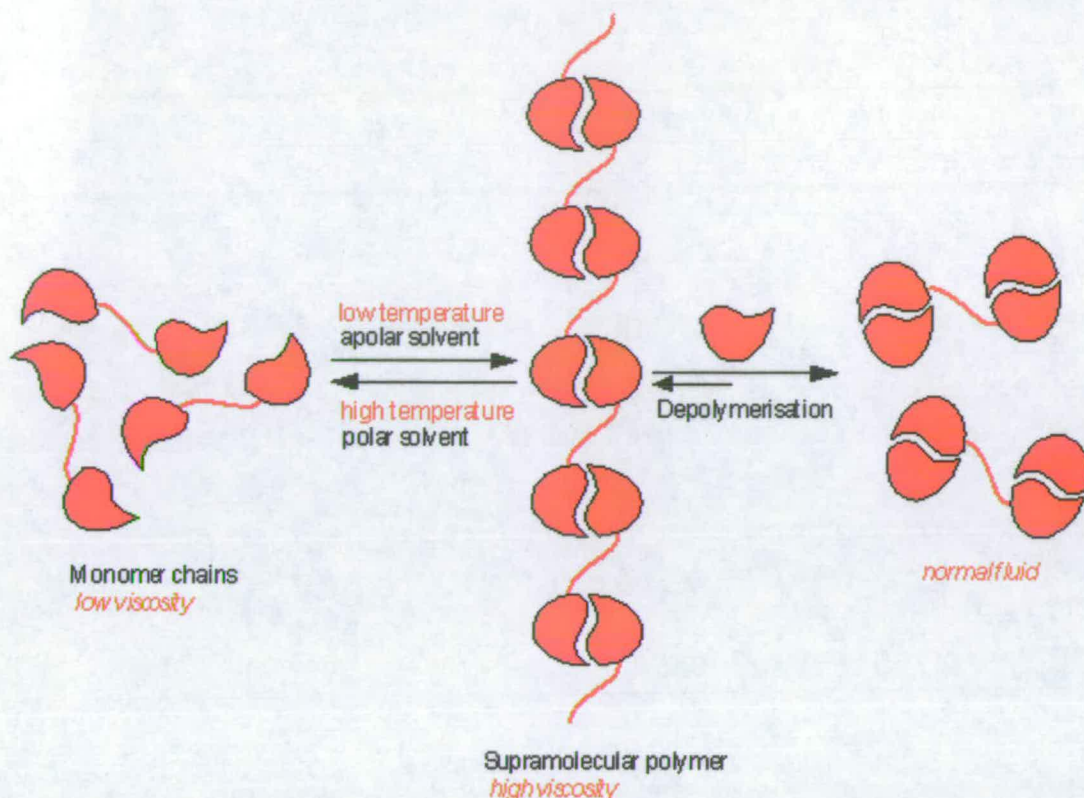
Figure 1.39 Formation of a supramolecular polymer and depolymerisation of bifuncional "Janus molecule"**65**.

The polymeric properties can be restored on decreasing the temperature. Similar effects are observed by addition of a polar solvent which also disrupts the hydrogen bonds. The addition of a small amount of trifluoroacetic acid also causes a dramatic decrease in the viscosity of the solution. This reversibility of the supramolecular polymerisation is a key difference that is not possible in conventional covalently linked polymers.

Another way to impose the depolymerisation is by the addition of the monofunctional ureidopyrimidone stopper **63** through a competitive association to a highly viscous solution of the bifunctional molecule **65** (Figure 1.39). The viscosity of the solution decreases dramatically with increasing concentration of stopper **63**.

1.6 Supramolecular copolymers

In 2005, Meijer and co-workers reported supramolecular copolymers based on strong and selective complexation[66-68] of the ureidopyrimidone **64** with 2,7-diamido-1,8-naphthyridines **66**, *via* quadruple hydrogen bonds between ADDA and DAAD arrays (Scheme 1.2). The association constant[69] measured for **64•66** heterocomplex was 5×10^6 M^{-1}.
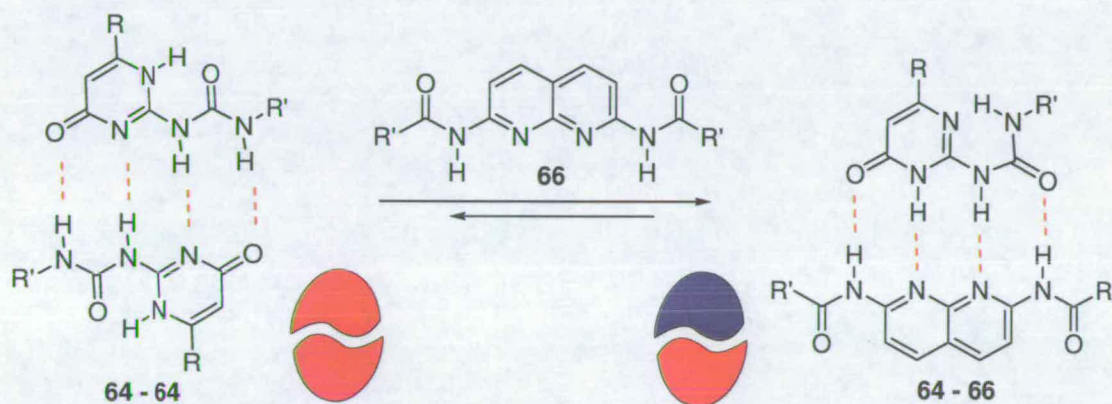
Scheme 1.2 Selective complexation of the ureidopyrimidone **64** and diamidonaphyridine **66** via quadruple hydrogen bonds between ADDA and DAAD arrays. Schematic representation of **64** -red and **66** –blue in heterocomplexes presented below.

One equivalent of **66** in CDCl$_3$ disrupts the **64•64** dimers and the high selectivity and strength of the **64•66** heterodimer was attractive for constructing complementary supramolecular copolymers. The study of supramolecular polymers based on the **64•66** heterodimer required bifunctional derivatives: **67** with ureidopyridinone telechelic polytetrahydrofuran core (Figure 1.40a) and **68** which contains 2-ethylhexamido substituents (Figure 1.40b) for increased solubility. The bifunctional derivative **68** was formed by a Buchwald amidation of 2-amido-7-chloro-1,8-naphthyridine **66** with hexanedioic amide.

a)

b)

68

67

Y=pTHF
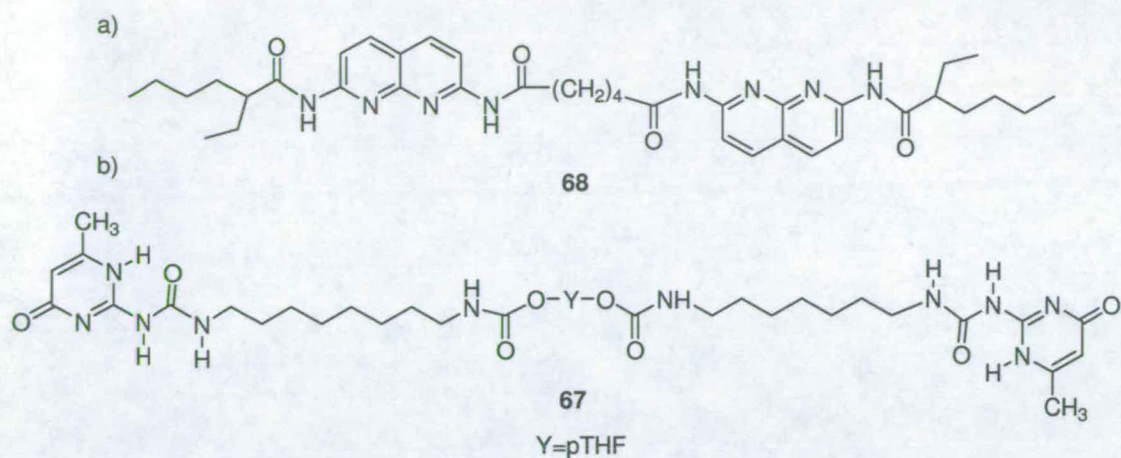
Figure 1.40 Units **67** and **68** of supramolecular copolymer.

Upon titration of macromonomer **68** with **67** only a limited amount of cyclic heterodimer is formed. Instead, **68** is incorporated in the supramolecular polymer chain until a strictly alternating copolymer is obtained in a 1:1 ratio of monomers (Figure 1.41).

macromonomer **67**

Insertion of   **68** (<1 eq.)

67-68 copolymer

End-capping with   **68** (>1eq.)
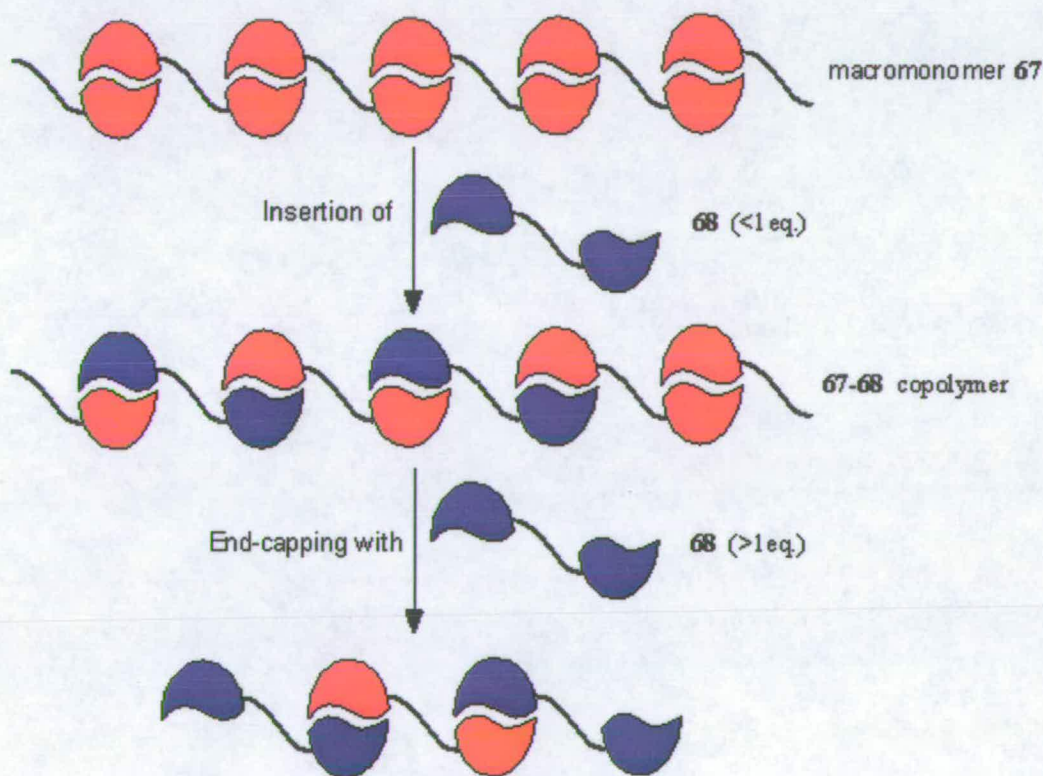
Figure 1.41 Formation of **67-68** supramolecular copolymer.

When 1:1 mixture is exceeded the additional molecules of **68** can no longer be incorporated into the polymer chain and act as end-cappers, and the length of the alternating copolymer is progressively reduced. This observed effect is very analogous to the effect of adding the monofunctional **64** or **66** to a solution of the bifunctional **64•64** in chloroform (Figure 1.39).

1.7 Conclusion and aims

There is great interest in designing heterocyclic units with multiple linear arrays of hydrogen bonding sites as described throughout the introduction. A number of literature examples are known for triple and quadruple hydrogen bonding motifs but there is a particular lack of systems with AAA and AAAA arrangements. Despite their importance and predicted high stability in AAA-DDD and AAAA-DDDD heterocomplexes, only a limited number of AAA and none of the AAAA units are known. This project aims towards a simple synthesis of triple hydrogen bonded units in AAA arrangement and strong binding stability with DDD counterparts in AAA-DDD systems.

Only two relevant examples of AAA-DDD heterocomplexes have been developed over the last 14-15 years, for directed self-assembly studies. In both cases the binding energy was very high and not accurately determined, but only estimated to be $K_a >$ 10^5 M^{-1} for Zimmerman and Murray's[52] **1•3** heterocomplex and $K_a > 5 \times 10^5$ M^{-1} Aslyn's[54] protonated AAA-DDD heterocomplex **61•3**.

The basis of this research project was to synthesise novel aromatic heterocyclic hosts, with two and three adjacent hydrogen bond sites in AA and AAA arrangements. In order to produce the targeted systems I employed new synthetic methods and techniques involving flash vacuum pyrolysis and high boiling solution reactions (Chapter 2), Buchwald-Hartwig coupling (Chapter 3), as well as Suzuki coupling chemistry (Chapter 4).

A further aim of this investigation was to study the binding affinity in AA-DDD and AAA-DDD heterocomplexes using ^{1}H NMR and fluorescence titrations (Chapter 5) together with molecular modelling studies for some of selected AAA-DDD heterocomplexes carried out by Dr Francesco Zerbetto and Gilberto Teobaldi from the University of Bologna. All binding constants have been determined by the _GasFit_ program, a specialized software program for determination of binding constants developed by Dr Dusan Djurdjevic from the University of Edinburgh. All relevant experimental and fitting data from titration experiments is presented in Appendix 2.

Chapter 2: Synthesis of multiple hydrogen bonded systems using Flash Vacuum Pyrolysis (FVP)

Trap assembly of FVP apparatus

2.1 Introduction

The synthetic objectives reported in this thesis are heterocycles with naphthyridine, anthyridine and naphthacene skeletons as represented in Scheme 2.1. These systems with two **69**, three **70** and four **71** annulated pyridine rings have the hydrogen bonded array in the most favourable AA, AAA and AAAA arrangement and are a very popular choice in supramolecular binding studies. In this chapter naphthyridine model systems were targeted employing the flash vacuum pyrolysis (FVP) technique as a new synthetic strategy.
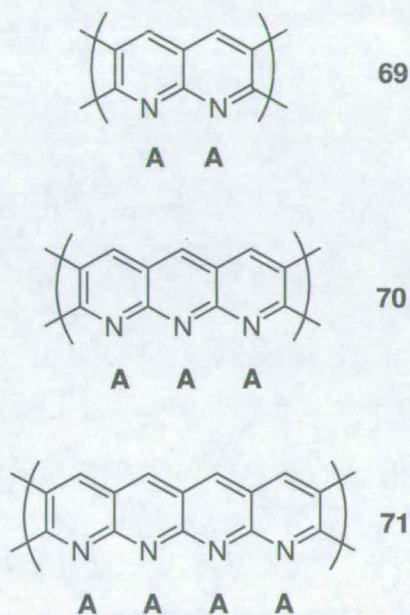
Scheme 2.1 Targeted hydrogen bonded systems

2.1.1 Flash vacuum pyrolysis technique

Flash vacuum pyrolysis (FVP) is described in IUPAC terminology as the thermal reaction of a molecule by exposing it to a short thermal shock at high temperature, usually in the gas-phase.[70] The characteristics of subjecting the

molecule to high temperature (350 – 900 °C) in a vacuum system ($\sim 10^{-2}$ Torr) for a short time ($\sim 10^{-2}$ s) make it possible to isolate kinetically controlled products and, in some cases, to avoid consecutive reactions.[71] Flash vacuum pyrolysis is therefore an interesting methodology for studying reaction mechanisms as well as for synthesis of new molecules. When the FVP technique is used in the synthesis of heterocyclic compounds we have a number of advantages over solution phase reactions. In general FVP is a clean technique which can give unusual disconnections, providing routes to complex molecules which are not available by solution chemistry (unless high boiling solvents are used). Short syntheses of targeted ring systems can be designed with as little as two steps, where many desired substituents can, in principle, be introduced in the precursors without fear of them affecting the cyclisation. Compared with high boiling solution reactions, the advantages of FVP are the absence of intermolecular reactions and no difficulties in removing high boiling solvents. On the other hand the major disadvantage of FVP can be substrate volatility problems; in such a case a clean reaction can not be guaranteed.

The apparatus used in FVP experiments is illustrated at Figure 2.1 and is based on the design of W. D. Crow of the Australian National University. The products are collected at the exit of the furnace tube in a trap surrounded by liquid nitrogen. A "U-shaped" trap is used for small scale pyrolysis (50 mg). The entire pyrolysate was washed through with a suitable deuteriated solvent for NMR analysis by ^{1}H and ^{13}C NMR spectroscopy.
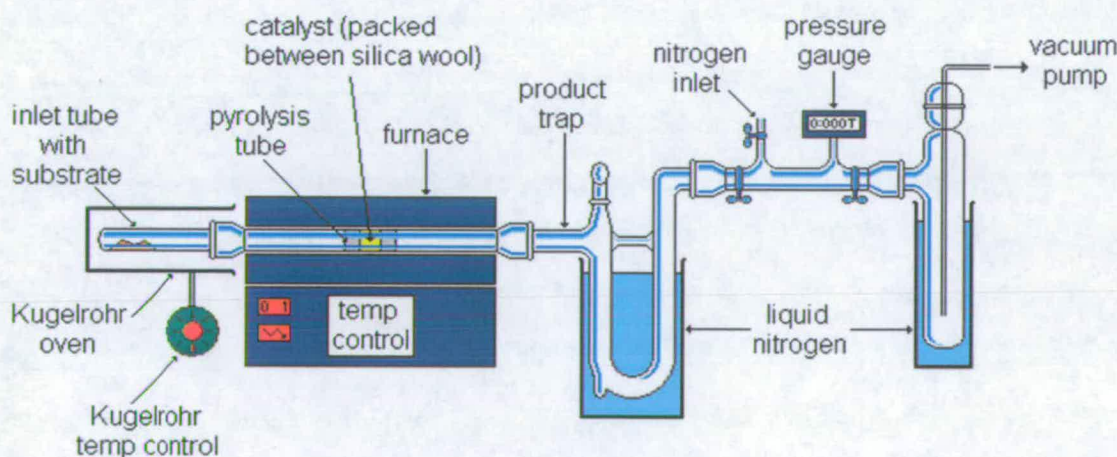
Figure 2.1 Flash vacuum pyrolysis apparatus.

FVP has been used in the past for the very efficient two step synthesis of quinolin-4-one[72] **75** represented in Scheme 2.2 and current work was initially inspired by this reaction.
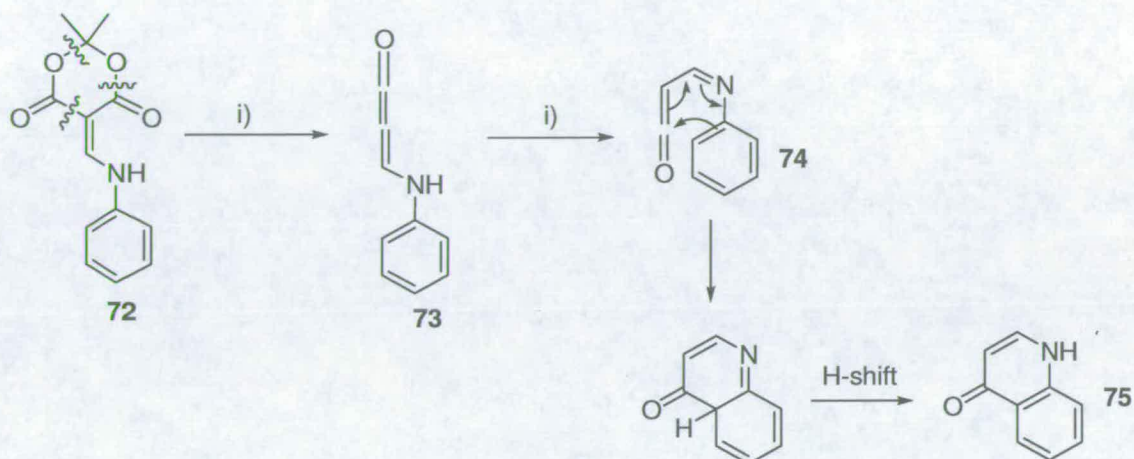
Scheme 2.2 i) FVP 600 °C.

Pyrolysis of Meldrum's acid derivative **72** in the gas phase takes place by loss of acetone and carbon dioxide to provide methyleneketene **73**. A hydrogen-shift generates the iminoketene intermediate **74** which acts as the substrate for an electrocyclisation. The final product **75** is formed after another hydrogen shift.[73, 74]

Matrix isolation studies[72, 73] have confirmed that both **73** and **74** (characterised by IR spectroscopy) are initially formed during pyrolysis, but at higher temperatures electrocyclisation and rearomatisation gives quinolin-4-one as a product.

Using heterocyclic substrates in which the amino group is adjacent to the heteroatom – as for example 2-aminopyridine – the pyridopyrimidinones **77** can be obtained using pyrolysis in solution[75] or neat thermal decomposition[76] of **76** as represented in Scheme 2.3.
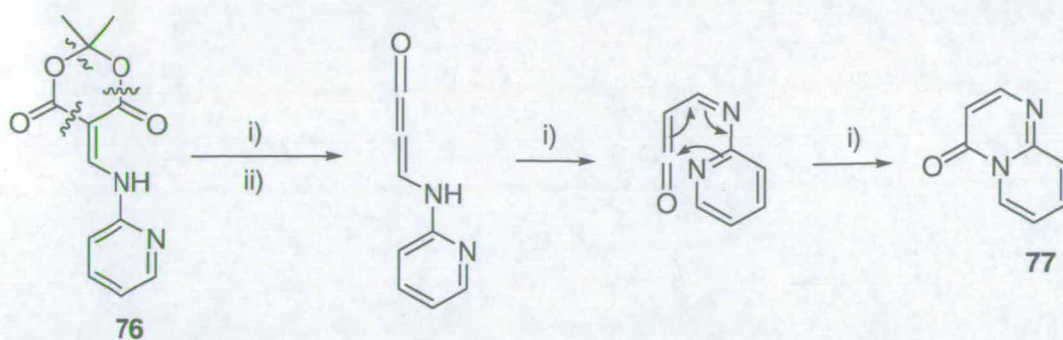
Scheme 2.3 i) Dowtherm[77] 200-220 °C or ii) Heating at ~200 °C

In this case the presence of a heteroatom with a lone pair of electrons allows cyclisation of the iminoketene intermediate onto the nitrogen atom as the more favourable option as found in related literature examples.[75, 78]

In principle, FVP of the 2-aminopyridine derivative **76** can give two possible products after generation of the methyleneketene and rearrangement to the ketenimine (Scheme 2.4). First, cyclisation at the heteroatom would be expected to give the pyridopyrimidine **77** (as found in solution). Alternatively, cyclisation can take place on carbon to provide the naphthyridine **78** (after hydrogen shift) – as found in the related case shown in Scheme 2.2.
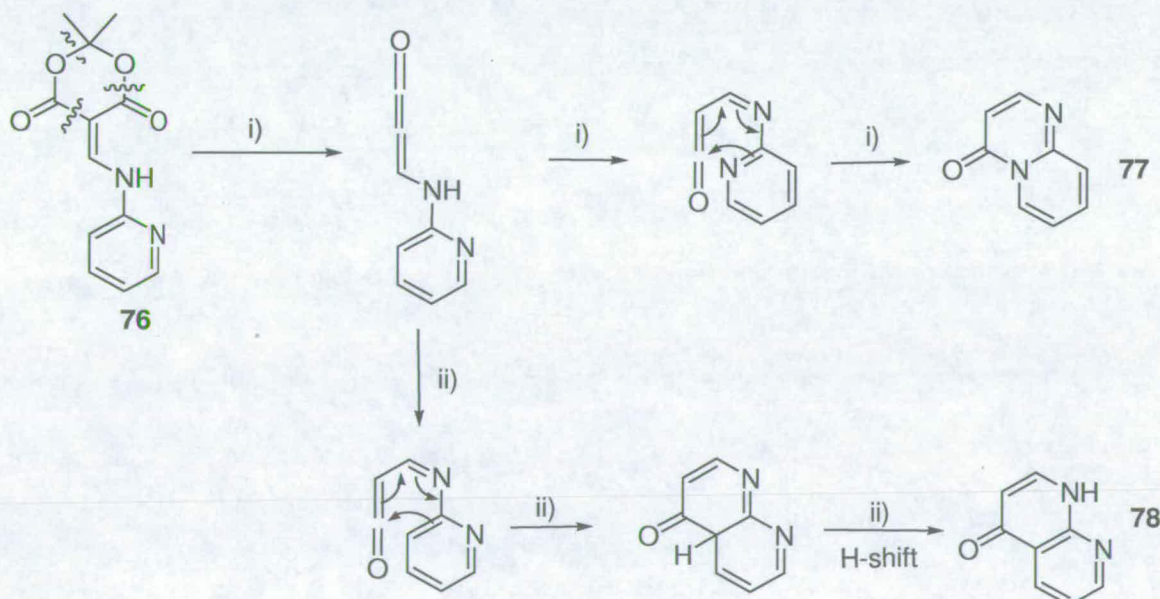
Scheme 2.4 i) FVP 600 °C, ii) FVP 950 °C.

If compound **78** could be formed using controlled conditions a naphthyridine targeted module in AD arrangement would be obtained subsequent rearomatisation *O*-alkylation step would result the desired double hydrogen bonded products in the AA arrangement (Scheme 2.5a). Employing diaminopyridine derivatives as pyrolysis precursors and following the previously described analogy would generate aminonaphthyridines as triple hydrogen bonded system in DAD or DAA arrangement (Scheme 2.5b). Finally for the quadruple hydrogen bonded naphthyridines would require bismethylsulfanylmethylene Meldrum's acid **80** as precursor and subsequent displacement of one methylthio group with ammonia and the second one with heteroarylamine we could afford in principle, naphthyridines in DADD or DAAD arrangement (Scheme 2.5c).
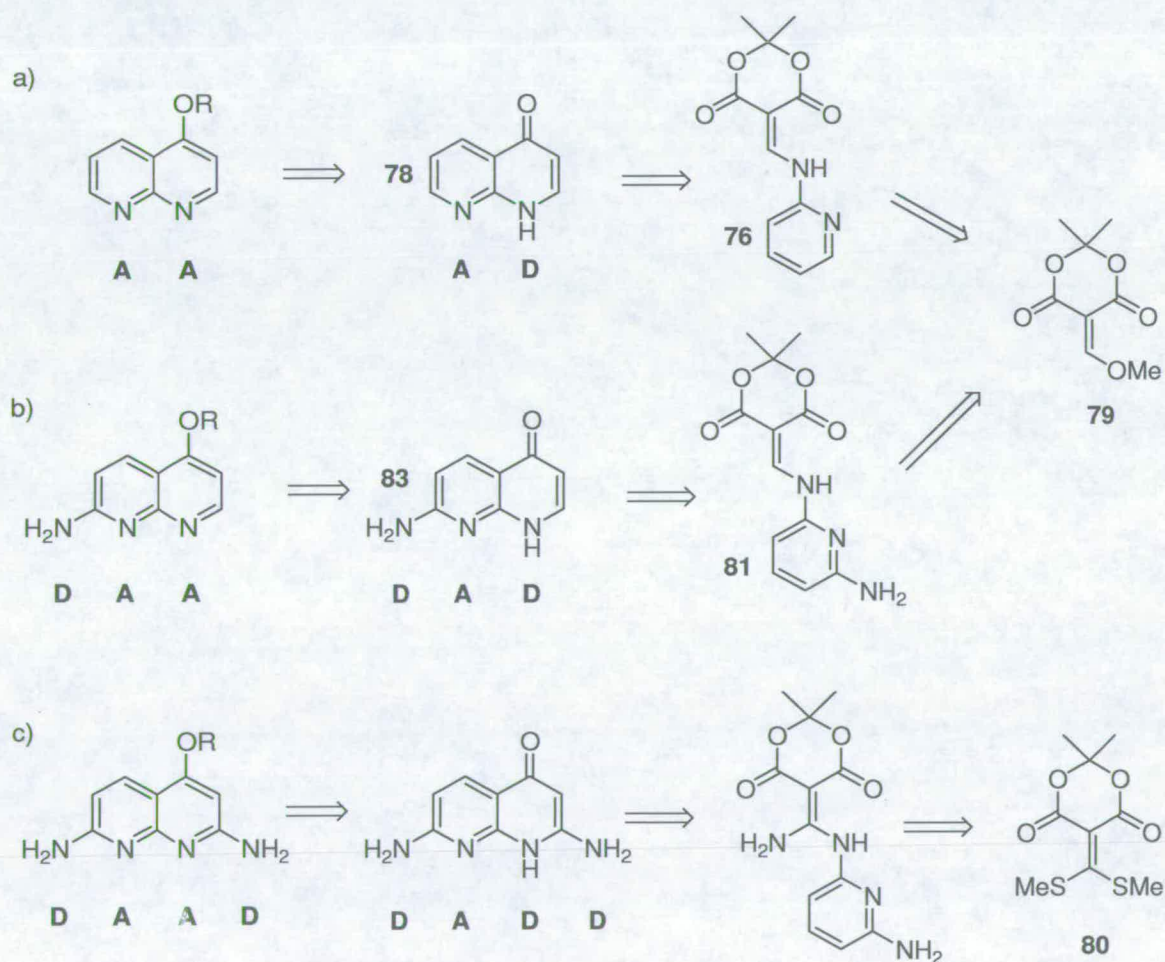
Scheme 2.5 Synthetic strategy of naphthyridine model system with a) double b) triple and c) quadruple hydrogen bonded modules; R-alkyl chain.

Synthetic strategies outlined at Scheme 2.5a and 2.5b have been successfully carried out but strategy 2.5c failed at the first step due to the low yield of pyrolysis precursors, difficulties in displacement of the second methylthio group *etc.*

2.2 Results and Discussion

2.2.1 Pyrolysis precursors

For the most part in carrying out the syntheses in Scheme 2.5a and 2.5b, the heterocycles used to create the pyrolysis precursors were readily available from the usual companies. The precursors themselves (Scheme 2.6) were prepared by reaction of the aminopyridine or aminopyrimidine heterocycles with methoxymethylene Meldrum's acid[79, 80] **79** (MMMA) following the literature methods.[81, 82] Most reactions have been performed under standard conditions at room temperature using acetonitrile as solvent except compounds **89** and **91** which, because of the poor solubility of the precursor were made in refluxing acetonitrile.

In general the pyridine based pyrolysis precursors were obtained in higher yields (67-95%) than pyrimidine analogues (32-67%) due both to the lower reactivity of pyrimidine derivatives and solubility issues.
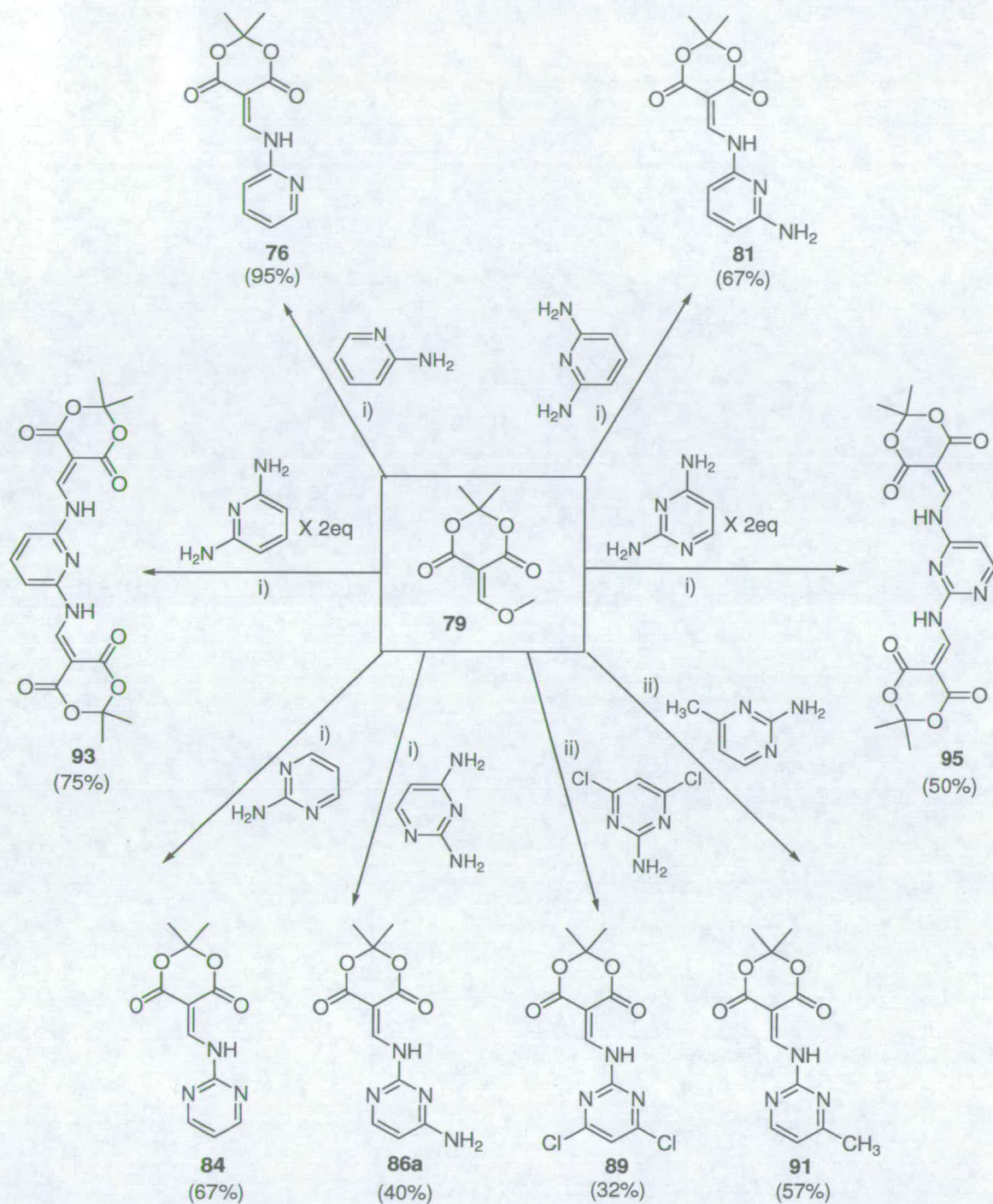
Scheme 2.6 i) Room temperature in acetonitrile; ii) Reflux in acetonitrile.

All pyrolysis precursors **76**, **81**, **84**, **86a**, **89**, **91**, **93** and **95** synthesised showed correct molecular ions in their mass spectra and characteristic doublets (J=13.4 Hz) in the range of δ_H 9.2-9.4 due to the H_e proton (highlighted red in Scheme 2.7).

61

In one particular case, when MMMA was reacted with 2,4-diaminopyrimidine under standard conditions, a mixture of two isomers **86a** and **86b** was produced regioselectively (Scheme 2.7).
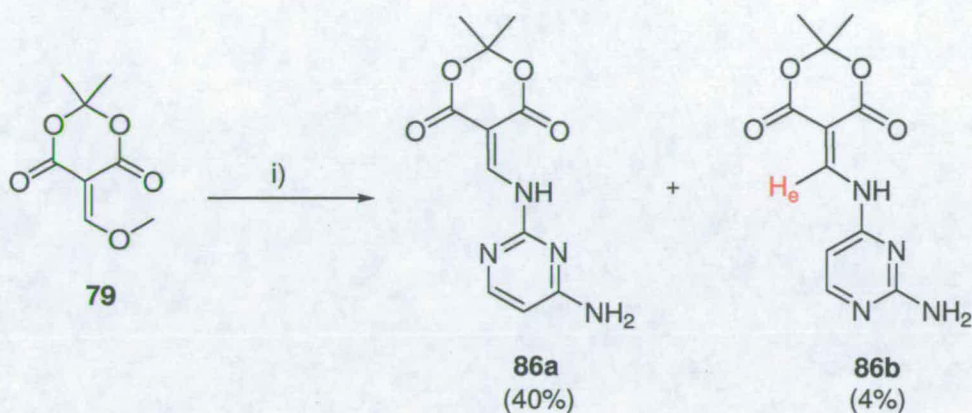
Scheme 2.7 i) 2,4-diaminopyrimidine, acetonitrile, reflux.

The structures **86a** and **86b** were difficult to distinguish by the usual spectroscopic methods, and but the single-crystal X-ray structure of compound **86a** (Figure 2.2a) established the structure of both compounds unequivocally.

In the structure of **86a** three hydrogen bonds were present with two of them being bifurcated (Figure 2.2b). One is an intermolecular hydrogen bond of amino N121-H121 group with O61 (2.902 Å) from the adjacent molecule. The second is the amino N121-H121 group that acts as a bifurcated hydrogen bond donor intermolecularly hydrogen bonded to O62 (2.985 Å) and to O42 (3.054 Å). The third one is the O42 atom that acts as hydrogen bond acceptor intramolecularly bonded to H82-N82 (2.719 Å) and intermolecularly to H121-N121 (3.054 Å).

It is interesting that the hydrogen bond of the amino N121-H121 group with O61 was not bifurcated with O41 (See Scheme 2.2b) and this can be explained by the slightly longer distance of 3.077 Å.

a)   b)
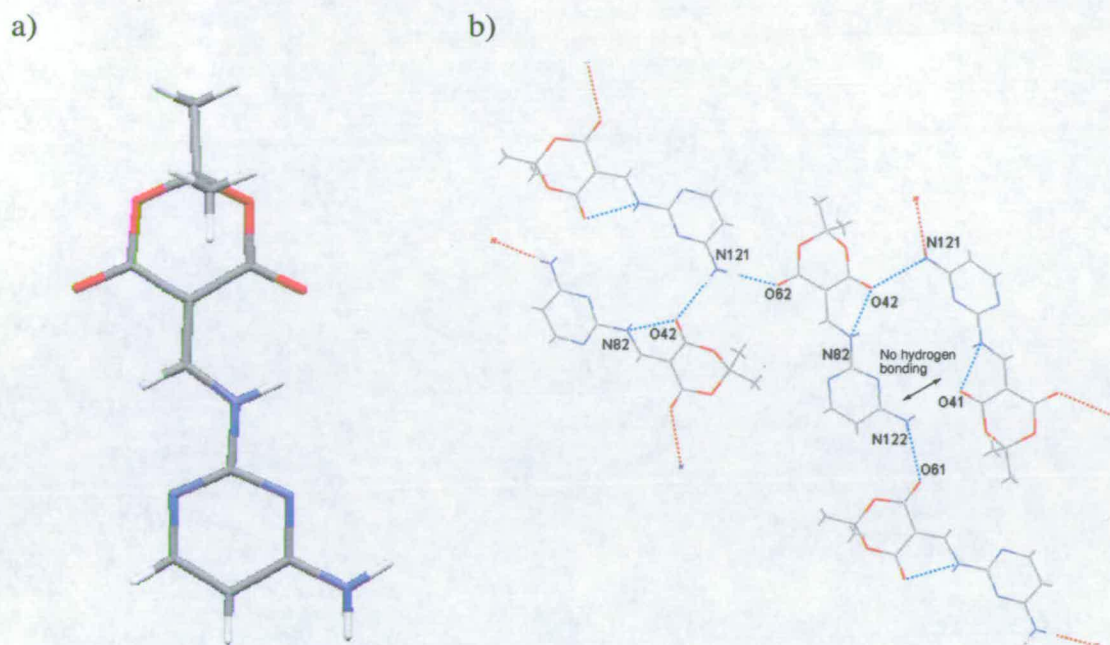
Figure 2.2 a) X-ray crystal structure of **86a** and b) insight into hydrogen bonds in packing diagram.

In the X-ray crystal structure of the analogous compound **91**, only one bifurcated hydrogen bond is observed (Figure 2.3). The amino N8-H8 group acts as a bifurcated hydrogen-bond donor, intramolecularly to O11 (2.709 Å) and intermolecularly to O51 (2.959 Å) from an adjacent centrosymmetrically related molecule.

a)   b)
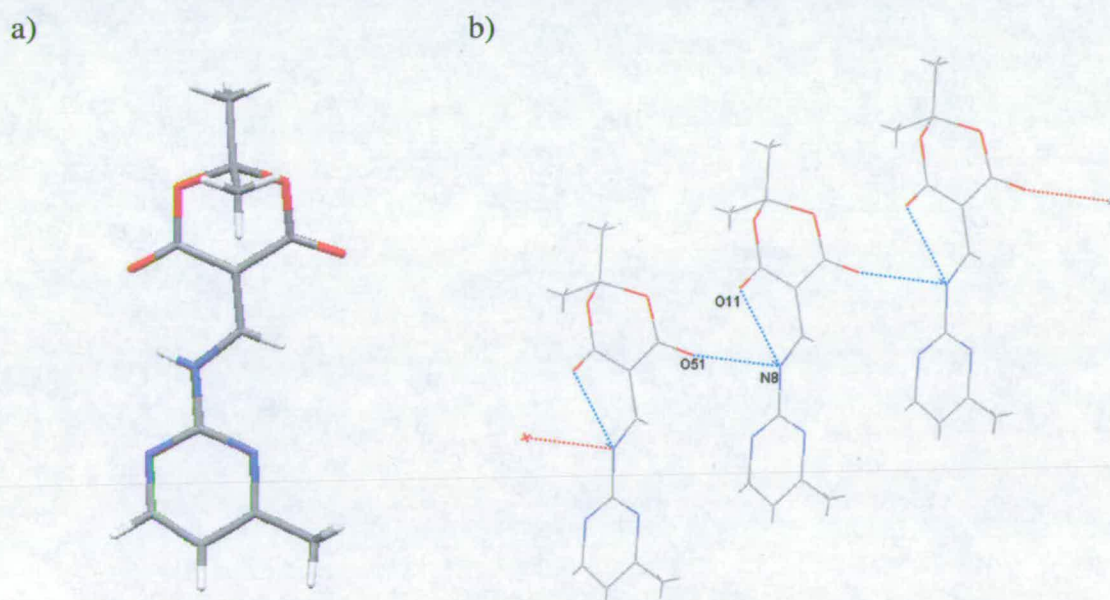
Figure 2.3 a) X-ray crystal structure of **91** and b) insight into hydrogen bonds in packing diagram.

The recently reported X-ray crystal structure of anilinomethylene Meldrum's acid analogues[83] (Figure 2.4) confirmed that amino group N1-H1 acts as a bifurcated hydrogen bond donor intramolecularly to O9 (2.760 Å) and intermolecularly to O9^i (3.259 Å) from an adjacent centrosymmetrically related molecule as found in structures **86a** and **91**.

a)
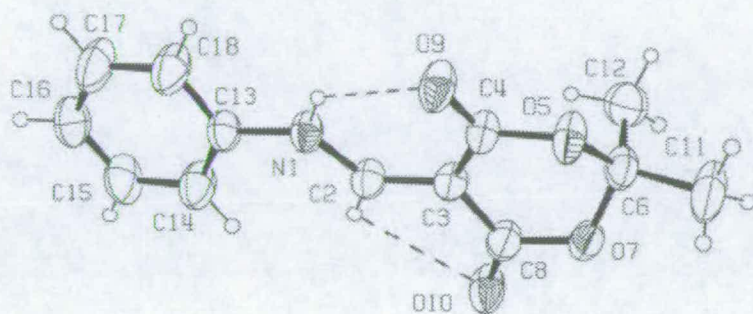
b)
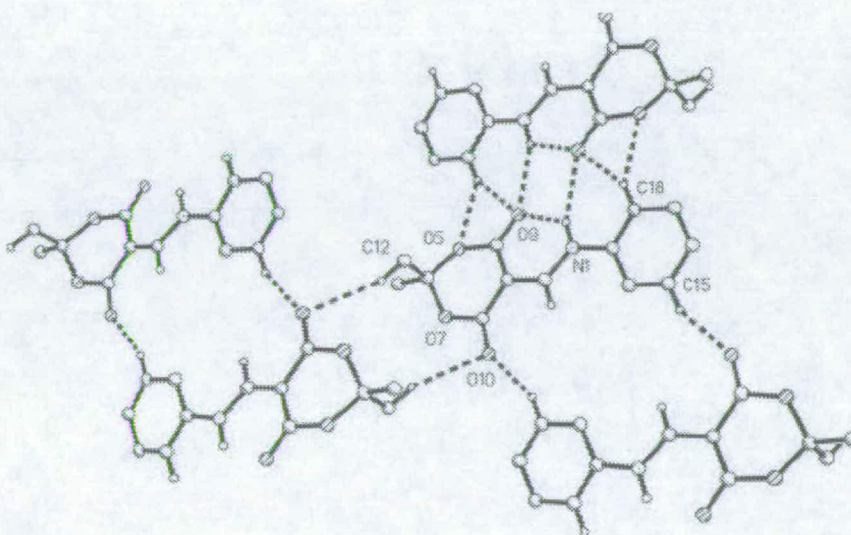
Figure 2.4 a) The X-ray crystal structure of anilinomethylene Meldrum's acid and b) insight into hydrogen bonds in packing diagram.

For 2,4-diaminopyrimidine, literature findings[84] confirmed that the reactivity of a 2-amino group is much greater than the 4- amino isomer and this therefore explains the higher yield of **86a** against **86b**.

The reaction of 1 equivalent of MMMA with 2,6-diaminopyridine or 2,4-diaminopyrimidine gave low yields (<5%) of side products **93** and **95** respectively. These products could be obtained in much higher yield by reaction of MMMA with

two equivalents of diamine giving compounds **93** and **95** in 75% and 50% yield respectively.

2.2.1.1 Pyrolysis precursors - pyridine based

In principle, FVP of the 2-aminopyridine derivative **76** can give two possible products after generation of the methyleneketene and rearrangement to the ketenimine (Scheme 2.4). First, cyclisation at the heteroatom would be expected to give the pyridopyrimidone **77** (as found in solution). Alternatively, cyclisation can take place on carbon to provide the naphthyridine **78** (after hydrogen shift) – as found in the related case shown in Scheme 2.3.

In practice, gas-phase pyrolysis of **76** under FVP conditions at 600-650 °C gave the pyridopyrimidine **77** (98%) as the only product, as found in solution-phase.[85] However, at higher pyrolysis temperatures the new product **78** was found in increasing amounts and was the sole product when the FVP was carried out at 900-950 °C. Clearly C=N ring closure to give **77** takes places under kinetic control while high temperature induced C=C ring closure takes place under thermodynamic control affording compound **78**. It is therefore likely that formation of **77** is reversible and that cyclisation to give **77**, though of higher energy barrier (perhaps because of the unfavourable 1,3-hydrogen shift in the final step), produces a thermodynamically more stable product. Few related thermal rearrangements seem to be known in the literature; however, the pyrazolo[1,2-*b*][1,2,3]triazin-5-ium-4-olate **97** is known to rearrange quantitatively to the pyrazolopyridazinone **98** at high furnace temperatures (Scheme 2.8).[78]

97 **98**
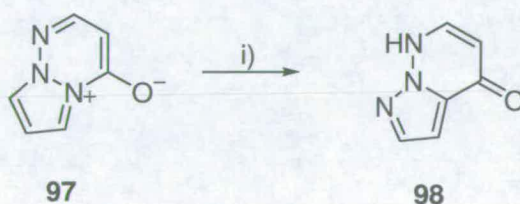
Scheme 2.8 Thermal rearrangement of **97** to **98**, i) 400-750 °C, 50-55%.

Starting from the Meldrum's acid derivative **76**, the synthetic strategy to provide the 1*H*-[1,8]naphthyridin-4-one **78** has been completed in only one step but in practice the isolated yield proved to be very low (25%).
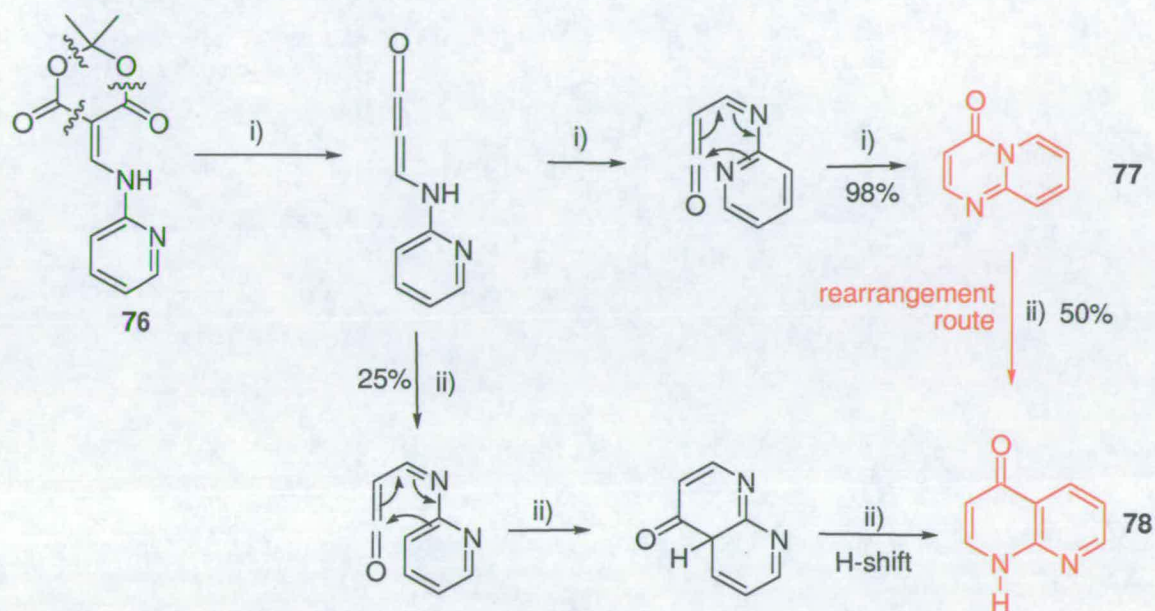
Scheme 2.9 i) FVP 600-650 °C, ii) FVP 900-950 °C.

The low yield of product **78** can be explained by decomposition of the acetone coproduct to give a ketene which may react with the product. Gas-phase pyrolysis of acetone is a well known route to ketene.[86] Increased pressure during pyrolysis of **76** at high temperatures supports this explanation. To overcome this problem repyrolysis of **77** at high temperature was employed and product **78** was afforded in higher yield (50%) using the rearrangement route highlighted red in Scheme 2.9. This rearrangement at high temperatures proved to be more efficient in general, presumably because of the absence of co-products which were formed from the Meldrum's acid precursor.

It was of interest to perform an experiment following the transformation of compound **77** to **78** as a function of temperature. The amounts of **77** and **78** were measured in the product mixture after pyrolysis at various temperatures (Figure 2.4); at 880 °C the ratio was 50:50 and at 1000 °C was 1:100. In this way, the optimum

temperature for preparative pyrolyses to give **77** and **78** could be determined. The low temperature regime to provide **6** and its analogues involved temperatures ranging from 600-650 °C and the high temperature regime to provide thermodynamic products (*e.g.* **78**) usually used temperatures from 900-950 °C.
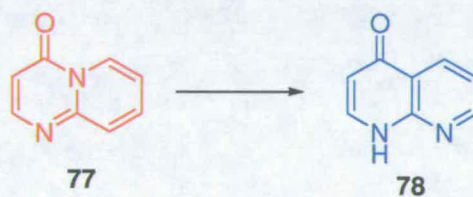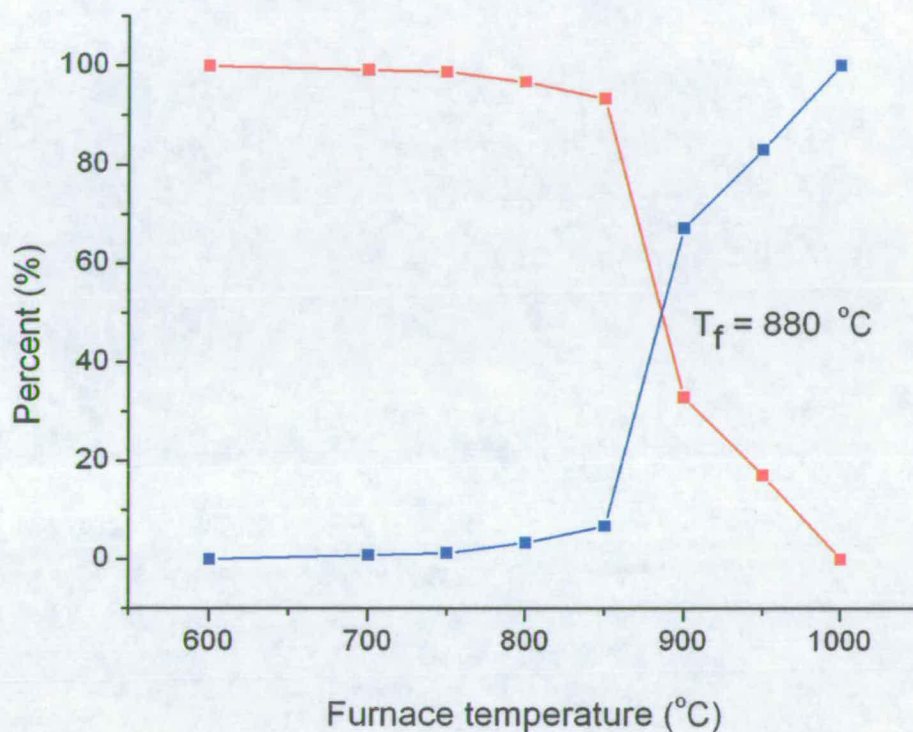
Figure 2.5 Product mixture of **77-78** at various temperatures

This work has successfully resulted in the synthesis of a DA hydrogen-bonding system. In order to extend the strategy to a DAD moiety, following the same strategy precursor **81** was pyrolysed under a low temperature regime, obtaining the product **82** in similar manner to that of **77** (99% yield). Repyrolysis of **82** gave the DAD product **83** in 40% yields as represented in the Scheme 2.10.
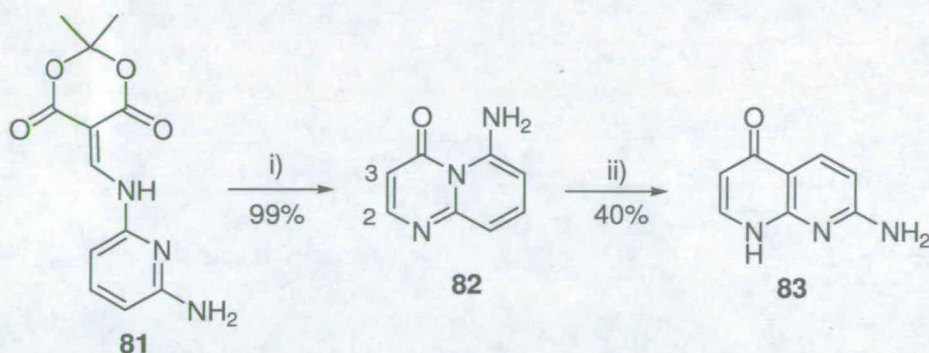
Scheme 2.10 i) FVP 600-650 °C, ii) FVP 900-950 °C.
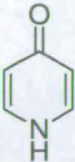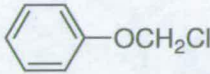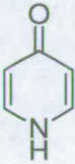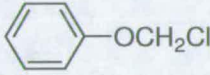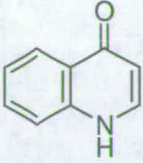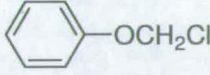
All compounds described so far (**77**, **78**, **81**, and **83**) obtained from pyrolysis experiments showed correct molecular ions in their mass spectra. The products synthesised under low temperature pyrolysis conditions (**77** and **82**) showed characteristic sets of doublets at δ_H 6.5 ppm and 8.2 ppm with *J*=6.5 Hz due to the coupling of the 2- and 3- protons (See Scheme 2.10). For compounds **78** and **83** (high temperature regime) the coupling constant for the corresponding protons was 7.6 Hz and a characteristic broad singlet in the range of δ_H 12.2-11.3 was observed due to the deshielded -NH proton.

In terms of molecular recognition studies this rearrangement route from the pyridopyrimidin-4-ones (**77** and **82**) to 1*H*-naphthyridin-4-one (**78** and **83**) is a one step transformation from only an A hydrogen bonding unit to the double and triple hydrogen bonding unit in DA (**78**) and DAD (**83**) arrangement (Scheme 2.11). However, there are some limitations in the strategy (high temperature regimes and moderate preparative yields-50 mg) as outlined in Scheme 2.5b.
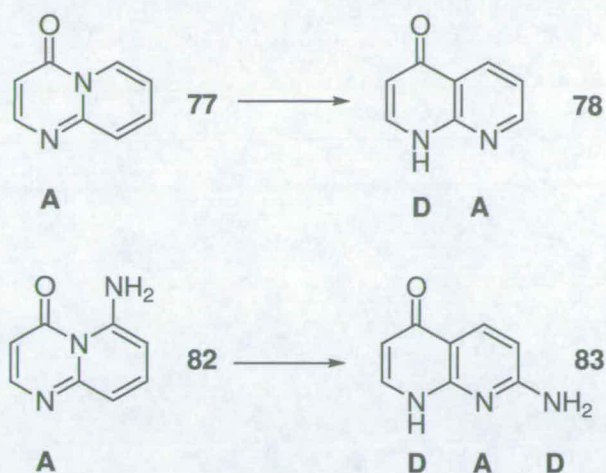
Scheme 2.11

In order to implement the strategy of Scheme 2.5a and Scheme 2.5b, it was necessary to functionalise the products **78** and **83** since they were only DMSO soluble due to the presence of the oxypyridine moiety and therefore not useful in binding studies. In theory, this could be achievable in many ways for example: chlorination by reaction with phosphoryl chloride,[87, 88] Mitsunobu reaction targeting the hydroxy-tautomer of the pyridine moiety,[89, 90] *O*-alkylation[91, 92] or *O*-acylation *etc*. In the latter cases, competitive reaction at *O*- and *N*-centres is possible as shown by literature precedent [93] (Table 2.1) but great importance is given to the HSAB rule for interpreting the results.[94] To promote *O*-alkylated product "hard" base and "hard" solvent are required to favour attack on the "harder" oxygen centre rather than the "softer" nitrogen centre.

Heterocycle	Conditions	*N*-alkylated product	*O*-alkylated product
	KOH, DMSO —OCH$_2$Cl	0%	23%
	NaH, THF —OCH$_2$Cl	35%	12%
	NaH, THF —OCH$_2$Cl	66%	15%

Table 2.1 *O* versus *N*-alkylation.[93]

In cases of 2-pyridones other literature resources[95] report that mixtures occur frequently although *N*-alkylation is much easier to achieve. The design of reaction conditions to maximise the amount of *O*-centred reaction required that the poor solubility of the substrates must be taken into account. Thus the use of the silver salt of the substrate in a non-polar solvent which is reported to give predominantly *O*-alkylation[95-98] in related cases was not considered.

The present preliminary experiments (Scheme 2.12) showed no indications that reaction takes place at all, although different conditions were used. Only unreacted starting material was isolated. This could be due to the long alkyl chain (octyl and nonyl) of the alkylating agent employed for attempted solubility improvement and possible further functionalisation.
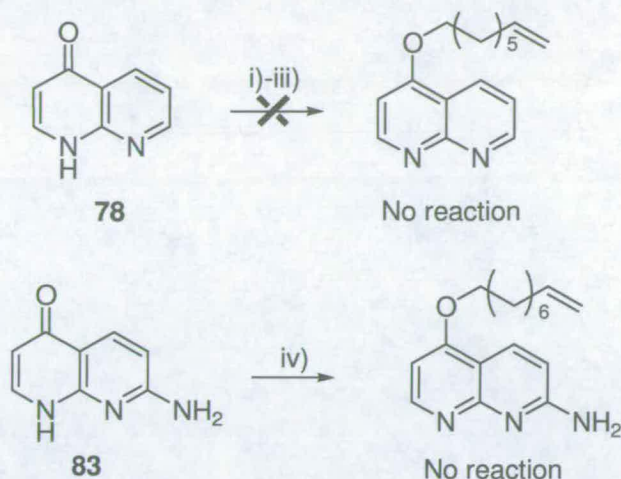
Scheme 2.12 i) 8-Bromo-1-octene, CH$_3$CN, K$_2$CO$_3$; ii) 8-Bromo-1-octene, DMSO, KOH; iii) 8-Bromo-1-octene, DMF, K$_2$CO$_3$; iv) 9-Bromo-1-nonane, DMSO, KOH.

In general two key problems have been identified with the pyridine strategy. First, the yields and very high temperatures of the pyrolyses do not give sufficient amount of product for investigating further reactions. Second, preliminary attempts to solublize these products by functionalization have been unsuccessful. The strategy was therefore modified by using pyrimidine templates, which we hoped would give soluble final products without further functionalization.

2.2.1.2 Pyrolysis precursors - pyrimidine based

Using the pyrimidine based precursors **84** and **89**, which pyrolysed under low temperature FVP conditions, the products **85** and **90** respectively were obtained in high yield (94-95%) by cyclisation onto one of the equivalent nitrogen atoms, in agreement with previous studies of **76** in solution (Scheme 2.1).[75] These products provide, in 2 steps, a defined AA binding surface and were chloroform soluble. In the case of compound **90** attempted displacements of the chlorine atoms using ammonia in ethanol to achieve an AAD (D-amino group) binding surface resulted in complex mixtures of products and were not pursued.

$$84 \xrightarrow[95\%]{i)} 85$$

$$86a \xrightarrow[10\%]{i)} 87$$

$$89 \xrightarrow[94\%]{i)} 90$$
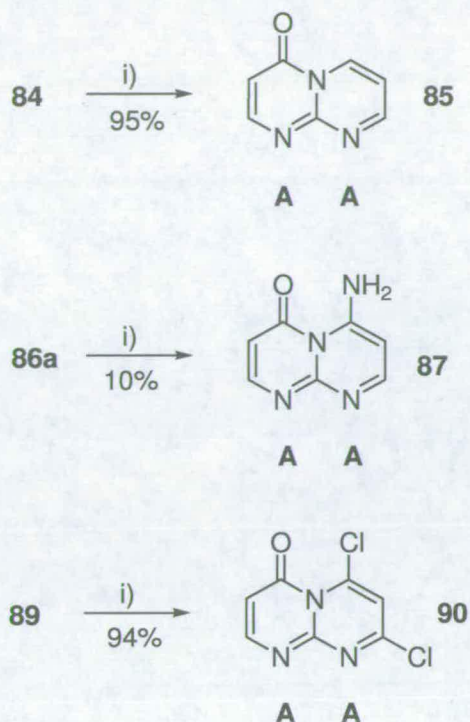
Scheme 2.13 i) FVP 600-650 °C.

Unlike **84** and **89**, FVP of **86a** could in principle provide two isomeric products by cyclisation onto the ring heteroatom adjacent to the amino group (Pathway B, providing **87**), or onto the other heteroatom (Pathway A, to give **88**) (Scheme 2.14). In practice pyrolysis of **86a** indeed produced a mixture of two products, but one proved to be 2,4-diaminopyrimidine. It is known that aromatic amines may be recovered from aminomethylene Meldrum's acid pyrolyses[82] and it is thought that this may be due to competitive free-radical cleavage of the CH-NH bond, perhaps in the inlet prior to evaporation. Compound **87**,[99] pathway B, was the only cyclised isomer isolated from the FVP of **86a**. The structure of product **87** was unambiguously assigned due to the two separate NH signals one at δ_H 6.27 ppm and the other shifted to high frequency (δ_H 10.05 ppm) due to intramolecular hydrogen bonding.
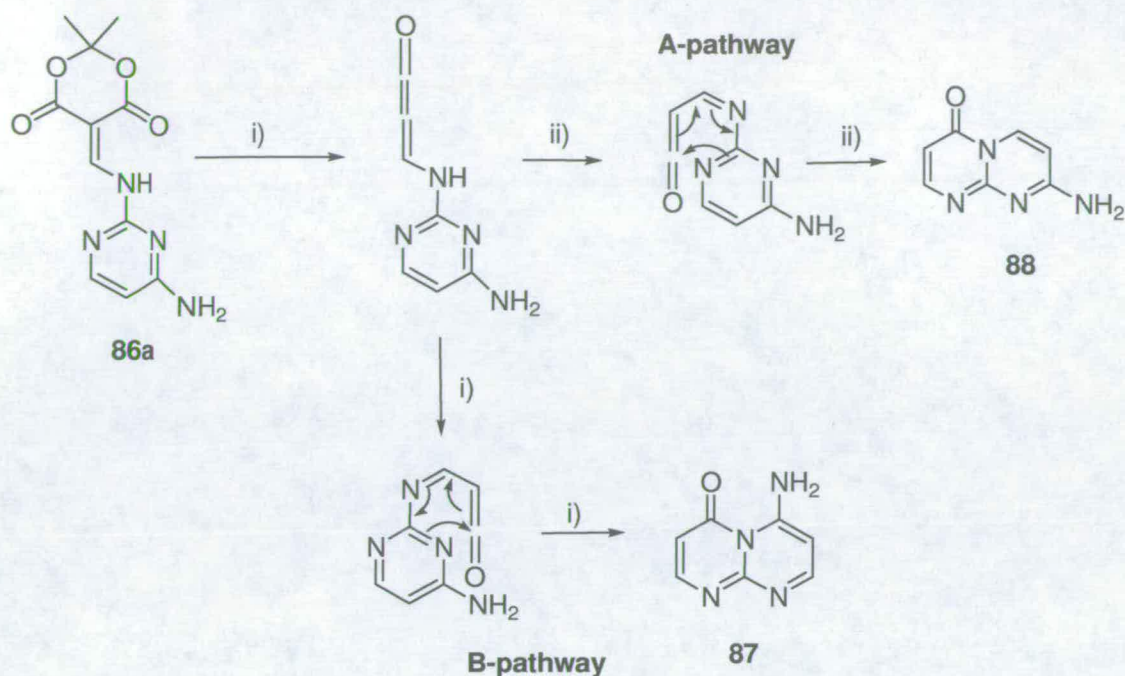
Scheme 2.14 i) FVP 600-650 °C, ii) Dowtherm A, 200-220 °C.

Because of the low yield of cyclised products, and because of decomposition of the substrate in the inlet tube, pyrolysis of **86a** was also carried out in Dowtherm solution[5] at 220 °C according to the method reported by Cassis *et al.*[85] Practical problems that we found with this reaction were: high temperatures that required heating of the reaction mixture with a Bunsen burner to achieve the desired temperature, difficulty in removing the solvent after completion and finally product purification. Under these conditions, the only product obtained was **88** in 9.3% (pathway A). This product has a linear array of the AAD hydrogen bonding motif. The structure of compound **88** was unambiguously assigned due to the presence of only one broad NH_2 signal at δ_H 8.03-8.11 ppm.

It is possible that, under FVP conditions, the kinetic product **87** is formed (*ca.* 10 ms contact time) due to hydrogen bonding between the ketene and the amino substituent in the transition state. Under the thermodynamic control of the solution conditions (*ca.* 20 min contact time), the less sterically hindered product **88** is formed. This result shows that different effects, hydrogen bonding in gas phase and sterics in solution are determining the cyclisation pattern.
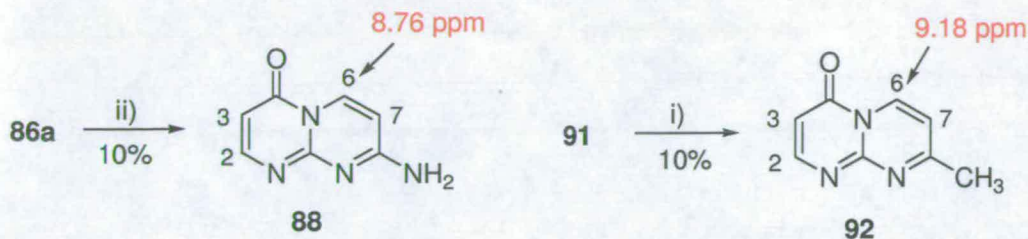
Scheme 2.15 i) FVP 600-650 °C, ii) Dowtherm A, 200-220 °C.

In order to test this hypothesis, pyrolysis of the methyl-substituted analogue **92** was carried out in the gas-phase and in solution (Scheme 2.15). Unfortunately FVP was unsuccessful, giving only 2-amino-4-methylpyrimidine by radical decomposition of **91** in the inlet tube while pyrolysis in solution gave a single isomeric product the structure of which was assigned as **92** from the following spectroscopic observations. By analogy with compound **88**, compound **92** shows a particularly characteristic doublet (δ_H 9.2 ppm, J= 7.7-7.5 Hz) in the range δ_H 8.7-9.2 ppm expected of the highly deshielded H_6 proton peri to the carbonyl group (See Experimental section). Support of the fact that protons peri to the carbonyl group are highly deshielded is found in literature examples[100] and is a key feature which enabled such isomeric structures to be distinguished.

For precursors **93** and **95**, FVP was unsuccessful due to precursor involatility so the thermal cyclisation was carried out using the high boiling solvent reaction. The products obtained (Scheme 2.16) were formed by cyclisation onto C=N, giving aromatic tri- and tetra-azatricycles in modest yield.
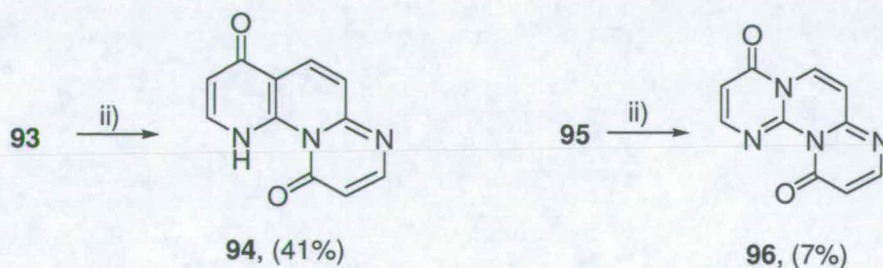
Scheme 2.16 ii) Dowtherm A, 200-220 °C

Compounds **94** and **96** showed the correct molecular ions in their mass spectra and have been characterised by comparison with previously assigned compounds. In the recent literature[9] the reaction **93 → 94** was reported with an X-ray crystal structure of pentachloro analogues of **94** but without clear characterisation data for compound **94**.

2.3 The quadruple hydrogen bond motif of naphthyridine systems

In view of the relatively low yields obtained by these methods, only preliminary studies on the 4-H-bonding strategy were carried out.

Synthesis of the ketene dithioacetal **80** from the reaction of MA with CS$_2$ followed by methylation has been reported previously.[101] Interest in this compound was based on the presence of two reactive methylthio groups ready for displacement by a variety of nucleophiles. The syntheses of three pyrolysis precursors **99**, **101** and **102** are presented at Scheme 2.17. All reactions were performed at reflux conditions in acetonitrile as a solvent.
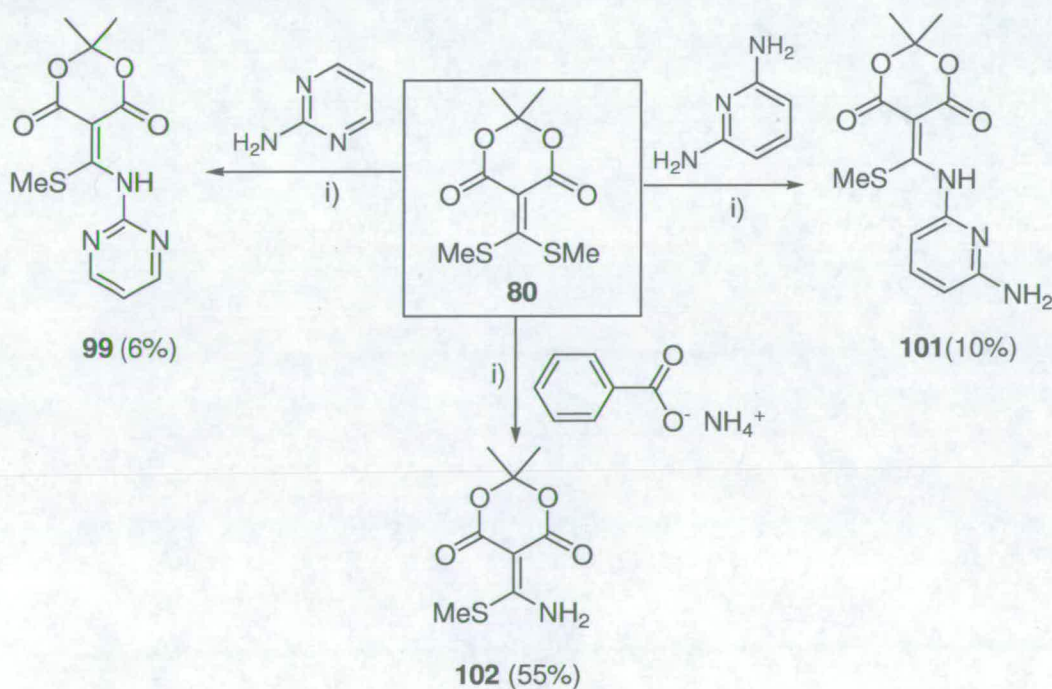
Scheme 2.17 i) acetonitrile at reflux.

Reactions to provide **99** and **101** were low yielding (6% and 10%) and with a number of side products, though formation of **102** (55%) was more efficient where the better nucleophile (ammonium benzoate) as a source of ammonia was used. In all cases attempts to displace the second methylthio group were unsuccessful and they will not be discussed in detail.

All products **99**, **101** and **102** showed correct molecular ions in their mass spectra and a characteristic broad singlet in the range δ_H 13.0-11.0 due to the deshielded hydrogen bonded -NH proton. In the compound **102** the two -NH signals appear at different chemical shifts (δ_H 6.31 and 11.04 ppm), due to differential hydrogen bonding with carbonyl oxygen of the Meldrum's ring. This has been proved by the X-ray crystal structure of **102** (See Experimental section). The only precursor that was pyrolysed was compound **99** at a low temperature regime and product **100** was obtained in 80% yield (Scheme 2.18).
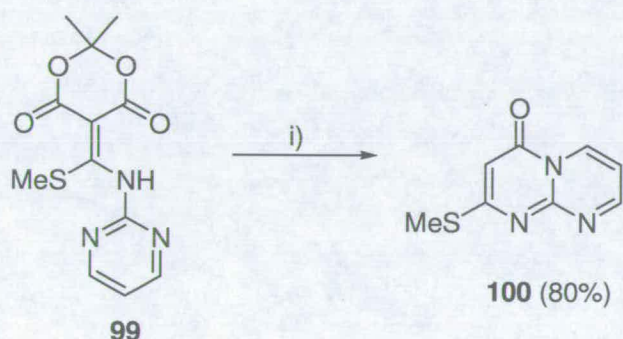
Scheme 2.18 i) FVP 600-650 °C.

This chemistry overall was not promising due to low yield of pyrolysis precursors (<10%) and problems that occurred in the displacement of second methylthio group, so it was abandoned as a strategy.

2.4 Conclusions

In conclusion, in this chapter we have demonstrated different ways for the synthesis of small aromatic heterocyclic units using pyrolysis in the gas phase and in

solution of pyridine and pyrimidine based precursors. In this way we produced a small library of two hydrogen bonding units: AD **78**, AA-pattern (**85**, **87**, **90** and **92**) and three three hydrogen bonding units: DAD-pattern **83** and AAD-pattern **88** (Scheme 2.19).

78

D   A

85

A   A

83

D   A   D

76

A   A   D

87

A   A

90

A   A

92

A   A
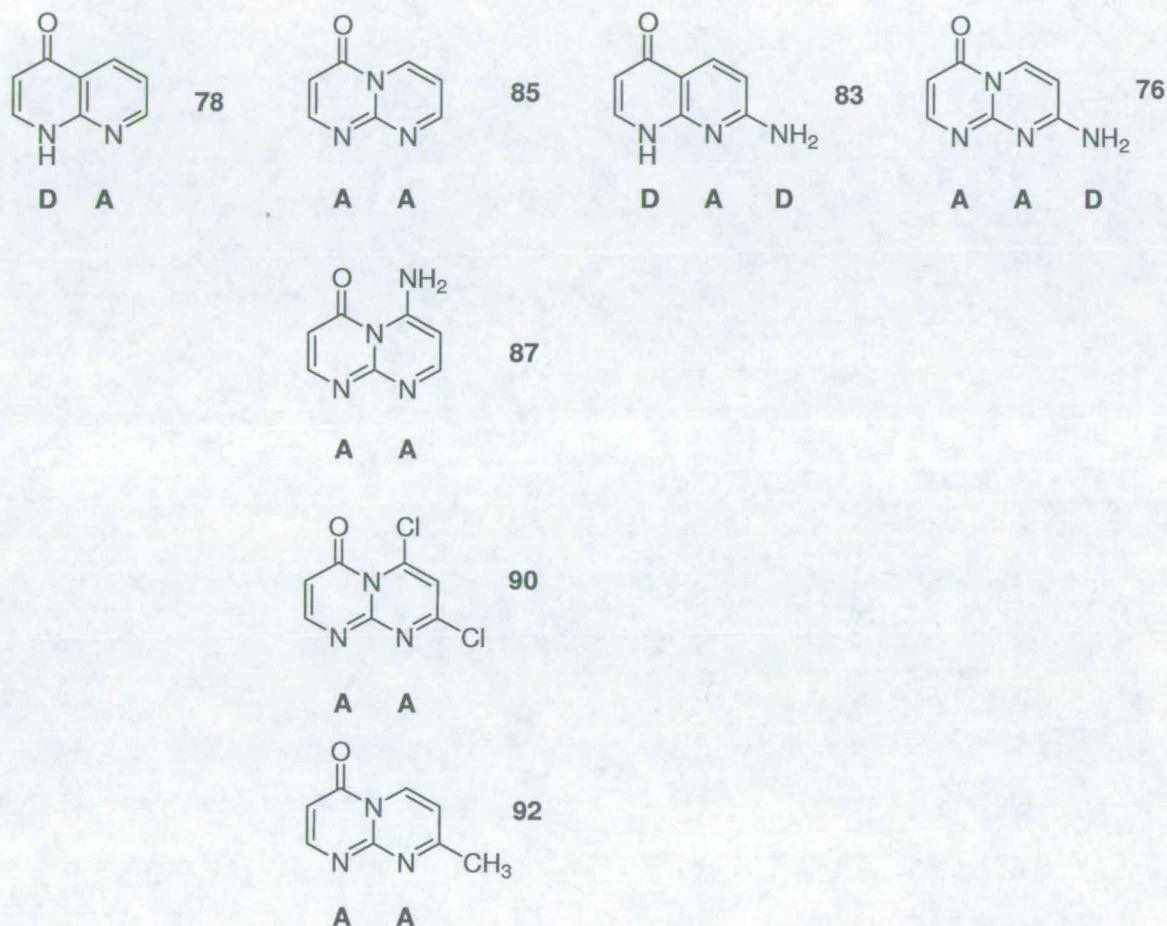
Scheme 2.19 Summary of synthesised compounds.

Unfortunately this strategic method was not applicable for the formation of three and four annelated heterocyclic units due to problems with involatility of pyrolysis precursors.

2.5 Experimental section

FVP General method: The FVP system is evacuated to a pressure of 10^{-2}-10^{-3} Torr by means of high capacity oil pump. Precursors (30-50 mg) are sublimed under reduced pressure through an empty silica tube (35 × 2.5 cm) heated by an electrical furnace. The products are collected in a U-tube cooled by liquid nitrogen (Figure 2.1) situated at the exit point of the furnace. Upon completion of the pyrolysis the trap is allowed to warm to room temperature under an atmosphere of dry nitrogen. The entire pyrolysate is then dissolved in solvent to enable removal from the trap.

2,2-Dimethyl-5-(pyridin-2-ylaminomethylene) -[1,3]dioxane-4,6-dione (76)
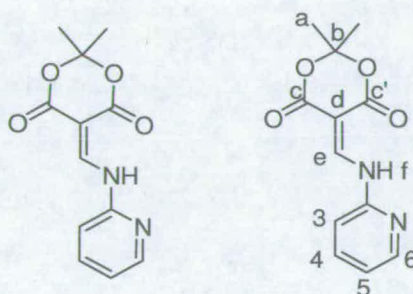
To a stirred solution of methoxymethylene Meldrum's acid **79** (0.47 g, 5 mmol) in anhydrous acetonitrile (15 cm^3) was added 2-aminopyridine (0.47 g, 5 mmol). The mixture was stirred at room temperature for 2 h (TLC, 1% MeOH in CHCl$_3$). The white precipitate was filtered, recrystallised from acetonitrile and dried in an oven to give **76** (1.18 g, 95%) as a white solid, mp 181-184 °C (decomp) [lit.,[102] 175-176 °C]. ^{1}H NMR (400 MHz, CDCl$_3$) δ ppm 11.28 (br d, $J_{f,e}$ = 13.4 Hz, 1H, $\underline{H}_f$-), 9.39 (d, $J_{e,f}$ = 13.4 Hz, 1H, $\underline{H}_e$-), 8.40 (dd, $J_{6,5}$ = 4.6 Hz, $J_{6,4}$ = 1.5 Hz, 1H, $\underline{H}_6$-), 7.75 (ddd, $J_{4,3}$ = 8.1 Hz, $J_{4,5}$ = 7.5 Hz, $J_{4,6}$ = 1.5 Hz, 1H, $\underline{H}_4$-), 7.17 (dd, $J_{5,4}$ = 7.5 Hz, $J_{5,6}$ = 4.6 Hz, 1H, $\underline{H}_5$-), 7.02 (d, $J_{3,4}$ = 8.1 Hz, 1H, $\underline{H}_3$-) and 1.76 (s, 6H, $\underline{H}_a$-); ^{13}C NMR (100 MHz, CDCl$_3$) δ ppm 165.6 (-$\underline{C}_{c'}$-), 163.2 ($\underline{C}_c$-), 151.7 ($\underline{C}_e$-), 149.2 (C_2-), 149.1 ($\underline{C}_6$-), 139.0 ($\underline{C}_4$-), 121.5 ($\underline{C}_5$-), 112.7 ($\underline{C}_3$-), 105.2 ($\underline{C}_b$-), 88.7 ($\underline{C}_d$-) and 27.1 ($\underline{C}_a$-); FAB-

MS m/z 249 (M+1, 26%), 191 (M+1-Acetone, 100%). Found C, 57.55; H, 4.8; N, 11.15). $C_{12}H_{12}N_2O_4$ requires: C, 58.05; H, 4.85; N, 11.3%.

Pyrido[1,2-*a*]pyrimidin-4-one (77)
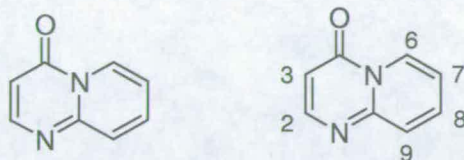
FVP of (**76**) (0.050 g, T_f = 650 °C, T_i = 180 °C, P = 1.5 x 10^{-3} Torr, t = 10 min) produced **77** in a quantitative yield. Compound **77** was recrystallised from diisopropyl ether (0.029 g, 98%) and was a white solid, mp 136-138 °C [lit.,[102] 130-131 °C]. ^{1}H NMR (400 MHz, CDCl$_3$) δ ppm 9.09 (d, $J_{6,7}$ = 7.3 Hz, 1H, H$_6$-), 8.31 (d, $J_{2,3}$ = 6.4 Hz, 1H, H$_2$-), 7.76 (dd, $J_{8,9}$ = 8.6 Hz, $J_{8,7}$ = 6.7 Hz, 1H, H$_8$-), 7.67 (d, $J_{9,8}$ = 8.6 Hz, 1H, H$_9$-), 7.17 (dd, $J_{7,6}$ = 7.3 Hz, $J_{7,8}$ = 6.7 Hz, 1H, H$_7$-) and 6.46 (d, $J_{3,2}$ = 6.4 Hz, 1H, H$_3$-); ^{13}C NMR (100 MHz, CDCl$_3$) δ 157.6 (C$_4$-), 154.8 (C$_2$-), 151.8 (C$_{9a}$-), 136.2 (C$_7$-), 127.4 (C$_6$-), 126.5 (C$_9$-), 115.6 (C$_7$-) and 104.8 (C$_3$-); FAB-MS: m/z 147 (M+1, 74%). Found C 65.7, H 4.0, N, 19.15. $C_8H_6N_2O$ requires: C, 65.75; H, 4.1; N, 19.2%.

1*H*-[1,8]Naphthyridin-4-one (78)
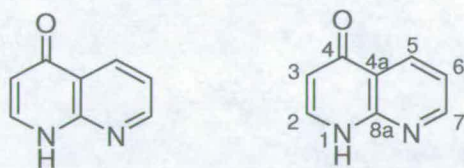
FVP of (**77**) (0.050 g, T_f = 950 °C, T_i = 200 °C, P = 1.5 x 10^{-3} Torr, t = 10 min) using a furnace tube packed in the centre with silica tubes produced (**78**) in 50% yield, mp 163-170 °C (decomp) [lit.,[103] 239 °C]. ^{1}H NMR (400 MHz, CDCl$_3$) δ ppm 12.20 (br, 1H, H$_1$-), 8.78 (dd, $J_{7,6}$ = 4.5 Hz, $J_{7,5}$ = 2.0 Hz, 1H, H$_7$-), 8.48 (dd, $J_{5,6}$ = 8.1 Hz, $J_{5,7}$ = 2.0 Hz, 1H, H$_5$-), 7.98 (dd, $J_{2,3}$ = 7.6 Hz, $J_{2,1}$ = 6.1 Hz, 1H, H$_2$), 7.44 (dd, $J_{6,5}$ = 8.1 Hz, $J_{6,7}$ = 4.5 Hz, 1H, H$_6$-), 6.14 (d, $J_{3,2}$ = 7.6 Hz, 1H, H$_3$-); ^{13}C NMR (100 MHz,

[D$_6$]DMSO) δ ppm 177.5 (C$_4$-), 153.0 (C$_7$-), 150.5 (C$_{4a}$-), 140.4 (C$_2$-), 134.6 (C$_5$-), 120.2 (C$_{8a}$-), 119.7 (C$_6$-) and 109.6 (C$_3$-); FAB-MS: *m/z* 147 (M+1, 76%); Found C, 65.5; H 4.2; N, 18.9. C$_8$H$_6$N$_2$O requires: C, 65.75; H, 4.1; N 19.2%.

5-[(6-Aminopyridin-2-ylamino)-methylene]-2,2-dimethyl-[1,3]dioxane-4,6-dione (81)
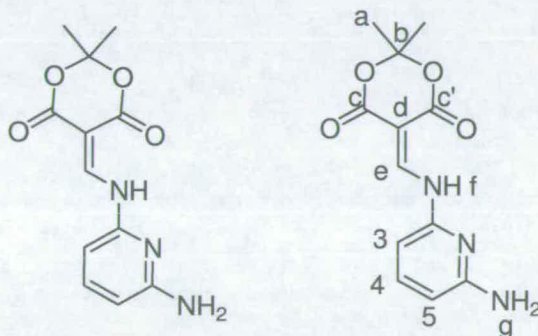
To a stirred solution of methoxymethylene Meldrum's acid **79**, (0.93 g, 5.00 mmol) in anhydrous acetonitrile (15 cm^3) was added 2,6-diaminopyridine (2.76 g, 25.0 mmol). The reaction was allowed to stir for 5 h at room temperature. The solvent was removed under reduced pressure and the residual oil purified by chromatography on silica gel using a solvent gradient of CHCl$_3$ to CHCl$_3$/methanol (10%) as eluent to obtain **93** (< 5%) as a first product from the column. Compound **81** eluted next from the column as the main product, (3.33 g, 67%), mp 192-193 °C ^{1}H NMR (400 MHz, CDCl$_3$) δ ppm 11.12 (br d, $J_{f,e}$ = 13.6 Hz, 1H, H$_f$-), 9.32 (d, $J_{e,f}$ =13.6 Hz, 1H, H$_e$-), 7.45 (t, J = 7.7 Hz, 1H, H$_4$-), 6.29-6.36 (m, 2H, H$_3$- and H$_5$-), 4.69 (br s, 2H, H$_g$-), and 1.75 (s, 6H, H$_a$-) ^{13}C NMR (100 MHz, CDCl$_3$) δ ppm 163.6 (C$_{c'}$), 163.0 (C$_c$), 159.1 (C$_6$), 150.2 (C$_e$), 147.7 (C$_2$), 139.7 (C$_4$), 106.0 (C$_5$), 104.1 (C$_b$), 100.4 (C$_3$), 86.8 (C$_d$) and 26.4 (C$_a$); FAB-MS *m/z* 264 (M+1, 100%). Found: C, 54.85; H, 4.0; N, 16.0. C$_{12}$H$_{13}$N$_3$O$_4$ requires: C, 54.75; H, 4.1; N, 15.95%.

6-Aminopyrido[1,2-*a*]pyrimidin-4-one (82)
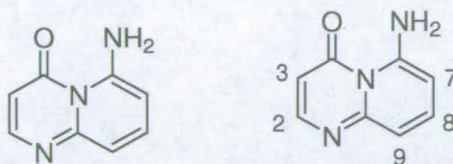
FVP of (**81**) (0.050 g, T_f = 650 °C, T_i = 200 °C, P = 1.5 x 10^{-3} Torr, t = 10 min) produced in essentially quantitative yield **82** (0.032 g, 99%), mp 192-193 °C. ^{1}H NMR (400 MHz, CDCl$_3$) δ ppm 8.00 (d, $J_{2,3}$ = 6.1 Hz, 1H, H$_2$-), 7.46 (br s, 2H, -NH$_2$), 7.40 (dd, $J_{8,7}$ = 7.9 Hz, $J_{8,9}$ = 8.4 Hz, 1H, -H$_8$), 6.82 (d, $J_{9,8}$ = 8.4 Hz, 1H, H$_9$-), 6.03 (d, $J_{3,2}$ = 6.1 Hz, 1H, H$_3$-) and 5.96 (d, $J_{7,8}$= 7.9 Hz, 1H, H$_7$-); ^{13}C NMR (100 MHz, CDCl$_3$) δ 164.6 (C$_4$), 157.6 (C$_{9a}$-), 153.6 (C$_2$-), 151.9 (C$_6$-), 138.1 (C$_8$), 112.1 (C$_9$), 102.9 (C$_3$), 98.7 (C$_7$); EI-MS m/z 161 (M$^+$, 100%), 106 (77), 93 (65), 80 (54), 66 (62) and 39 (75). Found: C, 59.7; H, 4.35; N, 26.15. C$_8$H$_7$N$_3$O requires: C, 59.6; H, 4.4; N, 26.05%.

7-Amino-1*H*-[1,8]naphthyridin-4-one (83)
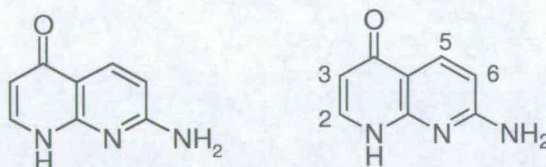
FVP of (**82**) (0.050 g, T_f = 900 °C, T_i = 200 °C, P = 1.0 x 10^{-3} Torr, t = 10 min) produced (**83**) in 40% yield (0.012 g). mp 200-204 °C, ^{1}H NMR (400 MHz, [D$_6$]DMSO) δ ppm 11.35 (br , 1H, H$_1$-), 8.01 (d, $J_{5,6}$ = 8.6 Hz, 1H, H$_5$-), 7.56-7.63 (br m, 1H, H$_2$-), 6.86 (br s, 2H, -NH$_2$), 6.49 (d, $J_{6,5}$ = 8.6 Hz, 1H, H$_6$-) and 5.92 (d, $J_{3,2}$ = 7.6 Hz, 1H, H$_3$-); ^{13}C NMR (100 MHz, [D$_6$]DMSO) δ ppm 177.9 (C$_4$-), 162.2

($\underline{C}_7$-), 152.3 ($\underline{C}_{4a}$-), 138.9 ($\underline{C}_2$-), 136.0 ($\underline{C}_5$-), 112.8 ($\underline{C}_{8a}$-), 110.4 ($\underline{C}_3$-) and 108.7 ($\underline{C}_6$-); EI-MS m/z = 161 (M$^+$, 25%), 43 (100), 105 (68), 57 (41). HMRS [M]$^+$ = 161.0589, $C_8H_7N_3O$ requires: 161.0563. FVP of (**81**) (0.050 g, T_f = 900 °C, T_i = 200 °C, P = 1.0 x 10^{-3} Torr, t = 10 min) under diffusion pump conditions produced (**83**) in 20% (0.006 g) yield.

2,2-Dimethyl-5-(pyrimidin-2-ylaminomethylene)-[1,3]dioxane-4,6-dione (84)
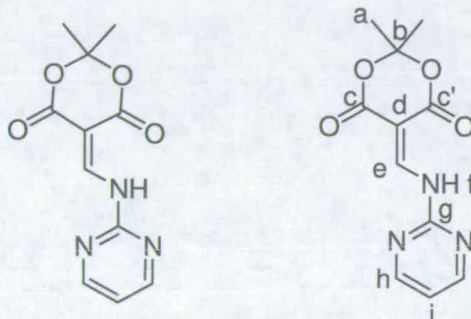
To a stirred solution of methoxymethylene Meldrum's acid **79** (0.47 g, 5 mmol) in anhydrous acetonitrile (15 cm^3) was added 2-aminopyrimidine (0.47 g, 5 mmol). The mixture was stirred at room temperature for 2 h (TLC, 1% MeOH in CHCl$_3$). The white precipitate was filtered, recrystallised from acetonitrile and dried in oven to give (1.65 g, 67%) as a white solid (**84**), mp 214-215 °C [lit.,[104] 206-208 °C]. ^{1}H NMR (400 MHz, CDCl$_3$) δ ppm 11.23 (br d, $J_{f,e}$ = 13.3 Hz, 1H, $\underline{H}_f$-), 9.40 (d, $J_{e,f}$ = 13.3 Hz, 1H, $\underline{H}_e$-), 8.61 (d, $J_{4,5}$ = 4.8 Hz, 2H, $\underline{H}_4$-), 7.16 (t, $J_{5,4}$ = 4.8 Hz, 1H, $\underline{H}_5$-), 1.74 (s, 6H, $\underline{H}_a$-); ^{13}C NMR (100 MHz, CDCl$_3$) δ ppm 164.7 ($\underline{C}_{c'}$-), 162.9 ($\underline{C}_c$-), 158.7 ($\underline{C}_4$-), 156.1 ($\underline{C}_g$-), 152.0 ($\underline{C}_e$-), 118.2 ($\underline{C}_5$-), 105.3 ($\underline{C}_b$-), 90.4 ($\underline{C}_d$-) and 27.2 ($\underline{C}_a$-); FAB-MS m/z 250 (M+1, 14%). Found: C, 52.90, H, 4.31, N, 16.92. $C_{11}H_{11}N_3O_4$ required: C, 53.0; H, 4.45; N, 16.85.

Pyrimido[1,2-*a*]pyrimidin-4-one (85)
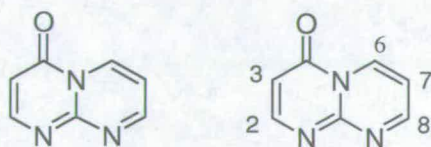
FVP of (**84**) (0.050 g, T_f = 600 °C, T_i = 180 °C, P = 1.5 x 10^{-3} Torr, t = 10 min) produced **85** in a quantitative yield. Compound **85** was recrystallised from acetonitrile (0.029 g, white solid), mp 185-186 °C [lit.,[104] 170-173 °C]. ^{1}H NMR (400 MHz, CDCl$_3$) δ ppm 9.36 (d, $J_{6,7}$ = 7.1 Hz, 1H, H$_6$-), 9.07 (d, $J_{8,7}$ = 3.9 Hz, 1H, H$_8$-), 8.44 (dd, $J_{2,3}$ = 6.7 Hz 1H, H$_2$-), 7.19 (dd, $J_{7,6}$ = 7.1 Hz, $J_{7,8}$ = 3.9 Hz 1H, H$_7$-) and 6.52 (d, $J_{3,2}$ = 6.7 Hz, 1H, H$_3$-); ^{13}C NMR (100 MHz, CDCl$_3$) δ ppm 162.0 (C$_8$-), 158.0 (C$_4$-), 157.1 (C$_2$-), 152.4 (C$_{10}$-), 136.4 (C$_6$-), 111.9 (C$_7$-), 106.0 (C$_3$-); FAB-MS m/z 147 (M+1, 55%). Found: C, 56.4; H, 3.55; N, 28.9%. C$_7$H$_5$N$_3$O required: C 57.1; H 3.4; N 28.55%.

5-[(4-Aminopyrimidin-2-ylamino)-methylene]-2,2-dimethyl-[1,3]dioxane-4,6-dione (86a)

and 5-[(2-Aminopyrimidin-4-ylamino)-methylene]-2,2-dimethyl-[1,3]dioxane-4,6-dione (86b)
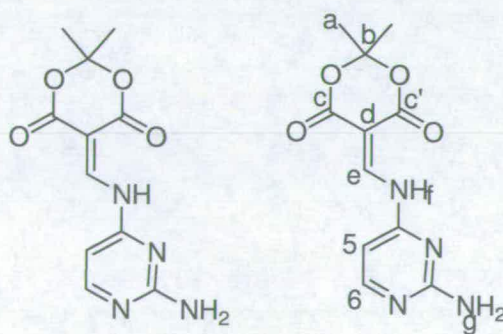
To a stirred solution of methoxymethylene Meldrum's acid **79** (1.86 g, 10.00 mmol) in anhydrous acetonitrile (15 cm^3) was added 2,4-diaminopyridine (1.10 g, 10.00 mmol). The reaction was allowed to stir for 5 h at room temperature. The solvent was removed under reduced pressure and the residual oil chromatographed on silica gel using a solvent gradient of DCM to DCM/THF (30%) as eluent to obtain as a (**86a**) white solid (1.05 g, 40%). The regiochemistry was established by X-ray crystallography (See supporting information), mp 204-206 °C ^{1}H NMR (400 MHz, CDCl$_3$) δ ppm 10.94 (br d, $J_{f,e}$ = 13.9 Hz, 1H, $\underline{H}_f$-), 9.30 (d, $J_{e,f}$ = 13.9 Hz, 1H, $\underline{H}_e$-), 8.10 (d, $J_{6,5}$ = 5.8 Hz, 1H, $\underline{H}_6$-), 6.26 (d, $J_{5,6}$ = 5.8 Hz, 1H, $\underline{H}_5$-), 5.16 (br s, 2H, -N$\underline{H}_2$), and 1.74 (s, 6H, $\underline{H}_a$-); ^{13}C NMR (100 MHz, CDCl$_3$) δ ppm 164.7 ($\underline{C}_{c'}$-), 163.7 ($\underline{C}_4$-), 163.3 ($\underline{C}_c$-), 157.2 ($\underline{C}_6$-), 155.8 ($\underline{C}_2$-), 152.4 ($\underline{C}_e$-), 105.2 ($\underline{C}_b$-), 102.4 ($\underline{C}_5$-), 89.4 ($\underline{C}_d$-) and 27.2 ($\underline{C}_a$-); FAB-MS *m/z* 265 (M+1, 20%). Found: C, 50.3; H 4.65; N, 21.05%. C$_{11}$H$_{12}$N$_4$O$_4$ required: C, 50.00; H 4.58; N, 21.2%. Compound **86b** was obtained as the second fraction from the column (0.105 g, 4%) and was identified by it is ^{1}H NMR spectrum. ^{1}H NMR (400 MHz, CDCl$_3$) δ ppm 10.94 (br d, $J_{f,e}$ = 13.9 Hz, 1H, $\underline{H}_f$-), 9.37 (d, $J_{e,f}$ = 13.9 Hz, 1H, $\underline{H}_e$-), 8.28 (d, $J_{6,5}$ = 5.7 Hz, 1H, $\underline{H}_6$-), 6.33 (d, $J_{5,6}$ = 5.7 Hz, 1H, $\underline{H}_5$-), 5.13 (br s, 2H, -N$\underline{H}_2$), and 1.57 (s, 6H, $\underline{H}_a$-).

6-Aminopyrimido[1,2-*a*]pyrimidin-4-one (87)
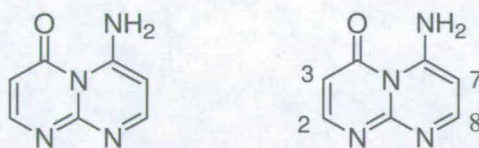
FVP of (**86a**) (0.127 g, T_f = 600 °C, T_i = 180 °C, P = 3.0 x 10^{-3} Torr, t = 10 min) produced **87** (0.013 g, 10%) as a white solid identified by ^{1}H NMR spectrum. ^{1}H NMR (400 MHz, CDCl$_3$) δ ppm 10.05 (br s, 1H, N$\underline{H}'$-), 7.92 (d, $J_{2,3}$ = 6.3 Hz, 1H, -$\underline{H}_2$) 7.65 (d, $J_{8,7}$ = 6.1 Hz, 1H, $\underline{H}_8$-), 6.51 (d, $J_{7,8}$ = 6.1 Hz, 1H, $\underline{H}_7$-), 6.27 (br s, 1H, -N$\underline{H}''$-) and 6.16 (d, $J_{3,2}$ = 6.3 Hz, 1H, $\underline{H}_3$-).

8-Aminopyrimido[1,2-*a*]pyrimidin-4-one (88)
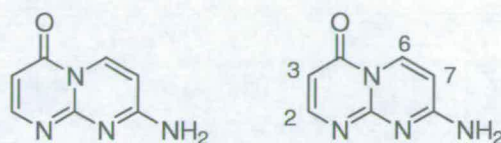
To a boiling solution of Dowtherm (Ph$_2$O and Ph$_2$) (70 cm^3) was added (**86a**) (0.5 g, 2 mmol). The resulting mixture was heated under reflux at 220 °C for 20 minutes and then filtered; the product (**88**) was precipitated from the solution with petroleum ether (3 x 50 cm^3). The white precipitate was collected and dried in oven to give **88** (0.03 g, 9.3%), mp 220-235 °C ^{1}H NMR (400 MHz, [D$_6$]DMSO) δ ppm 8.76 (d, $J_{6,7}$ = 7.7 Hz, 1H, $\underline{H}_6$-), 8.11-8.03 (br s, 1H, -N$\underline{H}_2$-), 8.04 (d, $J_{2,3}$ = 6.3 Hz, 1H, -$\underline{H}_2$), 6.57 (d, $J_{7,6}$ = 7.7 Hz, 1H, $\underline{H}_7$-) and 5.96 (d, $J_{3,2}$ = 6.3 Hz, 1H, $\underline{H}_3$-); ^{13}C NMR (100 MHz, [D$_6$]DMSO) δ ppm 162.3 ($\underline{C}_8$), 158.1 ($\underline{C}_4$), 157.6 ($\underline{C}_2$), 153.2 ($\underline{C}_{10}$), 134.4 ($\underline{C}_6$), 103.7 ($\underline{C}_7$), 99.9 ($\underline{C}_3$); EI-MS *m/z* 162 (M$^+$, 100%), 134 (53), 94 (51), 82 (28). Found: C, 51.9; H, 3.7; N, 34.1%. C$_7$H$_6$N$_4$O required: C, 51.85; H, 3.7; N, 34.55%.

## 5-[(4,6-Dichloropyrimidin-2-ylamino)-methylene]-2,2-dimethyl-[1,3]dioxane-4,6-dione (89)
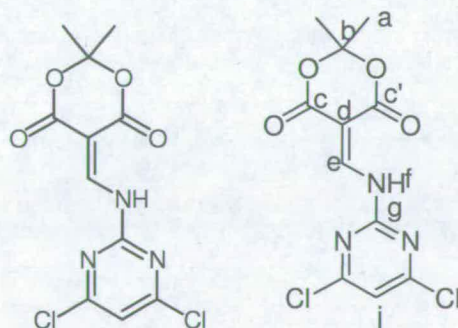
To a stirred solution of methoxymethylene Meldrum's acid **79**, (0.74 g, 4 mmol) in anhydrous acetonitrile (15 cm^3) was added 2-amino-4,6-dichloropyrimidine (0.65 g, 4 mmol). The mixture was stirred at reflux for 3 days (TLC, 1% MeOH in CHCl$_3$). The white precipitate was filtered and dried in oven to obtain (**89**) as a white solid

(0.403 g, 32%), mp 183-184 °C; ^{1}H NMR (400 MHz, CHCl$_3$) δ ppm 11.21 (d, $J_{f,e}$ = 12.8 Hz, 1H, $\underline{H}_f$-), 9.23 (d, $J_{e,f}$ = 12.8 Hz, 1H, $\underline{H}_e$-), 7.21 (s, 1H, $\underline{H}_j$-) and 1.74 (s, 1H, $\underline{H}_a$-); ^{13}C NMR (100 MHz, CHCl$_3$) δ ppm 164.3 ($\underline{C}_{c'}$-), 163.3 ($\underline{C}_i$-), 162.2 ($\underline{C}_c$-), 155.9 ($\underline{C}_g$-), 151.0 ($\underline{C}_e$-), 117.5 ($\underline{C}_j$-), 105.7 ($\underline{C}_b$-), 92.6 ($\underline{C}_d$-) and 27.6 ($\underline{C}_a$-); EI-MS *m/z* 318 (M$^+$, 48%), 259 (59), 215 (75), 187 (100), 147 (76) and 43 (86). Found C, 41.6; H, 2.75; N, 13.35. C$_{11}$H$_9$Cl$_2$N$_3$O$_4$ requires: C, 41.5; H, 2.85; N, 13.21%.

6,8-Dichloropyrimido[1,2-*a*]pyrimidin-4-one (90)
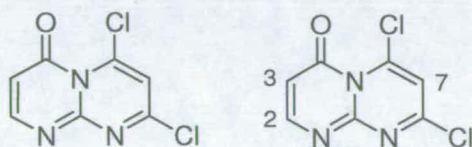
FVP of (**89**) (0.037 g, T_f 650 °C, T_i 200 °C, P 5.5 x 10^{-3} Torr, t 15 min) produced **90** in quantitative yield. Compound **90** was recrystallised from acetonitrile (0.025 g) as a yellow solid, mp 143-146 °C. ^{1}H NMR (400 MHz, CDCl$_3$) δ ppm 8.17 (d, $J_{2,3}$ = 6.6 Hz, 1H, $\underline{H}_2$-), 6.98 (s, 1H, $\underline{H}_7$-) and 6.38 (d, $J_{3,2}$ = 6.6 Hz 1H, $\underline{H}_3$-). ^{13}C NMR (100 MHz, CDCl$_3$) δ ppm 159.7 ($\underline{C}_8$-), 157.8 ($\underline{C}_4$-), 153.8 ($\underline{C}_2$-), 149.8 ($\underline{C}_{10}$-), 141.9 ($\underline{C}_6$-), 115.3 ($\underline{C}_7$-), 108.9 ($\underline{C}_3$-); EI-MS *m/z* 217 (M$^+$, 4.5%), 197 (100), 169 (71), 128 (84), 95 (89) and 44 (75). Found C, 38.4; H, 1.55; N, 19.3. C$_7$H$_3$Cl$_2$N$_3$O required: C 38.9; H 1.4; N 19.45%.

2,2-Dimethyl-5-[(4-methylpyrimidin-2-ylamino)-methylene]-[1,3]dioxane-4,6-dione (91)
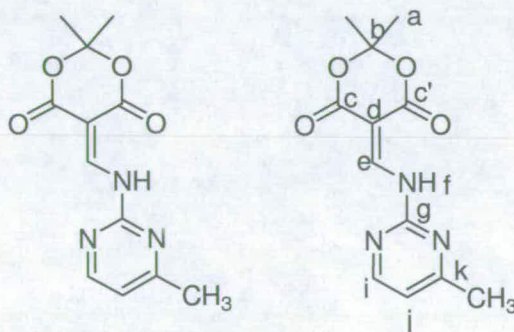
To a stirred solution of methoxymethylene Meldrum's acid **79**, (0.58 g, 5.3 mmol) in anhydrous acetonitrile (10 cm³) was added 2-amino-4-methylpyrimidine (1.0 g, 5.3 mmol). The mixture was stirred at reflux for 24 h (TLC, 1% MeOH in CHCl₃). The precipitate was filtered and dried in an oven to obtain (**91**) as a yellow solid (0.803 g, 57%), mp 144-145 °C; ^{1}H NMR (400 MHz, CHCl₃) δ ppm 11.17 (d, $J_{f,e}$ = 13.4 Hz, 1H, $\underline{H}_f$-), 9.40 (d, $J_{e,f}$ = 13.4 Hz, 1H, $\underline{H}_e$-), 8.42 (d, $J_{j,l}$ = 5.1 Hz 1H, $\underline{H}_j$-), 6.97 (d, $J_{i,j}$ = 5.1 Hz 1H, $\underline{H}_i$-), 2.50 (s, 6H, $\underline{H}_a$-) and 1.73 (s, 3H, $\underline{H}_{Me}$-); ^{13}C NMR (100 MHz, CHCl₃) δ ppm 169.7 ($\underline{C}_{c'}$-), 164.7 ($\underline{C}_c$-), 158.1 ($\underline{C}_i$-), 155.8 ($\underline{C}_g$-), 155.8 ($\underline{C}_k$-), 152.2 ($\underline{C}_e$-), 117.9 ($\underline{C}_j$-), 105.2 ($\underline{C}_b$-), 90.1 ($\underline{C}_d$-), 27.2 ($\underline{C}_a$-) and 24.1 ($\underline{C}_{Me}$-); EI-MS m/z 263 (M⁺, 62%), Found C, 54.8; H, 4.92; N, 15.90. $C_{12}H_{13}N_3O_4$ requires: C, 54.7; H, 4.98; N, 15.96%.

8-Methylpyrimido[1,2-*a*]pyrimidin-4-one (92)
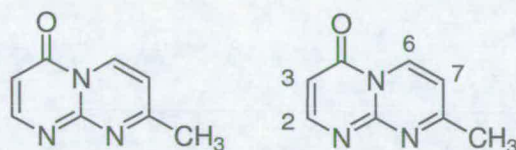
To a boiling solution of Dowtherm[99] (Ph₂O and Ph₂) (70 cm³) was added **91** (0.5 g, 2 mmol). The resulting mixture was heated under the reflux at 220 °C for 20 min. and then filtered; the product **92** was precipitated from the solution with petroleum ether (3 x 50 cm³). The white precipitate was collected and dried in an oven to give **92** (0.05 g, 10%) which was identified by its ^{1}H NMR spectrum. ^{1}H NMR (400 MHz, CDCl₃) δ 9.18 (d, $J_{6,7}$ = 7.3 Hz, 1H, $\underline{H}_6$-), 8.42 (d, $J_{2,3}$ = 6.3 Hz, 1H, -$\underline{H}_2$), 7.04 (d, $J_{7,6}$ = 7.3 Hz, 1H, $\underline{H}_7$-), 6.44 (d, $J_{3,2}$ = 6.3 Hz, 1H, $\underline{H}_3$-) and 2.74 (s, 3H, -$\underline{H}_{Me}$).

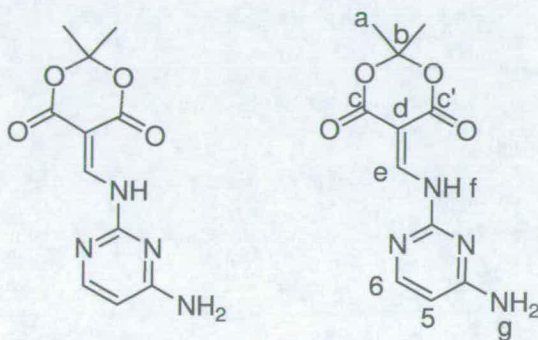## *N,N'*-Bis(5-methylene-4,6-diketo 2,2-dimethyl-[1,3]dioxane)-pyridine-2,6 diamine (93)
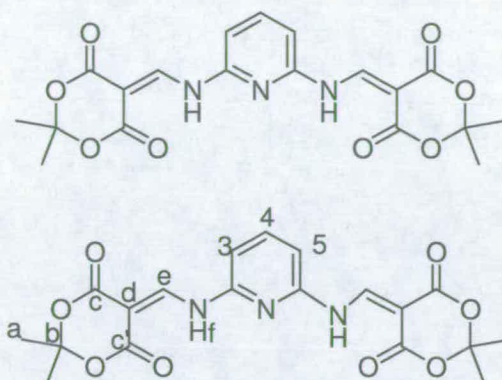
To a stirred solution of methoxymethylene Meldrum's acid **79**, (1.86 g, 10 mmol) in anhydrous acetonitrile (15 cm^3) was added 2,6-diaminopyridine (0.55 g, 5 mmol). The mixture was stirred at room temperature for 5 h (TLC, 1% MeOH in CHCl$_3$). The white precipitate was filtered and dried in oven to give **93** (2.04 g, 98%) as a white solid, mp 244-254 °C. ^{1}H NMR (400 MHz, CDCl$_3$) δ ppm 11.38 (d, $J_{f,e}$ = 13.4 Hz, 2H, $\underline{H}_f$-), 9.25 (d, $J_{e,f}$ = 13.4 Hz, 1H, $\underline{H}_e$-), 7.82 (t, $J_{4,3}$ = 7.8 Hz, 1H, $\underline{H}_4$-) 6.90 (d, $J_{3,4}$ = 7.8 Hz, 2H, $\underline{H}_3$-) and 1.77 (s, 12H, $\underline{H}_a$-); ^{13}C NMR (100 MHz, CDCl$_3$) δ ppm 165.6 ($\underline{C}_{c'}$), 165.5 ($\underline{C}_c$), 162.0 ($\underline{C}_5$), 151.2 ($\underline{C}_e$), 149.3 ($\underline{C}_2$), 142.0 ($\underline{C}_4$), 109.5 ($\underline{C}_3$), 105.5 ($\underline{C}_b$), 90.1 ($\underline{C}_d$), 27.2 ($\underline{C}_a$); FAB-MS *m/z* 418 (M+1, 1%). Found C, 54.35; H, 4.6; N, 9.75. C$_{19}$H$_{19}$N$_3$O$_8$ requires: C, 54.65; H, 4.6; N, 10.05%.

5H-1,4a,5-Triazaphenanthrene-4,8-dione (94)
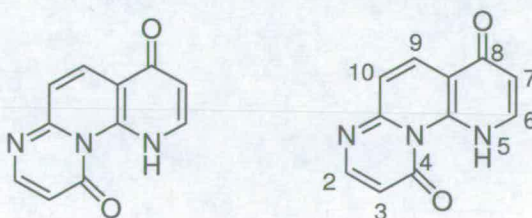
To a boiling solution of Dowtherm^{99} (Ph$_2$O and Ph$_2$) (70 cm^3) was added **93** (0.5 g, 2 mmol). The resulting mixture was boiled at 220 °C for 20 minutes and then filtered;

the product (**94**) was precipitated from the solution with petroleum ether (3 x 50 cm^3). The white precipitate was filtered and dried in an oven to give **94** (0.17 g, 41%), mp 210-218 °C. ^{1}H NMR (400 MHz, CDCl$_3$) δ ppm 14.36 (b, 1H, $\underline{H}_5$-), 8.26 (d, $J_{2,3}$ = 6.3 Hz, 1H, $\underline{H}_2$-), 8.27 (d, $J_{9,10}$ = 9.3 Hz, 1H, $\underline{H}_9$-), 7.95 (d, $J_{6,7}$ = 8.2 Hz, 1H, $\underline{H}_6$-), 7.31 (d, $J_{10,9}$ = 9.3 Hz, 1H, $\underline{H}_{10}$-), 6.53 (d, $J_{3,2}$ = 6.3 Hz, 1H, $\underline{H}_3$-) and 6.35 (d, $J_{7,6}$ = 8.2 Hz, 1H, $\underline{H}_7$-); ^{13}C NMR (100 MHz, CDCl$_3$) δ ppm 175.4 ($\underline{C}_4$), 165.7 ($\underline{C}_8$), 158.1 ($\underline{C}_{10a}$), 154.8 ($\underline{C}_2$), 152.0 ($\underline{C}_{4a}$), 134.6 ($\underline{C}_6$), 133.8 ($\underline{C}_9$), 120.8 ($\underline{C}_{8a}$), 114.7 ($\underline{C}_{10}$), 109.6 ($\underline{C}_7$), 108.6 ($\underline{C}_3$); FAB-MS *m/z* 214 (M+1, 17%). Found C, 62.1; H, 3.6; N, 19.95.C$_{11}$H$_7$N$_3$O$_2$ required: C, 62.0; H, 3.3; N, 19.7%.

### *N,N'*-Bis(5-methylene-4,6-diketo 2,2-dimethyl-[1,3]dioxane)-pyrimidine-2,6-diamine (95)
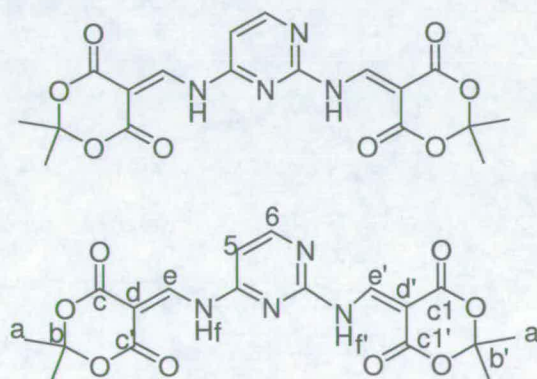
To a stirred solution of methoxymethylene Meldrum's acid **79**, (1.86 g, 10 mmol) in anhydrous acetonitrile (15 cm^3) was added 2,4-diaminopyrimidine (0.55 g, 5 mmol). The mixture was stirred at room temperature for 5 h (TLC, 1% MeOH in CHCl$_3$). The white precipitate was filtered and dried in oven to give **95** (1.32 g, 63% as a white solid), mp 194-196 °C. ^{1}H NMR (400 MHz, CDCl$_3$) δ ppm 11.29 (d, $J_{f,e'}$ = 12.9 Hz, 2H, $\underline{H}_{f'}$-), 11.20 (d, $J_{f,e}$ = 13.3 Hz, 1H, $\underline{H}_f$-), 9.33 (d, $J_{e',f'}$ = 12.9 Hz, 2H, $\underline{H}_{e'}$-), 9.27 (d, $J_{e,f}$ = 13.3 Hz, 1H, $\underline{H}_e$-), 8.57 (d, $J_{6,5}$ = 5.4 Hz, 1H, $\underline{H}_6$-), 6.82 (d, $J_{5,6}$ = 5.4 Hz, 1H, $\underline{H}_5$-) and 1.77 (s, 12H, $\underline{H}_a$-); ^{13}C NMR (100 MHz, CDCl$_3$) δ ppm 165.1 ($\underline{C}_{c1'}$), 164.5 ($\underline{C}_{c1}$), 162.6 ($\underline{C}_{c'}$),162.0 ($\underline{C}_c$),160.6 ($\underline{C}_6$), 158.0 ($\underline{C}_{5a}$), 157.4 ($\underline{C}_{7a}$), 151.6

($\underline{C}_{e'}$), 150.0 ($\underline{C}_e$), 105.9 ($\underline{C}_{b'}$), 105.7 ($\underline{C}_5$), 105.5 ($\underline{C}_b$), 92.5 ($\underline{C}_{d'}$), 91.5 ($\underline{C}_d$), 27.3 ($\underline{C}_{a'}$) and 27.3 ($\underline{C}_a$). EI-MS m/z 418 (M$^+$, 2%), 214 (31), 186 (38) and 43 (100). Found C, 51.1; H, 4.3; N, 13.35. $C_{18}H_{18}N_4O_8$ requires: C, 51.68; H, 4.34; N, 13.39%.

1,4a,5,8a-Tetraazaphenanthrene-4,8-dione (96)
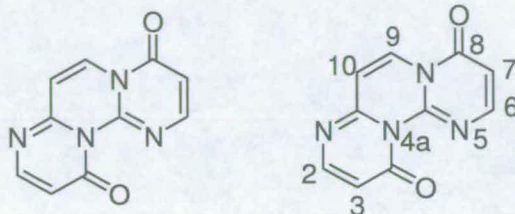
To a boiling solution of Dowtherm[99] (Ph$_2$O and Ph$_2$) (70 cm^3) was added (**95**) (0.5 g, 2.3 mmol). The resulting mixture was boiled under reflux at 220 °C for 20 minutes and then filtered; the product (**96**) was precipitated from the solution with petroleum ether. The crude product was washed 3-5 times with ether (50 cm^3 total). The white precipitate was filtered and dried in an oven to give **96** (0.03 g, 7%). ^{1}H NMR (400 MHz, CDCl$_3$) δ ppm 8.94 (d, $J_{2,3}$ = 8.1 Hz, 1H, $\underline{H}_2$-), 8.05 (d, $J_{6,7}$ = 6.7 Hz, 1H, $\underline{H}_6$-), 7.84 (d, $J_{9,10}$ = 6.8 Hz, 1H, $\underline{H}_9$-), 6.7 (d, $J_{3,2}$ = 8.1 Hz, 1H, $\underline{H}_3$-), 6.45 (d, $J_{10,9}$= 6.8 Hz, 1H, $\underline{H}_{10}$-) and 6.42 (d, $J_{7,6}$= 6.7 Hz, 1H, $\underline{H}_7$-); ^{13}C NMR (100 MHz, CDCl$_3$) δ ppm 186.9 ($\underline{C}_4$), 175.5 ($\underline{C}_8$), 158.0 ($\underline{C}_{10a}$), 152.4 ($\underline{C}_2$), 151.1 ($\underline{C}_6$), 150.4 ($\underline{C}_{4a}$), 128.6 ($\underline{C}_9$), 120.8 ($\underline{C}_{10}$), 114.7 ($\underline{C}_9$), 112.1 ($\underline{C}_7$) and 111.1 ($\underline{C}_3$); EI-MS m/z 214 (M$^+$, 19%), 213 (100), 185 (51) and 145 (59).

2,2-Dimethyl-5-(methylsulfanyl)-5-[(pyrimidin-2-ylamino)-methylene]-[1,3]dioxane-4,6-dione (99)
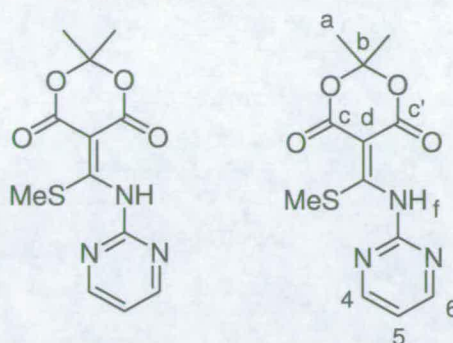
To a stirred solution of 5-(bis-methylsulfanylmethylene)-2,2-dimethyl-[1,3]dioxane-4,6-dione **80**,[101] (0.40 g, 1.78 mmol) in anhydrous acetonitrile (15 cm^3) with 1 drop of DMF, was added 2-aminopyrimidine (0.16 g, 1.78 mmol). The reaction was allowed to stir for 24 h at reflux; the solvent was removed under reduced pressure and the residual oil was purify by chromatography on silica gel using a solvent gradient of CHCl$_3$ to CHCl$_3$/methanol (10%) as eluent to obtain (**99**) as a yellow solid in a yield of 6%, mp 213-214 °C. ^{1}H NMR (400 MHz, CDCl$_3$) δ ppm 13.02 (br. s, 1H, $\underline{H}_f$-), 8.70 (d, $J_{4,5}$ = 4.8 Hz, 2H, $\underline{H}_4$ and $\underline{H}_6$-), 7.13 (d, $J_{5,4}$ = 4.8 Hz, 1H, $\underline{H}_5$-), 2.45 (s, 3H, $\underline{H}_{SMe}$-) and 1.78 (s, 1H, $\underline{H}_a$-); ^{13}C NMR (100 MHz, CDCl$_3$) δ ppm 178.8 ($\underline{C}_e$-), 164.7 ($\underline{C}_{c'}$-), 164.2 ($\underline{C}_c$-), 158.2 ($\underline{C}_4$-), 156.8 ($\underline{C}_g$-), 117.4 ($\underline{C}_5$-), 103.4 ($\underline{C}_b$-), 90.2 ($\underline{C}_d$-), 20.2 ($\underline{C}_a$-) and 16.6 ($\underline{C}_{SMe}$). EI-MS m/z 295 [(M-C$_2$H$_5$O)$^+$, 45%)], 212 (91), 159 (25), 79 (56), 41 (100). (Found C, 49.3; H, 4.15; N, 14.8; C$_{12}$H$_{13}$N$_3$O$_4$S requires: C, 48.8; H, 4.4; N, 14.2%).

2-Methylsulfanylpyrimido[1,2-*a*]pyrimidin-4-one (100)
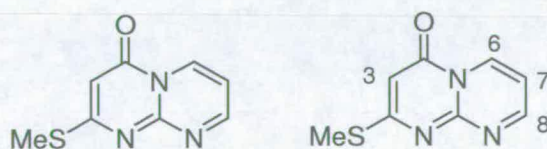
FVP of (**99**) (0.050 g, T_f = 600 °C, T_i = 180 °C, P = 1.5 x 10^{-3} Torr, t = 10 min) produced **100** in 80% yield. Compound **99** was recrystallised from acetonitrile (0.026 g), white solid after recrystallisation and characterized by its ^{1}H NMR spectrum. ^{1}H NMR (400 MHz, CDCl$_3$) δ ppm 9.26 (d, $J_{6,7}$ = 7.1 Hz, 1H, H$_6$-), 9.01 (d, $J_{8,7}$ = 3.8 Hz, 1H, $\underline{H}_8$-), 8.58 (d, $J_{3,a}$ = 4.8 Hz 1H, $\underline{H}_3$-), 7.13 (d, $J_{7,6}$ = 7.1 Hz, $J_{7,8}$ = 3.8 Hz 1H, $\underline{H}_7$-) and 2.21 (s, 3H, $\underline{H}_a$-).

5-[(6-Aminopyridin-2-ylamino)-5-[methylsulfanyl-methylene]-2,2-dimethyl-[1,3]dioxane-4,6-dione (101)
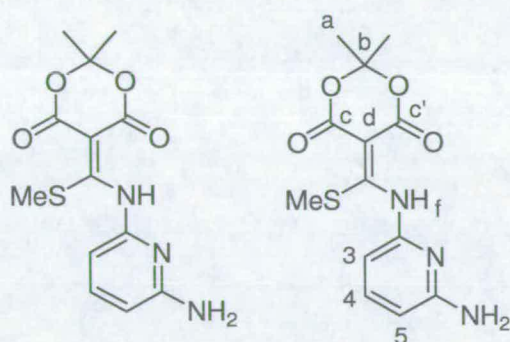
To a stirred solution of **80** (0.5 g, 2.01 mmol) in anhydrous acetonitrile (15 cm^3) was added 2,6-diaminopyrimidine (0.22 g, 2.01 mmol). The reaction was allowed to stir for 2 h at reflux; the solvent was removed under reduced pressure and the residual oil was purify by chromatography on silica gel using a solvent gradient of CHCl$_3$ to CHCl$_3$/methanol (10%) as eluent to obtain **101** (0.063 g, 10%) as a yellow solid, mp 166-168 °C. ^{1}H NMR (400 MHz, CDCl$_3$) δ ppm 12.99 (br. s, 1H, $\underline{H}_f$-), 7.51 (t, $J_{4,5}$ = 7.6 Hz, $J_{4,3}$ = 8.1 Hz, 1H, $\underline{H}_4$-), 6.60 (d, $J_{5,4}$ = 7.6 Hz, 1H, $\underline{H}_5$-), 6.39 (d, $J_{3,4}$ = 8.1 Hz, 1H, $\underline{H}_3$-), 4.56 (br. s, 2H, N$\underline{H}_2$-) 2.35 (s, 3H, $\underline{H}_{SMe}$-) and 1.76 (s, 3H, $\underline{H}_a$-); ^{13}C NMR (100 MHz, CDCl$_3$) δ ppm 178.0 ($\underline{C}_e$) 163.9 ($\underline{C}_{c'}$), 157.8 ($\underline{C}_c$), 157.8 ($\underline{C}_6$), 149.0 ($\underline{C}_2$), 139.9 ($\underline{C}_4$), 107.1 ($\underline{C}_5$), 106.3 ($\underline{C}_3$), 103.1 ($\underline{C}_b$), 87.4 ($\underline{C}_d$), 26.5 ($\underline{C}_a$), 19.7 ($\underline{C}_g$). FAB MS m/z 310 (M+1, 17%). (Found C, 50.7; H, 4.85; N, 13.0; C$_{13}$H$_{15}$N$_3$O$_4$S requires: C, 50.5; H, 4.9; N, 13.6%).

5-(Amino-5-methylsulfanylmethylene)-2,2-dimethyl-[1,3]dioxane-4,6-dione (102)
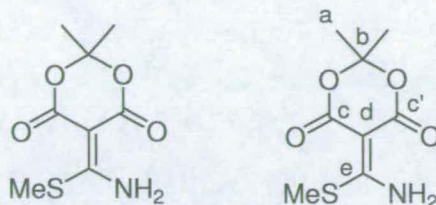
To a stirred solution of **80** (0.30 g, 1.4 mmol) in anhydrous ethanol (15 cm^3) was added ammonium benzoate (0.17 g, 1.4 mmol). The reaction was allowed to stir for 4 h at reflux. The precipitate was filtered and recrystallised to give **102** (0.17 g, 55%) as a yellow solid, mp 216 °C. ^{1}H NMR (400 MHz, CDCl$_3$) δ ppm 11.04 (br. s, 1H, N$\underline{H}$-), 6.31 (br s, 1H, N$\underline{H}$'-), 2.42 (s, 3H, $\underline{H}_{SMe}$-) and 1.71 (s, 3H, $\underline{H}_a$-). ^{13}C NMR (100 MHz, CDCl$_3$) δ ppm 177.7($\underline{C}_e$), 165.6 ($\underline{C}_{c1}$), 163.1 ($\underline{C}_c$), 103.4 ($\underline{C}_b$), 84.3 ($\underline{C}_d$), 26.5 ($\underline{C}_a$) and 13.4 ($\underline{C}_{SMe}$). EI-MS *m/z* 217 (M$^+$, 67%), 160 (62), 115 (82), 87 (75) and 68 (100). Found C, 45.2; H, 5.15; N, 6.4; C$_8$H$_{11}$NO$_4$S requires: C, 44.2; H, 5.1; N, 6.45%.

Details of X-ray Crystal Structure Determination

X-ray crystallographic data for compound 86a:

$C_{11}H_{12}N_4O_4$, M_r=264.24, colourless rod of dimensions 0.91×0.22×0.18 mm, monoclinic, p21, a= 7.081(1), b= 14.500(2), c= 11.9556(18) Å; β=103.689(3)°, V= 1192.7(3) Å^3, ρ_{calcd}=1.471 Mg/m^3, Z=4; λ=0.71073 Å, T=150(2) K, 7518 reflection measurements, 2917 unique. The structure was solved and refined using Direct (Sir92) program to yield final residuals R= 0.04086 and Rw= 0.1005. All hydrogen atoms on carbon atoms were placed in rigid fixed geometries.

X-ray crystallographic data for compound 91:

$C_{12}H_{13}N_3O_4$, M_r=263.25, colourless chip of dimensions 0.97×0.55×0.39 mm, monoclinic , p21; a= 5.2532(7), b= 11.7017(16), c= 10.2904(14) Å; β=102.686(9)°, V= 617.12(15) Å^3, ρ_{calcd}=1.417 Mg/m^3, Z=2; λ=0.71073 Å, T=150(2) K, 7231 reflection measurements, 1576 unique. The structure was solved and refined using SHELXL-86 program to yield final residuals R= 0.0486 and Rw= 0.1350. All hydrogen atoms on carbon atoms were placed in rigid fixed geometries.

X-ray crystallographic data for compound 102:

$C_8H_{11}NO_4S$, M_r=217.25, yellow block of dimensions 0.59×0.52×0.40 mm, triclinic , p-1; a= 5.8088(6), b= 7.1597(8), c= 11.1690(12) Å; β=90.703(2)°, V= 463.06(9) Å^3, ρ_{calcd}=1.558 Mg/m^3, Z=2; λ=0.337 Å, T=150 K, 4289 reflection measurements, 2221 unique. The structure was solved and refined using CRYSTALS program to yield final residuals R= 0.0311 and Rw= 0.0849.

Chapter 3:   Synthesis of multiple hydrogen bonded systems using Buchwald-Hartwig coupling chemistry
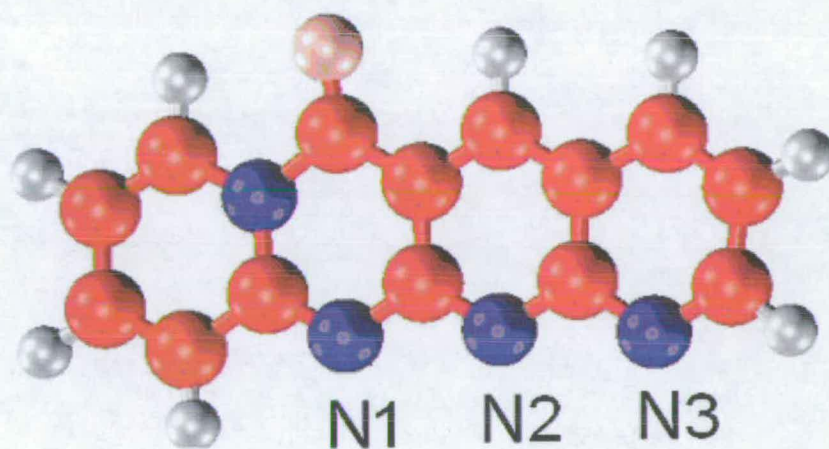
Molecular model of compound 110

3.1 Introduction

In chapter 2 the synthesis of naphthyridine model systems using the flash vacuum pyrolysis (FVP) technique as a new synthetic strategy was described. This technique was applied for the synthesis of heterocycles with anthyridine and naphthacene skeletons but due to problems of involatility of the pyrolysis precursors a different approach was required. The systems represented in Scheme 2.1 remain as targeted compounds but particular attention has been directed towards heterocycles with three **70** and four **71** annelated pyridine rings: anthyridines and naphthacenes. In this chapter we aimed primarily at anthyridine systems employing Buchwald-Hartwig coupling chemistry.
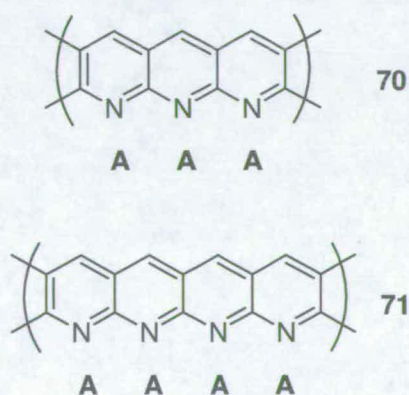
Scheme 3.1 Targeted hydrogen bonded systems.

3.1.1 Anthyridines in literature

Interestingly very few compounds containing the anthyridine heterocyclic system of **70** (Scheme 3.1) have been reported[40, 53, 105] and there are no examples of tetraazanaphthacenes (**71**) in the recent literature. The first example of the 1,9,10-anthyridine parent compound was reported by Carboni and Settimo in 1970 using the

Ullmann reaction between 2,6-diaminopyridine and 2-bromonicotinic acid.[105] A new synthetic strategy to approach the anthyridine skeleton using the Friedlander condensation of 2,6-diaminopyridine-3,5-dicarboxaldehyde and ketones was introduced 7 years later by Caluwe and Majewicz[53] as outlined in Scheme 3.2.
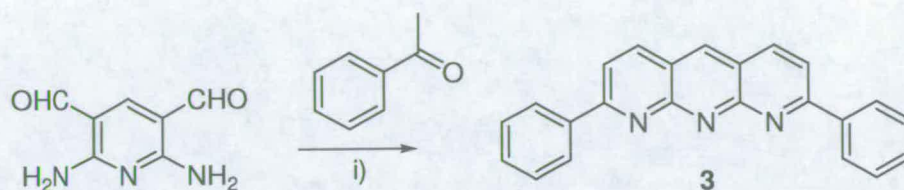
Scheme 3.2 Synthesis of **3** using Caluwe and Majewicz[53] strategy; i) EtOH, KOH, 85%.

The 2,8-diphenyl-1,9,10-anthyridine **3** was the most widely used in binding studies experiments[15] although a few other 1,9,10-anthyridine based compounds were synthesised by the same principle.[53] Therefore some of the chemical properties of **3** will be addressed taking into account some of the findings discovered during binding studies.

3.1.2 Chemical properties of 2,8-diphenyl-1,9,10-anthyridine (3)

The chemical properties of compound **3** were outlined by the authors[105] highlighting the instability of the central ring in all 1,9,10-anthyridine based compounds. They found that compound **3** can be easily reduced to 5,10-dihydroanthyridines **37** by hydride transfer from the solvent and spontaneously oxidised to 1,9,10-anthyridone **35** at room temperature and atmospheric conditions[106] as shown in Scheme 3.3.
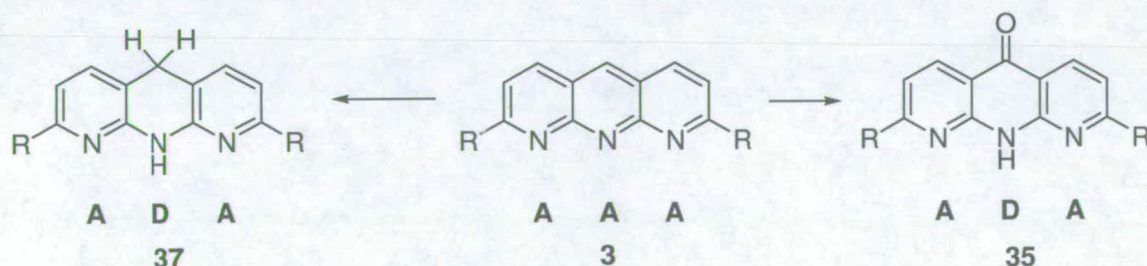
Scheme 3.3 Stability issues of **3**.

Obviously these transformations were very problematic, especially in binding studies where the binding surface is changed from the most favourable AAA to the least favourable ADA arrangement.

This problem has been recognised by Murray and Zimmerman.[40] During binding studies of 2,8-diphenyl-1,9,10-anthyridine **3** with 1,4-dihydro-2,6-diaminopyridines **1** the complex formed was unstable in the presence of acid undergoing clean hydride transfer from C4 of **3** to C10 of **1** (Scheme 3.4).
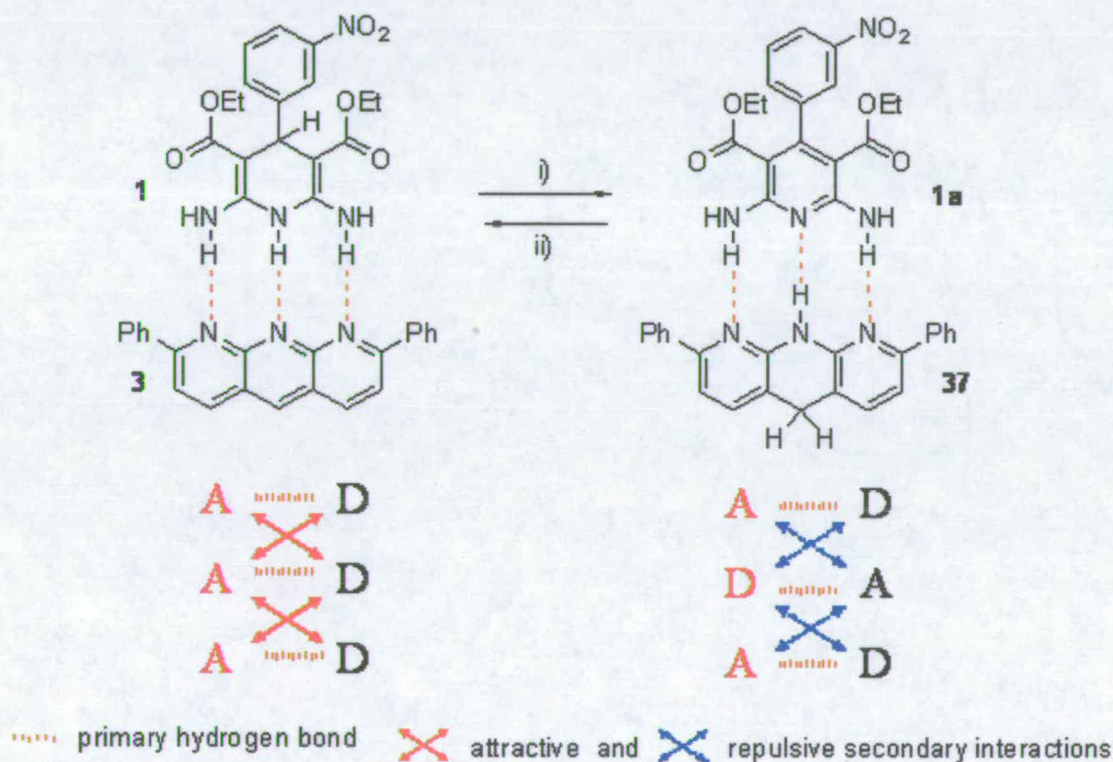
Scheme 3.4 i) chloroform-*d*, ii) 1,8-bis(dimethylamino)naphthalene.

In order to complete complexation studies they used 1,8-bis(dimethylamino)-naphthalene (proton sponge) to neutralise acid from solution and prevent the hydride shift happening. The binding constants have been determined in its presence.

Later publications by Murray and Zimmerman[40] tackle this issue and the synthesis of 5-arylanthyridines was undertaken in order to inhibit reduction of the central ring. Two approaches were developed, the first of which was analogous to the Caluwe

approach. This route required 2,6-diamino-4-phenylpyridine-3,5-dicarboxaldehyde **103**[40] in the double Friendlander condensation (Scheme 3.5) using a wide range of ketones to form anthyridines **3a-3g** directly.
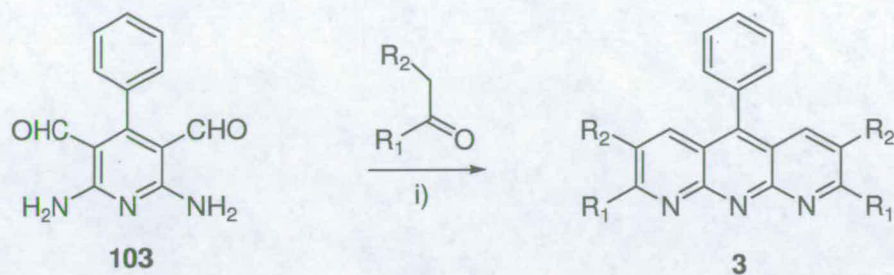
Compound	R$_1$	R$_2$	Yield
3a	Ph	H	85%
3b	2-pyridyl	H	88%
3c	6-Br-2-pyridyl	H	66%
3d	2-thienyl	H	70%
3e	4-Br-2-thienyl	H	41%
3f	Me	H	72%
3g	Pr	Et	54%

Scheme 3.5 Synthesis of 5-arylanthyridines **3a-3g** using the first approach.[40] i) EtOH, KOH.

The second approach to synthesise 5-arylanthyridines involved the addition of an aryl Grignard reagent to a 5-unsubstituted anthyridine.[40] 4-Trimethylsilylphenyl magnesium bromide reacted with **3** to form anthyridan **104** (Scheme 3.6) and its oxidation with DDQ produced anthyridine **3h** in high yield.
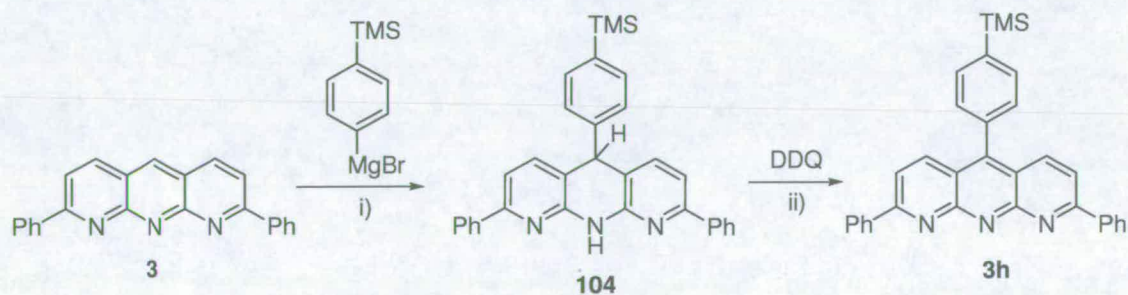
Scheme 3.6 Synthesis of 5-arylanthyridine **3h** using the second approach.[40] i) THF, 66%; ii) dioxane, 90%.

Taking into account both approaches, the total synthesis of 5-arylated anthyridines required five steps and interestingly none of these compounds has been used in binding model studies although they were reported to be much more stable in AAA-DDD heterocomplexes.

The target of the present work was to prepare stable anthyridine derivatives with less synthetic steps involved. Herein we describe an attempt to implement this synthetic strategy (Scheme 3.7) using palladium catalyzed Buchwald-Hartwig coupling reactions followed by rearrangement and rearomatisation.
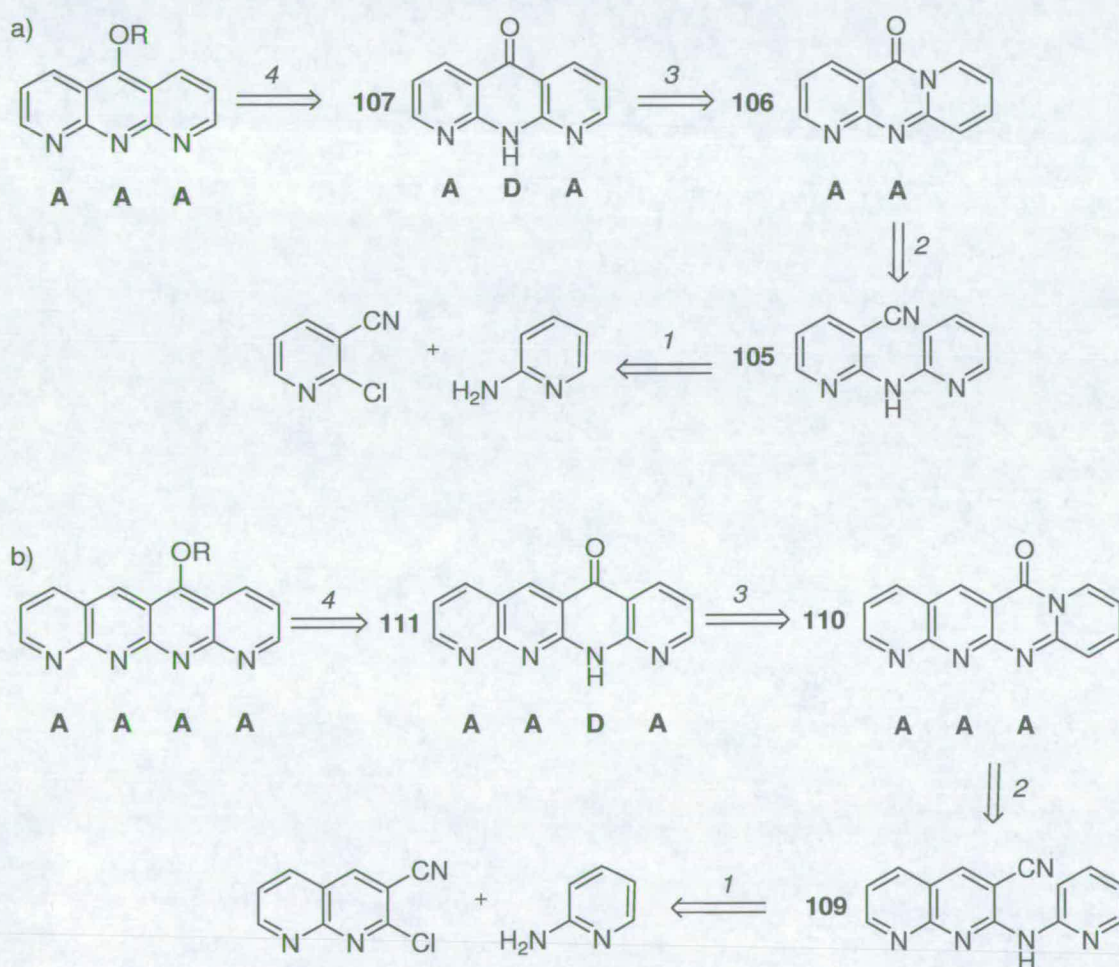
Scheme 3.7 Synthetic strategy of a) anthyridine in AAA and b) naphthacene model system in AAAA arrangement.

The first step (*1*) in both synthetic strategies involves a palladium catalyzed coupling of the heterocyclic diarylamine **105** or **109**.[107] Step *2* uses the ring closure of heterocyclic diarylamines under acidic conditions as seen in similar literature examples[108] to obtain **106** (AA) or **110** (AAA) hydrogen bonded modules. If this part of synthetic strategy was to be successful the AA hydrogen bonding unit could be prepared in only two steps and AAA unit in four synthetic steps.

Further possibilities are to employ FVP technique as in step *3*, using the thermal electrocyclisation to form products **107** (ADA) and **111** (AADA). The analogous transformation was elaborated in Chapter 2 together with the final rearomatisation (step *4*).

3.2 Results and discussion

The synthesis of heterocyclic diarylamine **105** and **109** involved palladium catalyzed coupling of, commercially available, 2-aminopyridine with 2-chloro-3-cyanopyridine or 2-chloro-3-cyano-1,8-naphthyridine[107] precursors (Scheme 3.8).
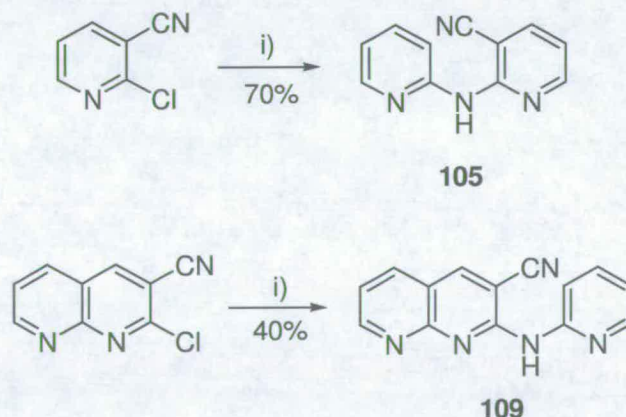
Scheme 3.8 Conditions and reagents: i) 2-aminopyridine, Pd(OAc)$_2$, BINAP, K$_2$CO$_3$, toluene under reflux.

When the 2-chloro-3-cyanopyridine or 2-chloro-3-cyano-1,8-naphthyridine[107] precursors were refluxed in DMF for 3-5 days with 2-aminopyridine, no products were formed. The reason is the poor nucleophilicity of the amine precursors and

therefore the palladium catalyzed carbon-nitrogen coupling reaction was employed to make the reaction work.

Buchwald and Hartwig[109] reported a C-N biaryl coupling reactions by use of bidentate phosphine ligands (BINAP and _etc._)[110, 111] and catalyst (Pd(OAc)$_2$ or Pd$_2$(dba)$_3$) loadings of typically 0.5-1.0 mol% to accelerate the reactions. The reaction conditions using Pd(OAc)$_2$/BINAP coupling agents have been successfully applied for the synthesis of compounds **105** and **109**. Products have been obtained in 70% for **105** and 40% for **109**.

Compounds **105** and **109** showed correct molecular ions in their mass spectra and characteristic NH signals in the range of δ_H 8.5-9.4 ppm depending on the solvent present indicating coupling product. (See experimental section).

Since 1998, major improvement in scope and yields in this area have been described by a number of research groups and the method has been widely used in synthesis of biaryl heterocyclic systems.[112-114] In our case when different reaction conditions were used as for example Pd$_2$(dba)$_3$ /Xantphos[115] no significant difference in product yields were found.

The cyclisation step to obtain **106** and **110** (Scheme 3.9) involved heating of **105** and **109** in polyphosphoric acid (PPA) for 5 h and the products were obtained without requiring further purification and in high yields (>85%).
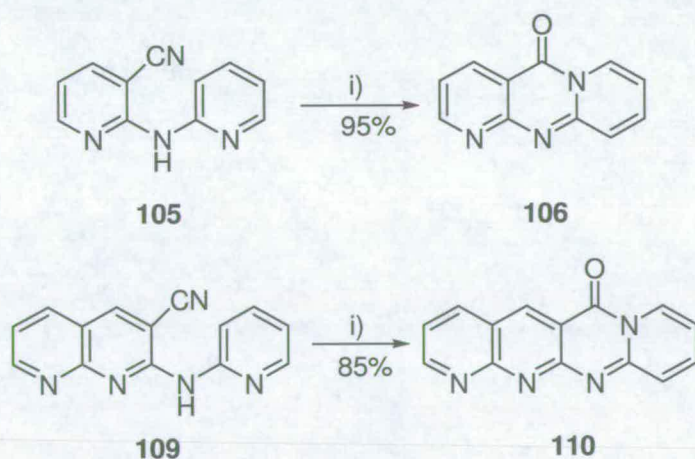
Scheme 3.9 Conditions and reagents: i) polyphosphoric acid.

The constitution of compounds **106** and **110** has been confirmed by the presence of the correct molecular ions in their mass spectra and, in the ^{13}C NMR spectra, a

characteristic carbonyl signal at δ_C 159.2-159.7 ppm. Additional conformation that cyclisation takes place was obtained from their fluorescence in the excited state with λ_{max} at 430 nm for compound **106** and 518 nm for compound **110** (see Appendix).

Use of PPA or paraffin oil in thermal reactions was described in 1984 by Kalinowski and coworkers[116] involving the temperatures ranging from 160-330 °C. Heating compounds in PPA was used to form different heterocyclic products that easily separated from the reaction mixture. In 1987 the synthesis of partially saturated dipyridopyrimidinones, analogous to **106**, have been reported by Fulop and coworkers.[108]

The mechanism of the acid catalyzed cyclisation step to afford products **106** and **110** involves hydrolysis of the nitrile group in the first stage, cyclisation onto the nitrogen followed by dehydration. A controlled temperature of 150 °C and a reaction time of only a few hours in both cases gave the best yields. Prolonged reaction time (overnight) and higher temperatures induced ring opening of **106** and **110** and formation of heterocyclic diarylamine carboxylic acids.

Compound **110** is a novel example of an AAA system, obtained in 85% overall yield in four steps from commercially available precursors. Binding studies with counterpart DDD will be discussed in Chapter 5.

As mentioned in Chapter 2 a novel rearrangement route from pyridopyrimidin-4-ones **77** to 1*H*-naphthyridin-4-one **78** in the gas phase was discovered, therefore we investigated this option on our present systems **106** and **110** (Scheme 3.10).
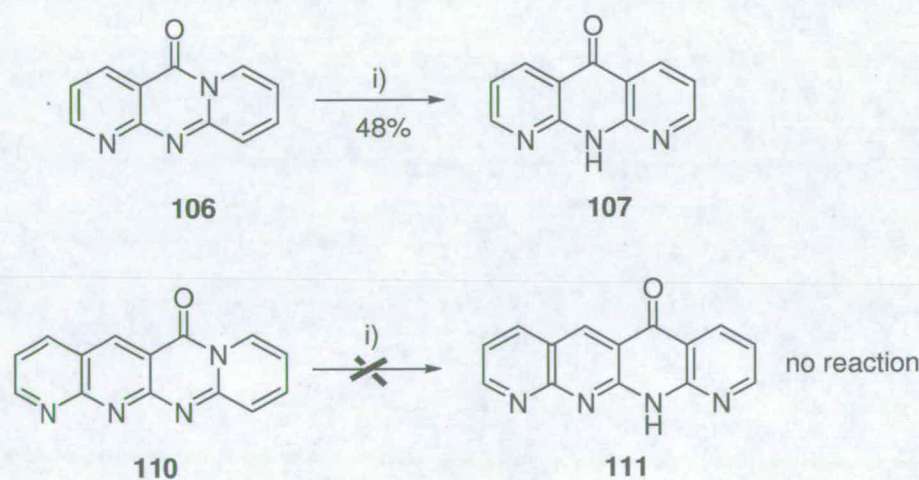
Scheme 3.10 FVP conditions i) $T_f = 980$ °C (with silica wool), $T_i = 300$ °C, p = 2 × 10^{-3} Torr, 20 min.

The first attempt to pyrolyse **106** at 980 °C gave a low conversion (20%) to the product **107**. In order to improve conversion to **107** two options were available, increasing the furnace temperature or increasing the contact time. An increase in furnace temperature was not very practical due to decomposition of vacuum grease and loss of pressure.[117] Increase of contact time can be achieved by inserting silica tubes (which did not have a great effect) or placing a loose plug of silica wool at the exit point of the furnace tube.[117] That gave satisfactory conversion of 48% but another product **108** was formed due to decarbonylation.

It was of interest to perform an experiment following the transformation of compound **106** to **107** as a function of temperature, observing the formation of the **108** side product. The amounts of **106** and **107** were measured in the product mixture after pyrolysis at various temperatures (Figure 3.1); at 980 °C the ratio was 40:40:20 (**106** → **107** → **108**) with further increase of **108** with temperature rise.
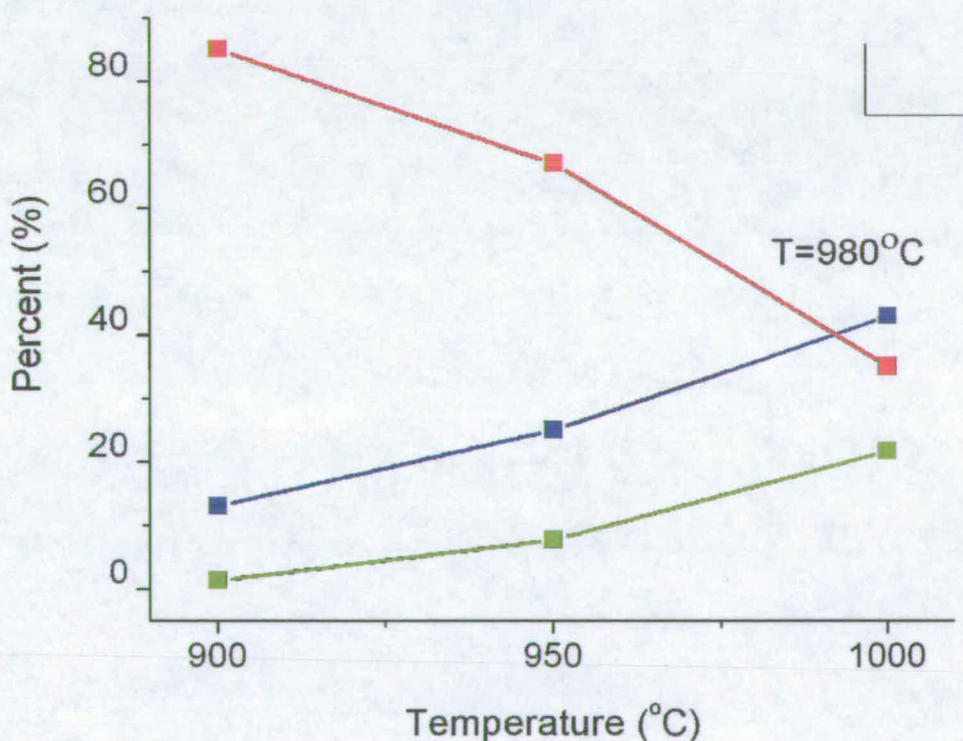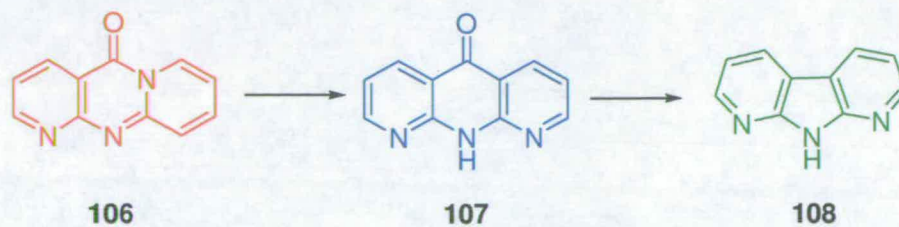
Figure 3.1 Temperature profile for the **106** → **107** → **108** transformation

The general mechanism of the cyclisation process for the **106** → **107** → **108** systems has been outlined in Scheme 3.11. The amide bond of **106** has been broken under FVP conditions by a reverse electrocyclisation forming an iminoketene intermediate which undergoes electrocyclisation and H-shift to form product **107**. The high temperature employed (900-980 °C) allows ring closure onto the C=C bond under thermodynamic control. Thermal decarbonylation affords **108** as seen in some similar literature examples.[118]
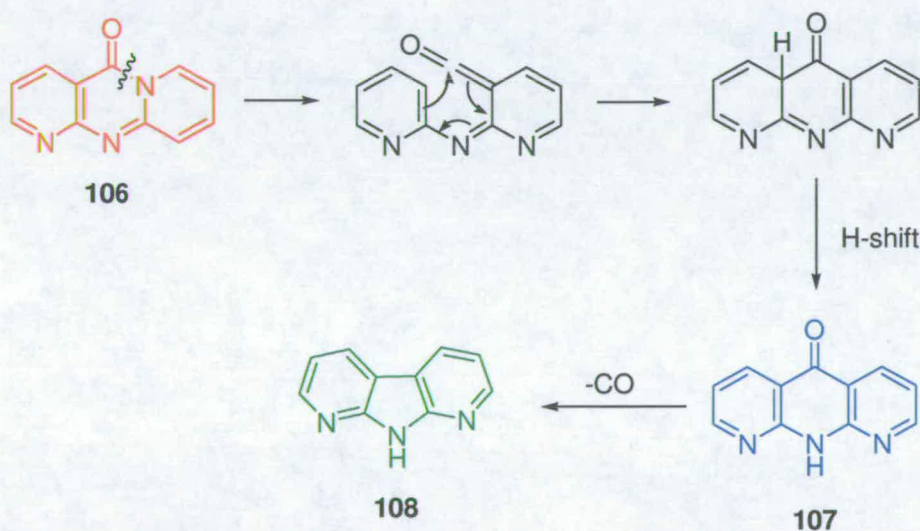
Scheme 3.11 Mechanism of **106** → **107** → **108** cyclisation.

Unfortunately, in the pyrolysis of **110** it was not clear whether or not compound **111** was produced. The crude NMR spectra after pyrolysis indicated new signals but it was not clear if this was due to product formation or to decomposition. The yield was very poor and solubility issues did not allow any further investigations.

It is interesting to compare the temperature trends for the transformation between the present system and the one described in Chapter 2 (Figure 3.2).

a)

$T_f = 880\,°C$

77   **78**

b)

$T_f = 980\,°C$

106   **107**

c)

$T_f = 1080\,°C$

?
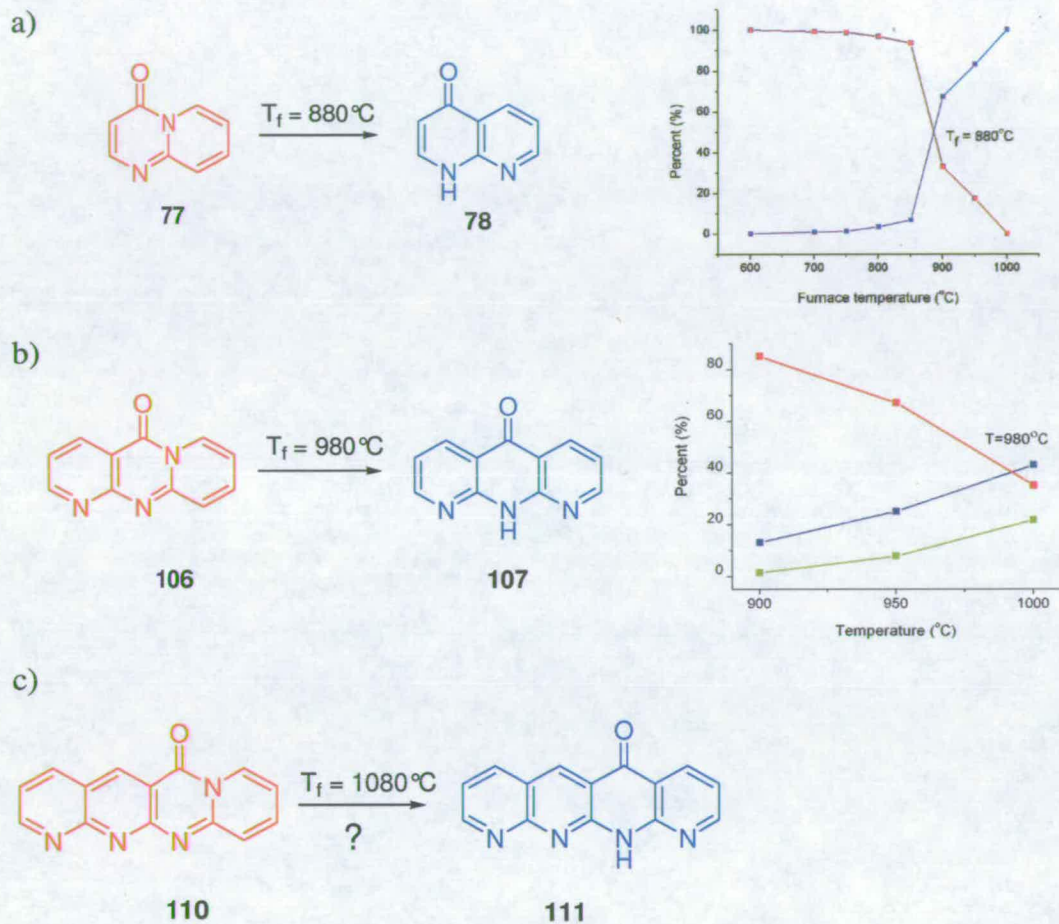
110   **111**

Figure 3.2 Temperature profiles for the a) **77→ 78** (Chapter 1) b) **106 → 107 → 108** (this Chapter) and c) **110→111** transformation.

Exactly 100 °C more was required to get to the 50:50 ratio by adding one more aromatic ring into the system **106→ 107** with **108** as decarbonylation product. Following the same analogy for 50:50 ratio of the **110→ 111** system the temperature of 1080 °C or higher could be required with possibility of more decarbonylation.

3.3 Conclusion

Overall, the Buchwald-Hartwig coupling approach was successful in obtaining the AA and AAA units **106** and **110**. The FVP technique was employed for rearranging compound into ADA unit **107** (Scheme 3.11).
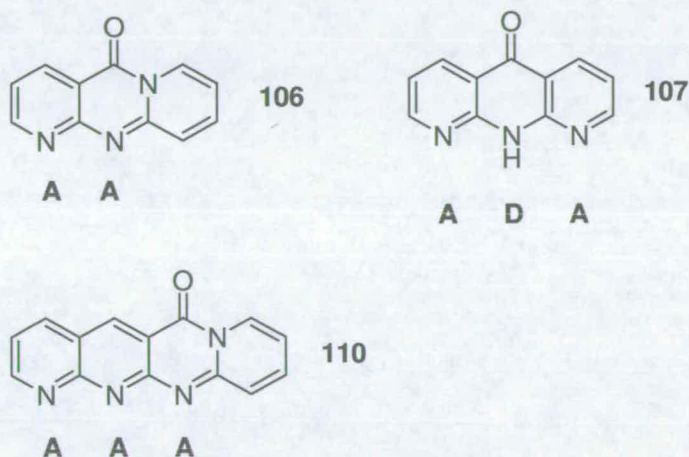
Scheme 3.11 Summary of synthesized compounds.

Limitations in temperature range did not allow successful transformation of compound **110** → **111** and in that respect an initial attempt to generate a tetraaza-naphthacene unit in AAAA arrangement failed. The low yield of **107** and the presence of a side product in crude mixture, made the next rearomatisation step towards AAA unit not practical.

3.4 Experimental section

2-(Pyridin-2-ylamino) nicotinonitrile (105)
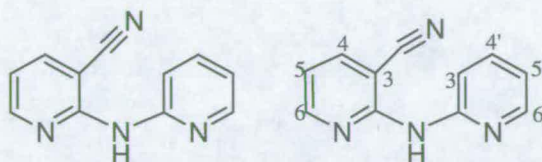
A round bottomed flask was flushed with nitrogen and charged with palladium (II)-acetate (13.5 mg, 0.06 mmol, 2%), (±)-BINAP (37.5 mg, 0.06 mmol, 2%) and toluene (10 cm^3). The mixture was stirred under nitrogen for 10 min. In another round bottomed flask, 2-chloro-3-cyanopyridine (0.41 g, 3 mmol), 2-aminopyridine (0.34 g, 3.6 mmol) and potassium carbonate (8.28 g, 60 mmol) were weighed. Then, the palladium (II)-acetate/BINAP solution was added, and the flask rinsed with an additional portion of toluene (17 cm^3). The resulting mixture was subsequently heated under reflux in an oil bath under nitrogen with vigorous stirring until the starting material had disappeared. After cooling down, the solid material was filtered off and washed with dichloromethane (100 cm^3). The solvent was evaporated and the resulting crude product was purified by recrystallisation using isopropyl alcohol to yield 2-(pyridin-2-ylamino) nicotinonitrile (**105**) (0.42 g, 70%), mp 138-140 °C; ^{1}H NMR (400 MHz, CDCl$_3$) δ ppm 9.06 (d, $J_{3',4'}$= 7.6 Hz , 1H, $\underline{H}_{3'}$-), 8.88 (d, $J_{4,5}$= 4.5 Hz, 1H, $\underline{H}_4$-), 8.50 (br s, 1H, N$\underline{H}$-), 8.21 (d, $J_{6,5}$= 8.3 Hz, 1H, $\underline{H}_6$-), 7.50 (dd, $J_{4',3'}$= 7.6 Hz, $J_{4',5'}$= 6.3 Hz 1H, $\underline{H}_{4'}$-), 7.43 (d, $J_{6',5'}$= 8.8, 1H, $\underline{H}_{6'}$-), 7.26 (dd, $J_{5,6}$= 8.3 Hz, $J_{5,4}$= 4.5 Hz, $\underline{H}_5$-) and 6.78 (t, $J_{5',6'}$= 8.8 Hz, $J_{5',4'}$= 6.3 Hz, 1H, $\underline{H}_{5'}$-). ^{13}C NMR (100 MHz, CDCl$_3$) δ ppm 157.8 ($\underline{C}_2$-), 151.9 ($\underline{C}_4$-), 138.0 ($\underline{C}_{ipso}$-), 135.8 ($\underline{C}_{4'}$-), 133.4 ($\underline{C}_6$-), 127.9 ($\underline{C}_{3'}$-), 126.5 ($\underline{C}_{6'}$-), 119.6 ($\underline{C}_5$-), 115.1 ($\underline{C}_{CN}$-), 112.1 ($\underline{C}_{5'}$-) and 95.0 ($\underline{C}_3$-); EI-MS *m/z* 196 (M$^+$, 64%), 195 (100), 170 (81), 78 (65), 51 (59) 103 (41) and 272 (28). HRMS [M$^+$]: 196.0747, C$_{11}$H$_8$N$_4$ requires: 196.0749.

Dipyrido[1,2-a;2',3'-a] pyrimidin-5-one (106)
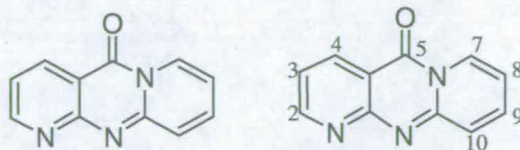
A mixture of 2-(pyridin-2-ylamino)nicotinonitrile (1.28 g, 6.5 mmol) and polyphosphoric acid (10 cm^3) was heated to 150 °C for 5 h. The reaction mixture was cooled, diluted with water and neutralized with 10% NH_3. The water layer was extracted three times with DCM to give **106** (1.0 g, 84%), mp 205-207 °C; ^{1}H NMR (400 MHz, CDCl$_3$) δ ppm 9.11 (d, $J_{4,3}$ =6.5, 1H, $\underline{H}_4$-), 8.88 (d, $J_{7,8}$= 7.7 Hz, 1H, $\underline{H}_7$-), 8.76 (d, $J_{2,3}$ = 7.9 Hz, 1H, $\underline{H}_2$-), 7.71-7.69 (m, 2H, $\underline{H}_9$- and $\underline{H}_{10}$-), 7.41 (d, $J_{3,2}$ = 7.9 Hz, 1H, $\underline{H}_3$-) and 6.98 (t, $J_{8,7}$= 7.7 Hz, $J_{8,9}$= 6.1 Hz, 1H, $\underline{H}_8$-); ^{13}C NMR (100 MHz, CDCl$_3$) δ ppm 159.7 ($\underline{C}_{c=o}$-), 157.8 ($\underline{C}_4$-), 157.4 ($\underline{C}_{4a}$-), 149.8 ($\underline{C}_{10a}$-), 137.0 ($\underline{C}_2$-), 135.7 ($\underline{C}_9$-), 127.0 ($\underline{C}_7$-), 126.7 ($\underline{C}_{10}$-), 120.6 ($\underline{C}_3$-), 113.5 ($\underline{C}_8$-) and 111.3 ($\underline{C}_{2a}$-). EI-MS m/z 197 (M$^+$, 95%), 78 (100), 169 (93), 142 (52), 168 (47) and 143 (44). Found: C, 67.0; H, 3.58 N, 20.5. C$_{11}$H$_7$N$_3$O requires: C, 67.00; H, 3.58; N, 20.31%.

9H-1,8,9-Triaza-anthracen-10-one (107)
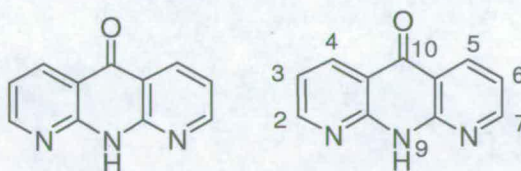
FVP of (**106**) (0.043 g, T_f = 850 °C, T_i = 300 °C, P = 2.0 x 10^{-3} Torr, t = 20 min) produced in a good yield of compound **107** (0.034 g, 70%), mp 305-307 °C [lit.,[104] 320 °C].; ^{1}H NMR (400 MHz, CDCl$_3$) δ ppm 10.17 (s br, 1H, -$\underline{N}$H-) 8.48 (d, $J_{4,3}$= 4.8 Hz, 1H, $\underline{H}_4$-), 8.28 (d, $J_{2,3}$ = 7.8 Hz, 1H, $\underline{H}_2$-) and 7.21 (d, $J_{3,2}$ = 7.8 Hz, $J_{3,4}$ = 4.8 Hz, 1H, $\underline{H}_3$-). ^{13}C NMR (100 MHz, CDCl$_3$) δ ppm 157.9 ($\underline{C}_{c=o}$-), 151.3 ($\underline{C}_{4a}$-), 147.2 ($\underline{C}_2$-), 129.3 ($\underline{C}_4$-), 116.4 ($\underline{C}_3$-) and 114.5 ($\underline{C}_{2a}$-). EI-MS m/z 197 (M$^+$, 40%), 169 (100),

142 (66), 115 (52), 85 (48) and 39 (45). HRMS $[M]^+$: 197.0587, $C_{11}H_7N_3O$ requires: 197.0589.

3-Cyano-1,8-naphthyridin-2-one
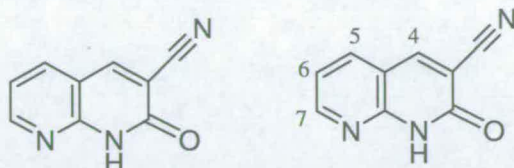
A mixture of 2-aminonicotinaldehyde[119] (2.44 g, 0.02 mol), ethyl 2-cyanoacetate (4.25 g, 0.04 mmol), absolute ethanol (50 ml) and piperidine (0.5 cm^3) was stirred and heated at reflux. After 1 h, the solution was cooled and the precipitate filtered to yield 3-cyano-1,8 naphthyridin-2-one in 73% yield (2.5 g), mp >300°C [lit.,[104]300 °C]; ^{1}H NMR (400 MHz, [D$_6$]DMSO) δ ppm 12.88 (br s, N$\underline{H}$-), 8.88 (s, 1H $\underline{H}_4$-), 8.67 (d, $J_{7,6}$= 4.6 Hz 1H, $\underline{H}_7$-), 8.23 (d, $J_{5,6}$= 4.6 Hz, 1H, $\underline{H}_5$-) and 7.37 (dd, $J_{6,5}$= 7.6 Hz, $J_{6,7}$= 4.6 Hz 1H, $\underline{H}_6$-). ^{13}C NMR (100 MHz, [D$_6$]DMSO) δ ppm 159.5 ($\underline{C}_{c=o}$-), 153.9 ($\underline{C}_4$-), 150.3 ($\underline{C}_{4a}$-), 148.9 ($\underline{C}_7$-), 138.2 ($\underline{C}_5$-), 119.4 ($\underline{C}_6$-), 125.5 ($\underline{C}_{1a}$-), 113.0 ($\underline{C}_3$-) and 107.3 ($\underline{C}_{CN}$-). EI-MS m/z 171 (M$^+$, 23%), 108 (100), 137 (94), 109 (69) and 91 (53). (Found: C, 63.10; H, 3.01; N, 24.76. $C_9H_5N_3O$ requires: C, 63.16; H, 2.95; N, 24.55%).

2-Chloro-3-cyano-1,8-naphthyridine
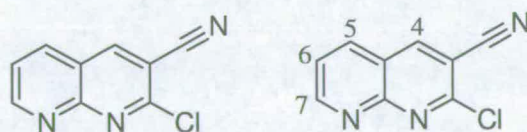
A mixture of PCl$_5$ (12.2 g, 0.06 mmol), POCl$_3$ (44 cm^3), and 3-cyano-1,8-naphthyridin-2-one (2.3 g, 0.013 mmol) was stirred and heated at reflux. After 1 h excess POCl$_3$ was distilled off using Kugelrohr apparatus. The residue was treated with ice, neutralized with solid Na$_2$CO$_3$, and extracted with CHCl$_3$. The organic

extracts were dried, filtered and concentrated to dryness. The residue was sublimed at low pressure (*ca* 0.01 Torr) to yield 2-chloro-3-cyano-1,8-naphthyridine (1.2 g, 81%), mp 300°C [lit.,[104]300 °C]; ^{1}H NMR (400 MHz, [D$_6$]DMSO) δ ppm 9.36 (s, $\underline{H}_4$-), 9.26 (dd, $J_{7,6}$= 4.3 Hz, $J_{7,5}$= 2.0 Hz, 1H, $\underline{H}_7$-), 8.61 (dd, $J_{5,6}$ = 8.1 Hz $J_{5,7}$= 2.0 Hz, 1H, $\underline{H}_5$-) and 7.84 (dd, $J_{6,5}$= 8.1 Hz, $J_{6,7}$= 4.3 Hz, 1H, $\underline{H}_6$-). ^{13}C NMR (100 MHz, [D$_6$]DMSO) δ ppm 157.6 ($\underline{C}_4$-), 154.6 ($\underline{C}_2$-), 150.4 ($\underline{C}_{4a}$-), 148.9 ($\underline{C}_7$-), 138.5 ($\underline{C}_5$-), 124.4 ($\underline{C}_6$-), 120.7 ($\underline{C}_{1a}$-), 115.1 ($\underline{C}_3$-) and 108.0 ($\underline{C}_{CN}$-). EI-MS *m/z* 189 (M$^+$, 100%), 154 (83), 127 (32), 122 (49), 94 (64) and 93 (59). Found: C, 57.10; H, 2.15; N, 19.06. C$_9$H$_4$ClN$_3$ requires: C, 57.01; H, 2.13; N, 18.70%.

2-(Pyridin-2-ylamino)-[1,8]naphthyridine-3-carbonitrile (109)
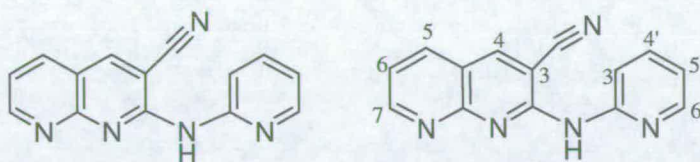
A round bottomed flask was flushed with nitrogen and charged with palladium (II)-acetate (13.5 mg, 0.06 mmol, 2%), (±)-BINAP (37.5 mg, 0.06 mmol, 2%) and toluene (10 cm^3). The mixture was stirred under nitrogen for 10 min. In another round bottomed flask 2-chloro-3-cyano-1,8-naphthyridine (0.41 g, 3 mmol), 2-aminopyridine (0.34 g, 3.6 mmol) and potassium carbonate (8.28 g, 60 mmol) were weighed. Then, the palladium (II)-acetate/BINAP solution was added, and the flask was rinsed with an additional amount of toluene (17 cm^3). The resulting mixture was subsequently heated under reflux in an oil bath under nitrogen with vigorous stirring until the starting material had disappeared. After cooling the solid material was filtered off and washed with dichloromethane (100 cm^3). The solvent was evaporated and resulting crude product was purified by column chromatography (Al$_2$O$_3$-neutral, 70:30 DCM-MeOH) to yield 2-(pyridin-2-ylamino)-[1,8]naphthyridine-3-carbonitrile (**109**) (0.164 g, 40%), mp 189-190 °C; ^{1}H NMR (400 MHz, [D$_6$]DMSO) δ ppm 9.41 (br s, N$\underline{H}$-), 9.06-9.02 (s, 2H, $\underline{H}_4$ and $\underline{H}_5$-), 8.37 (d, $J_{6',5'}$= 6.3 Hz 1H, $\underline{H}_{6'}$-), 8.33 (d,

$J_{7,6}$= 4.1 Hz, 1H, $\underline{H}_{7'}$-), 8.21 (d, $J_{3',4'}$= 7.6 Hz 1H, $\underline{H}_{3'}$-), 7.86 (t, $J_{4',3'}$= 7.6, $J_{4',5'}$= 8.1 Hz, 1H, $\underline{H}_{4'}$-), 7.54 (dd, $J_{6,7}$= 4.1 Hz, $J_{6,5}$= 6.3 Hz 1H, $\underline{H}_{6'}$-), 7.11 (dd, $J_{5',6'}$= 6.3 Hz, $J_{5',4'}$= 8.1 Hz, 1H, $\underline{H}_{5'}$-). ^{13}C NMR (100 MHz, [D$_6$]DMSO) δ ppm 156.3 ($\underline{C}_{5'}$-), 155.2 ($\underline{C}_{2'}$-), 153.3 ($\underline{C}_{4a'}$-), 152.4 ($\underline{C}_{ipso'}$-), 147.8 ($\underline{C}_{4'}$-), 147.0 ($\underline{C}_{7'}$-), 138.1 ($\underline{C}_{6'}$-), 137.8 ($\underline{C}_{3''}$-), 121.0 ($\underline{C}_{5''}$-), 118.9 ($\underline{C}_{4''}$-), 117.1 ($\underline{C}_{1a'}$-), 115.7 ($\underline{C}_{CN'}$-) and 113.6 ($\underline{C}_{6''}$-); EI-MS m/z 247 (M$^+$, 25%), 185 (100), 189 (21) and 186 (16). Found: C, 64.10; H, 3.18; N, 25.76. $C_{14}H_9N_5 \times H_2O$ requires: C, 63.4; H, 4.15; N, 26.4%.

1, 6a,11,12 –Tetraazanaphthacene-6-one (110)
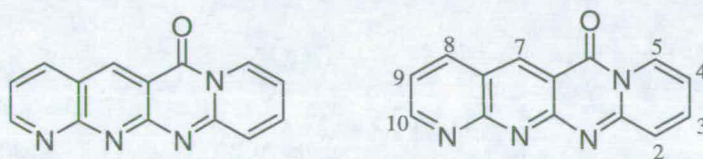
A mixture of 2-(pyridin-2-ylamino)-[1,8]naphthyridine-3-carbonitrile (**109**) (0.16 g, 0.66 mmol) and polyphosphoric acid (5 cm^3) were heated into the liquid at 150 °C for 5 h. The reaction mixture was cooled, diluted with water and neutralized with 10% NH$_3$. The water layer was extracted three times with DCM to give **110** (0.14 g, 85%), mp 300 °C (dec); ^{1}H NMR (400 MHz, CDCl$_3$) δ ppm 9.46 (s, 1H, $\underline{H}_{7'}$-), 9.36 (dd, $J_{8,9}$= 4.0 Hz, $J_{8,10}$= 2.0 Hz 1H, $\underline{H}_8$-), 8.81 (d, $J_{5,4}$ = 7.3 Hz, 1H, $\underline{H}_5$-), 8.42 (dd, $J_{10,9}$= 8.1Hz, $J_{10,8}$= 2.0 Hz 1H, $\underline{H}_{10}$-), 7.68-7.65 (m, 2H, $\underline{H}_2$- and $\underline{H}_3$-) 7.52 (dd, $J_{9,10}$= 8.1Hz, $J_{9,8}$= 4.0 Hz 1H, $\underline{H}_9$-) and 6.93 (t, $J_{4,3}$= 7.8 Hz, $J_{4,5}$= 7.3 Hz, 1H, $\underline{H}_4$-); ^{13}C NMR (100 MHz, CDCl$_3$) δ ppm 160.3 ($\underline{C}_{6a'}$-), 159.2 ($\underline{C}_{c=o'}$-), 158.6 ($\underline{C}_{7'}$-), 157.1 ($\underline{C}_{1a'}$-), 156.2 ($\underline{C}_{11a'}$-), 151.5 ($\underline{C}_{2a'}$-), 142.3 ($\underline{C}_8$-), 138.3 ($\underline{C}_{10}$-), 136.6 ($\underline{C}_3$-), 127.2 ($\underline{C}_5$-), 126.7 ($\underline{C}_2$-), 121.4 ($\underline{C}_9$-), 112.9 ($\underline{C}_4$-) and 112.7 ($\underline{C}_{8a'}$-). EI-MS m/z 248 (M$^+$, 6%), 69 (100), 81 (53), 180 (43), 149 (34), 246 (23). Found: C, 67.24; H, 3.19 N, 21.67. $C_{14}H_8N_4O \times 0.1H_2O$ requires: C, 67.25; H, 3.28; N, 22.41%.

3.5 Appendix

Absorption (blue) and fluorescence (red) spectra of compounds **106** and **110** are represented in Figure A1 and A2.

a)
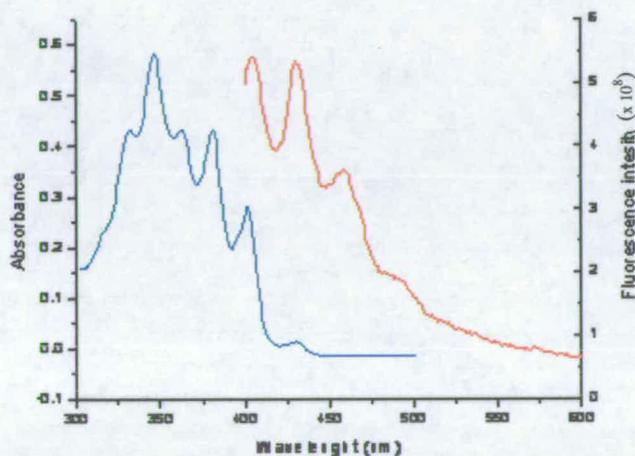
Figure A1. Absorption and fluorescence spectra of **106.**

b)
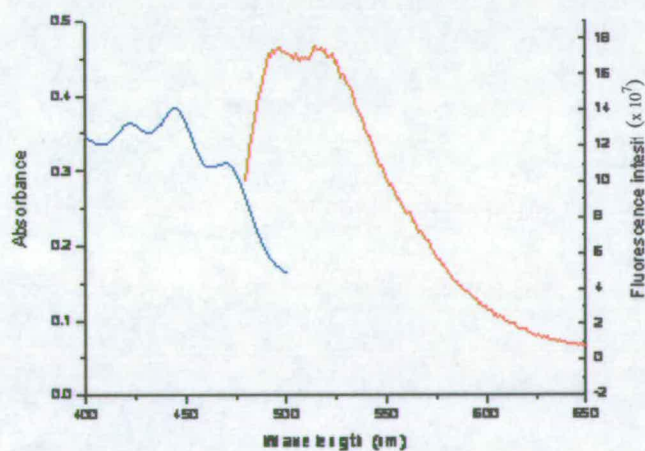
Figure A2. Absorption and fluorescence spectra of **110**.

Compound **106** showed multiple absorption bands with λ_{max} at 341 nm and for **110** λ_{max} was at 445 nm; for fluorescence **106** has λ_{max} at 445 nm and **110** at 518 nm.

Chapter 4: Synthesis of multiple hydrogen bonded systems with extended aromatic framework using Suzuki-coupling chemistry

X-ray "Pringles" packing of 117 compound

4.1 Introduction

In the previous chapter we described the synthesis of anthyridine systems using Buchwald-Hartwig palladium catalyzed coupling chemistry. Using that methodology AA and AAA units were successfully produced in two step syntheses. The only limitations with these systems are the presence of carbonyl groups that can potentially act as the second acceptor and intervene in binding studies.

In this chapter the targets are differently designed systems with two (**112**), three (**113**) and four (**114**) annulated pyridine rings extended by annelation in positions 3 and 4 (Scheme 4.1) which might help in adding stability during binding studies.
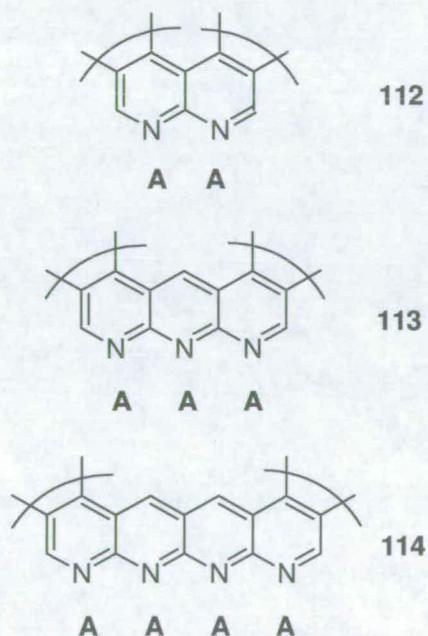
Scheme 4.1 New targeted systems.

The goal was to produce stable targeted systems (Scheme 4.1) soluble in chloroform involving as few synthetic steps as possible. Herein we describe the synthetic strategy (Scheme 4.2) using Suzuki coupling reactions for **120** AAA and **123** AAAA systems (Scheme 4.2b and 4.2c) and a slightly modified approach for the synthesis of the AA **117** unit (Scheme 4.2a) involving an FVP cyclisation step.

Suzuki coupling reaction has been known since 1979[120] and has been widely used in the synthesis of substituted biphenyls.[121] An advantage of using this strategy is to allow the condensation of the aldehyde groups from commercially available 2-formylphenylboronic acid with amino groups (step *5*) after Suzuki coupling to create "left hand" and "right hand" heterocyclic rings such as **120** and **123** (Scheme 2.4b and 2.4c).
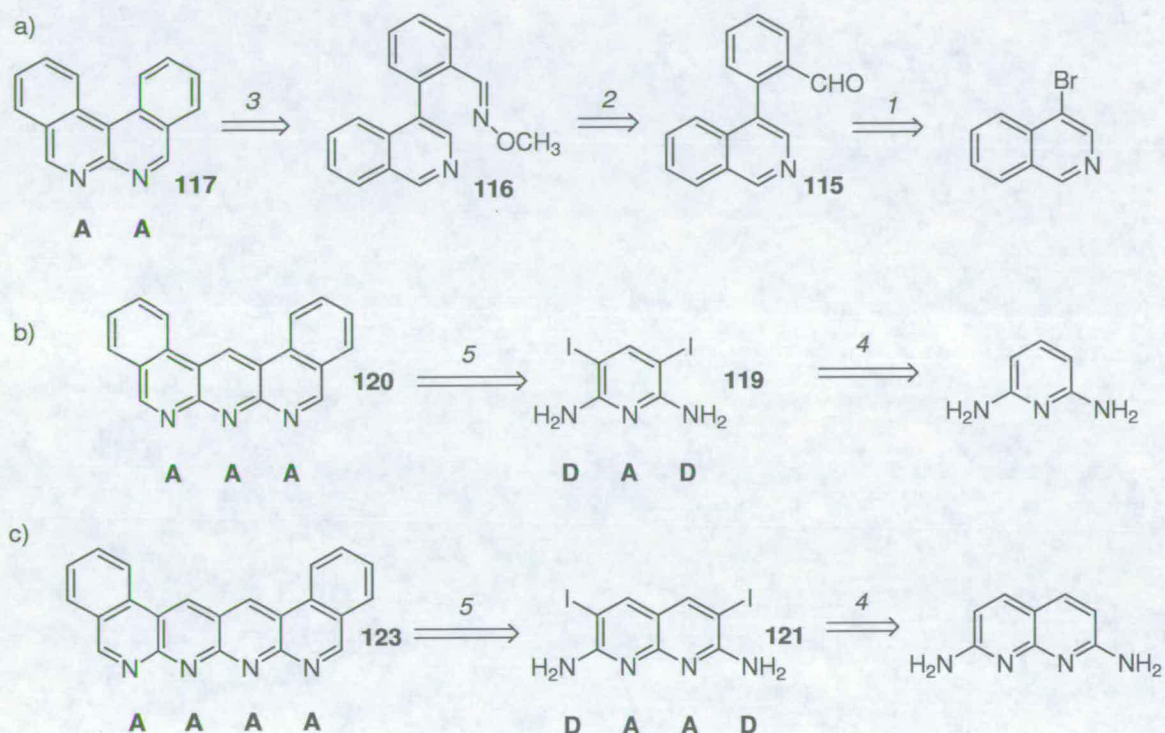
Scheme 4.2 New synthetic strategies for targeted systems with an extended aromatic framework in AA, AAA and AAAA arrangement.

In case of AA unit **117** a modified strategy was required involving Suzuki coupling of the 4-bromoisoquinoline with 2-formylphenylboronic acid to form **115**, followed by oxime formation **116** and flash vacuum pyrolysis (FVP) in step *3*. This strategy was developed by Fiona McMillan from University of Edinburgh.

Although this strategy had limitations and restriction for the complete synthesis of AAAA model, two heterocyclic analogues AA (**117**) in three steps and AAA (**120**) system in two steps were produced in high yields. In that sense this has been the most

successful approach that we developed so far and the systems proved to be extremely stable in binding studies (Chapter 5).

4.2 Results and discussion

4.2.1 Synthesis of 1,13,14-Triazadibenz[*a,j*]anthracene (120)

The synthesis of **120** was achieved in only two steps (Scheme 4.3). Diiodination of 2,6-diaminopyridine under standard conditions[17] gave **119** followed by Suzuki coupling with commercially available 2-formylphenylboronic acid, provided the fully aromatized compound **120** in 80% yield.
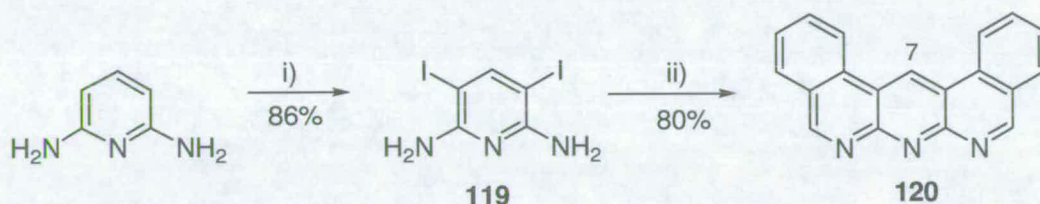
Scheme 4.3 Reaction conditions: i) *N*-Iodosuccinimide, DMF; ii) 2-formylphenyl boronic acid, Pd(PPh$_3$)$_4$, Cs$_2$CO$_3$, dioxane/water.

Compounds **119** and **120** showed correct molecular ions in their mass spectra. Compound **120** had characteristic aromatic proton signals in the range of δ_H 7.8-10.15 including the signal of the H$_7$ proton at a very high chemical shift of δ_H 10.15 ppm (Scheme 4.3). Additional confirmation that cyclisation took place in the final step was the fluorescence of **120** in excited state with λ_{max} at 430 nm (See Appendix).

4.2.2 Synthesis of Dibenzo[*c,f*][1,8]naphthyridine (117)

A modified approach (Scheme 4.4) was required for the synthesis of **117** and involved gas-phase generation and cyclization of an iminyl radical under flash vacuum pyrolysis (FVP) conditions,[122] in the final step.
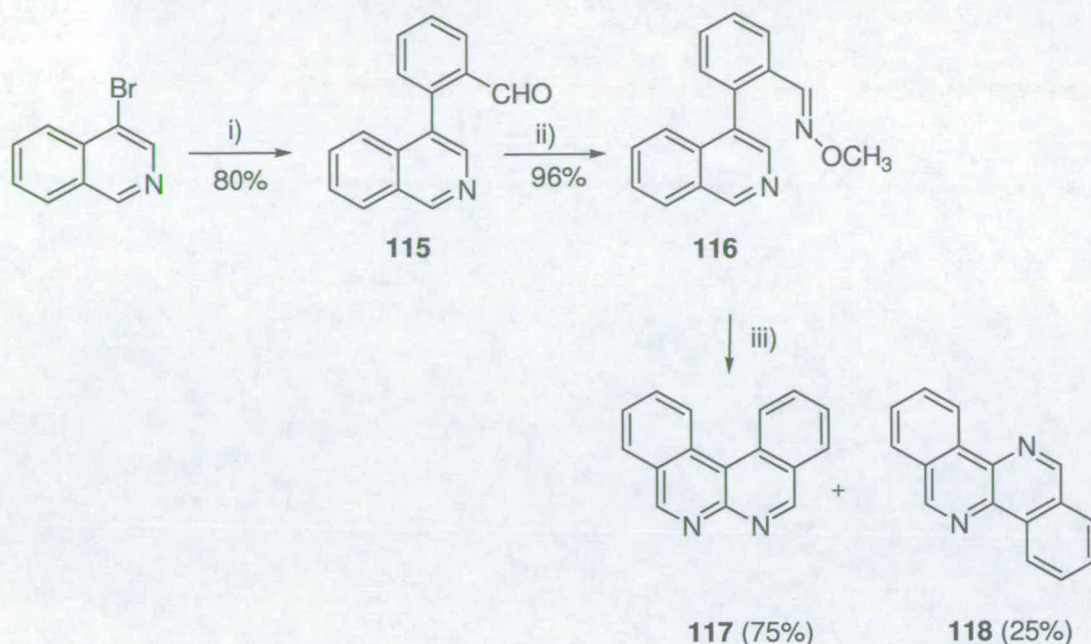
Scheme 4.4 Reaction conditions: i) Pd(PPh$_3$)$_4$, K$_2$CO$_3$, dioxane/water (1:1), 80%; ii) methoxyamine hydrochloride, EtOH, 96%; iii) FVP (T$_f$= 700 °C, T$_i$= 182 °C, p= 4.8 × 10^{-2} Torr, 10 min, 75%.

The oxime ether precursor **116** was made by Suzuki coupling of 4-bromoisoquinoline with 2-formylphenylboronic acid followed by reaction with *O*-methylhydroxylamine. FVP of the oxime ether **116** at 700 °C gave **117** as the main product (75%),[123] though a substantial by-product, identified as dibenzo[*c,h*]1,5-naphthyridine **118**, was also obtained in 25% yield. The crude ratio of the two products **117** and **118** was 3:1 as reported by Fiona McMillan.[122]

The formation of the two isomeric tetracycles is best rationalized by *ipso*-attack of the iminyl to give a spirodienyl intermediate (Scheme 4.5), followed by competitive C-N migration to give **117**, or C-C migration to give **118**.
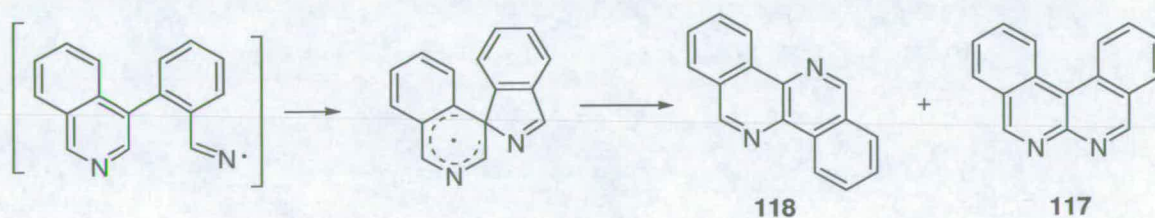
Scheme 4.5 Mechanism for formation of **117** and **118**.

118

Although the involvement of spirodienyl radicals is common in gas-phase iminyl chemistry,[124] previously, in such cases, C-N migration has been observed exclusively.[117] The C-C migration route may be able to compete in this example because of the increased steric congestion in the bay region of the transition state leading to **117**.

The structure of **115**, **116**, **117** and **118** has been confirmed by the correct molecular ions in their mass spectra and ^{13}C NMR signals have been used to distinguish compounds **117** and **118** (Scheme 4.6), by making use of the different symmetries of the two isomers.

118   **117**

Scheme 4.6 Highlighted (*) quaternary carbons.

Compound **117** has four quaternary carbon atoms at δ_C 126.5, 133.1, 153.2 and 157.7 ppm while compound **118** has only three quaternary carbon atoms at δ_C 128.4, 134.0 and 135.0 ppm. These findings are confirmed by X-ray crystallography (Section 4.2.3).

It was interesting that binding studies with counterpart **1** can distinguish the two isomers also. Using ^{1}H NMR titration experiments (10^{-3} M, 273 K, CDCl$_3$) a very high association constant value for the **1·117** heterocomplex was determined (Chapter 5) but no binding occurred ($K_a = 0$ M^{-1}) for heterocomplex **1·118**.

4.2.3 X-ray crystal structures of 1,13,14-Triazadibenz[*a,j*] anthracene (120) and Dibenzo[*c,f*][1,8] naphthyridine (117)

Crystals appropriate for single crystal X-ray structural determination (see experimental section) of **120** and **117** (Figure 4.1) were obtained in both cases by slow evaporation of a dichloromethane/methanol solution of the substrate. Dr Simon

Parsons from the University of Edinburgh solved and analyzed the X-ray crystal structure data for both compounds. The atom labels are colour-coded as follows: red for C, blue for N, white for H and yellow for C atoms.

a)

b)
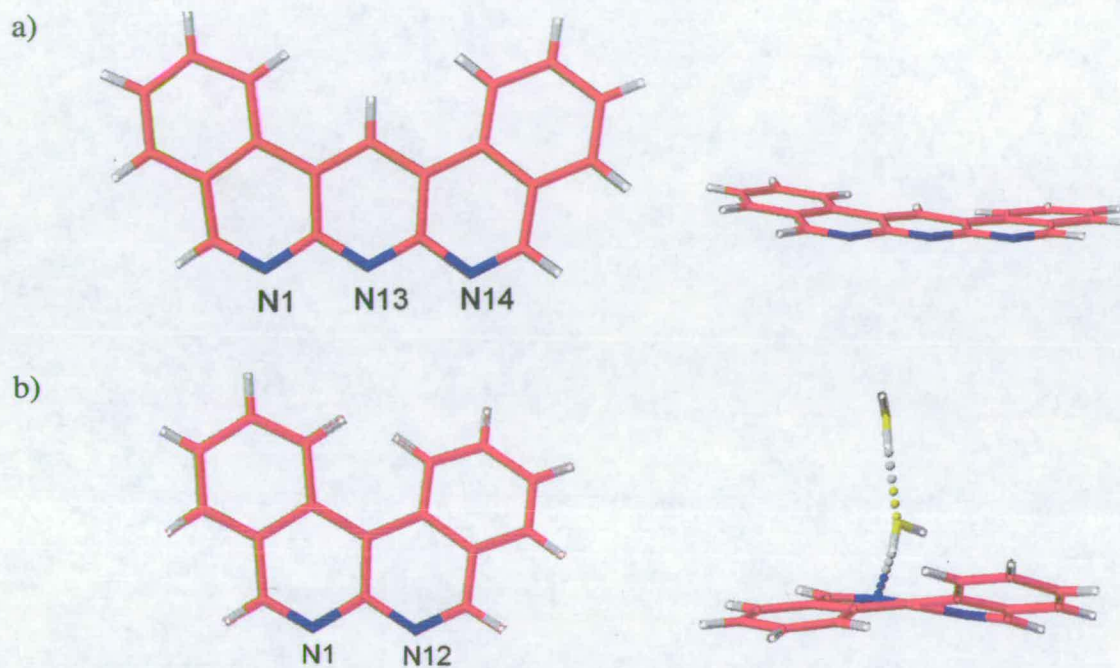
Figure 4.1 X-ray crystal structure of compounds a) **120** and b) solvate **117** $C_{16}H_9N_2 \times 2H_2O$ (C red, N blue, H white) from front and side view.

Selected N-N distances in the binding surface are for **120** N13-N14 2.294 Å and N1-N14 2.290 Å and for compound **117** N1-N12 2.300 Å. The crystal structure of compound **120** has slight deviation from planar geometry (Figure 4.1a) with different C-N bonds lengths: C12-N13 1.302 Å, C14-N13 1.340 Å and N13-C13 1.388 Å respectively.

Solvate **117** crystallized with a helical twist at the central C-C bond establishing a link from one water molecule to one nitrogen atom (Figure 4.1b). The other nitrogen makes a link a with different water molecule.
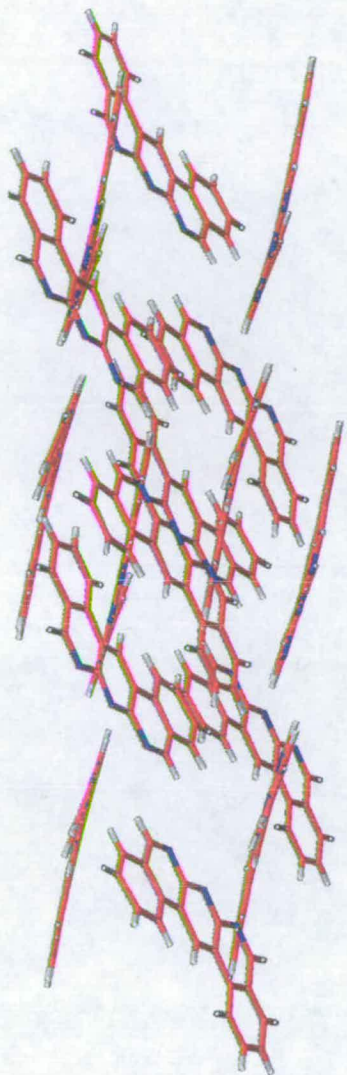
a)   b)
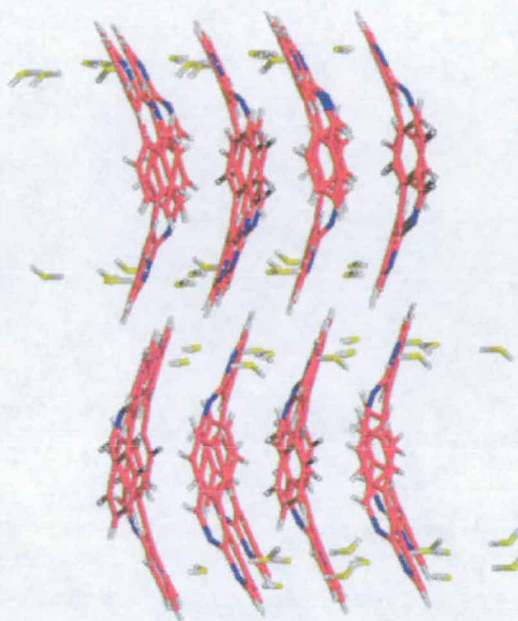
Figure 4.2 Packing diagrams for compounds a) **120** and b) **117** along the a-axis.

Well defined and strong π- π interactions are seen in both packing diagrams for **120** (Figure 4a) and **117** (Figure 4b).

4.2.4 Attempted synthesis of 1,14,15,16-Tetraazadibenz[*a,j*] anthracene (123)

The strategy for synthesizing compound **123** was analogous to the synthesis of **120**, using 2,7-diaminonaphthyridine available in several steps[125] to make 3,6-diiodo-2,7-diaminonaphthyridine **121** using standard methods.[126] When this step was carried out, the product formed that could potentially be **121** was very insoluble even in polar solvents such as DMSO or DMF and therefore the final cyclisation step failed, only starting material was recovered, from the crude mixture.

To overcome this problem we used dibromo-2,7-diaminonaphthyridine **122**, instead of **121** as the latter was more soluble in DMSO solvent (Scheme 4.7).
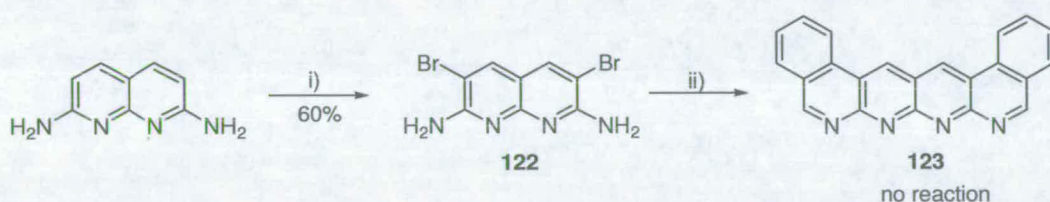
Scheme 4.7 i) *N*-bromosuccinimide, DMF; ii) 2-formylphenylboronic acid, Pd(PPh$_3$)$_4$, Cs$_2$CO$_3$, dioxane/water.

When the final Suzuki coupling step was performed, ambiguous results were obtained and it was not clear if compound **123** was formed. Although ^{1}H NMR spectra were obtained which were consistent with the structure of **123** [δ_H ppm 10.22 (s, 2H), 9.71 (s, 2H), 8.98 (d, 2H), 8.30 (d, 2H), 8.09 (t, 2H) and 7.90 (t, 2H)] it was not unexpectedly much less soluble then its AAA analogue **120**. The results were difficult to reproduce results and the structure of **123** could not be confirmed by other analytical methods, *e.g.* ^{13}C NMR or MS.

4.3 Conclusion

Overall, the Suzuki-coupling approach was the most successful approach so far and gave access to the most stable AA and AAA units **117** and **120** in only few steps and in high yields and their structures were confirmed by X-ray crystallography.
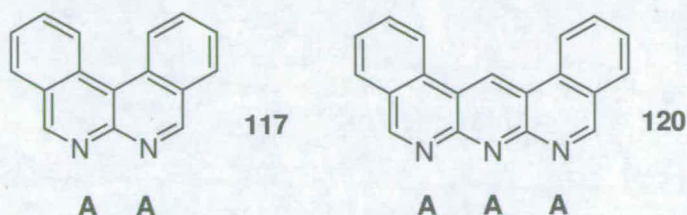
Scheme 4.8 Summary of synthesized compounds

The synthesis of an AAAA unit was not completed but the suggested approach appears viable once the solubility problems of the precursors can be overcome.

4.4 Experimental section

General method: The FVP system was evacuated to a pressure of 10^{-2}-10^{-3} Torr by means of a high capacity oil pump. Precursors (50-150 mg) were sublimed under reduced pressure through an empty silica tube (35 cm × 2.5 cm) heated by an electrical furnace. The products were collected in a U-tube cooled by liquid nitrogen situated at the exit point of the furnace. Upon completion of the pyrolysis the trap was allowed to warm to room temperature under an atmosphere of dry nitrogen. The entire pyrolysate was then dissolved in solvent to enable removal from the trap.

T_f- Temperature of furnace

T_i- Temperature of inlet tube

P- Pressure of FVP system

t- Time needed to complete pyrolysis

1,13,14-Triazadibenz[_a,j_]anthracene (120)
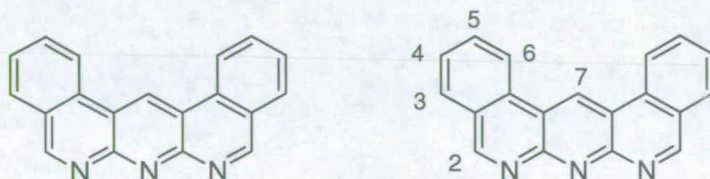
A mixture of 2-formylphenylboronic acid (1.5 g, 0.01 mol), 3,5-diiodo-2,6-pyridinediamine (1.8 g, 0.005 mol), potassium carbonate (8.28 g, 0.06 mol) and

tetrakis(triphenylphosphine) palladium (0.11 g, 0.01 mmol) was heated under reflux in a solution of dioxane (75 cm^3) and water (25 cm^3) for 3 h under a nitrogen atmosphere. After the solution was cooled to room temperature the precipitate was filtrated and subjected to silica gel chromatography using a solvent mixture of chloroform and MeOH (1:5) as eluent to obtain (**120**) (2.0 g, 70%), mp >340 °C; ^{1}H NMR (400 MHz,CDCl$_3$) δ ppm 7.89 (t, 2H, $J_{5,4}$ = 8.3 Hz, $J_{5,6}$ = 7.8 Hz, H$_5$), 8.04 (dd, 2H, $J_{4,3}$ = 8.3 Hz, $J_{4,5}$ = 7.0 Hz, H$_4$), 8.19 (d, 2H, $J_{3,4}$ = 7.8 Hz, H$_3$), 8.90 (d, 1H, $J_{6,5}$ = 8.34 Hz, H$_6$), 9.67 (s, 2H, H$_2$) and 10.15 (s, 1H, H$_7$); ^{13}C NMR (100 MHz, CDCl$_3$) δ ppm 118.4 (C$_{6b}$), 122.3 (C$_6$), 126.3 (C$_{2a}$), 127.2 (C$_4$), 128.8 (C$_7$), 129.6 (C$_5$), 132.0 (C$_3$), 132.4 (C$_{6a}$), 157.6 (C$_{1a}$) and 159.6 (C$_2$). EI-MS m/z 281 [M]. Anal. calcd. for C$_{19}$H$_{11}$N$_3$: C, 81.12; H, 3.94; N, 14.94. Found: C, 80.9; H, 3.85; N, 15.0.

2-(Isoquinolin-4-yl) benzaldehyde (115)
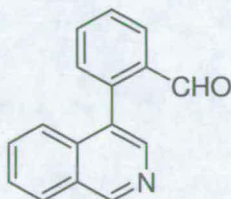
2-Formylphenylboronic acid (0.510 g, 3.40 mmol), 4-bromoisoquinoline (0.700 g, 3.36 mmol), potassium carbonate (2.778 g, 0.020 mol) and tetrakis(triphenylphosphine) palladium (0.077 g, 0.067 mmol) were mixed in a solution of dioxane (24 cm^3) and water (8 cm^3) and the mixture heated under reflux under a nitrogen atmosphere for 4 h. After cooling to room temperature, the solution was diluted with ether and filtered through a silica plug. The solvent was removed leaving a yellow oil which was purified by dry flash chromatography eluted with 20% ethyl acetate in hexane to produce **115** (0.631 g, 80%), mp 80-81 °C; ^{1}H NMR (400 MHz,CDCl$_3$) δ = 7.76 (m, 6H), 8.145 – 8.19 (s, 1H), 8.23 (ddd, 1H, J =0.5, 1.6, 7.7 Hz), 8.57 (s, 1H), 9.43 (s, 1H) and 9.75 (s, 1H); ^{13}C NMR (100 MHz, CDCl$_3$) δ = 124.8 (CH), 128.0 (CH), 128.2 (CH), 128.4 (2CH-overlap), 129.2 (quat), 129.5 (CH), 131.7 (CH), 132.3 (quat), 134.4 (CH), 135.3 (quat), 135.6 (quat), 140.4 (quat), 143.8

(CH), 153.4 (CH) and 191.5 (CH). EI-MS *m/z* 233 [M]. HRMS [M]$^+$: 233.0841, $C_{16}H_{11}NO$ requires: 233.0852.

2-(1-Phenylisoquinolin-4-yl)-*O*-methyl oxime (116)
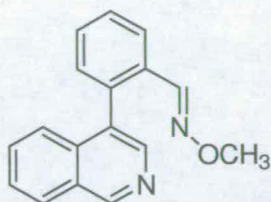
2-(Isoquinolin-4-yl)benzaldehyde (0.173 g, 0.741 mmol) and methoxylamine hydrochloride (0.110 g, 1.32 mmol) were added to ethanol (10 cm^3) and the solution heated to reflux for 2 h. The solution was then concentrated under vacuum and dissolved with ether (3 × 20 cm^3) and washed with NaOH (0.25 M, 10 cm^3) and water (10 cm^3) and dried over MgSO$_4$. The solvent was removed to produce **116** as a white solid (0.187 g, 96%), mp 108–110 °C (from ethanol). ^{1}H NMR (400 MHz,CDCl$_3$) δ ppm 3.75 (s, 3H), 7.23 (ddd, 1H, *J* =0.5, 3.4, 6.0 Hz), 7.40 (dd, 3H, *J* =3.7, 5.7 Hz), 7.49 – 7.57 (m, 3H), 7.94 (ddd, 1H, *J* =1.8, 4.8, 6.5 Hz), 8.00 (dd, 1H, *J* =3.7, 5.5 Hz), 8.32 (s, 1H) and 9.21 (s, 1H); ^{13}C NMR (100 MHz, CDCl$_3$) δ ppm 60.9 (CH$_3$), 123.8 (CH), 124.7 (CH), 126.4 (CH), 126.8 (CH), 127.6 (CH), 128.6 (CH), 130.0 (CH), 130.3 (2CH-overlap), 130.3 (quat), 133.9 (quat), 135.4 (quat), 142.3 (quat), 142.3 (CH), 145.8 (CH), 151.5 (quat); EI-MS *m/z* 262 [M]. HRMS [M]$^+$: 262.1106, $C_{17}H_{14}N_2O$ requires: 262.1110.

Dibenzo[*c*,*f*][1,8]naphthyridine (117)
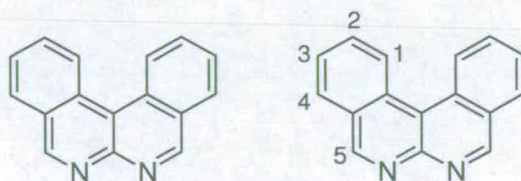
Flash vacuum pyrolysis (FVP) of 2-isoquinolin-4-ylbenzaldehyde-O-methyl oxime (0.15 g, T_f = 700 °C, T_i = 166 °C, P = 4.8 × 10^{-3} Torr, t = 10 min) produced a mixture of two components. They were purified by column chromatography on silica gel using a solvent gradient of hexane to hexane/EtOAc (1:1) as eluent to obtain **118** (0.04 g, 25%) and **117** (0.11 g, 75%). mp 169 – 170 °C ^{1}H NMR (400 MHz, CDCl$_3$) δ ppm 7.83 (t, 2H, $J_{2,1}$= 7.9 Hz, $J_{2,3}$= 7.2, H$_2$), 7.99 (t, 2H, $J_{3,4}$ = 8.5 Hz, $J_{3,2}$= 7.2, H$_3$), 8.27 (d, 2H, $J_{3,4}$= 7.9 Hz, H$_3$), 9.16 (d, 2H, $J_{1,2}$ = 8.5 Hz, H$_1$) and 9.55 (s, 2H, H$_5$). ^{13}C NMR (100 MHz, CDCl$_3$) δ ppm 126.5 (C$_{4a}$), 127.6 (C$_{3}$-), 127.9 (C$_{4a}$-), 129.3 (C$_2$-), 131.6 (C$_4$-), 133.1 (C$_{12a}$-), 153.2 (C$_{12b}$-), 154.5 (C$_5$-), 157.7 (C$_{6a}$-), EI-MS m/z 230 [M]. HRMS [M]$^+$: 230.0844, C$_{16}$H$_{10}$N$_2$ requires: 230.0834.

Dibenzo[*c*,*h*][1,5]naphthyridine (118)
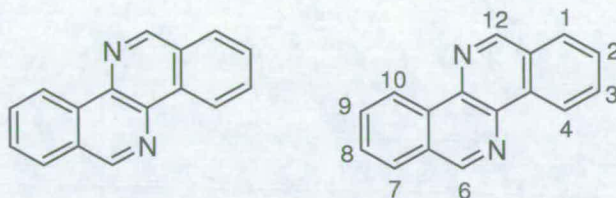
mp 166–167 °C [lit.[122], 166 – 167 °C] ^{1}H NMR (400 MHz, CDCl$_3$) δ =7.82 (t, 2H, $J_{2,1}$= 8.0 Hz, $J_{2,3}$= 7.1 Hz, H$_2$), 8.00 (t, 2H, $J_{3,4}$ = 8.1 Hz, $J_{3,2}$= 7.2 Hz, H$_3$), 8.20 (d, 2H, $J_{1,2}$= 8.0 Hz, H$_1$), 9.27 (d, 2H, $J_{4,3}$ = 8.4 Hz, H$_4$), 9.53 (s, 2H, H$_6$). ^{13}C NMR (100 MHz, CDCl$_3$) δ =123.5 (CH), 127.8 (CH), 128.2 (CH), 128.4 (quat), 131.3 (CH), 134.0 (quat), 135.0 (quat), 152.6 (CH). EI-MS m/z 230 [M]. HRMS [M]$^+$: 230.0849, C$_{16}$H$_{10}$N$_2$ requires: 230.0834.

3,6-Dibromo-1,8-naphthyridine-2,7-diamine (122)
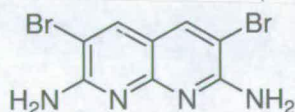
To 2,6-diaminonaphthyridine[125] (0.7 g, 4.3 mmol) dissolved in DMF (10 cm^3) was added dropwise NBS (1.55 g, 8.75 mmol) dissolved in DMF (10 cm^3) at -30 °C over 1 h and the mixture was then left to stir at room temperature for a further 2 h. The solution was concentrated under vacuum and DCM (10 cm^3) was added to form a brown precipitate which was washed with hexane (10 cm^3) and acetone (10 cm^3) to obtain yellow crystals of **122** (0.8 g, 60%), mp > 300 °C (dec). ^{1}H NMR (400 MHz, [D$_6$]DMSO) δ ppm 8.37 (s, 2H) and 8.08 (br s, 4H); ^{13}C NMR (100 MHz, [D$_6$]DMSO) δ ppm 100.9 (2 quat), 110.1 (2 quat), 141.7 (2 CH), 146.3 (2 quat) and 155.8 (2 quat); EI-MS *m/z* 318 [M+H]$^+$: HRMS [M]$^+$: 317.8940, C$_8$H$_6$Br$_2$N$_4$ requires: 317.8980.

1,14,15,16-Tetraazadibenz[*a,j*]anthracene (123)
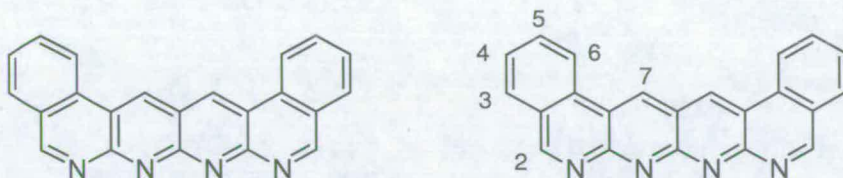
A mixture of 2-formylphenylboronic acid (1.5 g, 0.01 mol), 3,6-dibromo-1,8-naphthyridine-2,7-diamine (1.8 g, 0.005 mol), potassium carbonate (8.28 g, 0.06 mol) and tetrakis(triphenylphosphine) palladium (0.11 g, 0.01 mmol) was heated under reflux in a solution of dioxane (75 cm^3) and water (25 cm^3) for 5 h under a nitrogen atmosphere. After the solution was cooled to room temperature, the precipitate indicating compound **123** was filtered and characterized using ^{1}H NMR spectra, only. ^{1}H NMR (400 MHz, CDCl$_3$) δ ppm 10.22 (s, 2H), 9.71 (s, 2H), 8.98 (d, 2H), 8.30 (d, 2H), 8.09 (t, 2H) and 7.90 (t, 2H).

X-ray crystallographic data for compound 120:

Crystal data for **120**: $C_{19}H_{11}N_3$, $M = 281.31$, colorless needle 0.90 mm × 0.17 mm × 0.13 mm, monoclinic, space group $P21/c$; $a = 13.7096(9)$, $b = 7.1732(5)$, $c = 14.1350(9)$ Å; $\beta = 110.494(4)°$, $V = 1302.08(15)$ Å^3, ρ_{calcd}=1.435 Mg/m^3, $Z = 4$; $\lambda = 0.71073$Å, $T = 150(2)$ K, 10583 reflection measurements, 2309 unique. The structures were solved and refined using SHELXL-97 to yield final residuals $R = 0.0431$ and $R_w = 0.1087$. All hydrogen atoms were placed in rigid fixed geometries.

X-ray crystallographic data for compound 117-solvate:

Crystal data for **117**-solvate: $C_{16}H_{14}N_2O_2.2H_2O$, $M = 266.29$, colorless block 1.05 mm × 0.34 mm × 0.14 mm, orthorhombic, space group $Pbca$; $a = 13.3373(9)$, $b = 7.1636(5)$, $c = 26.4564(18)$ Å; $\beta = 90°$, $V = 2527.7(3)$ Å^3, ρ_{calcd}=1.399 Mg/m^3, $Z = 8$; $\lambda = 0.71073$ Å, $T = 150(2)$ K, 22710 reflection measurements, 2226 unique. The structures were solved and refined using SHELXL-97 to yield final residuals $R = 0.0437$ and $R_w = 0.1041$. All hydrogen atoms were placed in rigid fixed geometries.

Appendix

Absorption (yellow) and fluorescence (red) spectra of compound **120** are represented in Figure A1.

a)
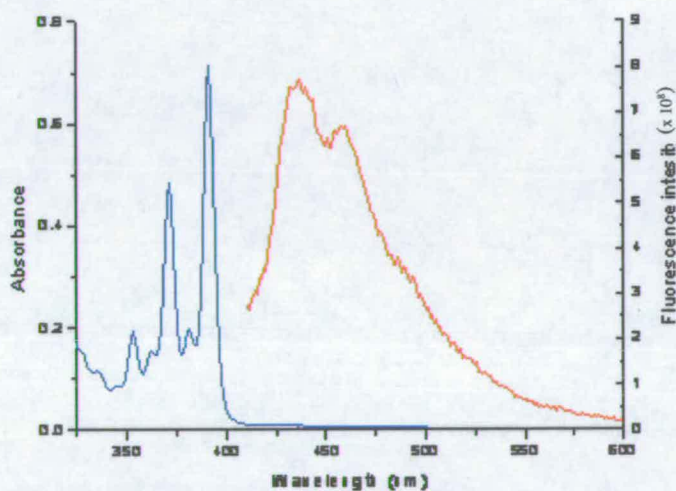
Figure A1. Absorption and fluorescence spectra of **120**.

Compound **120** showed multiple absorption bands with λ_{max} at 390 nm whereas the fluorescence spectrum exhibited a λ_{max} at 430 nm.

Chapter 5: Binding studies
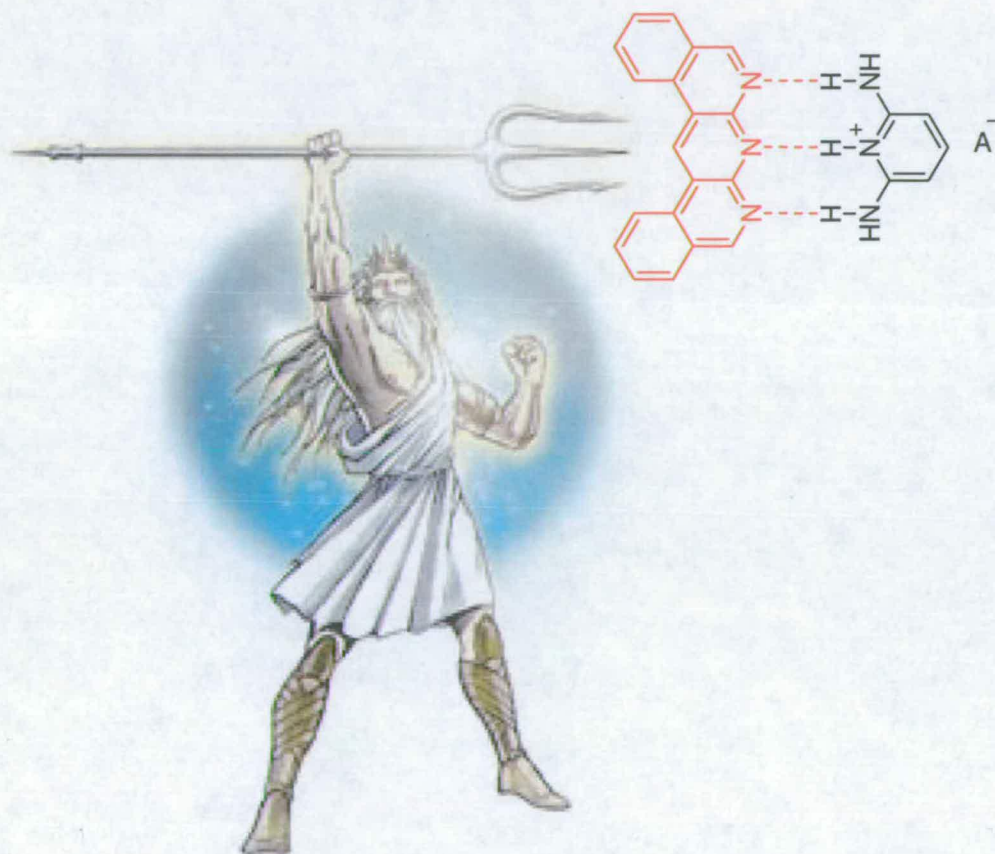
*The strongest **125•120** heterocomplex*

5.1 Introduction

The previous three chapters covered different synthetic strategies for obtaining new AA and AAA units. The compounds that have been synthesised can be found in the Glossary of compounds. Only selected examples (Figure 5.1) have been used in binding studies with appropriate DDD counterparts (Figure 5.2) and will be discussed in this chapter.
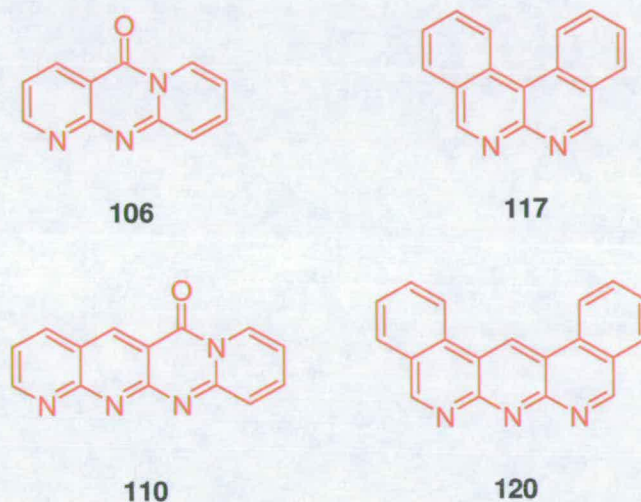
Figure 5.1 Selected AA and AAA units for the binding studies.

Counterparts 1^{15} and **124** were readily available and the cationic DDD counterpart **125** was synthesized by analogy with Aslyn's 61^{54} (Figure 1.28).
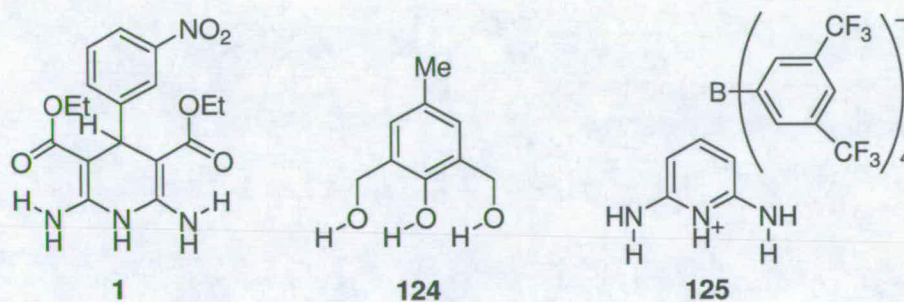
Figure 5.2 Selected DDD units for the binding studies.

Different techniques[127] have been used for the determination of association constants of AA-DDD heterocomplexes **1•106**, **1•117** and **124•120** and AAA-DDD heterocomplexes **1•110**, **1•120** and **125•120**. Most of the K_a values were determined by ^{1}H NMR titration experiments in chloroform-*d* solution. For the other AAA-DDD heterocomplexes that display very high binding stabilities fluorescence spectroscopy in dichloromethane solution was employed. To determine the stoichiometry of host-guest in all heterocomplexes, method of continues variations (Job's plot experiments) were used.[128]
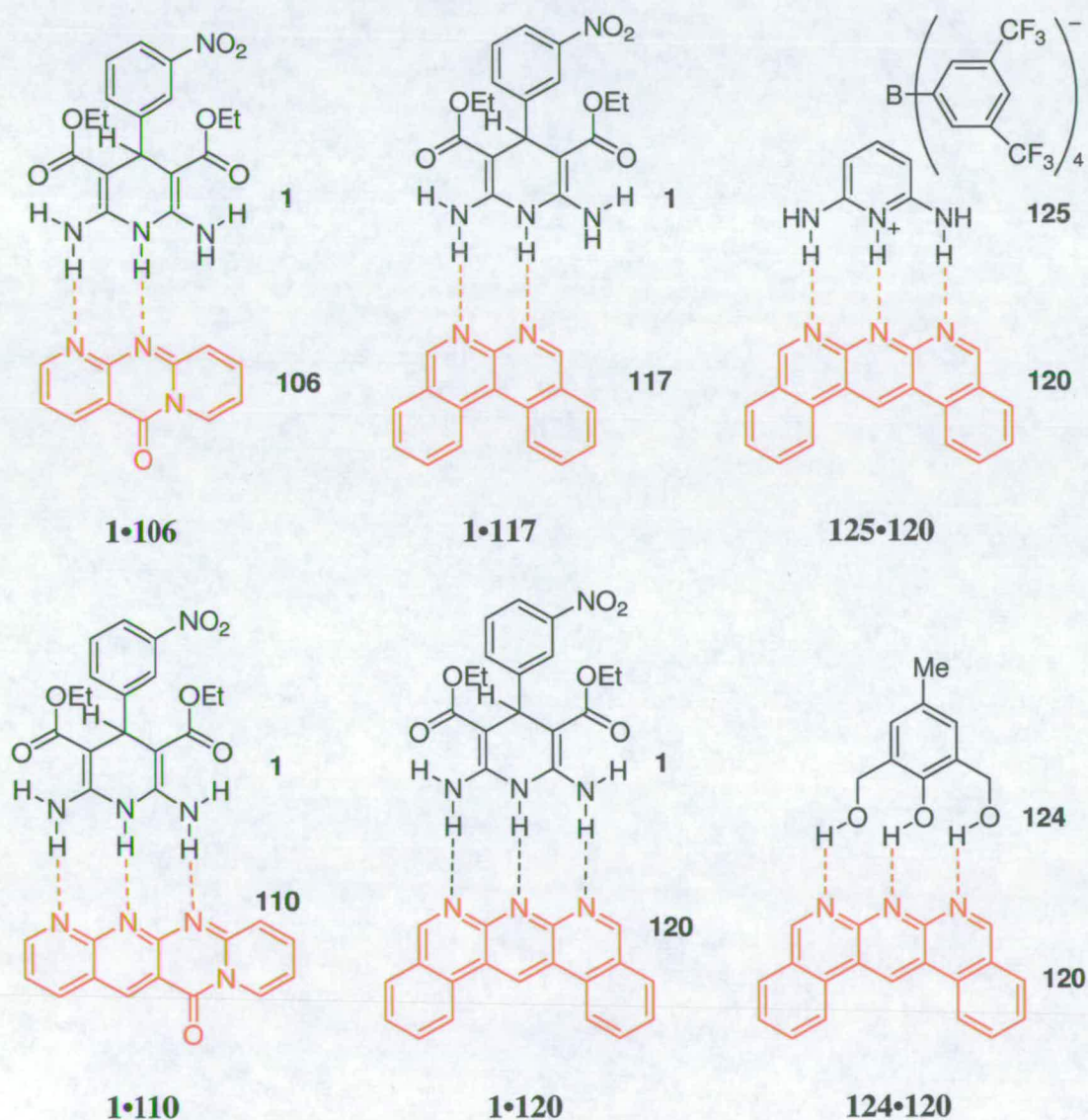
Scheme 5.1 Heterocomplexes used in the binding studies.

Experimental data obtained from titration experiments of all heterocomplexes were modelled with a specially designed software program GasFit developed by Dr Dusan Djurdjevic[129] to obtain binding constants using standard equations for the binding methods (Scheme 5.1).[97, 130]

Calculated K_a values determined by fluorescence spectroscopy were in good agreement with a molecular model study for the heterocomplex 1•120.

5.2 Results and discussion

5.2.1 DDD-Counterparts

Counterparts 1, 124 and 125 (Scheme 5.2) were used in binding study experiments. The DDD receptor 124 was commercially available and the cationic counterpart 125 was prepared in the same way as 61 and outlined in Scheme 5.2. The protonation of 2,6-diaminopyridine with gaseous HCl followed by anion exchange with commercially available sodium tetrakis[3,5-bis(trifluoromethyl)phenyl]borate, afforded 125 in 75% yield.

125
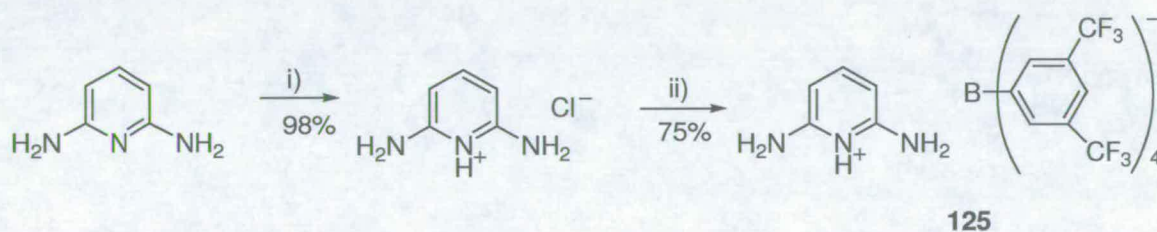
Scheme 5.2 Synthesis of 125 DDD-counterpart: i) HCl(g), DCM, 98%; ii) $Na^+B^-[C_6H_3(CF_3)_2]_4$, acetonitrile, 75%.

Compound 1 has been already used by Zimmerman and Murray and can be prepared by known methods.[15] The authors reported[40] that use of 1 in binding studies has been complicated by tautomerism, and it is known that 1 exists as a mixture of 1,4-dihydro (DDD-unit) and 3,4-dihydro (DAD) tautomeric forms (Figure 5.3) in slow exchange in chloroform-*d*.
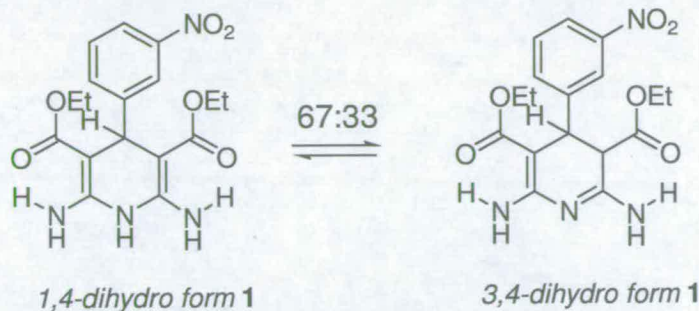
Scheme 5.3 Tautomeric mixture of **1** in chloroform-*d*.

These DDD units were selected because of their availability and their previous use in a comparable study with known literature examples **1•2**, **1•3** and cationic **61•3** (Figure 1.28). At the same time we can make comparison of –OH (**124**) and –NH (**1**) donor sites in binding ability within **1•120** and **124•120** heterocomplexes.

5.2.2 ^{1}H NMR Titration experiments

Initial complexation studies for all heterocomplexes (Scheme 5.1) were preformed by the ^{1}H NMR technique in chloroform-*d* at 293 K under conditions where self-association of **1**, **106**, **110**, **117**, **120**, **124** and **125** was negligible (see experimental section). The association constants were determined using standard methods[97] by titrating **1** and **125** with **106**, **110**, **117** or **120** and monitoring the high frequency shift of the amino hydrogen. For the complex **124•120** the chemical shift of the hydroxy proton has been monitored upon addition of **120** to the **124**.

In each binding experiment, the [DDD]/[AA or AAA] ratio was incrementally increased by adding **106**, **110**, **117** or **120** to **1**, **124** or **125**.

System	AA-DDD			AAA-DDD		
Complex	**1•106**	**1•117**	**1•110**	**1•120**	**124•120**	**125•120**
K_a (M^{-1})	6.2×10^3	8.6×10^4	$>10^5$	$>10^5$	2.4×10^4	$>10^5$
Proton monitored	-NH$_2$	-NH$_2$	-NH$_2$	-NH$_2$	-OH	-NH$_2$

Table 5.1 The K_a values determined by the ^{1}H NMR titration experiments for all heterocomplexes. Repetition of the binding experiments for each of heterocomplexes gave K_a within 10% of the values shown (the error in data fitting for each run was <1%).

Plots of chemical shifts of amino/hydroxyl protons versus guest to host ratio confirmed the typical 1:1 binding isotherm for all heterocomplexes except for **1•120** where the ratio of 1:2 was formed at the concentration (10^{-3} M) used in ^{1}H NMR titration experiments. This has been confirmed by the Job plot experiment with max mole ratio at 0.76 (see experimental section).

The explanation for this could be very strong π- π stacking at high concentration with the possibility of three stacks in complex, potentially forming three bifurcated H-bonds in stacked complex. When the **1•120** complex is diluted from *ca.* 10^{-3} M to 10^{-9} M, 1:1 stoichiometry is formed. The low concentration of 10^{-9} M for **120** is not practical for determining K_a by the ^{1}H NMR technique, but it can be used in fluorescence titration experiments (See 5.2.3 Section).

Experimental data for all heterocomplexes were modeled with a computer program[129] and the K_a values were determined for the **124•120** heterocomplex[14] K_a= 2.4×10^4 M^{-1}; for the **1•117** heterocomplex K_a= 8.6×10^4 M^{-1}; and for the **1•106** heterocomplex K_a= 6.2×10^3 M^{-1} (Figure 5.4).
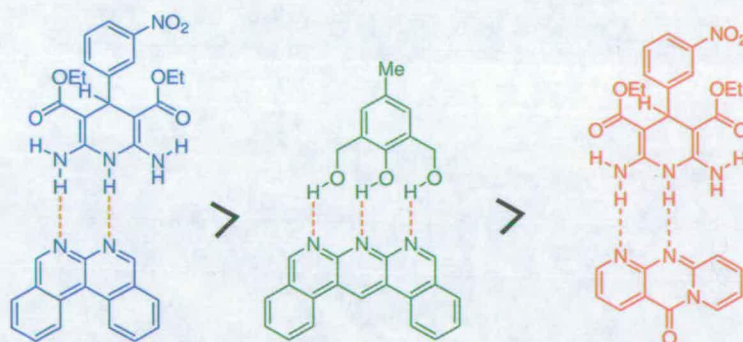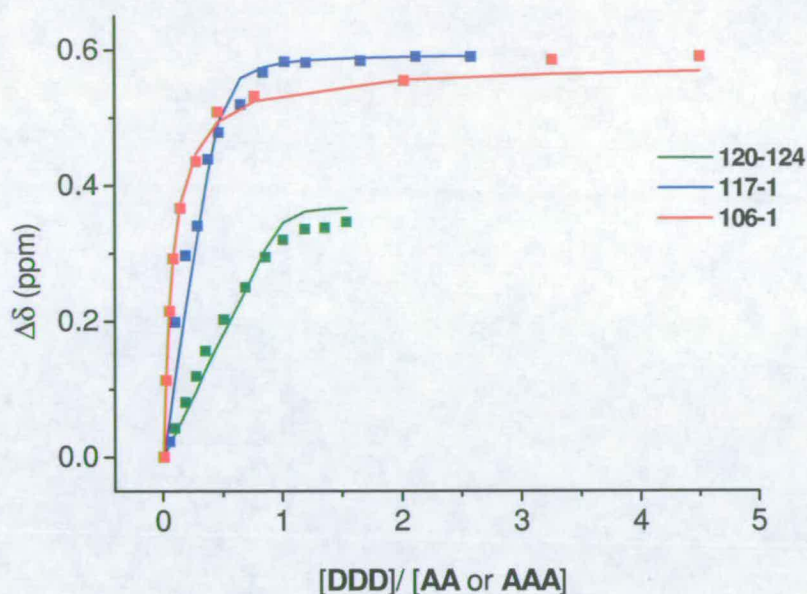
Figure 5.4 Binding isotherms in chloroform-*d* using the change in chemical shift (Δδ) of the amino NH$_2$ protons of **1** (10^{-3} M) upon addition of **117** or **106** and the hydroxyl protons of **124** (10^{-3} M) upon addition of **120**. The lines indicate best-fitting K_a for **1•117** (blue), **1•106** (red) and **124•120** (green) heterocomplexes.

The lack of curvature for heterocomplexes **1•110**, **1•120** and particularly **125•120** indicated exceptionally strong association constants (>10^5 M^{-1}) which cannot be determined by the NMR technique (Figure 5.5). These last results were in agreement with Zimmerman's[40] analogues **1•3** and the cationic analogues **4•3** developed by Aslyn.[54] Comparison of K_a values for **1•106** and **1•117** with Zimmerman's **1•2** AA-DDD heterocomplex indicated good agreement although our systems appeared to be 1.8 to 2.0 kcal mol^{-1} more stable.
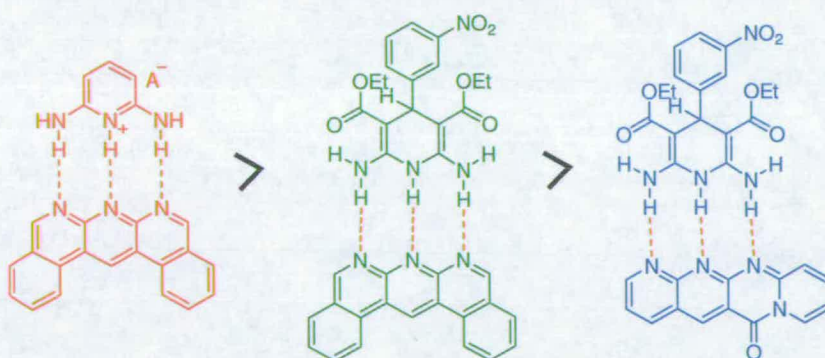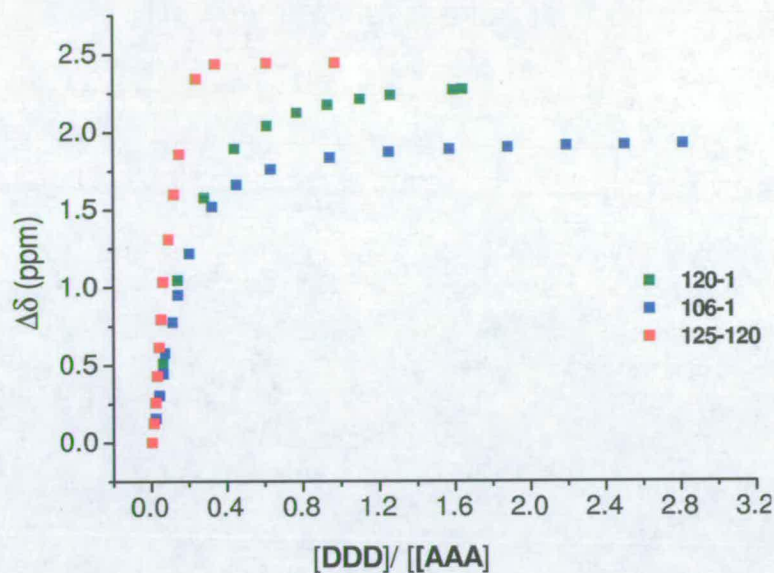
Figure 5.5 Binding isotherms in chloroform-*d* using the change in chemical shift ($\Delta\delta$) of the amino NH$_2$protons of **1** (10^{-3} M) or **125** (10^{-3} M) upon addition of **110** or **120**. The experimental data indicated $K_a > 10^5$ M^{-1} for **1•120** (green), **1•110** (blue) and **125•120** (red) heterocomplexes.

In heterocomplexes **1•106**, **1•110**, **1•117** and **1•120** the use of receptor **1** in the binding experiments is complicated by its tautomerism (see Figure 5.3). Murray and Zimmerman reported[40] that 10 eq. of **3** at mM concentration was required to convert **1** fully into the 1,4-dihydro form involved in DDD H-bonding. In contrast, in our ^{1}H NMR titration experiments less than 3 eq of AAA (10^{-3} M) receptor was needed to convert the initial 67:33 ratio of the 1,4-dihydro:3,4-dihydro forms of **1** to >98: 2. In decreasing order, this was achieved at 3 eq of **106** in the **1•106** heterocomplex (Figure 5.6); 2 eq of **110** in the **1•110** heterocomplex (Figure 5.7); 1 eq of **117** in the **1•117** heterocomplex (Figure 5.8) and only 0.5 eq of **120** in the **1•120** heterocomplex (Figure 5.9).
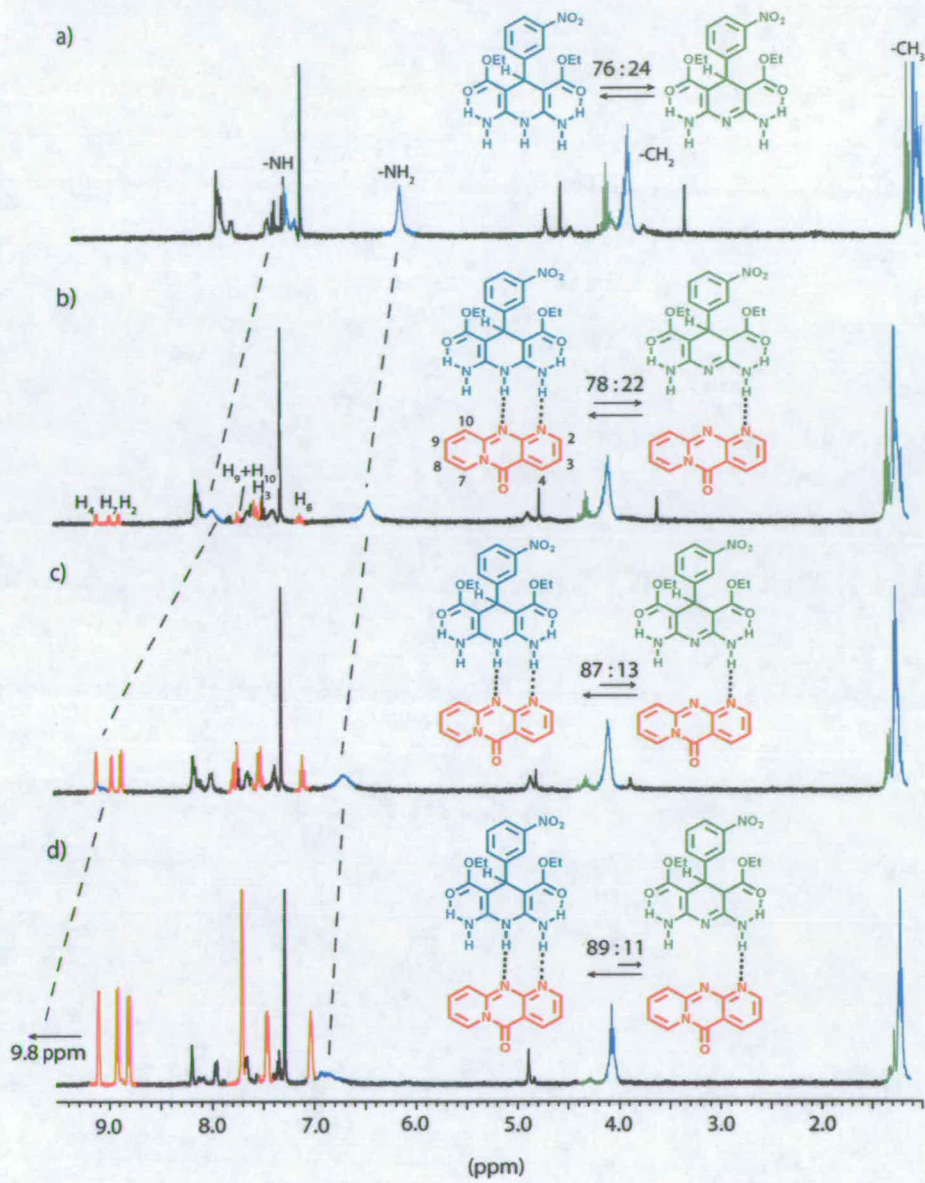
Figure 5.6 ^{1}H NMR (400 MHz, CDCl$_3$, 298 K) spectra of **1** (10^{-3} M^{-1}) in the (a) absence of **1**, (b) presence of 0.35 eq, (c) 0.7 eq and (d) 1.5 eq of **106**.
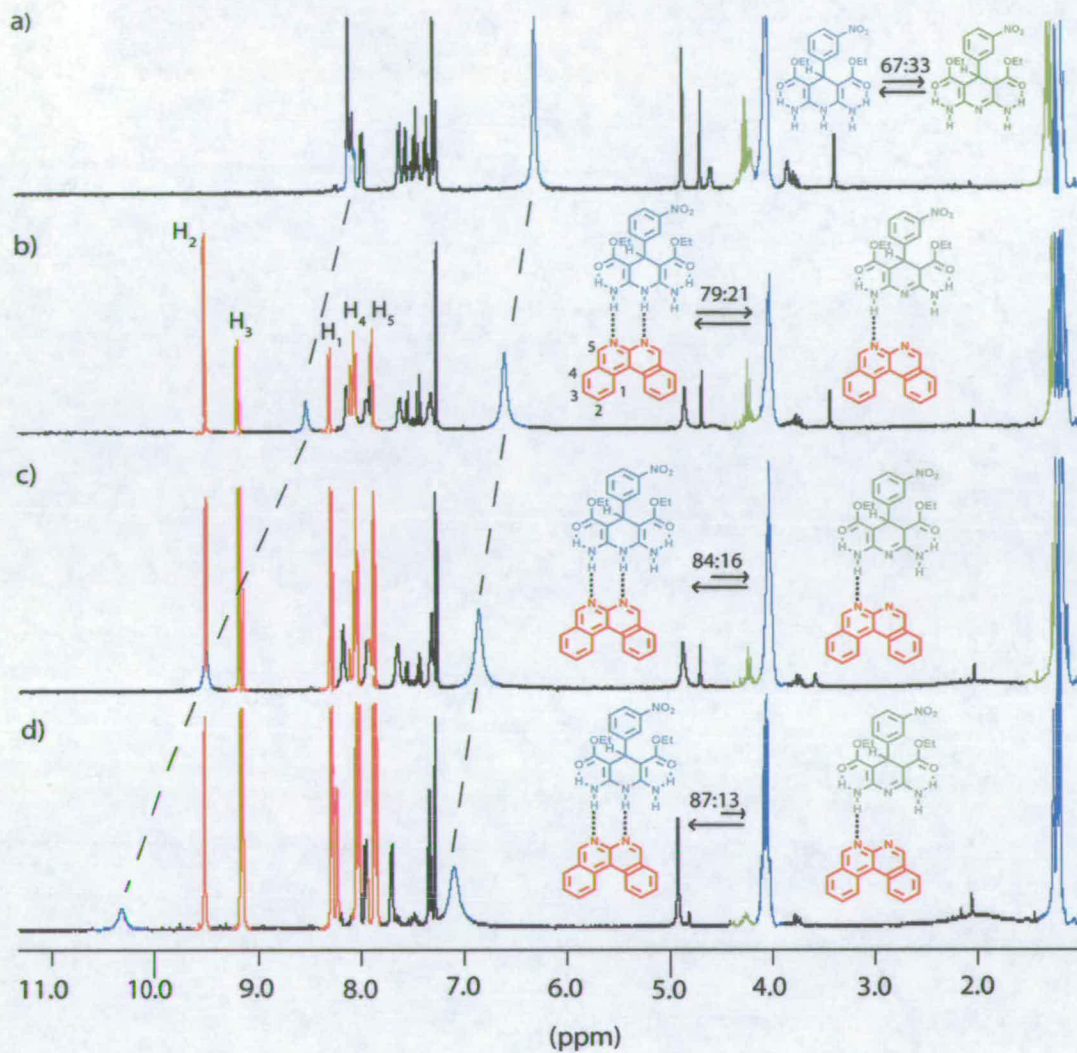
Figure 5.7 ^{1}H NMR (400 MHz, CDCl$_3$, 298 K) spectra of **1** (10^{-3} M^{-1}) in the (a) absence of **117**, (b) presence of 0.8 eq, (c) 0.9 eq and (d) 1 eq of **117**.
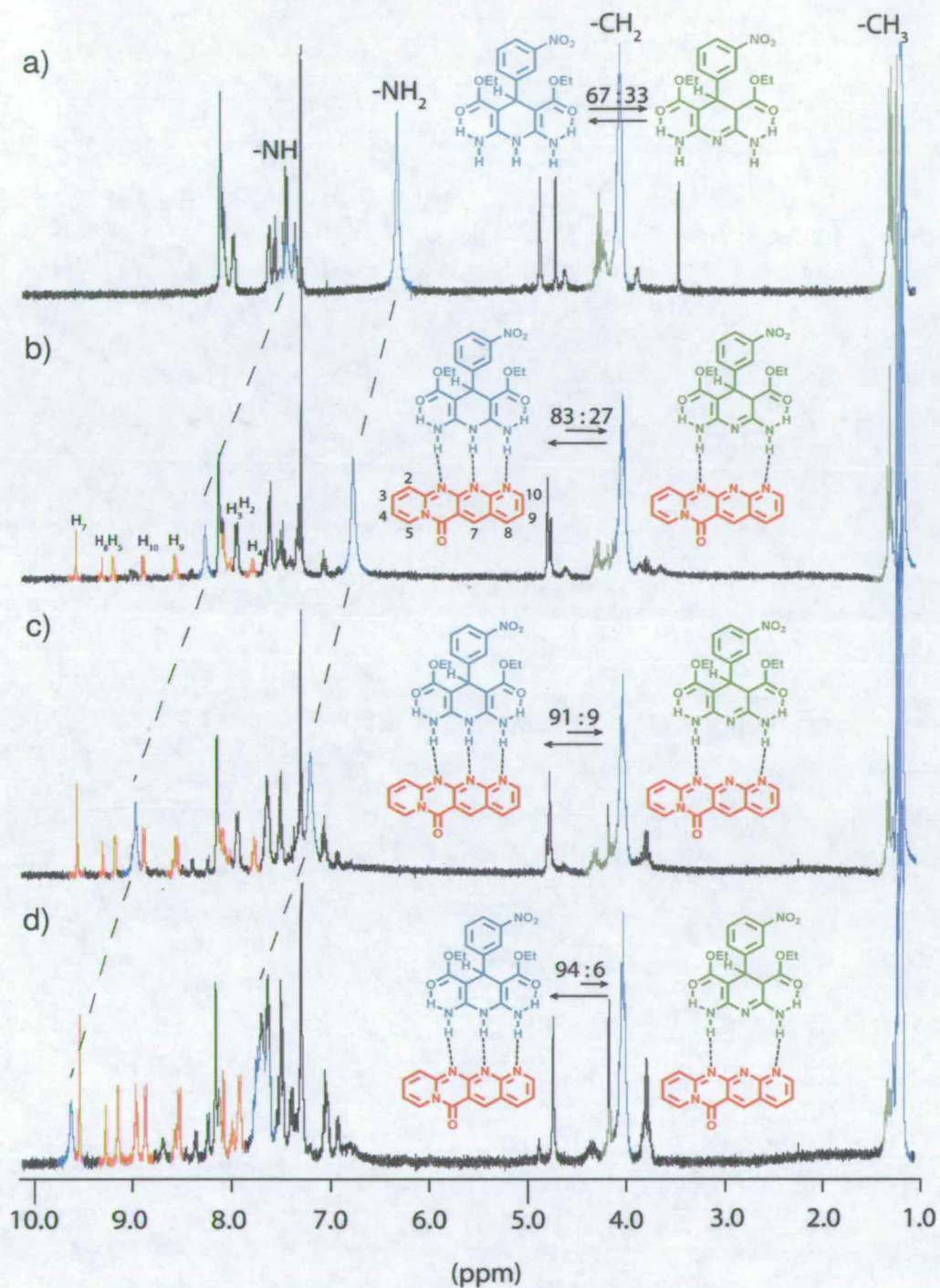
Figure 5.8 ^{1}H NMR (400 MHz, CDCl$_3$, 298 K) spectra of **1** (10^{-3} M^{-1}) in the (a) absence of **1**, (b) presence of 0.3 eq, (c) 0.4 eq and (d) 0.9 eq of **110**.
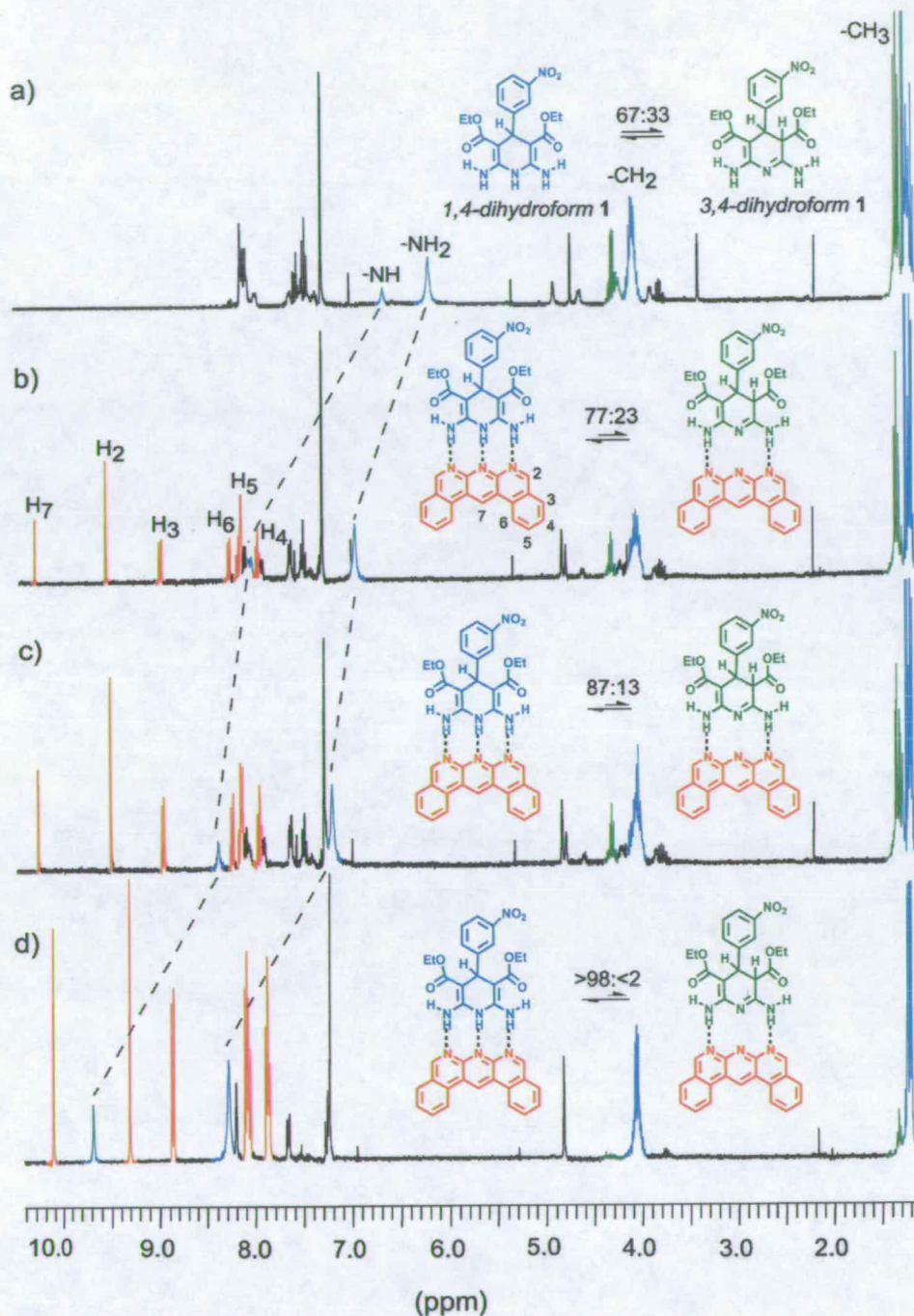
Figure 5.9 ^{1}H NMR (400 MHz, CDCl$_3$, 298 K) spectra of **1** (10^{-3} M^{-1}) in the (a) absence of **120**, (b) presence of 0.13 eq, (c) 0.25 eq and (d) 0.5 eq of **120**.

A further indication of the powerful hydrogen bonding accepting ability of the new heterocycles **106-120** is seen by direct comparison of the AA-DDD complexes in CDCl$_3$ at RT; **1•117** is >2 and **1•120** is >27 times stronger than **1•3** (Figure 1.32).
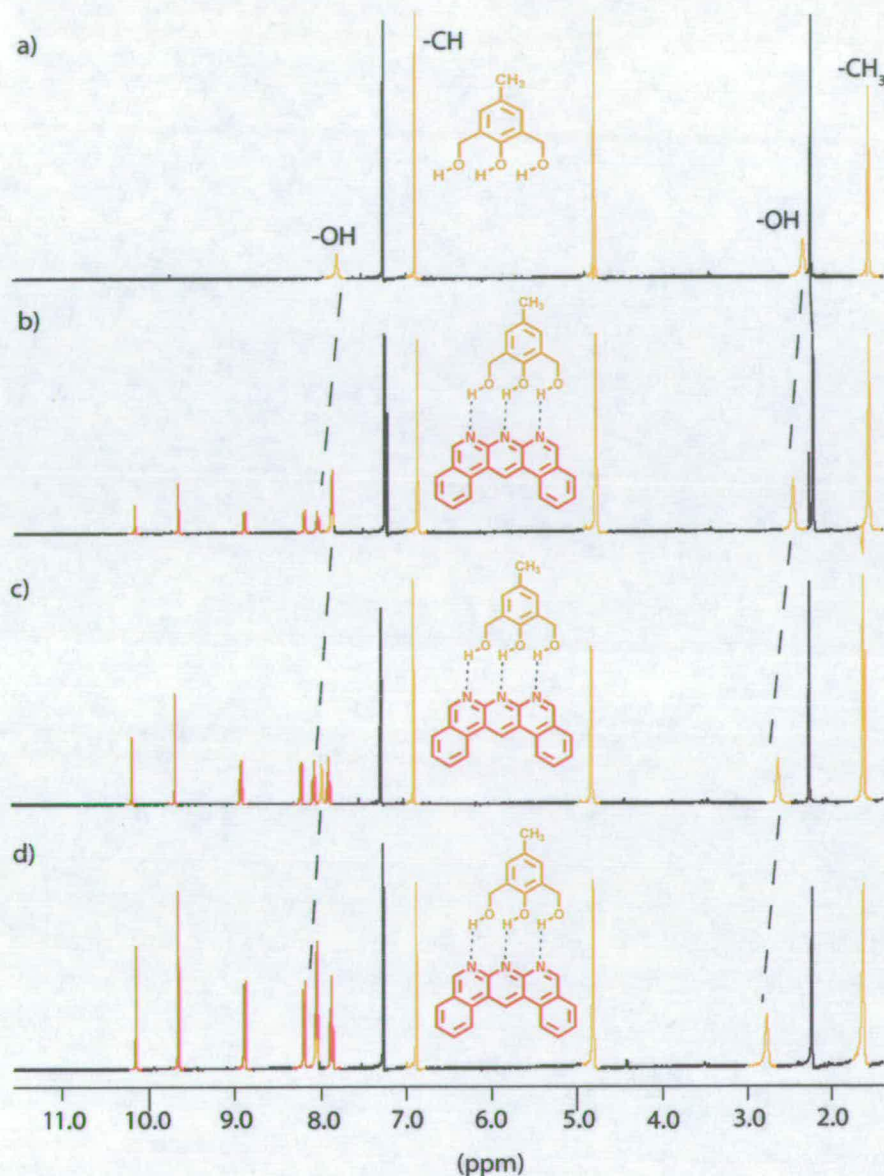
Figure 5.10 ^{1}H NMR (400 MHz, CDCl$_3$, 298 K) spectra of **124** (10^{-3} M^{-1}) in the (a) absence of **120**, (b) presence of 0.3 eq, (c) 0.45 eq and (d) 0.6 eq of **120**.

The two last ^{1}H NMR stack plots present the heterocomplexes **124•120** (Figure 5.10) and the cationic **125•120** (Figure 5.11). It was interesting that complex **124•120** has a high binding constant although hydroxyl groups have been used as H-bond donors. Hydroxyl groups are much poorer H-bond donors than amides, anilines, or pyrrole

like NH's,[131] and the hydroxyl protons of **124** are also involved in intramolecular H-bonding. It is therefore remarkable that the K_a for **124•120** is 2.4×10^4 M^{-1}.[132]
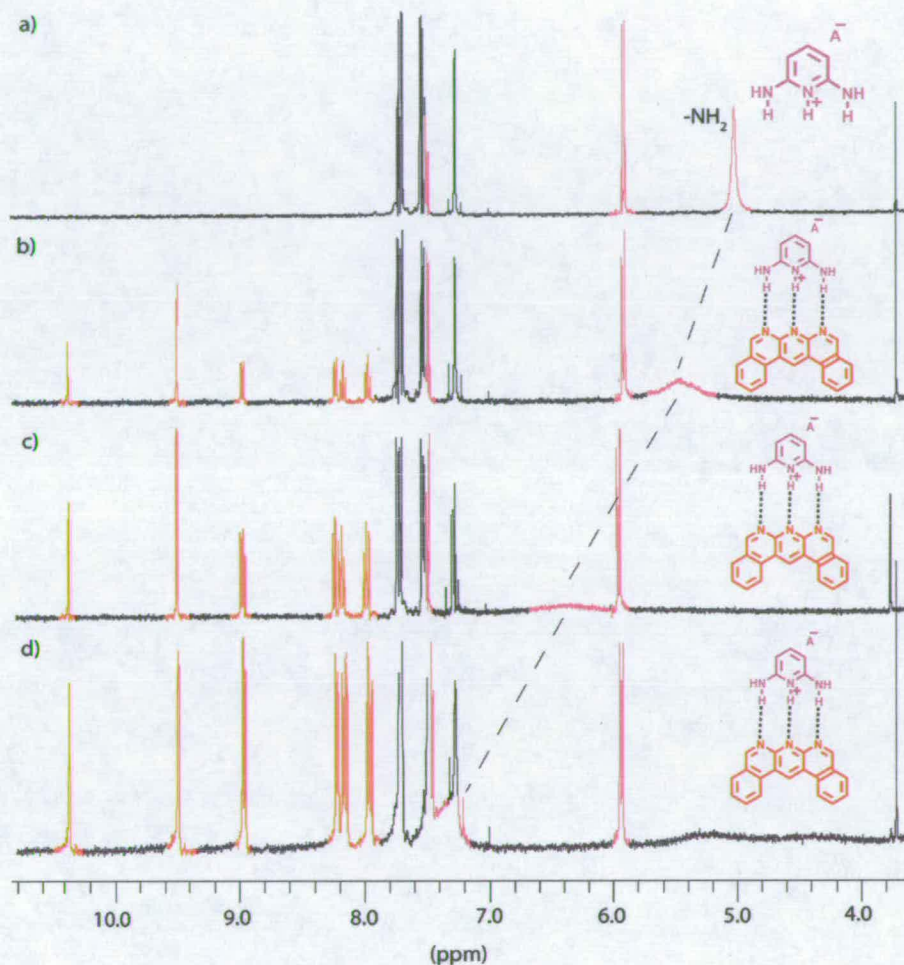
Figure 5.11 ^{1}H NMR (400 MHz, CDCl$_3$, 298 K) spectra of **125** (10^{-3} M^{-1}) in the (a) absence of **120**, (b) presence of 0.4 eq, (c) 0.5 eq and (d) 0.6 eq of **120**.

The last stack plot (Figure 5.11) is for the cationic AAA-DDD system **125•120**, following the –NH$_2$ proton to high frequency upon addition of **120** (10^{-3} M, 273 K, CDCl$_3$).

5.2.3 Fluorescence titration experiments

In order to determine more accurate K_a values for the **1•120**, **1•110** and **120•125** heterocomplexes, fluorescence spectroscopy was employed. Compounds **110**, **120** and **125** are fluorescent with fluorescent quantum yields of 0.94 for **120** and 0.25 for **110** in CH_2Cl_2 determined by standard methods,[18] while **1** is non-fluorescent. Fluorescence titrations were performed in CH_2Cl_2 at 293 K by adding a solution of **1** (10^{-7} M for **1•110** and 10^{-8} M) to **120** (initial concentrations 1×10^{-9} M) or **110** (10^{-8} M) and monitoring the increase in fluorescence intensity at 410 nm (for **1•120**) and 517 nm (for **1•110**).
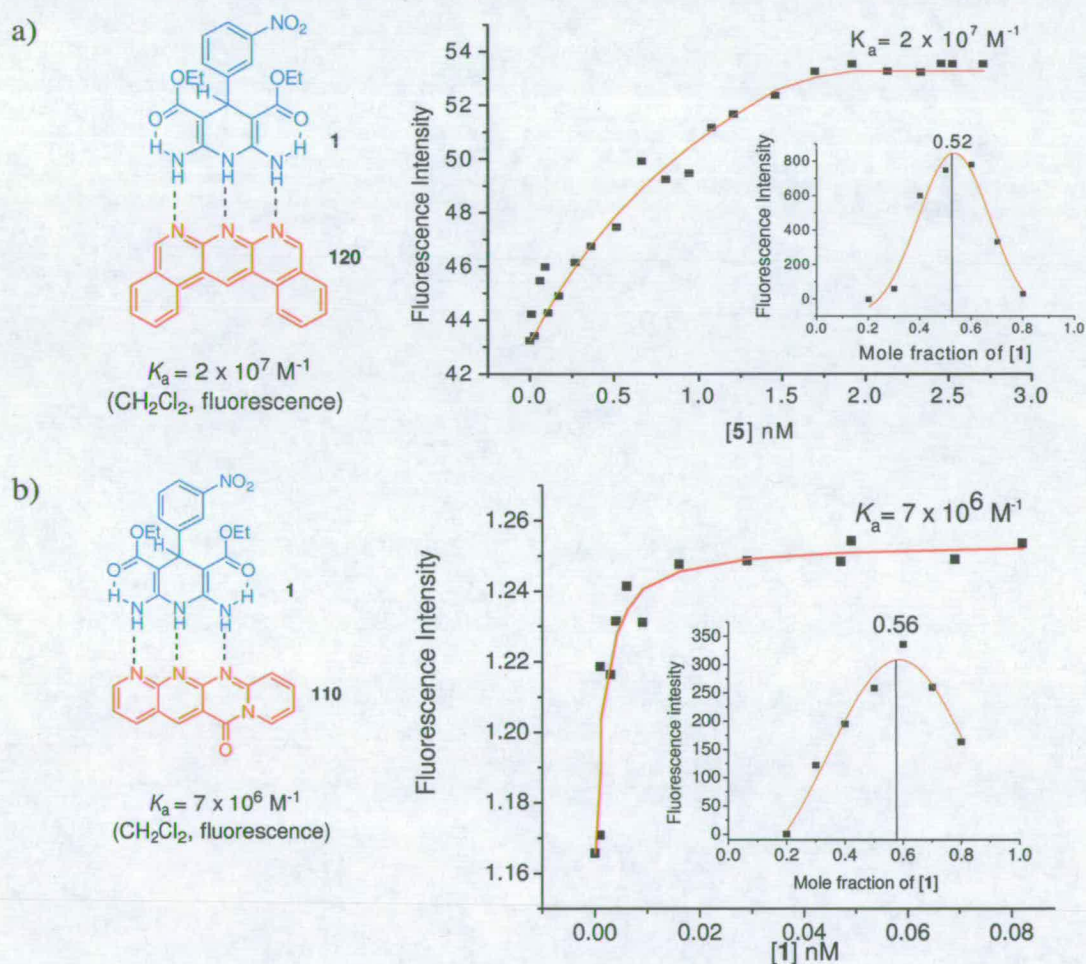
Figure 5.12 Fluorescence intensities of a) **120** (ca. 10^{-9} M) at 410 nm and b) **110** (ca. 10^{-9} M) at 517 nm in CH_2Cl_2 at 293 K upon addition of **1** (0→2 equiv.) using 1:1 complexation model. Insets: Job's plot under the same conditions as titration experiments.

144

A curve-fitting program[11] gave K_a values for **1•120** of 2×10^7 M^{-1} as previously reported[13] (Figure 5.12a) and 7×10^6 M^{-1} for the **1•110** complex (Figure 5.12b). Job's plot experiments confirmed the 1:1 stoichiometry for both complexes (See insets in Figure 5.12).

Although Job plot experiment confirmed 1:1 binding mode for **1•120** isosbestic points could not be seen during the fluorescence titration, so the titration experiment was repeated using UV-vis spectroscopy. Upon addition of **1** to **120** (ca. 10^{-5} M, CH$_2$Cl$_2$, 293 K) the absorption intensity at 395 nm increased with a clear isosbestic point at 390 nm, suggesting a 1:1 binding mode in this concentration range (Figure 5.13).
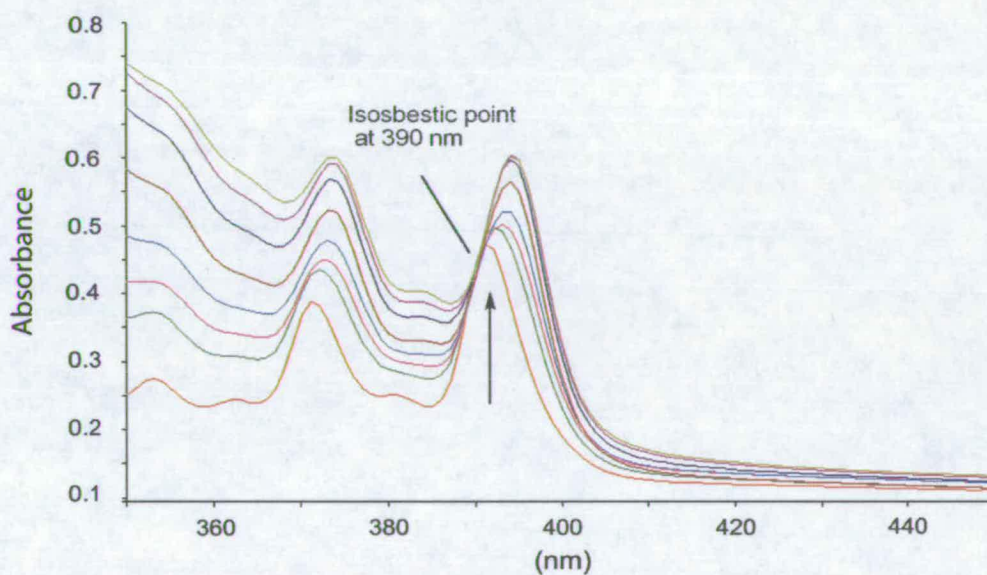
Figure 5.13 UV/vis spectra in CH$_2$Cl$_2$ at 293 K upon the addition of **1** (0→1.2 equiv) to **120** (1×10^{-5} M). The arrow indicates the change in absorption at 390 nm with increasing **120**.

It has been mentioned that complex **1•120** shows 1:2 binding mode at 10^{-3} M concentrations (^{1}H NMR titration exp.) but as seen when diluted 100 times (UV-vis titration exp.) or more (fluorescence titration exp. *ca* 10^{-9} M) the ratio is 1:1.

For heterocomplex **125•120** upon addition of **120** (*ca*. 10^{-9} M) to **125** (*ca*. 10^{-8} M) in CH$_2$Cl$_2$ at 293 K the fluorescence intensity at 360 nm decreased with one clear isosbestic point at 380 nm, suggesting a 1:1 binding mode in this concentration range (Figure 5.14). The same results have been confirmed by UV-vis experiments (ca. 10^{-5} M, CH$_2$Cl$_2$, 293 K) with an isosbestic point at 394.2 nm (Figure 5.15).
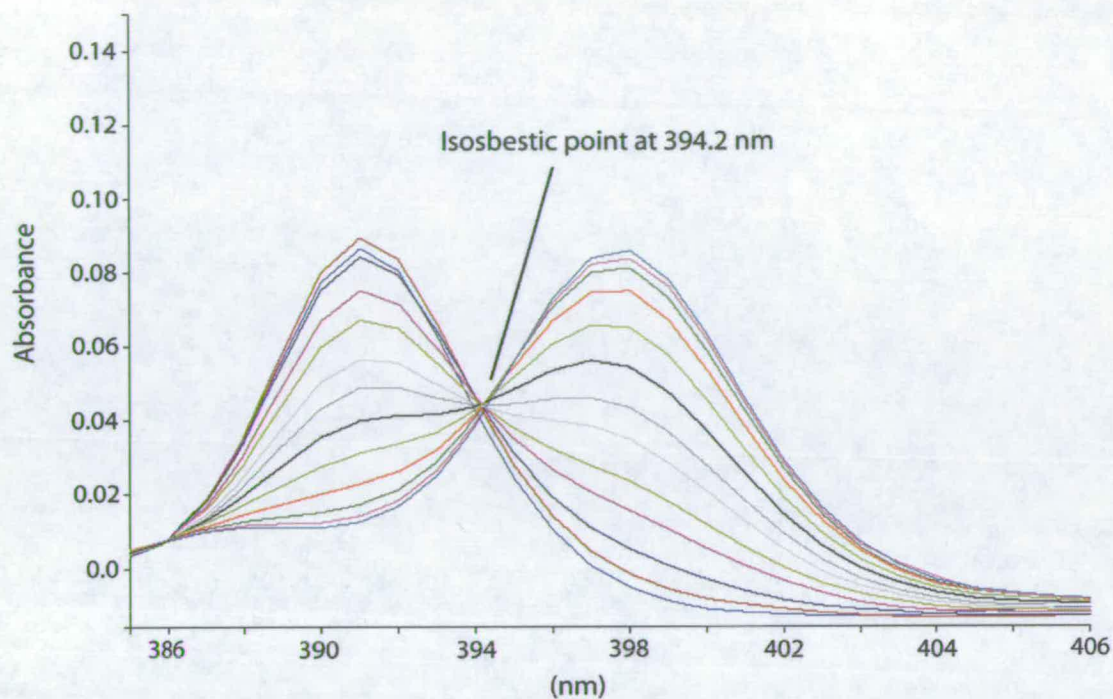
Figure 5.14 UV/vis spectra in CH_2Cl_2 at 293 K upon the addition of **125** (0→1.2 equiv) to **120** (1×10^{-5} M). Clear isosbestic point at 394.2 nm.
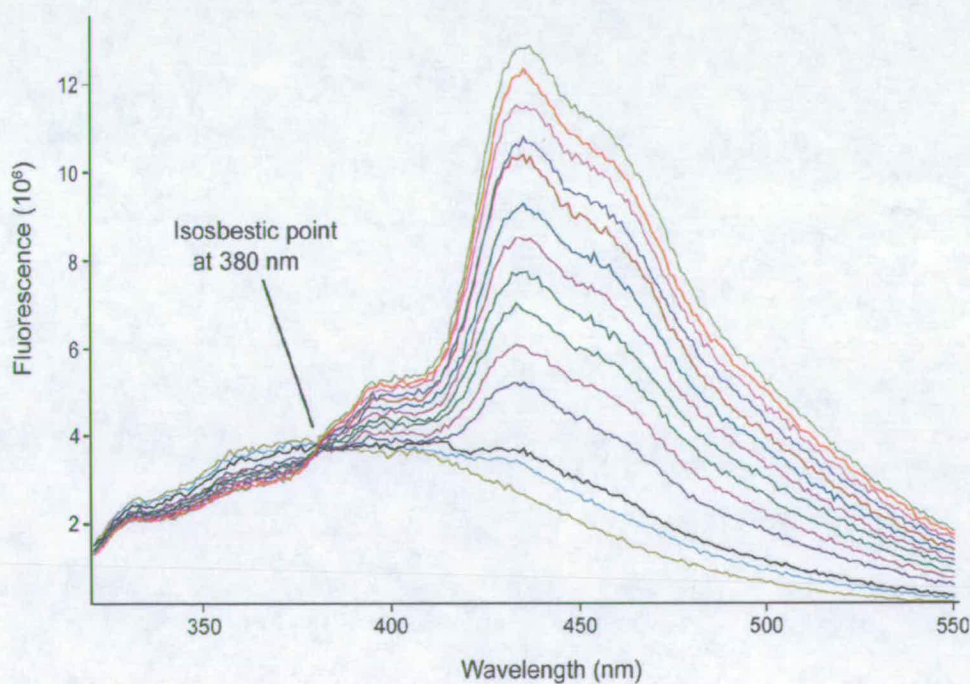
Figure 5.15 Fluorescence spectra of **125** (ca. 10^{-9} M) upon addition of **120** (0→ 2.5 equiv.) in CH_2Cl_2 at 293K with isosbestic point at 380 nm.

Plots of fluorescence intensity change as a function of the guest concentration **120** produced association constants 3.8×10^9 M^{-1} for the **125•120** heterocomplex (Figure 5.16) using the computer fitting program.[9] The Job plot experiments[74] were done under the same conditions as the titration experiments, confirming the 1:1 binding (max at mole ratio = 0.48).
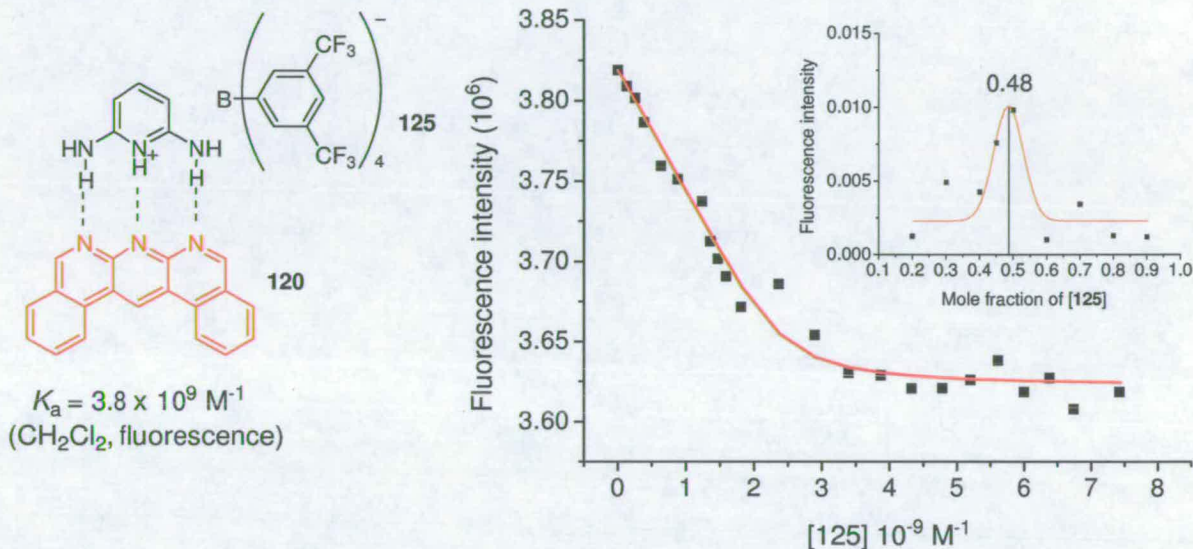
Figure 5.16 Fluorescence intensities of **125** (ca. 10^{-9} M) at 380 nm in CH$_2$Cl$_2$ at 293 K upon addition of **120** (0→2.5 equiv.) using 1:1 complexation model. Insets: Job's plot under the same conditions as titration experiments.

The very high binding constants of 3.8×10^9 M^{-1} (13.4 kcal/mol) is one of the highest reported for the triple hydrogen bonded complexes, when compared with the only cationic example **61•3** the K_a value for our system is 4 times higher than Aslyn's one. It should be noted that we measure binding strength using different methods, we employed fluorescence and Aslyn used UV-vis spectroscopy due to some indication that during fluorescence experiments excited state proton transfer has been seen as in some similar examples.[133]

The spectral changes during the UV-experiment were due to complex formation rather than solely proton transfer as reported by Aslyn. The pK_a values of 12.2 for **3** and 12.6 for **61** measured in non-aqueous solvents indicate that the complex should best be viewed as a cationic AAA-DDD system. The charged character of the

hydrogen bonds in this system is hypothesized to be perturbing the electronic structure of the chromophore **3** in a manner analogous to this complex.

Our results during fluorescence titrations for the **125•120** complex indicated that binding takes place with increasing fluorescence intensity, showing clear isosbestic points at 380 nm and 394.2 nm (by UV-vis) upon addition of **120** to **125**.

5.3 Structural studies

To assess the high binding constant for heterocomplex **1•120**, molecular modelling studies were done by Dr Francesco Zerbetto and Gilberto Teobaldi from University of Bologna. The heterocomplex has been modelled in vacuum and in CH_2Cl_2 solution to make comparison with experimental results obtained from fluorescence titration.

Geometry optimization and vibrational frequency calculations were carried out at _B3LYP/6-31G*_ level with Gaussian03 program[134] for **1•120** both in the vacuum and in CH_2Cl_2 solution. The solvent was modelled by the self-consistent reaction field method (SCRF),[135] with the dielectric permittivity set to the experimental value of 8.93. The radii of the cavities were 6.81, 5.62, 5.16 Å for **1•120**, **1**, and **120** and were determined from the electron density contours with a threshold set to 0.001 _e_ _bohr_$^{-3}$. This step was performed with the "Volume=tight" options switched on. The optimized **1•120** (in CH_2Cl_2) is pictorially represented in Figure 5.17. As reported for similar systems,[80, 136-139] the complex is not perfectly planar (see Table 5.2 and Figure 5.17b) with a larger deviation for the complex optimized in the absence of solvent. The calculated binding free energies, see Table 5.2, are in qualitative agreement with the experiments that give 9.8 kcal mol^{-1}. In particular, in the vacuum the calculated 9.0 kcal mol^{-1} underestimates the binding by nearly 10%, while in the solvent the binding free energy is overestimated by ~25%. Variation of the cavity radii by 5% allows one to provide an improved assessment of the free energy, which comes to 11.4 ± 2.3 kcal mol^{-1}.

The purely electrostatic binding energy is remarkably large. Upon going from the individual molecules to the complex, three rotational and translational degrees of freedom are changed into vibrational ones and become less thermally populated. This

affects the ΔG that is found to agree with the experimental one within the limitation of a implicit solvent description. The loss of external degrees of freedom can have profound effects, for instance, in protein association[140] and is also present here.

a)   b)
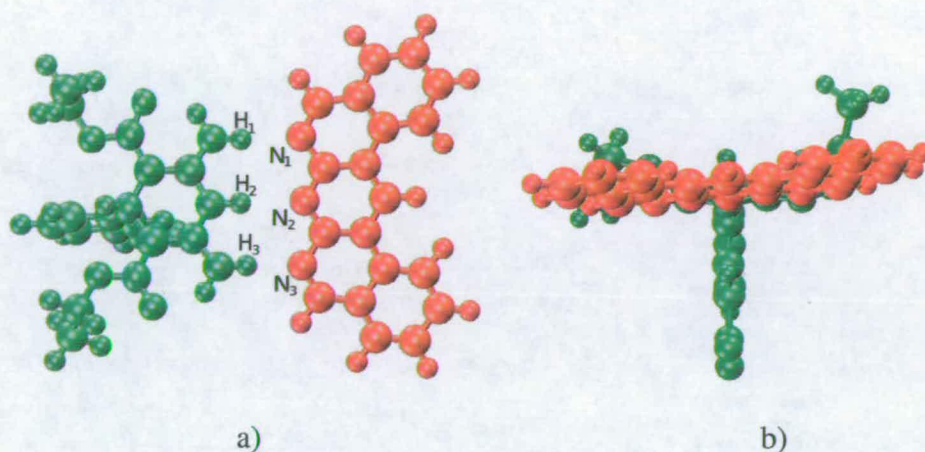
Figure 5.17. Calculated structure of **1•120** in CH_2Cl_2: a) front view and b) side view.

	$N_1 \cdots H_1$	$N_2 \cdots H_2$	$N_3 \cdots H_3$	H_1-N_1-N_3-H_3	E_{bind}	ΔH_{bind}	ΔG_{bind}
Vacuum	2.08 (172.2°)	2.21 (178.0°)	2.07 (176.8°)	-20.5°	-22.9	-20.9	-9.0
CH_2Cl_2	1.98 (172.0°)	2.26 (167.2°)	1.98 (172.5°)	-4.6°	-25.6±2.3	-23.3±2.3	-11.4±2.3

Table 5.2 Selected quantum chemical results for **1•120** in vacuum and CH_2Cl_2: $N_i \cdots H_i$ distances, Å, in brackets the hydrogen bond angles; Tilt dihedral angle (tilt angles, see pictures with the molecular orientation, are positive when the atoms are encountered clockwise); Electrostatic binding energy, E_{bind}, enthalpy, ΔH_{bind} and free energy, ΔG_{bind}, kcal mol^{-1}. Error bars of the calculation have been estimated changing (±5%) the cavity radius a_0.

5.4 Conclusion and discussion

In conclusion, very high binding constants were observed for all systems but particularly high binding stabilities in **120•1** and **110•1** heterocomplexes were found for neutral AAA-DDD heterocomplexes were found. The calculated K_a value determined by fluorescence spectroscopy gave good agreement with molecular modelling studies for the **120•1** heterocomplex. The cationic AAA-DDD system **120•125** was the tightest complex with $K_a = 3.8 \times 10^9$ M^{-1} determined by fluorescence spectroscopy. This is the first time that an accurate K_a value for a cationic AAA-DDD system has been determined. These findings and accurate determinations of binding constants showed that previous results[54, 15] underestimated K_a values of heterocomplexes (particularly cationic) in AAA-DDD arrangements.

5.5 Experimental section

2,6-Diaminopyridinium tetrakis[3,5-bis(trifluoromethyl)phenyl]borate (125)
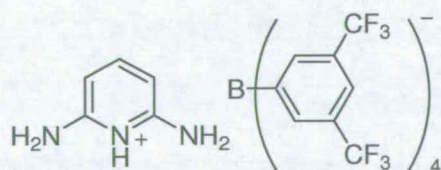
To a suspenstion of 2,6-diaminopyridine hydrochloride (2.5 mg, 0.017 mmol) in acetonitrile (5 cm^3) was added a solution of sodium tetrakis[3,5-bis(trifluoromethyl)phenyl]borate (20 mg, 0.0226 mmol) in acetonitrile (5 cm^3). The solution was warmed to 40 °C and stirred for 1h. The acetonitrile solution was filtered through celite to remove the NaCl precipitate. Addition of aliquots of CH$_2$Cl$_2$ (5 × 1 cm^3) followed by "pumping off" the CH$_2$Cl$_2$ was required to facilitate the removal of acetonitrile from the product. Salt **125** (11 mg, 75%) was collected as a gray/tan solid, mp 165-166 °C ^{1}H NMR (400 MHz, CDCl$_3$) δ ppm 7.70 (s, 8H, aryl

anion-), 7.53 (s, 4H, aryl anion-), 7.51 (t, *J*= 8.3 Hz, aryl cation-), 5.93 (d, *J*= 8.3 Hz, aryl cation) and 5.00 (s, br 4H, NH_2-). ^{13}C NMR (100 MHz, $CDCl_3$) δ ppm 157.9, 147.1, 98.2 (cation), 134.8, 121.2, 117.8, 111.9, 103.5 (anion). FAB-MS *m/z* 110 (MH^+, cation component).

^1H NMR Binding studies

^1H NMR binding studies were performed with a Bruker AV 400 NMR spectrometer at constant temperature (293 K), using $CDCl_3$ that had been dried over molecular sieves and stored under a dry N_2 atmosphere. A ^1H NMR binding study consists of incremental additions of small volume (3-100 mm^3) of a concentrated guest solution (mM) to a 600 mm^3 volume of a host solution (mM). No more than 10% volume change has been allowed. After each addition of titrant (the guest solution), the ^1H NMR spectrum of the system was recorded. Changes in the spectrum of the host were plotted against the concentration of the added guest. The guest concentration was known from the amount of guest solution added at the resulting volume change and/or from integration of each recorded ^1H NMR spectrum. The resulting isothermic curve was used to determine the association constant by fitting the curve with the specially developed *GasFit* program[129] based on an evolutionary algorithm (see Appendix 2) by solving the Equations (1)-(3).

(1) $$[HG] = \frac{1 + K[H]_0[G]_0 - \sqrt{\left\{(1+[H]_0[G]_0)^2 - 4K[H]_0[G]_0\right\}}}{2K}$$

(2) $$[H] = [H]_0 - [HG]$$

(3) $$\delta_{obs} = \frac{[HG]}{[H]_0}\delta_b + \frac{[H]}{[H]_0}\delta_f$$

$[H]_0$ - the total concentration of host;
$[G]_0$ - the total concentration of guest;
$[H]$ - concentration of unbound free host;
$[HG]$ - the concentration of host-guest complex;
K - the association constant for formation of host-guest complex;
δ_f - the free chemical shift of the host;
δ_b - the limiting bound chemical shift of the host-guest complex.

Fluorescence Binding Studies

The fluorescence experiments were performed using a Hitachi F-4500 spectrofluorimeter. The experiments were carried out in analytical grade dichloromethane at a constant temperature (293 K). A quartz cuvette capable of holding 4 cm^3 of sample and possessing a ground glass stopper was employed in all of the binding studies. A binding study consisted of incremental additions of small volume (3-100 cm^3) of a highly diluted guest solution (μM) to a 2 cm^3 volume of a host solution (μM). No more than 10% volume change has been allowed. After each addition of the guest, the fluorescence spectrum of the system was recorded along with the changes in fluorescence intensity. The guest concentration in the cuvette at each addition was calculated based on the guest's stock solution concentration. Changes in the fluorescence intensity were plotted against the guest concentration to obtain the binding isotherm. The fitting of the curve used to determine the association constant was calculated using the *GasFit* program[129] by solving Equation (4).

$$(4) \quad \frac{F}{F_0} = \frac{1+\left(k_{11}/k_s\right)K_{11}[L]}{1+K_{11}[L]}$$

F – Fluorescence intensity of complex
F_0 –Fluorescence intensity of the substrate
k_i – proportionality constant
K_{11}- the association constant for formation of 1:1 substrate-ligand complex
L- ligand

Job's plot experiments

The method of continuous variations (Job's plot method) was used to determine the stoichiometry of the complex (1:1, 1:2, *etc.*) using ^{1}H NMR or fluorescence spectroscopy. A series of solutions with constant total concentration of guest and host (mM or μM), together with guest concentration fractions, [G]/([G]+[H]), varying from about 0.1 to 0.9. Changes of chemical shifts or fluorescence intensities have been recorded for each solution and plotted against the molar fractions of [G]. The maximum of the plotted curve corresponds to the stoichiometry of the complex.

Job plot experiments
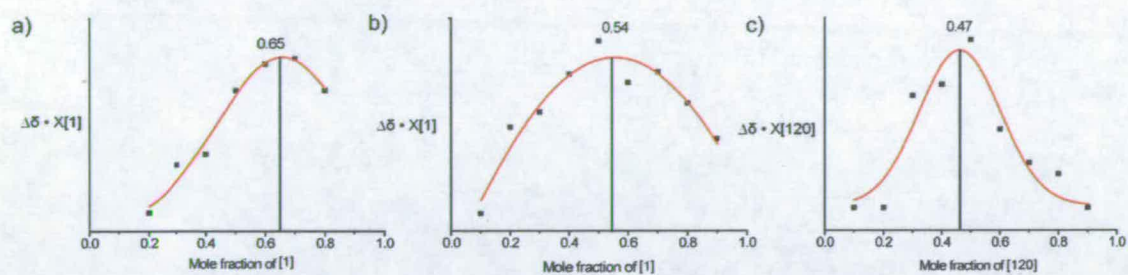
Figure 5.18 Job plot experiments performed at the same conditions as titration experiments using ^{1}H NMR technique and confirmed 2:1 binding mode for a) **120•1** and 1:1 binding mode for b) **117•1** and c) **124•120** heterocomplex.

Chapter 6:   Conclusions

Nature has provided a number of examples of hydrogen bonding interactions, particularly with the heteroaromatic hosts seen in RNA and DNA base pairings. This offers a special challenge for supramolecular chemists to synthesise heteroaromatic modules that can mimic properties and stabilities of naturally occurring molecules.

In the introduction of my thesis I discussed a number of heterocyclic units with triple linear arrays of hydrogen bonding sites in all possible arrangements. Some selected quadruple hydrogen bonding motifs were also mentioned as supramolecular polymer units, with some insight into properties and behaviour of supramolecular polymers.

The theoretical studies of Jörgensen showed that the hydrogen bonding pattern, acceptor, acceptor, acceptor – donor, donor, donor (AAA-DDD) provides the most stable binding array for three contiguous hydrogen bonding centres. However, the only experimental investigation of such a system to date comes from Zimmerman who determined *via* ^{1}H NMR spectroscopy that the AAA host 2,8-diphenyl-1,9,10-anthyridine (**3**) binds to a DDD guest (**1**) with an association constant greater than 10^5 M^{-1}. Since these studies, little progress in developing AAA-DDD hydrogen bonding motifs has been described. The limited number of AAA units in the literature and the stability problems during binding studies (as seen in the **1•3** heterocomplex) were taken into account before the synthesis of targets with AA and AAA modules began.

Three synthetic methodologies to obtain AA and AAA heteroaromatic units were used: Flash Vacuum Pyrolysis (Chapter 2), Buchwald-Hartwig coupling chemistry (Chapter 3) and Suzuki coupling chemistry (Chapter 4). The Flash Vacuum Pyrolysis (FVP) approach allowed the synthesis of naphthyridine ring systems in only two steps from substituted Meldrum's acid derivatives after cyclisation at high temperature. Different heteroaromatic compounds – predominantly double (DA and AA) and a few triple (DAD and AAD) hydrogen bonding units – were produced, but this technique was not applicable for formation of three annelated heterocyclic units in the AAA arrangement, due to volatility problems.

In the second approach, palladium catalyzed coupling was used to provide heterocyclic diarylamines from readily available pyridine or naphthyridine precursors, with subsequent ring closure under acidic conditions. This approach led to the synthesis of new compounds: dipyrido[1,2-*a*;2',3'-*a*]pyrimidin-5-one **106** (AA) and 1,6a,11,12–tetraaza-naphthacene-6-one **110** (an AAA hydrogen bonding unit) in high yields.

Suzuki coupling chemistry was used as the last synthetic route, obtaining dibenzo[*c*,*f*][1,8]naphthyridine **117** (AA) and 1,13,14-triazadibenz[*a*,*j*]anthracene **120** (AAA) which have extended aromatic frameworks to overcome stability problems during binding studies.

Binding studies of all AA and AAA units with the selected DDD counterparts: dihydropyridine **1**, 2,6-bis(hydroxy-methyl)-*p*-cresol **124** and protonated 2,6-diaminopyridine (with a lipophilic tetraarylborate counter-ion) **125** were described in chapter 5. Association constants for **1•117** (8.6×10^4 M^{-1}), **1•106** (6.2×10^3 M^{-1}) and **124•120** (2.4×10^4 M^{-1}) were determined by ^{1}H NMR titration experiments in chloroform-*d* solution. The K_a values for the AAA-DDD heterocomplexes **1•110**, **1•120** and **125•120** display very high binding stabilities ($K_a > 10^5$ M^{-1}) and they were determined using fluorescence spectroscopy. In this way, accurate assignment of $K_a = 1.4 \times 10^6$ M^{-1} for the **1•110** heterocomplex, $K_a = 2.6 \times 10^7$ M^{-1} for the **1•120** heterocomplex and $K_a= 3.8 \times 10^9$ M^{-1} for the cationic **125•120** heterocomplex were determined. Our experimental binding constants were in qualitative agreement with molecular modelling calculations for **1•110** and **1•120** heterocomplexes.

The extremely high binding stability found in the **125•120** heterocomplex was due to the combination of cooperative secondary interactions and strong electrostatic energy and the additional cationic charge. The most stable cationic AAA-DDD heterocomplex **125•120** reported in this thesis may be used as a supramolecular unit in the formation of pH controllable supramolecular polymers/copolymers.

Chapter 7:   References and Notes

1.   Zimmerman, S. C.; Corbin, P. S., _Structure and bonding.,_ **2000**, 96, 63.
2.   Breslow, R., _Chem. Bio._ **1998**, 5, R27.
3.   Eigen. M.; De Maeyer. L., _Nature.,_ **1966**, 53, 50.
4.   A., K., _Angew. Chem. Int. Ed. Engl._ **1983**, 22, 565.
5.   Capsomers- protein subunits of the viral structure
6.   Zimmerman, S.; Wu, W., _J. Am. Chem. Soc._ **1989**, 111, 8054.
7.   Hamilton, A.; Pant, N.; Muehldorf, A., _Pure. Appl. Chem._ **1988**, 60, 533.
8.   Kelly, T.; Maguire, M., _J. Am. Chem. Soc._ **1987**, 109, 6549.
9.   Kyogoku, Y.; Lord, R.; Rich, A., _Proc. Natl. Acad. Sci._ USA: **1967**, 57, 250.
10.   Bell, T.; Hou, Z.; Zimmerman, S.; Thiessen, P., _Angew. Chem. Int. Ed. Engl._
1995, 34, 2163.
11.   Stone, A. J., _The Theory of Intermolecular Forces._ Oxford, **1996**, 115.
12.   Jeffrey, G. A.; Saenger, W., _Hydrogen Bonding in Biological Structures._
Springer-Verlag: Berlin, **1991**.
13.   Scheiner, S., _Hydrogen bonding: A Theoretical Perspective._ Oxford
University Press: New York, **1997**.
14.   Wilcox, C. S.; Kim, E.; Romano, D.; Kuo, L. H.; Burt, A. L.; Curran, D. P.,
Tetrahedron **1995**, 51, 620.
15.   Zimmerman, S. C.; Murray, T. J., _Tetrahedron Lett._ **1994**, 35, 4077.
16.   Corbin, P. S.; Zimmerman, S. C.; Thiessen, P.; Hawryluk, N. A.; Murray, T.
J., _J. Am. Chem. Soc._ **2001**, 123, 10475.
17.   Jorgensen, W. L.; Pranata, J., _J. Am. Chem. Soc._ **1990**, 112, 2008.
18.   Pranata, J.; Wierschke, S. G.; Jorgensen, W. L., _J. Am. Chem. Soc._ **1991**, 113,
2810.
19.   Sartorius, J.; Schneider, H. J, _Chem. Eur. J._ **1996**, 2, 1446.
20.   Murray, T. J.; Zimmerman, S. C., _J. Am. Chem. Soc._ **1992**, 114, 4010.
21.   Cooperativity is a phenomenon in biology displayed by enzymes or receptors
that have multiple binding sites. When substrate bonds to the active site of one
enzymatic subunit, the rest of the subunits are stimulated and become active.
22.   Bisson, A. P.; Hunter, A. C., _Chem. Commun._ **1996**, 1723.
23.   Adams, H.; Carver, F. J.; Hunter, C. A.; Morales, J. C.; Seward, E. M.,
Angew. Chem. Int. Ed. Engl. **1996**, 108, 1628.
24.   Gong, B.; Yan, Y.; Zeng, H.; Skrzypczak-Jankunn, E.; Kim, Y. W.; Zhu, J.;
Ickes, H., _J. Am. Chem. Soc._ **1999**, 121, 5607.
25.   Hamilton, A.; Van Engen, D., _J. Am. Chem. Soc._ **1987**, 109, 5035.
26.   Park, T.; Schroeder, J.; Rebek, J. J., _J. Am. Chem. Soc._ **1991**, 113, 5125.
27.   Beijer, F.; Sijbesma, R. P.; Vekemans, J.; Meijer, E. W.; Koojiman, H.; Spek,
A., _J. Org. Chem._ **1996**, 61, 6371.
28.   Leonard, N.; McCredie, R.; Logue, M.; Cunddall, R., _J. Am. Chem. Soc._
1973, 95, 2320.
29.   Hamilton, A.; Little, D., _J. Chem. Soc. Chem. Commun._ **1990**, 297.
30.   Sessler, J.; Wang, R., _J. Org. Chem._ **1998**, 63, 4079.
31.   Kotera, M.; Lehn, J.; Vigneron, J., _Tetrahedron._ **1995**, 51, 1953.

32.   Hamilton, A.; Fan, E.; Van Arman, S.; Vicent, C.; Tellado, F.; Geib, S., _Supramolec. Chem._ **1993**, 1, 247.

33.   Fife, T. H.; Jaffe, S. H.; Natarajan, R., _J. Am. Chem Soc._ **1991**, 113, 7640.

34.   Beer, P. D.; Gale, P. A.; Smith, G. S., _Supramolecular Chemistry._ Oxford University Press: New York, **1999**.

35.   Kimizuka, N.; Kawasaki, T.; Hirata, K.; Kunitake, T., _J. Am. Chem. Soc._ **1995**, 117, 6360.

36.   Durham, A. C. H.; Finch, J. T.; Klug, A., _Nature._ **1971**, 229, 37.

37.   Kotera, M.; Lehn, J.; Vigneron, J., _J. Chem. Soc. Chem. Commun._ **1994**, 197.

38.   Kelly, T.; Bridger, G.; Zhao, C., _J. Am. Chem. Soc._ **1990**, 112, 8024.

39.   Berstein, J.; Sterns, B.; Shaw, E.; Lott, W., _J. Am. Chem. Soc._ **1974**, 69, 1151.

40.   Murray, T. J.; Zimmerman, S. C.; S.V., K., _Tetrahedron._ **1995**, 51, 635.

41.   Kral, V.; Sessler, J., _Tetrahedron._ **1995**, 51, 539.

42.   Hisatome, M.; Ikeda, K.; Kishibata, S.; Yamakawa, K., _Chem. Lett._ **1993**, 1357.

43.   Berman, A.; Izreali, E.; Levanon, H.; Wang, B.; Sessler, J., _J. Am. Chem. Soc._ **1995**, 117, 8252.

44.   Sessler, J.; Wang, B.; Harriman, A., _J. Am. Chem. Soc._ **1993**, 115, 10418.

45.   Sessler, J.; Wang, B., _Angew. Chem. Int. Ed. Engl._ **1998**, 37, 1726.

46.   Fenlon, E.; Murray, T.; Baloga, M.; Zimmerman, S., _J. Org. Chem._ **1993**, 58, 6625.

47.   Marsh, A.; Nolen, E.; Gardinier, K.; Lehn, J., _Tet. Lett._ **1994**, 35, 397.

48.   Kolotuchin, S.; Zimmerman, S., _J. Am. Chem. Soc._ **1998**, 120, 9092.

49.   Petersen, P.; Wu, W.; Fenlon, E.; Kim, E.; Zimmerman, S. C., _Bioorg. Med. Chem._ **1996**, 4, 1107.

50.   Marsh, M.; Silvestri, M.; Lehn, J. M., _Chem. Commun._ **1996**, 1527.

51.   Mascal, M.; Hext, N. M.; Wartmuth, R.; Moore, M. H.; Turkemburg, J. P., _Angew. Chem. Int. Ed._ **1996**, 35, 2204.

52.   Murray, T. J.; Zimmerman, S. C.; Kolotuchin, S. V., _Tetrahedron._ **1994**, 51, 635.

53.   Caluwe, P.; Majewicz, T., _J. Org. Chem._ **1977**, 42, 3410.

54.   Anslyn, E. V.; Bell, D. A., _Tetrahedron._ **1995**, 51, 7161.

55.   Adachi, K.; Sugiyama, Y.; Yoneda, K.; Nozaki, K.; Fuyuhiro, A.; Kawata, S., _Chem. Eur. J._ **2005**, 11, 6616.

56.   Beijer, F. H.; Kooijman, H.; Spek, A. L.; Sijbesma, R. P.; Meijer, E. W., _Angew. Chem. Int. Ed. Eng._ **1998**, 37, 75.

57.   Hirschberg, J. H. K. K.; Brunsveld, L.; Ramzi, A.; Vekemans, J.; Sijbesma, R. P.; Meijer, E. W., _Nature.,_ **2000**, 407, 167.

58.   Sijbesma, R. P.; Meijer, E. W., _Chem. Commun._ **2003**, 5.

59.   H, B. F.; Kooijman, H.; Spek, A. L.; Sijbesma, R. P.; Meijer, E. W., _Angew. Chem. Int. Ed._ **1998**, 110, 79.

60.   Rispent, M. T.; Sanchez, L.; Knol, J.; Hummelen, J. C., _Chem. Commun._ **2001**, 161.

61.   Gonzalez, J. J.; Gonzalez, S.; Priego, E. M.; Luo, C.; Guldi, D. M.; de Mendoza, J.; Martin, N., _Chem. Commun._ **1999**, 163.

62.   Folmer, B. J. B.; Sijbesma, R. P.; Kooijman, H.; Spek, A. L.; Meijer, E. W., _J. Am. Chem. Soc._ **1999**, 121, 9001.

63.   Bostman, A. W.; Sijbesma, R. P.; Meijer, E. W., _Materials Today._ **2004**, 34.

64.   Sijbesma, R. P.; Beijer, F. H.; Brunsveld, L.; Folmer, B. J. B.; Ky Hirschberg, J. H., _Science._ **1997**, 278, 1601.

65.   Sontjes, S. H. M.; Sijbesma, R. P.; van Genderen, M. H. P.; Meijer, E. W., _Macromolecules._ **2001**, 34, 3815.

66.   Sijebesma, R.; Beijer, F.; Brunsveld, L.; Folmer, B. J. B.; Hirschberg, J. H. K. K.; Lange, R. F.; Lowe, J. K. L.; Meijer, E. W., _Science._ **1997**, 278, 1601.

67.   Hirschberg, J. H. K. K.; Beijer, F. H.; van Aert, H. A.; Magusin, P. C. M. M.; Sijbesma, R. P.; Meijer, E. W., _Macromolecules._ **1999**, 32, 2696.

68.   Folmer, B. J. B.; Sijbesma, R. P.; Versteegen, R. M.; van der Rijt, J. A. J.; Meijer, E. W., _Adv. Materials._ **2000**, 12, 874.

69.   Corbin, P. S.; Zimmerman, S. C., _J. Am. Chem. Soc._ **1998**, 120, 9710.

70.   IUPAC, _Compendium of Chemical Terminology._ **1993**, 65, 2407.

71.   Yranzo, G. I.; Moyano, E. L., _Current Org. Chem._ **2004**, 8, 1071.

72.   Rao Ramana, V. V.; Wenrup, C., _J.Chem. Soc. Perkin Trans._ **1998**, 2583.

73.   Briehl, H.; Lukosch, A.; Wentrup, C., _J. Org. Chem._ **1984,** 49, 2772.

74.   Bruneau, E.; Lavabre, D.; Levy, G.; Micheau, J. C., _J. Chem. Educ._ **1992**, 69, 1992.

75.   Clarke, D.; W. Mares, R.; McNab, H., _J. Chem. Soc. Perkin Trans. 1,_ **1997**, 1799.

76.   Zicane, D.; Raviniya, I.; Tetere, Z.; Rijkure, I.; Gudriniece, E.; Kalejs, U., _J. Heterocyc. Comp._ **2000**, 36, 754.

77.   Rebek, J. J., _Angew. Chem. Int. Ed. Engl._ **1990**, 29, 245.

78.   Blake, A. J.; McNab, H.; Morrow, M.; Rataj, H., _J. Chem. Soc. Chem. Commun._ **1993**, 840.

79.   Jourdain, F.; Pommelet, _Synth. Commun._ **1997**, 27, 483.

80.   Kabelac, M.; Hobza, P., _J. Phys. Chem. B._ **2001**, 105, 5804.

81.   Derbyshire, P. A.; Hunter, G. A.; McNab, H.; Monahan, L. C., _J. Chem. Soc. Perkin Trans._ **1993**, 2017.

82.   McNab, H.; Monahan, L. C., _J. Chem. Soc. Perkin Trans. 1._ **1988**, 1, 863.

83.   Vencato, I.; Cunha, S.; Ferrari, J.; Sabino, J. R., _Acta Crystallographica Section E._ **2006**, E62, o4062.

84.   Rupert, K. C.; Henry, J. R.; Dodd, J. H.; Wadsworth, S. A.; Cavender, D. E.; Druie, E.; Olini, G. C.; Fahmy, B.; Siekierka, J. J., _Bioorg. Med. Chem. Lett._ **2003**, 13, 347.

85.   Cassis, R.; Tapia, R.; Valderamma, A., _J. Synth. Commun._ **1984**, 15, 125.

86.   Hurd, C. D., _Organic Synthesis._ **1941**; Collective Volume I, 330.

87.   Morak, B.; Pluta, K.; Suwinska, K.; Grymel, M.; Besnard, C.; Schiltz, M.; Kloc, C.; Siegrist, T., _Heterocycles_ **2005**, 65, 2619.

88.   Hong, F.; Hollenback, D.; Singer, J. W.; Klein, P., _Bioorg. Med. Chem. Lett._ **2005**, 15, 4703.

89.   Hovinen, J.; Turku Site, _Tet. Lett._ **2004**, 45, 5707.

90.   Azzouz, R.; Bischoff, L.; Fouquet, M.-H.; Marsais, F., _Synlett._ **2005**, 2808.

91.   Andres, P. R.; Hofmeier, H.; Lohmeijer, B. G. G.; Schubert, U. S., _Synthesis._ **2003**, 2865.

92.   Velasco, T.; Lecollinet, G.; Ryan, T. D., _Org. Biomol. Chem._ **2004**, 2, 645.

93.   Crawford, L. A. _PhD Thesis_, The University of Edinburgh, Edinburgh, **2002**.

94.   March, J., _Advanced Organic. Chemistry._ **1985**, 228.

95.   Comins, D., L; Jianhua, G., _Tet. Lett._ **1994**, 35, 2819.

96.   Comins, D., L; LaMunyon, D., H, *Tet. Lett.* **1988**, 29, 773.

97.   Connors, K. A., *Binding Constants: The Measurement of Molecular Complex Stability.* Wiley-Interscience: New York, **1987**; 24 and 141.

98.   Guillier, F.; Nivoliers, F.; Bourguignon, J.; Dupas, G.; Marsais, F.; Godard, A.; Quequiner, G., *Tet. Lett.* **1992**, 33, 7355.

99.   Dowtherm A- eutectic mixture of 26.5% diphenyl + 73.5% diphenyl oxide.

100.   Huang., X.; *J. Org. Chem.* **2002**, 67, 6731.

101.   Ye, F. C.; Chen, B. C.; Huang, X., *Synthesis.* **1989**, 317.

102.   Lesher, G. (Sterling Drug), USA Patent, **1975**, 3907798, 84, 44130.

103.   Sucharda, *J. Chem. Soc.* **1928**, 98, 2948.

104.   GB Patent, (Sterling Drug), **1969**, 1147759, 71, 70125j.

105.   Carboni, S.; Dasettim.A; Tonetti, I., *J. Heterocy. Chem.* **1970**, 7, 875.

106.   Madhavi, N. N. L.; Senthivel, P.; Nangia, A., *J. Phys. Org. Chem.* **1999**, 12, 665.

107.   Gorecki, D. K. J.; Hawes, E. M., *J. Med. Chem.* **1977**, 20, 124.

108.   Fulop, F.; Huber, I.; Dombi, G.; Bernath, G., *Tetrahedron.* **1987**, 43, 1160.

109.   Wolfe, J. P.; Ahman, J.; Sadighi, J. P.; Singer, R. A.; Buchwald, S. L., *Tet. Lett.* **1997**, 38, 6367.

110.   Wolfe, J. P.; Wagaw, S.; Buchwald, S. L., *J. Am. Chem. Soc.* **1996**, 118, 7215.

111.   Driver, M.; Hartwig, J., *J. Am. Chem. Soc.* **1996**, 118, 7217.

112.   Beller, M., *Angew. Chem. Int. Ed. Engl.* **1995**, 34, 1316.

113.   Yang, B.; Buchwald, S. L., *J. Organomet. Chem.* **1999**, 576, 125.

114.   Wolfe, J. P.; Buchwald, S. L., *J. Org. Chem.* **2000**, 65, 1144.

115.   Yin, J.; Zhao, M. M.; Huffman, M. A.; McNamara, J. M., *Org. Lett.* **2002**, 4, 3481.

116.   Kalinowski, J.; Rykowski, A.; Nantka-Namirski, P., *Polish Journal of Chemistry.* **1984**, 58, 125.

117.   Duffy, E. F.; Foot, J. S.; McNab, H.; Miligan, A. A., *Org. Biomol. Chem.* **2004**, 2, 2077.

118.   Gaber, A. M.; McNab, H., *Synthesis.* **2001**, 14, 2059.

119.   Majewich, T. G.; Caluwe, P. P., *J. Org. Chem.* **1974**, 39, 720.

120.   Miyaura N; A., S., *Tet. Lett.* **1979**, 3437.

121.   Miyaura N; Suzuki, A., *Chem. Rev.* **1995**, 95, 2457.

122.   McMillan, F. *PhD Thesis.* University of Edinburgh, **2007**.

123.   Djurdjevic, S.; Leigh, D. A.; McNab, H.; Parson, S.; Teobaldi, G.; Zerbetto, F., *J. Am. Chem. Soc.* **2006**, 129, 476.

124.   McNab, H.; Smith, G. S., *J. Chem. Soc. Perkin Trans. 1.* **1984**, 381.

125.   Park, T.; Mayer, M. F.; Nakashima, S.; Zimmerman, S. C., *Synlett.* **2005**, 9, 1435.

126.   Koradin, C.; Dohle, W.; Rodriguez, A. L.; Schmid, B.; Knochel, P., *Tetrahedron.* **2003**, 59, 1571.

127.   Atwood, J. L.; Davies, J. E.; Macnicol, D. D.; Vogtle, F., *Comprehensive Supramolecular Chemistry.* Oxford, UK, **1996**; 8, 426.

128.   Likussar, W.; Boltz, D. F., *Anal. Chem.* **1971**, 43, 1265.

129.   Djurdjevic, D., *GAs-Fit (www.djurdjevic.org.uk/software/GAsFit).* **2005**; A custom-written program, suitable even for large binding constants, that uses an evolutionary algorithm to solve the standard equations for titration methods. In tests,

for data in the Ka= 10^2-10^5 M^{-1} range, GAs-Fit gave similar results to the binding constant determination program available from the group of H.-J. Schneider (www.uni-saarland.de/fak8/schneider/Links/download.html).

130.   Wilcox, C. S., Schneider, H. J. Durr, H. *Frontiers in Supramolecular Organic Chemistry and Photochemistry,* New York, **1991**, 123.

131.   Hunter, C. A., *Angew. Chem. Int. Ed. Engl.* **2004,** 43, 5310.

132.   There is no evidence of deprotonation of **120** by **124** in UV/vis spectra.

133.   Balzani, V.; Scandola, F., *Supramolecular Photochemistry.* New York, **1991**, 342.

134.   Frisch, M. J.; Trucks, G. W.; Schlegel, H. B.; Scuseria, G. E.; Robb, M. A.; Cheeseman, J. R.; Montgomery, J., J. A.; Vreven, T.; Kudin, K. N.; Burant, J. C.; Millam, J. M.; Iyengar, S. S.; Tomasi, J.; Barone, V.; Mennucci, B.; Cossi, M.; Scalmani, G.; Rega, N.; Petersson, G. A.; Nakatsuji, H.; Hada, M.; Ehara, M.; Toyota, K.; Fukuda, R.; Hasegawa, J.; Ishida, M.; Nakajima, T.; Honda, Y.; Kitao, O.; Nakai, H.; Klene, M. L., X.; Knox, J. E.; Hratchian, H. P.; Cross, J. B.; Bakken, V.; Adamo, C.; Jaramillo, J.; Gomperts, R.; Stratmann, R. E.; Yazyev, O.; Austin, A. J.; Cammi, R.; Pomelli, C.; Ochterski, J. W.; Ayala, P. Y.; Morokuma, K.; Voth, G. A.; Salvador, P.; Dannenberg, J. J.; Zakrzewski, V. G.; Dapprich, S.; Daniels, A. D.; Strain, M. C.; Farkas, O.; Malick, D. K.; Rabuck, A. D.; Raghavachari, K.; Foresman, J. B.; Ortiz, J. V.; Cui, Q.; Baboul, A. G.; Clifford, S.; Cioslowski, J.; Stefanov, B. B.; Liu, G.; Liashenko, A.; Piskorz, P.; Komaromi, I.; Martin, R. L.; Fox, D. J.; Keith, T.; Al-Laham, M. A.; Peng, C. Y.; Nanayakkara, A.; Challacombe, M.; Gill, P. M. W.; Johnson, B.; Chen, W.; Wong, M. W.; Gonzalez, C.; Pople, J. A., *Gaussian 03.* **2004**.

135.   Wong, M. W.; Wiberg, K. B.; Frisch, M. J., *J. Am. Chem. Soc.* **1992**, 114, 1645.

136.   Hobza, P.; Sponer, J., *Chem. Rev.* **1999**, 99, 3247.

137.   Sponer, J.; Hobza, P., *J. Am. Chem Soc.* **1994**, 116, 709.

138.   Sponer, J.; Kypr, J., *Int. J. Biol. Macromol.* **1994**, 16, 3.

139.   Spirko, V.; Sponer, J.; Hobza, P., *J. Chem. Phys.* **1997**, 106, 1472.

140.   Minh, D. D. L.; Bui, J. M.; Chang, C. E.; Jain, T.; Swanson, J. M. J.; McCammon, J. A., *Biophys. J.* **2005**, 89, L25.

141.   Goldberg, D. E., *Genetic Algorithms.* Addison Wesley Longman, Reading, Massachussets. **1989**.

142.   Schwefel, P. H. *Evolutionsstrategie und numerische Optimierung.* Technische Universitat Berlin., **1975**.

143.   Djurdjevic, D. *PhD Thesis*, The University of Edinburgh, Edinburgh, **2006**.

144.   Mammen, M.; Simanek, E.E.; Whitesides, G.M.; *J. Am. Chem, Soc.* **1996**, 118, 12614.

Appendix 1: Glossary of synthesized compounds

This appendix will cover all synthesized AA and AAA hydrogen bonded systems and the chapters where these can be found. Highlighted in red are all those used in the binding studies.

We present all DDD counterparts used in binding studies and the AA-DDD and AAA-DDD heterocomplexes studied in this thesis.

AA Hydrogen bonded systems
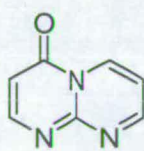
85
Chapter 2
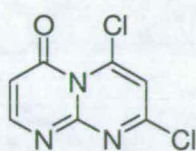
90
Chapter 2
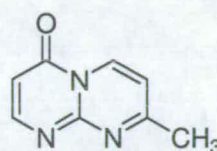
92
Chapter 2
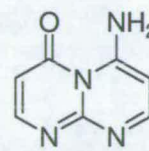
87
Chapter 2
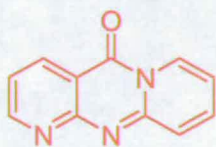
106
Chapter 3
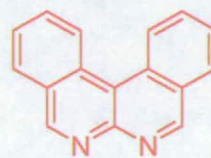
117
Chapter 4

AAA Hydrogen bonded systems
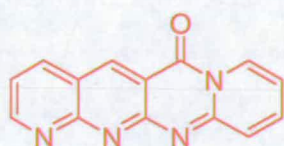
110
Chapter 3
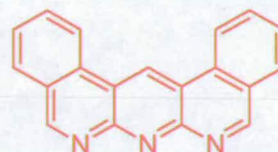
120
Chapter 4

DDD Hydrogen bonded systems
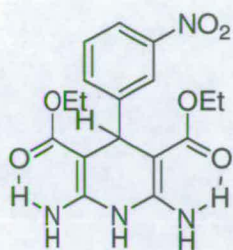
1
Chapter 5
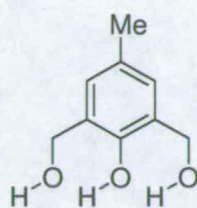
124
Chapter 5
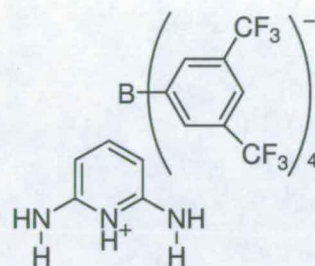
125
Chapter 5

AA-DDD Hydrogen bonded heterocomplexes
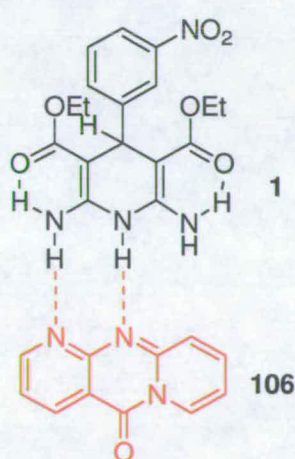
1·106
Chapter 5
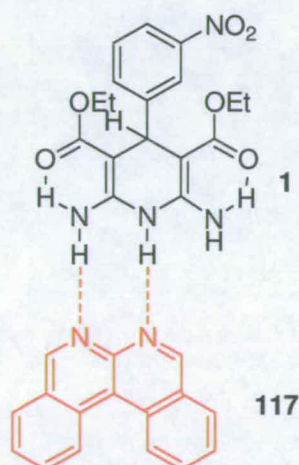
1·117
Chapter 5

AAA-DDD Hydrogen bonded heterocomplexes
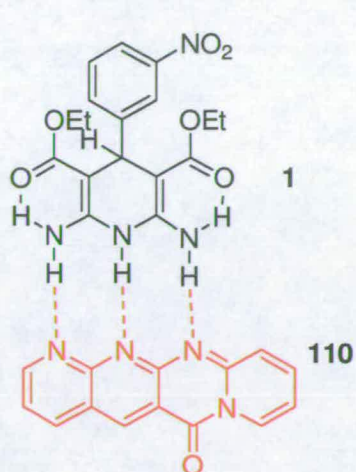
1•110
Chapter 5
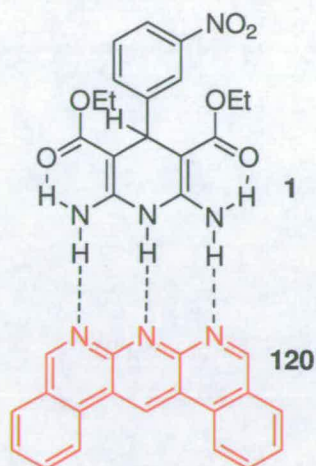
1•120
Chapter 5
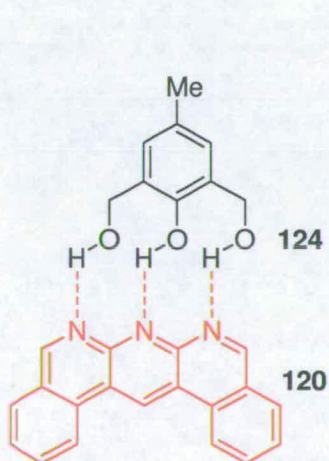
124•120
Chapter 5
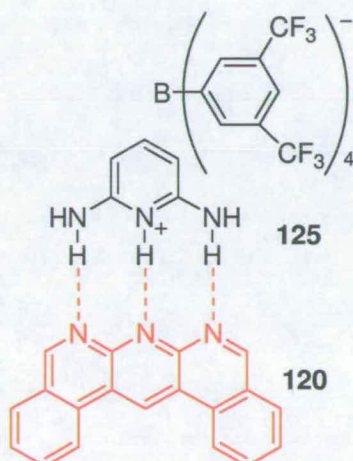
125•120
Chapter 5

Appendix 2:

Custom-written program _GasFit_ was designed by Dr Dusan Djurdjevic and it is suitable for determination of large association constants (K_a) using an evolutionary algorithms to solve the standard equations (1)-(4) (see Chapter 5.5) for titration methods.

Evolutionary algorithms (EAs) are a class of optimization methods based on the principles of evolution[141-143] and are widely used as a global optimization technique ranging from stock market predictions and portfolio planning to biochemistry, signal processing to artificial intelligence. Main advantages of EAs over other popular optimization methods include:

- The parameter space needs not to be continuous at any level.
- Derivatives of the 'object function' are not required.
- Population of solutions is created.
- It is capable of avoiding local minima going towards the global optimum.
- Can be used on extremely non-linear problems where other methods fail.

Considering EAs stochastic nature, usually EAs are coupled with local optimization methods (Marquardt-Levenberg, BFGS, Newton-Raphson, Simplex ...) where EAs are used to obtain first guesses and local optimizer is applied afterwards to distil the end result.

All other programs used to calculate binding constants employ one (or more) of the local optimization methods, and for high values of binding constants it was not possible to obtain a good result. Of course, results obtained from GasFit were later verified using other programs (_ie_. Origin, SigmaPlot).

GAsFit 2.3b - Project: AAb-DDD [Fit: AAb-DDD nmr]

Files Tools Help

New   Open   Save   Settings   Program For Fitting Experimental Data using GAs

Data :

X	Y
0	6.3112
3	6.4242
8	6.5264
13	6.6035
23	6.678
43	6.7468
73	6.8194
123	6.8428
323	6.8655
523	6.8958
723	6.8996

Fitting Model:

Adsorption
Exponential
Ligand Binding
Polynomial

Fluorescence 1:1
Fluorescence 1:1 general
Fluorescence 1:1 v1
Fluorescence 1:1 v2
Fluorescence 1:1 v3
NMR 1:1
NMR 1:2

Model Info :

Determination of Ligand Binding [1:1] using NMR

$$\Delta = \frac{\Delta_{11}K_{11}[L]}{1+K_{11}[L]}$$

$$\Delta = \delta - \delta_S$$

$$\Delta_{11} = \delta_{complex} - \delta_S$$

Parameters :

Var	Fix	Min	Max	Result
Co,h	☑	2.216E-5	100	2.216E-5
Vo,h	☑	600	100	600
shift,h	☑	6.3112	10	6.3112
Co,g	☐	8.223E-5	1	0.0078927
K	☐	1	10000	6244.6
shift,cplx	☐	6.5	6.9	6.9

Graph :

Import Data   Clear Data

Linear Object Function   Execute

Fits: Add Fit   Remove Fit   Messages: clear

AAb-DDD nmr

```
----------------------------------------
Gradient Method Results:
----------------------------------------
       Co,h =        2.216E-005
       Vo,h =               600
     shift,h =           6.3112
       Co,g =         0.0078927
         K =            6244.6
  shift,cplx =              6.9
----------------------------------------


Chi_Sqr =  1.113E-002
########################################
```

GasFit results of 1•106 complex

(^{1}H NMR, CDCl$_3$, 293K)

```
################################################################################
#! GAsFit Generated File: author: Dusan P Djurdjevic                           #
# Project Name: AAb-DDD                                                         #
# Fit Name:     AAb-DDD nmr                                                     #
#                                                                              #
# Model Used:   Ligand Binding->NMR 1:1                                         #
# Model Info:   Determination of Ligand Binding (1:1) using NMR                 #
#                                                                              #
# --------- PARAMETERS: ---------                                              #
#       Co,h = 2.216E-005                                                       #
#       Vo,h = 600                                                              #
#       shift,h = 6.3112                                                        #
#       Co,g = 0.0078927                                                        #
#       K = 6244.6                                                              #
#       shift,cplx = 6.9                                                        #
# --------------------------------                                             #
################################################################################
```

Volume added	Y(exp)	Y(fit)
0	6.3112	6.3112
3	6.4242	6.4175
8	6.5264	6.5314
13	6.6035	6.6024
23	6.678	6.6847
43	6.7468	6.7597
73	6.8194	6.8057
123	6.8428	6.8366
323	6.8655	6.8676
523	6.8958	6.8753
723	6.8996	6.8789

GAsFit 2.3b - Project: 10X less AA-DDD [Fit: prave vrednosti]

Files   Tools   Help

New   Open   Save   Settings   Program For Fitting Experimental Data using GAs

Data :

X	Y
0	6.07242
5E-6	6.09474
1E-5	6.27086
2E-5	6.3687
3E-5	6.41304
4E-5	6.51088
5E-5	6.55063
7E-5	6.59161
9E-5	6.639
0.00011	6.65429
0.00013	6.65337
0.00018	6.65582
0.00023	6.66162
0.00028	6.66162

Fitting Model:

Adsorption	Fluorescence 1:1
Exponential	Fluorescence 1:1 general
Ligand Binding	Fluorescence 1:1 v1
Polynomial	Fluorescence 1:1 v2
	Fluorescence 1:1 v3
	NMR 1:1
	NMR 1:2

Parameters :

Var	Fix	Min	Max	Result
Co,h	☑	0.00047	100	0.00047
Vo,h	☑	0.001	0.005	0.001
shift,h	☑	6.07242	10	6.0724
Co,g	☐	0.00435	0.009	0.009
K	☐	10000	500000	85992
shift,cplx	☐	1	7	6.6672

Model Info :

Determination of Ligand Binding [1:1] using NMR

$$\Delta = \frac{\Delta_{11} K_{11}[L]}{1 + K_{11}[L]}$$

$$\Delta = \delta - \delta_S$$

$$\Delta_{11} = \delta_{complex} - \delta_S$$

Graph :

Linear Object Function   ☑   Execute

Import Data   Clear Data

Fits   Add Fit   Remove Fit

prave vrednosti

Messages:

```
---------------------------------------
Gradient Method Results:
---------------------------------------
        Co,h =          0.00047
        Vo,h =          0.001
     shift,h =          6.0724
        Co,g =          0.009
           K =          85992
 shift,cplx =          6.6672
---------------------------------------


Chi_Sqr =   3.516E-002
########################################################
```

clear

```
###############################################################################
#! GAsFit Generated File: author: Dusan P Djurdjevic              #
# Project Name: 10X less AA-DDD                                   #
# Fit Name:      prave vrednosti                                  #
#                                                                 #
# Model Used:    Ligand Binding->NMR 1:1                          #
# Model Info:    Determination of Ligand Binding (1:1) using NMR  #
#                                                                 #
# --------- PARAMETERS: ----------                                #
#         Co,h = 0.00047                                          #
#         Vo,h = 0.001                                            #
#         shift,h = 6.0724                                        #
#         Co,g = 0.009                                            #
#         K = 85992                                               #
#         shift,cplx = 6.6672                                     #
# --------------------------------                                #
###############################################################################
```

Volume added	Y(exp)	Y(fit)
0	6.0724	6.0724
5.	6.0947	6.1278
10	6.2709	6.1829
20	6.3687	6.2915
30	6.413	6.396
40	6.5109	6.4915
50	6.5506	6.5663
70	6.5916	6.6305
90	6.639	6.6468
110	6.6543	6.6531
130	6.6534	6.6564
180	6.6558	6.6602
230	6.6616	6.6619
280	6.6616	6.6629

GAsFit 2.3b - Project: sd NMR ring 3oh [Fit: fit1]

Files   Tools   Help

New   Open   Save   Settings   Program For Fitting Experimental Data using GAs

Data :

X	Y
0	7.8111
50	7.8534
100	7.8913
150	7.9298
200	7.967
283	8.013
383	8.0611
483	8.105
566	8.1304
666	8.1463
766	8.1478
866	8.1563

Import Data   Clear Data

Fitting Model:

Adsorption	Fluorescence 1:1
Exponential	Fluorescence 1:1 general
Ligand Binding	Fluorescence 1:1 v1
Polynomial	Fluorescence 1:1 v2
	Fluorescence 1:1 v3
	NMR 1:1
	NMR 1:2

Parameters :

Var	Fix	Min	Max	Result
Co,h	✔	0.02	0.021	0.02
Vo,h	✔	600	601	600
shift,h		7.8	7.9	7.8339
Co,g		0.021	0.0211	0.0211
K		1	10000000	24421
shift,cplx		7.8	9	8.1601

Linear Object Function   Execute

Model Info :

Determination of Ligand Binding [1:1] using NMR

$$\Delta = \frac{\Delta_{11} K_{11}[L]}{1 + K_{11}[L]}$$

$$\Delta = \delta - \delta_s$$

$$\Delta_{11} = \delta_{complex} - \delta_s$$

Graph :

Fits: Add Fit   Remove Fit

- fit1
- fit2
- fit3
- fit4

Messages: clear

```
-------------------------------------
Gradient Method Results:

       Co,h =            0.02
       Vo,h =             600
     shift,h =          7.8339
       Co,g =           0.0211
          K =           24421
  shift,cplx =          8.1601
-------------------------------------


Chi_Sqr =  1.177E-002
#################################################################
```

```
###############################################################################
#! GAsFit Generated File: author: Dusan P Djurdjevic                          #
# Project Name: sd NMR ring 3oh                                               #
# Fit Name:      fit1                                                         #
#                                                                            #
# Model Used:    Ligand Binding->NMR 1:1                                      #
# Model Info:    Determination of Ligand Binding (1:1) using NMR              #
#                                                                            #
# --------- PARAMETERS: ---------                                             #
#       Co,h = 0.02                                                           #
#       Vo,h = 600                                                            #
#       shift,h = 7.8339                                                      #
#       Co,g = 0.0211                                                         #
#       K = 24421                                                             #
#       shift,cplx = 8.1601                                                   #
# -------------------------------                                             #
###############################################################################
```

Volume added	Y(exp)	Y(fit)
0	7.8111	7.8339
50	7.8534	7.8626
100	7.8913	7.8911
150	7.9298	7.9197
200	7.967	7.9482
283	8.013	7.9953
383	8.0611	8.0514
483	8.105	8.105
566	8.1304	8.1394
666	8.1463	8.153
766	8.1478	8.1559
866	8.1563	8.1571

GAsFit 2.3b - Project: Project_1 [Fit: sdring ddd fluo]

Files   Tools   Help

New   Open   Save   Settings   Program For Fitting Experimental Data using GAs

Data:

X	Y
0	43221
2.5	44211
7.5	43401
17.5	45454
27.5	45966
32.5	44262
52.5	44892
82.5	46135
112.5	46736
162.5	47456
212.5	49910
262.5	49235
312.5	49451
362.5	51168
412.5	51662
512.5	52354
612.5	53523
612.5	53523

Import Data   Clear Data

Fitting Model:

Adsorption
Exponential
Ligand Binding
Polynomial

Fluorescence 1:1
Fluorescence 1:1 general
Fluorescence 1:1 v1
Fluorescence 1:1 v2
Fluorescence 1:1 v3
NMR 1:1
NMR 1:2

Parameters:

Var	Fix	Min	Max	Result
Co,h	☐	1.64E-9	100	0.0063378
Vo,h	☑	0.003	100	0.003
Fo,h	☑	43221	100	43221
Co,g	☑	1E-8	1	1E-8
k11/ks	☐	0.5	5	2.7269
K	☐	1	10000000	26447000

Linear Object Function ▼   Execute

Model Info:

Determination of Ligand Binding (1:1) using Fluorescence (Ligand not fluorescent)

$$\frac{F}{F_0} = \frac{1 + (k_{11}/k_s)K[L]}{1 + K[L]}$$

Graph:

Fits: Add Fit   Remove Fit

good sd ring
sd ring high
sdring ddd fluo
very goog fit

Messages   clear

```
------------------------------------------------
Gradient Method Results:
------------------------------------------------
        Co,h  =        0.0063378
        Vo,h  =            0.003
        Fo,h  =            43221
        Co,g  =          1E-008
      k11/ks  =           2.7269
           K  =        2.6447E007
------------------------------------------------

Chi_Sqr  =   7.111E+002
################################################
```

```
################################################################################
#! GAsFit Generated File: author: Dusan P Djurdjevic                            #
# Project Name: Project_1                                                       #
# Fit Name:     sdring ddd fluo                                                 #
#                                                                              #
# Model Used:   Ligand Binding->Fluorescence 1:1                               #
# Model Info:   Determination of Ligand Binding (1:1) (Ligand not fluorescent) #
#                                                                              #
# --------- PARAMETERS: ----------                                            #
#        Co,h = 0.0063378                                                      #
#        Vo,h = 0.003                                                          #
#        Fo,h = 43221                                                          #
#        Co,g = 1E-008                                                         #
#        k11/ks = 2.7269                                                       #
#        K = 26447000                                                          #
# --------------------------------                                            #
################################################################################
```

Volume added	Y(exp)	Y(fit)
0	43221	43221
2.5	44211	43319
7.5	43401	43511
17.5	45454	43885
27.5	45966	44244
32.5	44262	44418
52.5	44892	45083
82.5	46135	45988
112.5	46736	46797
162.5	47456	47964
212.5	49910	48944
262.5	49235	49775
312.5	49451	50486
362.5	51168	51101
412.5	51662	51635
512.5	52354	52517
612.5	53523	53213
612.5	53523	53213
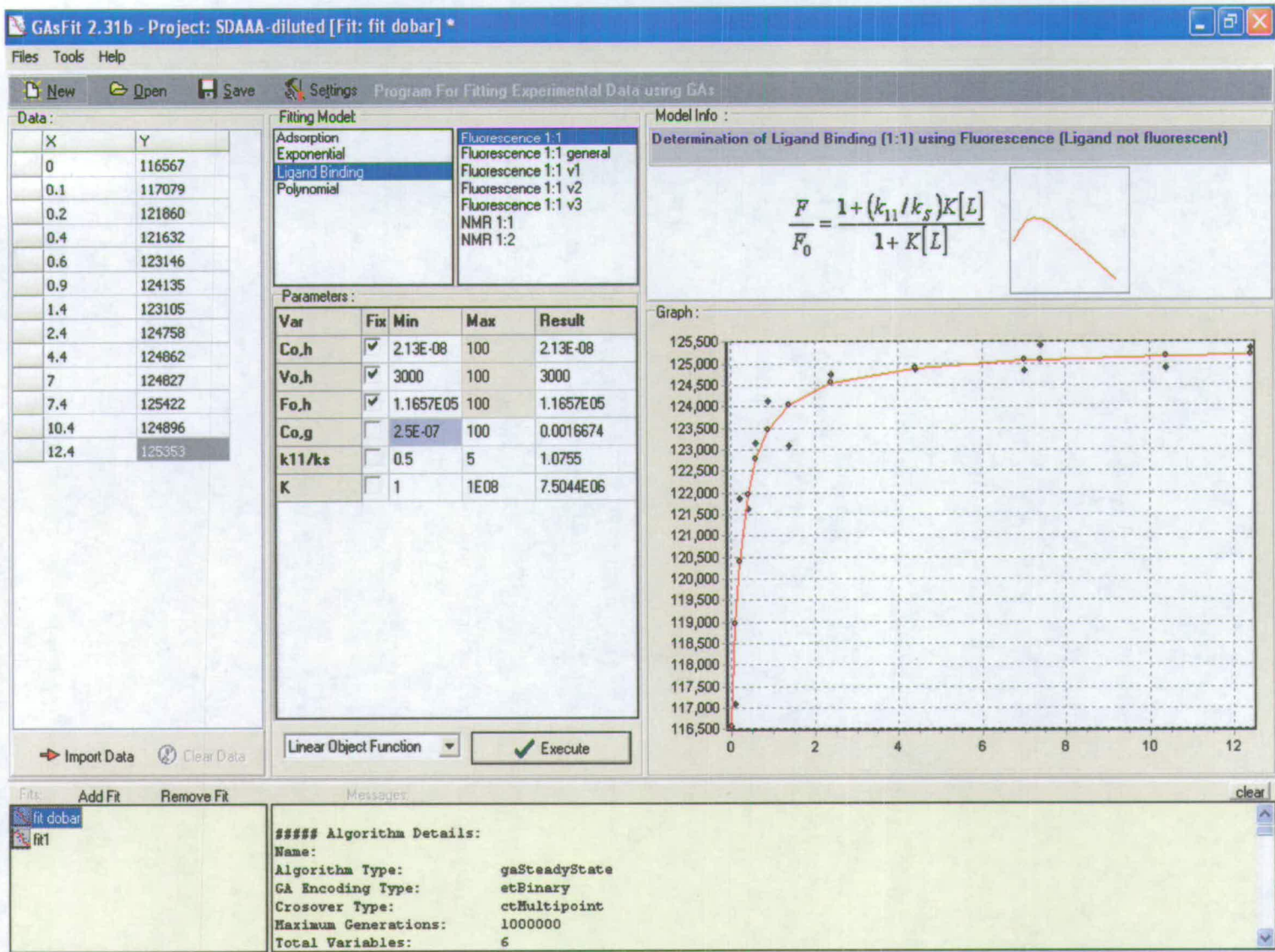
GasFit results of 1·110 complex (fluorescence, CH$_2$Cl$_2$, 293K)

GAsFit 2.31b - Project: SDAAA-diluted [Fit: fit dobar] *

Files   Tools   Help

New   Open   Save   Settings   Program For Fitting Experimental Data using GAs

Data :

X	Y
0	116567
0.1	117079
0.2	121860
0.4	121632
0.6	123146
0.9	124135
1.4	123105
2.4	124758
4.4	124862
7	124827
7.4	125422
10.4	124896
12.4	125353

Import Data   Clear Data

Fitting Model:

Adsorption
Exponential
Ligand Binding
Polynomial

Fluorescence 1:1
Fluorescence 1:1 general
Fluorescence 1:1 v1
Fluorescence 1:1 v2
Fluorescence 1:1 v3
NMR 1:1
NMR 1:2

Parameters :

Var	Fix	Min	Max	Result
Co,h	✔	2.13E-08	100	2.13E-08
Vo,h	✔	3000	100	3000
Fo,h	✔	1.1657E05	100	1.1657E05
Co,g	☐	2.5E-07	100	0.0016674
k11/ks	☐	0.5	5	1.0755
K	☐	1	1E08	7.5044E06

Linear Object Function   ✔ Execute

Model Info :

Determination of Ligand Binding (1:1) using Fluorescence (Ligand not fluorescent)

$$\frac{F}{F_0} = \frac{1 + (k_{11}/k_s)K[L]}{1 + K[L]}$$

Graph :

Fits: Add Fit   Remove Fit   Messages: clear

fit dobar
fit1

```
##### Algorithm Details:
Name:
Algorithm Type:        gaSteadyState
GA Encoding Type:      etBinary
Crosover Type:         ctMultipoint
Maximum Generations:   1000000
Total Variables:       6
```

```
################################################################################
# Fit Name:      fit dobar                                                     #
#                                                                              #
# Model Used:    Ligand Binding->Fluorescence 1:1                              #
# Model Info:    Determination of Ligand Binding (1:1) (Ligand not fluorescent) #
#                                                                              #
# --------- PARAMETERS: ---------                                              #
#       Co,h = 2.13E-008                                                       #
#       Vo,h = 3000                                                            #
#       Fo,h = 116570                                                          #
#       Co,g = 0.0016674                                                       #
#       k11/ks = 1.0755                                                        #
#       K = 7504400                                                            #
# ------------------------------                                               #
################################################################################
```

X	Yexp	Yfit
0	1.17E+05	1.17E+05
0.1	1.17E+05	1.19E+05
0.2	1.22E+05	1.20E+05
0.4	1.22E+05	1.22E+05
0.6	1.23E+05	1.23E+05
0.9	1.24E+05	1.23E+05
1.4	1.23E+05	1.24E+05
2.4	1.25E+05	1.25E+05
4.4	1.25E+05	1.25E+05
7	1.25E+05	1.25E+05
7.4	1.25E+05	1.25E+05
10.4	1.25E+05	1.25E+05
12.4	1.25E+05	1.25E+05

GAsFit 2.3b - Project: Cationic Fluo [Fit: dodate tacke 2]

Files   Tools   Help

New   Open   Save   Settings   Program For Fitting Experimental Data using GAs

Data :

X	Y
0	3818832.2
1E-5	3808989.2
2E-5	3801727.7
3E-5	3786575.14
5E-5	3759645.9
7E-5	3751127.2
0.0001	3737472.7
0.00011	3712500
0.00012	3701705.2
0.00013	3690802.02
0.00015	3671637
0.0002	3685988
0.00025	3654147.4
0.0003	3620390.8
0.00035	3628702.8
0.0004	3620568.7
0.00045	3620794.6
0.0005	3626088.8
0.00055	3638256.2
0.0006	3618422.7

Import Data   Clear Data

Fitting Model:

Adsorption
Exponential
Ligand Binding
Polynomial

Fluorescence 1:1
Fluorescence 1:1 general
Fluorescence 1:1 v1
Fluorescence 1:1 v2
Fluorescence 1:1 v3
NMR 1:1
NMR 1:2

Parameters :

Var	Fix	Min	Max	Result
Co,h	✓	7.7E-9	8E-9	7.7E-9
Vo,h	✓	0.002	100	0.002
Fo,h	✓	3818832	100	3818800
Co,g		2.6E-8	8E-8	7.8097E-8
k11/ks		0.5	5	0.94824
kl/ks		0.5	10000000	0.5
K		1	1E15	3814700000

Linear Object Function   ✓ Execute

Model Info :

Determination of Ligand Binding (1:1) using Fluorescence (general equation)

$$\frac{F}{F_0} = \frac{1 + (k_{11}/k_S)K[L]}{1 + K[L]} + \frac{k_L}{k_S}[L]$$

Graph :

Fits: Add Fit   Remove Fit

dodate tacke
dodate tacke 2
pravi
solidan

Messages: clear

```
------------------------------------------
Gradient Method Results:
------------------------------------------

     Co,h =          7.7E-009
     Vo,h =          0.002
     Fo,h =       3.8188E006
     Co,g =       7.8097E-008
   k11/ks =          0.94824
    kl/ks =          0.5
        K =       3.8147E009
------------------------------------------

Chi_Sqr =  1.056E+004
##############################################################
```

```
###############################################################################
#! GAsFit Generated File: author: Dusan P Djurdjevic                          #
# Project Name: Cationic Fluo                                                 #
# Fit Name:      dodate tacke 2                                               #
#                                                                             #
# Model Used:    Ligand Binding->Fluorescence 1:1 general                     #
# Model Info:    Determination of Ligand Binding (1:1) using Fluorescence     #
#                                                                             #
# --------- PARAMETERS: ----------                                            #
#       Co,h = 7.7E-009                                                       #
#       Vo,h = 0.002                                                          #
#       Fo,h = 3818800                                                        #
#       Co,g = 7.8097E-008                                                    #
#       k11/ks = 0.94824                                                      #
#       k1/ks = 0.5                                                           #
#       K = 3814700000                                                        #
# --------------------------------                                            #
###############################################################################
```

Volume added	Y(exp)	Y(fit)
0	3.82E+06	3.82E+06
10	3.81E+06	3.81E+06
20	3.80E+06	3.80E+06
30	3.79E+06	3.79E+06
50	3.76E+06	3.77E+06
70	3.75E+06	3.75E+06
100	3.74E+06	3.73E+06
110	3.71E+06	3.72E+06
120	3.70E+06	3.71E+06
130	3.69E+06	3.70E+06
150	3.67E+06	3.68E+06
200	3.69E+06	3.65E+06
250	3.65E+06	3.64E+06
300	3.62E+06	3.63E+06
350	3.63E+06	3.63E+06
400	3.62E+06	3.63E+06
450	3.62E+06	3.63E+06
500	3.63E+06	3.63E+06
550	3.64E+06	3.63E+06
600	3.62E+06	3.63E+06
650	3.63E+06	3.63E+06
700	3.61E+06	3.62E+06
800	3.62E+06	3.62E+06

Appendix 3: Published Paper

Extremely Strong and Readily Accessible AAA−DDD Triple Hydrogen Bond Complexes

Smilja Djurdjevic, David A. Leigh,* Hamish McNab,* Simon Parsons, Gilberto Teobaldi, and Francesco Zerbetto*

School of Chemistry, University of Edinburgh, The King's Buildings, West Mains Road, Edinburgh EH9 3JJ, U.K., and Dipartimento di Chimica "G. Ciamician", Università di Bologna, v. F. Selmi 2, 40126 Bologna, Italy

Received October 16, 2006; E-mail: david.leigh@ed.ac.uk; h.mcnab@ed.ac.uk; francesco.zerbetto@unibo.it

The development of multipoint hydrogen bonding motifs that form complexes with high stability and selectivity is important both for the understanding of biology and in the design of new materials.[1] There is a particular lack of building blocks that can be used to form acceptor, acceptor, acceptor−donor, donor, donor (AAA−DDD) hydrogen bonding patterns, believed to be the strongest contiguous triple hydrogen bond arrangement as a result of multiple favorable secondary electrostatic interactions.[2] Murray and Zimmerman provided the first experimental example of such a system when they reported that the K_a for complex 1·2 is >10^5 M^{-1} in CDCl_3, as evidenced by ^{1}H NMR spectroscopy (Figure 1).[3] They also found, however, that 1·2 is chemically unstable, and the presence of 1,8-bis(dimethylamino)naphthalene (proton sponge) was required to prevent hydride shift from C-4 of 2 to C-10 of 1 during their binding experiments.[3,4] No attempt to quantify the K_a beyond the limit measurable by NMR methods was reported and since these important and seminal studies relatively little progress[5] has been made in developing less reactive AAA−DDD systems. Here we report extremely high association constants for chemically stable AAA−DDD and AA−DDD complexes that feature the novel and readily accessible multiple hydrogen bond acceptors 3 and 4 (Figure 1).

We wondered whether the chemical stability of the Zimmerman AAA unit might be improved by extending the anthyridine aromatic framework. Accordingly, a pentacene analogue, 3, was prepared in only two steps by the diiodination of 2,6-diaminopyridine followed by a double Suzuki coupling with 2-formylphenyl boronic acid and spontaneous cyclization and aromatization (Scheme 1). A modified approach yielded the equivalent AA system, 4, the key step being flash vacuum pyrolysis (FVP) of an oxime (Scheme 1, step v). Single crystals suitable for X-ray analysis were obtained for each of 3 and 4 from saturated CH_2Cl_2/MeOH solutions. The solid state structures (Figure 2) confirmed the molecular geometries and provided data regarding the acceptor heteroatom separations for computer modeling of contiguous H-bond arrays with various prospective H-bond donors.

Experimentally, we first examined the ability of 3 to form complexes with DDD partners 2[6] and 5 in CDCl_3 by ^{1}H NMR spectroscopy, using a standard titration method[7] under conditions where the self-association of each component was negligible (K_{dimer} < 20 M^{-1}). To assess the effect of the extended aromatic system on binding other than chemical reactivity, we also determined the K_a of 4·2 to compare with 6·2[3] ($K_a = 3 \times 10^3$ M^{-1} in CDCl_3). Plots of the chemical shifts of the amino/hydroxyl groups of 2 or 5 versus the [DDD]/[AA or AAA] ratio for 4·2 and 3·5 showed typical 1:1 binding isotherms (Figure 3; confirmed by Job plots, see Supporting Information), and the data were computationally matched to the best-fitting association constant: 4·2, $K_a = 8 \times 10^4$ M^{-1}; 3·5, $K_a = 2.4 \times 10^4$ M^{-1}.[8] However, the Job plot for 3·2
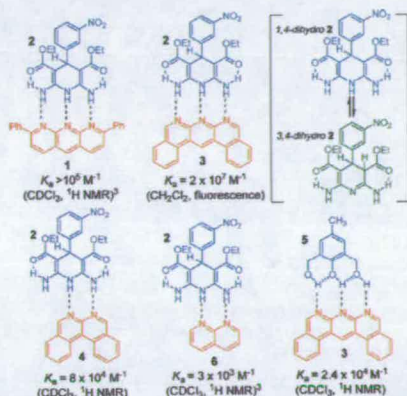
Figure 1. AAA−DDD (1·2,[3] 3·2, and 3·5) and AA−DDD (4·2 and 6·2[3]) heterocomplexes and their 1:1 stability constants (K_a's) in CDCl_3 or CH_2-Cl_2 at room temperature. Repetitions of the binding experiments for each of 3·2, 3·5, and 4·2 gave K_a's within 10% of the values shown (the error in data-fitting for each run was <1%). Inset: In the absence of an additional H-bonding partner, 2 exists in a 2:1 ratio of 1,4-dihydro/3,4-dihydro tautomers at millimolar concentrations in CDCl_3 at room temperature.[3]

Scheme 1. Synthesis of AAA and AA Systems 3 and 4[a]
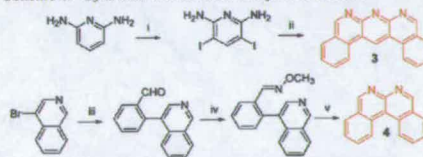
[a] Reagents and conditions: (i) N-Iodosuccinamide, DMF, 86%, (ii) 2-formylphenyl boronic acid, Pd(PPh_3)_4, Cs_2CO_3, dioxane/water (1:1), 80%; (iii) 2-formylphenyl boronic acid, Pd(PPh_3)_4, K_2CO_3, dioxane/water (1:1), 80%; (iv) MeONH_2·HCl, EtOH, 96%, (v) FVP (furnace temperature = 700 °C, inlet temperature = 182 °C, p = 4.8 × 10^{-2} Torr, 10 min), 75%.

showed a 2:1 complex at millimolar concentrations (see Supporting Information), and curve-fitting suggested at least one association constant beyond the range that could be reliably determined by our NMR experiments, consistent with the $K_a > 10^5$ M^{-1} previously reported[3] for 1·2.

Some of the results and observations from the ^{1}H NMR binding experiments deserve further comment. First, hydroxyl groups are much poorer H-bond donors than amides, anilines, or pyrrole-like NH's,[9] and the hydroxyl protons of 5 are also involved in

COMMUNICATIONS
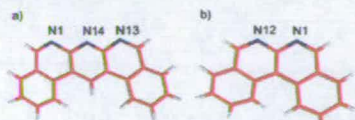
Figure 2 X-ray crystal structures of (a) **3** and (b) **4** (C red, N blue, H white). Nitrogen—nitrogen distances: (a) N13—N14 2.294 Å, N1—N14 2.290 Å and (b) N1—N12 2.300 Å (see Supporting Information).
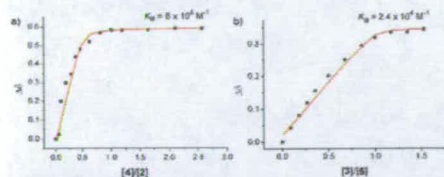
Figure 3. Binding isotherms using the change in chemical shift (Δδ) of (a) the amino NH_2 groups of **2** (10^{-4} M) upon addition of **4** and (b) the hydroxyl groups of **5** (10^{-3} M) upon addition of **3**. The red lines indicate best-fitting K_a's [8]
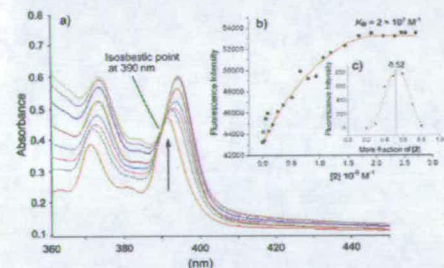
Figure 4. (a) UV/vis spectra in CH_2Cl_2 at 293 K upon the addition of **2** (0→1.2 equiv) to **3** (1×10^{-5} M). The arrow indicates the change in absorption at 390 nm with increasing **2**. (b) Fluorescence intensity at 410 nm in CH_2Cl_2 at 293 K upon the addition of **2** (0→3 equiv) to **3** (1×10^{-9} M). (c) Job plot under similar conditions to (b).

intramolecular H-bonding. It is therefore somewhat remarkable that the K_a (CDCl$_3$, room temperature) for **3·5** is sub-millimolar.[10] Second, the use of **2** in the binding experiments is complicated by its tautomerism (see Figure 1 inset). Murray and Zimmerman reported[3] that 10 equiv of **1** was required to fully convert **2** into the 1,4-dihydro form involved in DDD H-bonding. In contrast, in our NMR titration experiments only 0.5 equiv of **3** proved sufficient to convert the initial 2:1 ratio of the 1,4-dihydro/3,4-dihydro forms of **2** to >98:2 (see Supporting Information). A further indication of the powerful hydrogen bond accepting ability of these new heterocycles is seen in the direct comparison of the AA—DDD complexes in CDCl$_3$ at room temperature; **4·2** is at least 20 times more strongly bound than **6·2** (Figure 1).

We next investigated the binding in complex **3·2** by UV/vis and fluorescence spectroscopy. Upon addition of **2** to **3** (ca. 10^{-5} M, CH_2Cl_2, 293 K), the absorption intensity at 395 nm increased with a clear isosbestic point at 390 nm, suggesting a 1:1 binding mode in this concentration range (Figure 4a). Fluorescence titrations (**3** has a fluorescence quantum yield of 0.94 in CH_2Cl_2, while **2** is nonfluorescent) were performed in CH_2Cl_2 at 293 K by adding a

solution of **2** (10^{-8} M) to **3** (initial concentration 1×10^{-9} M) and monitoring the increase in fluorescence intensity at 410 nm (Figure 4b). Curve-fitting gave a K_a for **3·2** of 2×10^7 M^{-1}. A Job plot confirmed the 1:1 stoichiometry (Figure 4c).

Geometry optimization and frequency calculations were carried out on **3·2**, both in vacuum and in CH_2Cl_2 solution, at the B3LYP/6-31G* level using the Gaussian03 program[11] (see Supporting Information). In the isolated molecules approximation the binding free energy was underestimated by ~10%, while in solution it was overestimated by ~25%. Both types of calculations showed an extremely large electrostatic contribution to complex formation. The simulations also suggest that the AAA—DDD complex is near planar, particularly in solution: a tilt angle of ~5° between the planes of **2** and **3** in CH_2Cl_2 (~21° in vacuum) provides the optimum H-bonding arrangement and the strongest AAA—DDD interaction.

In conclusion, heterocycles **3** and **4** are novel, readily accessible, and chemically stable AA and AAA hydrogen bonding units that form extremely strong supramolecular complexes with DDD partners. The importance of secondary electrostatic interactions in contiguous multipoint hydrogen bonding arrays is well-illustrated by comparison of the relative binding strengths of AAA—DDD complex **3·2** ($K_a = 2 \times 10^7$ M^{-1} in CH_2Cl_2 at room temperature) and the previously reported[12] ADA—DAD complex between 1-butylthymine and 2,6-dibutyramidopyridine ($K_a = 90$ M^{-1} in CDCl$_3$ at room temperature).

Supporting Information Available: Experimental procedures and spectral data for **3** and **4** and complexes **3·2**, **3·5**, and **4·2**, details of X-ray analysis of **3** and **4**, including cif files, and additional experimental details on computational and complexation studies. This material is available free of charge via the Internet at http://pubs.acs.org.

References

(1) (a) Zimmerman, S. C.; Corbin, P. S. *Struct. Bonding (Berlin)* **2000**, *96*, 63—94. (b) Brunsveld, L.; Folmer, B. J. B.; Meijer, E. W.; Sijbesma, R. P. *Chem. Rev.* **2001**, *101*, 4071—4097. (c) Prins, L. J.; Reinhoudt, D. N.; Timmerman, P. *Angew. Chem., Int. Ed.* **2001**, *40*, 2383—2426. (d) Schmuck, C.; Wienand, W. *Angew. Chem., Int. Ed.* **2001**, *40*, 4363—4369. (e) Sherrington, D. C.; Taskinen, K. A. *Chem. Soc. Rev.* **2001**, *30*, 83—93. (f) Sijbesma, R. P.; Meijer, E. W. *Chem. Commun.* **2003**, 5—16. (g) Zimmerman, S. C.; Park, T. *Polym. Prepr.* **2005**, *42*, 1159—1160.
(2) (a) Jorgensen, W. L.; Pranata, J. *J. Am. Chem. Soc.* **1990**, *112*, 2008—2010. (b) Pranata, J.; Wierschke, S. G.; Jorgensen, W. L. *J. Am. Chem. Soc.* **1991**, *113*, 2810—2819.
(3) (a) Murray, T. J.; Zimmerman, S. C. *J. Am. Chem. Soc.* **1992**, *114*, 4010—4011. (b) Zimmerman, S. C.; Murray, T. J. *Tetrahedron Lett.* **1994**, *35*, 4077—4080.
(4) The reductive instability of **1** can also be overcome by using a protonated 2,6-aminopyridine derivative as the DDD partner. See: Bell, D. A.; Anslyn, E. V. *Tetrahedron* **1995**, *51*, 7161—7172.
(5) (a) Sugiyama, Y.; Adachi, K.; Kawata, S.; Kumagai, H.; Inoue, K.; Katada, M.; Kitagawa, S. *CrystEngComm* **2000**, *2*, 174—176. (b) Sugiyama, Y.; Adachi, K.; Kabir, M. K.; Kitagawa, S.; Suzuki, T.; Kaizaki, S.; Kawata, S. *Mol. Cryst. Liq. Cryst.* **2002**, *379*, 419—424. (c) Adachi, K.; Sugiyama, Y.; Yoneda, K.; Yamada, K.; Nozaki, K.; Fuyuhiro, A.; Kawata, S. *Chem.—Eur. J.* **2005**, *11*, 6616—6628.
(6) Compound **2** was prepared according to Murray, T. J.; Zimmerman, S. C. *Tetrahedron* **1995**, *51*, 635—648.
(7) Connors, K. A. *Binding Constants: The Measurement of Molecular Complex Stability*; Wiley-Interscience: New York, 1987.
(8) GAs-Fit (www.djurdjevic.org.uk/software/GAsFit): A custom-written program, suitable even for large binding constants, that uses an evolutionary algorithm to solve the standard equations for titration methods (see ref 7). In tests, for data in the K_a 10^2—10^6 M^{-1} range, GAs-Fit gave similar results to the widely used binding constant determination program available from H.-J. Schneider's group (www.uni-saarland.de/fak8/schneider/Links/download.html).
(9) Hunter, C. A. *Angew. Chem., Int. Ed.* **2004**, *43*, 5310—5324.
(10) There is no evidence of deprotonation of **5** by **3** in the UV/vis spectra.
(11) Frisch, M. J.; et al. *Gaussian 03*, revision C.02; Gaussian, Inc.: Wallingford, CT, 2004.
(12) Hamilton, A. D.; Van Engen, D. *J. Am. Chem. Soc.* **1987**, *109*, 5035—5036.

JA067410T